UNIVERSITAT DE
BARCELONA

Biomedical applications of PolyPurine Reverse Hoogsteen hairpins: immunotherapy and gene repair

Alejandro Jiménez Félix

UNIVERSITAT DE BARCELONA

FACULTAT DE FARMÀCIA I CIÈNCIES DE L'ALIMENTACIÓ

DEPARTAMENT DE BIOQUÍMICA I FISIOLOGIA
SECCIÓ DE BIOQUÍMICA I BIOLOGIA MOLECULAR

Programa de Doctorat en Biomedicina

BIOMEDICAL APPLICATIONS OF POLYPURINE REVERSE HOOGSTEEN HAIRPINS: IMMUNOTHERAPY AND GENE REPAIR

Alejandro Jiménez Félix

Barcelona, 2020

UNIVERSITAT DE BARCELONA

FACULTAT DE FARMÀCIA I CIÈNCIES DE L'ALIMENTACIÓ

DEPARTAMENT DE BIOQUÍMICA I FISIOLOGIA
SECCIÓ DE BIOQUÍMICA I BIOLOGIA MOLECULAR

Programa de Doctorat en Biomedicina

BIOMEDICAL APPLICATIONS OF POLYPURINE REVERSE HOOGSTEEN HAIRPINS: IMMUNOTHERAPY AND GENE REPAIR

Memòria presentada per Alejandro Jiménez Félix per optar al títol de Doctor
per la Universitat de Barcelona

Dr. Carlos J. Ciudad Gómez
Director

Dra. Verónica Noé Mata
Directora

Alejandro Jiménez Félix
Barcelona, 2020

ABBREVIATIONS

+AAT	Containing adenine, aminopterin and thymidine
2,8-DHA	2,8-dihydroxyadenine
A	Adenine
AGO2	Argonaute RISC Catalytic Component 2
ALAS1	Aminolevulinic acid synthase I
ALDH1A1	Aldehyde dehydrogenase 1
AMP	Adenosine monophosphate
APC	Antigen presenting cell
APOB	Apolipoprotein B
APOE	Apolipoprotein E
aprt	Adenine phosphoribosyl transferase
ASO	Antisense oligonucleotide
ATXN3	Ataxin 3
BCL2	B-cell CLL/lymphoma 2
bp	base pairs
C	Cytosine
C_2H_2	Two pairs of cysteine and histidine residues
CAR	Chimeric antigen receptor
Cas	CRISPR-associated protein
CCNG2	Cyclin G2
CCR5	C-C motif chemokine receptor 5
CD47	CD47 molecule
CDC2	Cyclin dependent kinase 1
CFTR	Cystic fibrosis transmembrane conductance regulator
Chimeraplasts	Chimeric RNA/DNA oligonucleotides
CHO	Chinese hamster ovary
CMV	Citomegalovirus
COL7A1	Type VII collagen
CREB-1	cAMP-responsive element-binding protein 1
CRISPR	Clustered regularly interspaced short palindromic repeats
crRNA	CRISPR RNAs
CTLA4	Cytotoxic T lymphocyte antigen 4
CXCR4	C-X-C motif chemokine receptor 4
cyc1	Cytochrome C1
D	Aspartic acid
DEB	Diepoxybutane
dhfr	dihydrofolate reductase
D-loop	Displacement loop
DMD	Duchenne muscular dystrophy
DOTAP	N-[1-(2,3-dioleoyloxy)propil]-N,N,N-trimethylammonium methylsufate
DSB	Double-strand DNA breaks
dsDNA	Double-stranded DNA

Abbreviations

dsRNA	Double-stranded RNA
ERCC1	Excision repair cross-complementation group 1
ESRD	End-stage renal disease
F9	Clotting factor IX
FA	Fanconi anemia
FAH	Fumarylacetoacetate hydrolase
FANCA	Fanconi anemia complementation group A
FANCF	Fanconi anemia complementation group F
FBS	Fetal bovine serum
FDA	Food and drug administration
FMR1	Fragile X mental retardation 1
G	Glycine
G	Guanine
GATA-3	GATA binding protein 3
gDNA	Genomic DNA
-GHT	lacking glycine, hypoxanthine and thymidine
glb1	β-galactosidase
GM-CSF	Granulocyte-macrophage colony-stimulating factor
GTF2E2	General transcription factor IIE
H	Histidine
HDR	Homology directed repair
HER-2	Erb-B2 receptor tyrosine kinase 2
HIV-1	Human immunodeficiency virus
hprt	Hypoxanthine phosphoribosyl transferase
HSC	Hematopoietic stem cell
HTT	Huntingtin
HUVEC	Human umbilical vein endothelial cells
I	Isoleucine
ICL	Interstrand cross-link
IE2	Immediate-early-2
IFN	Interferon
IL	Interleukin
IL2RG	Interleukin 2 receptor subunit gamma
LDLR	Low-density lipoprotein receptor
MCL-1	Myeloid cell leukemia 1
MMC	Mitomycin C
mTOR	Mechanistic target of rapamycin kinase
MTT	3-(4,5-dimethylthiazol-2-yl)-2,5-diphenyltetrazolium bromide
N	Asparagine
NER	Nucleotide excision repair
NF-Kβ	Nuclear factor kappa β
NGS	Next generation sequencing
NHEJ	Non-homologous end joining

NK	Natural killer
nt	Nucleotide
PAM	Protospacer adjacent motif
PCNA	Proliferating cell nuclear antigen
PCR	Polymerase chain reaction
PD-1	Programmed cell death 1
PD-L1	Programmed cell death 1 ligand 1
PKLR	Pyruvate kinase 1
PMA	Phorbol 12-myristate 13-acetate
PNA	Peptide nucleic acid
POLR2G	RNA polymerase II subunit G
PPRH	PolyPurine Reverse Hoogsteen hairpin
PRPP	Phosphoribosyl pyrophosphate
PTOV1	Prostate tumor overexpressed 1
RFC	Replication factor C
RISC	RNA-induced silencing complex
RNAi	RNA interference
RPA	Replication protein A
rRNA	Ribosomal RNA
RVD	Repeat-variable di-residues
SELEX	Systematic evolution of ligands by exponential enrichment
sgRNA	single-guide RNA
siRNA	Small interfering RNA
SIRPα	Signal regulatory protein alpha
SMN2	Survival of motor neuron 2
SOD1	Superoxid dismutase 1
ssDNA	Single-stranded DNA
ssODN	Single-stranded oligonucleotide
ssRNA	Single-stranded RNA
STAT3	Signal transducer and activator of transcription 3
T	Thymine
TALEN	Transcription activator-like effector nucleases
TAM	Tumor-associated macrophages
TF	Transcription factor
TFIIH	Transcription factor IIH
TFO	Triplex-forming oligonucleotide
TH	Tyrosine hydroxylase
TNF-α	Tumor necrosis factor Alpha
TOP1	DNA topoisomerase 1
TOP3	Topoisomerase 3
tracrRNA	Transactivating crRNA
TRY	Tyrosinase
TTR	Transthyretin

Abbreviations

UGT1A1	UDP-glucuronosyltransferase
VEGF	Vascular endothelial growth factor
WC	Watson-Crick
XPA	xeroderma pigmentosum complementary group A
ZF	Zinc-finger
ZFN	Zinc-finger nucleases

TABLE OF CONTENTS

PRESENTATION

This thesis is centered on the study of PolyPurine Reverse Hoogsteen (PPRH) hairpins technology as a tool for both gene silencing and gene editing.

PolyPurine Reverse Hoogsteen (PPRH) hairpins are nonmodified single-stranded DNA molecules formed by two antiparallel polypurine mirror repeat domains linked by a five-thymidine loop that are bound through intramolecular reverse Hoogsteen bonds, thus allowing the formation of the hairpin structure. PPRHs can bind in a sequence specific manner to their polypyrimidine target sequence in the dsDNA by Watson-Crick bonds, thus producing a triplex structure and inhibiting the expression of the targeted gene (de Almagro *et al.* 2009; Ciudad *et al.* 2017).

As a first part of this thesis, we increased our knowledge about the usage of PPRHs as gene silencing tools. On the one hand, we explored the pharmacogenomic response in PC3 prostate cancer cells upon the treatment with a PPRH designed against the antiapoptotic *survivin* gene that we had previously validated in our laboratory (Rodríguez *et al.* 2013). The analyses demonstrated that the PPRH was specific towards its intended target gene and the genomic response involved a deregulation of vital cell processes such as Apoptosis, Regulation of cell proliferation, Cellular response to stress and Prostate cancer, thus severely affecting cell viability. We also determined the lack of hepatotoxicity and nephrotoxicity of PPRH molecules *in vitro* in hepatic and renal human cell lines, respectively.

On the other hand, we were able to apply the PPRHs technology for immunotherapy approaches. We centered our studies in the inhibition of the CD47/SIRPα and the PD-1/PD-L1 pathways that promote the escape of tumor cells from host's immunosurveillance system. PPRHs were designed to silence those genes in macrophage/cancer cells co-culture experiments, showing an increase in the killing of cancer cells by macrophages. We also determined that apoptosis was the mechanism responsible for this cancer cell death.

The second part of this thesis is focused on the usage of PPRHs as gene editing tools. Repair-PPRHs are hairpins that bear an extension sequence at one end of the molecule which is homologous to the DNA sequence to be repaired but containing the wild-type nucleotide instead of the mutated one. Previous works performed in our laboratory demonstrated that repair-PPRHs were able to correct a representative collection of point mutations (substitutions, double substitutions, deletions and insertions) in the endogenous *locus* of the

dihydrofolate reductase (dhfr) gene in different Chinese Hamster Ovary (CHO) mutant cell lines (Solé *et al.* 2014, 2016).

In this work we have demonstrated the generality of action of the repair-PPRHs by correcting different single-point mutations in the *adenine phosphoribosyltransferase (aprt)* gene in CHO mutant cells. Moreover, we determined that the correction was specific since we did not detect any off-target effect in the repaired genome. We also gained insight into the mechanism responsible for the repair event, showing the formation of a D-loop structure upon the binding of the PPRH to its target sequence that stimulates homologous recombination.

Finally, we used repair-PPRHs to try to correct a single point mutation in the *FANCA* gene responsible for Fanconi anemia in a patient-derived human cell line, to extend the potential of PPRHs to correct mutations responsible for human monogenic diseases.

1. INTRODUCTION

1.1 Therapeutic oligonucleotides

The discovery of the DNA double-helix structure in 1953 set a milestone in field of molecular biology (Franklin & Gosling 1953; Watson & Crick 1953; Wilkins *et al.* 1953). Double-stranded DNA (dsDNA) is formed by two complementary strands where, through Watson-Crick (WC) hydrogen bonds, adenine pairs with thymine and guanine with cytosine, producing A·T and G·C base pairs. This fact implied that DNA replication is possible due to the complementary nature of both strands and corroborated that the DNA is the carrier of the genetic information, as previously stated by Avery and colleagues in 1944 (Avery *et al.* 1944). In 1957, Felsenfeld and collaborators found that a chain of polyribouridylic acid could bind to a double-stranded polyriboadenylic-polyribouridylic acid structure in the presence of Mg^{2+}, leading to a three-stranded structure (Felsenfeld *et al.* 1957). Two years later, Karst Hoogsteen proposed the model that described the existence of this triple stranded structure (Hoogsteen 1959). For that reason, the hydrogen bonds involved in triple-helix formation, which were different from those of Watson-Crick base pairing, were named as Hoogsteen hydrogen bonds (Hoogsteen 1963). The first example of sequence-specific functional use of a third strand of DNA was shown by Morgan and Wells in 1968, when they described the ability of a poly(U) to bind to a poly(dA:dT) dsDNA, effectively reducing the transcription of the dsDNA (Morgan & Wells 1968). In 1987, two significant studies showed that short oligonucleotides could be used to induce DNA cleavage at specific sites through DNA triplex formation (Le Doan *et al.* 1987; Moser & Dervan 1987). At the same time, both Fresco and Wells teams contributed to this field by studying different triple helical structures, proposing their implication in the control of gene expression (Broitman *et al.* 1987; Wells *et al.* 1988).

All these discoveries during the 20th century eventually led to the development of different types of oligonucleotides with the ability to modulate gene expression. These therapeutic oligonucleotides included triplex forming oligonucleotides (TFOs), antisense oligonucleotides (ASOs), small interfering RNAs (siRNAs), aptamers, ribozymes and decoys.

1.1.1 TFOs

TFOs are DNA oligonucleotides of 10-30 nucleotides (nt) that bind in a sequence-specific manner to the major groove of the dsDNA at

polypurine/polypyrimidine stretches (Knauert & Glazer 2001; Duca *et al.* 2008). This binding can occur either in parallel or antiparallel orientation towards the purine strand of the duplex (Figure 1). Their specificity of binding is based on the base triplets formed either by Hoogsteen or reverse Hoogsteen hydrogen bonds between the third strand and the purine strand of the duplex. The first triplex-mediated inhibition of transcription *in vitro* was demonstrated in 1988 with the *C-MYC* gene (Cooney *et al.* 1988). Since then, TFOs have been used for inhibition of gene transcription either by distorting the standard double helix structure or by blocking the binding of transcription factors (TFs) (Curcio *et al.* 1997; Vasquez & Wilson 1998). Also, there are some examples of TFOs that have been used to inhibit the replication process (Guieysse *et al.* 1995; Diviacco *et al.* 2001; Pesce *et al.* 2005).
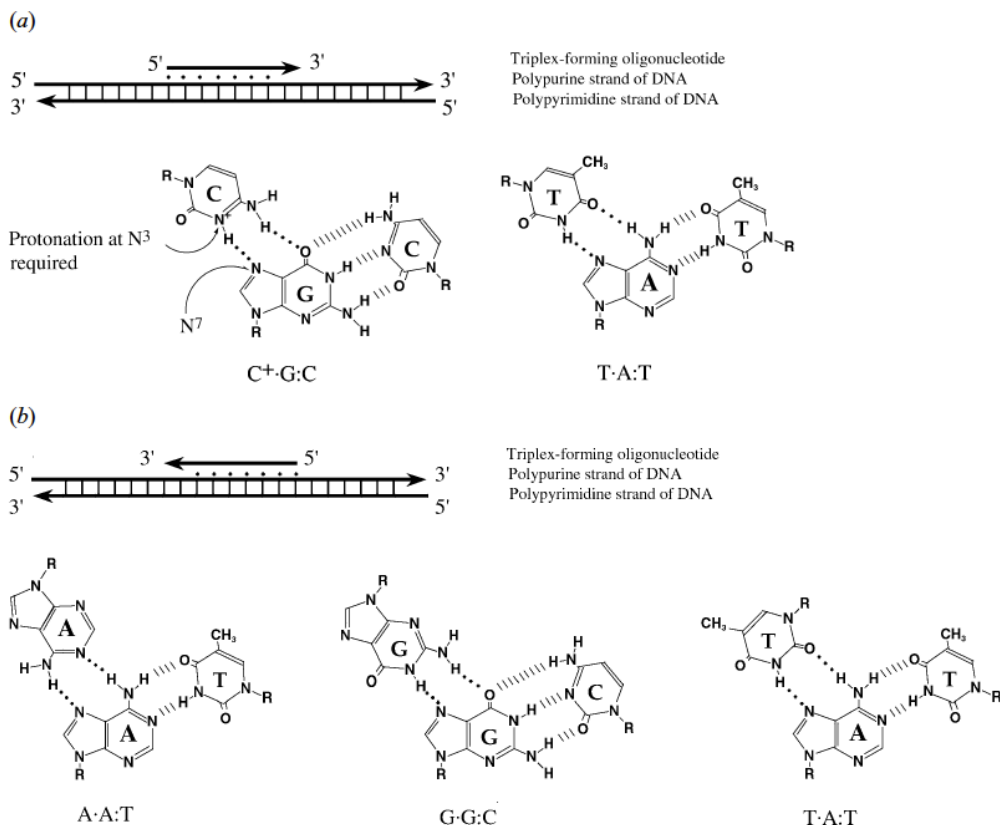
Figure 1. Motifs for triplex formation. Triplex formation occurs at polypurine/polypyrimidine sites in duplex DNA. At such sites, third strands can bind in either (a) the pyrimidine (Y·R:Y) motif or (b) the purine (R·R:Y) motif. In the pyrimidine motif, the third strand is parallel in polarity to the purine strand of the duplex. In the purine motif, it is anti-parallel. The canonical base triplets in each motif are shown. Obtained from (Vasquez & Glazer 2002).

1.1.2 ASOs

In 1978, Stephenson and Zamecnik showed that an oligodeoxynucleotide complementary to a target sequence located in the RNA of Rous sarcoma virus inhibited its replication *in vitro* (Stephenson & Zamecnik 1978). Nowadays, these kinds of molecules are called ASOs, which are single-stranded oligonucleotides typically around 20 nt in length that bind by WC bonds to a target mRNA and induce RNAse H endonuclease activity that cleaves the RNA-DNA heteroduplex, thus reducing the translation of the target gene (Crooke 2017). In other cases, ASOs have also been designed to interfere with alternative splicing by targeting splice sites, exons or introns, resulting in exclusion or inclusion of the targeted exon (Goyal & Narayanaswami 2018).

The advances in organic chemistry have made possible the synthesis of chemical modifications in the backbone of the oligonucleotides to favor their effect, increase the resistance to nucleases or improve the delivery into the cells (Rinaldi & Wood 2018). The most relevant chemical modifications and their main properties are shown in Figure 2.

Until date, five different ASOs have been approved by the Food and Drug Administration (FDA): fomivirsen targeting the *immediate-early-2* (*IE2*) gene for cytomegalovirus (CMV) retinitis (Jabs & Griffiths 2002); mipomersen targeting the apolipoprotein B (*APOB)* gene for homozygous familiar hypercholesterolemia (Bell *et al.* 2011); eteplirsen targeting the *dystrophin* gene for Duchenne muscular dystrophy (DMD) (Lim *et al.* 2017); nusinersen targeting the *survival of motor neuron 2* (*SMN2*) gene for spinal muscular atrophy (Wurster & Ludolph 2018) and inotersen targeting the *transthyretin* (*TTR*) gene for hereditary transthyretin amyloidosis (Mathew & Wang 2019).
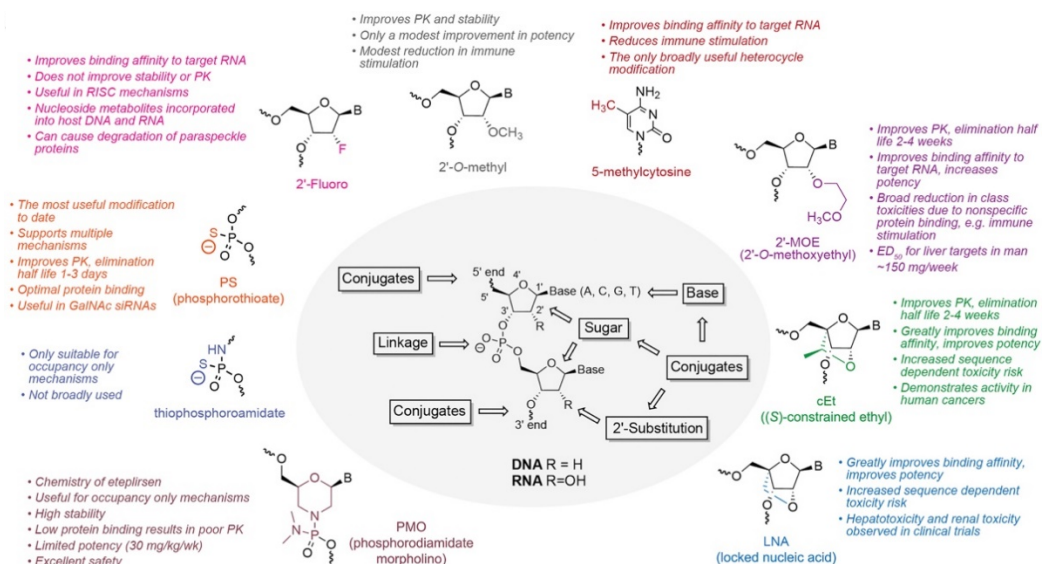
Figure 2. Nucleic acid analogs of RNA and DNA developed in ASOs. These consist of base modifications, sugar modifications, internucleoside linkage modifications, and conjugates of small and large molecules to every position of a dinucleotide. Structures and properties of several key modifications which have been used in clinical trials and/or approved products are shown. Obtained from (Crooke *et al.* 2018).

1.1.3 siRNAs

siRNAs are double-stranded RNA (dsRNA) oligonucleotides of 21-22 nt in length with two nucleotides protruding at the 3′-end of each strand that are designed against a specific mRNA target sequence. One of the strands is called the antisense (or guide) strand whereas the other one is the sense (or passenger) strand (Chernikov *et al.* 2019). When the molecule is delivered into the cell, the duplex siRNA enters the RNA interference (RNAi) pathway where the antisense strand is recognized by a protein complex named RNA-induced silencing complex (RISC). Within the RISC, the siRNA is unwound and the sense strand is discarded whereas the antisense strand serves as the guide for the recognition of complementary mRNAs. After the target sequence is recognized, the mRNA is cleaved 10 nucleotides downstream from the 5' end of the antisense strand by the endonuclease argonaute 2 (AGO2) of the RISC complex (Figure 3), thus reducing the protein levels of the targeted gene (Dana *et al.* 2017; Ahmadzada *et al.* 2018). This entire mechanism, which is highly conserved in eukaryotic organisms, was first demonstrated in 1998 in the

nematode *C. elegans* when the delivery of a dsRNA effectively decreased the mRNA levels of the target gene (Fire *et al.* 1998). It is known that the main function of the RNAi pathway is the defense against viruses or other exogenous genetic elements and the regulation of gene expression (Shabalina & Koonin 2008).

In the last two years, 2 siRNA-based therapies have been approved by the FDA: patisiran for the treatment of hereditary transthyretin amyloidosis (target gene *TTR*) in 2018 (Mullard 2018), and givosiran, which targets the *aminolevulinic acid synthase I (ALAS1)* gene, for the treatment of acute hepatic porphyria in 2019 ("FDA approves first treatment for inherited rare disease | FDA" 2019).

Figure 3. RNA interference pathway. dsRNA molecules are processed by the endonuclease Dicer into short, active siRNAs. The siRNA is loaded by Dicer onto AGO2, which selects the siRNA guide strand and cleaves the passenger strand. Then, the guide strand pairs with its complementary target mRNA and AGO2 cleaves the target. Obtained from (Dana *et al.* 2017).

1.1.4 Aptamers

Aptamers are short, single-stranded sequences of either DNA or RNA that have been evolved *in vitro* to bind to a desired target (small molecule or protein) with high affinity and specificity after an iterative process called Systematic Evolution of Ligands by Exponential Enrichment (SELEX) (Figure 4). Both Szostak and Gold laboratories described this process simultaneously in 1990 (Ellington & Szostak 1990; Tuerk & Gold 1990). In a similar way that antibodies bind to antigens, the action of aptamers rely on their tertiary structure. Aptamers can contain different types of secondary structures including stems, loops, bugles, pseudoknots and G-quadruplexes that form unique three-dimensional structures that can recognize their cognate targets (Zhou & Rossi 2017). Therefore, chemical modifications or changes in the sequence may alter their activity. In addition, aptamers present

some advantages such as short generation times, low variability and costs of manufacturing, thermal stability and high target potential ranging from ions to live animals.

Several aptamers have been developed for cancer therapy due to the particularities of cancer cells (e.g. overexpression of membrane proteins). In this case, whole living cells can be employed as selection targets. This methodology to obtain aptamers against specific living cells is called Cell-SELEX, where the aptamers can recognize the native conformation of the target molecule (Zhang *et al.* 2019). The only aptamer that has been approved by the FDA so far is pegaptanib (2004), an anti-vascular endothelial growth factor (anti-VEGF) RNA aptamer for the treatment of all types of neovascular age-related macular degeneration (Ng *et al.* 2006).
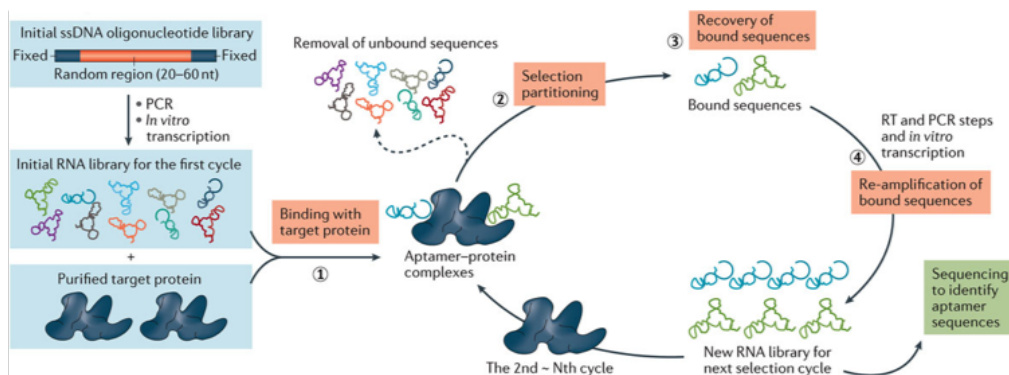
Figure 4. Example of SELEX to obtain RNA aptamers. A ssDNA pool is used as initial template for generating a dsDNA library by PCR and is subsequently converted into a corresponding RNA library via *in vitro* transcription for the first selection cycle. Step 1, the RNA library is incubated with the target protein. Step 2, bound species are isolated from unbound species through different partitioning strategies. Step 3, target-bound species are recovered. Step 4, sequences are re-amplificated (reverse transcription, PCR and *in vitro* transcription) into a new RNA library for the next selection cycle. Adapted from (Zhou & Rossi 2017).

1.1.5 Ribozymes

Ribozymes are single-stranded RNA molecules (ssRNA) that catalyze the formation and cleavage of phosphodiester bonds at specific sites in RNA strands (Jose 2002). These sites can be located in an RNA linked to the ribozyme (self-cleavage) or in an external RNA (trans-cleavage). The cleavage

occurs by nucleophilic attack of the 2'-OH group onto the neighboring phosphorus (Müller 2015). This fact makes RNA the only molecule with information-carrying capacity and inherent catalytic activity. In 1982, Cech and coworkers first described RNA self-splicing of the 413-nucleotide group I intron of the 26S ribosomal RNA (rRNA) from *Tetrahymena thermophila* (Kruger *et al.* 1982). Four years later, they also described a variant of the *T. thermophila* ribozyme that could act in trans (i.e. acting upon other RNA substrates) (Zaug *et al.* 1986).

The hammerhead ribozyme, which is the smallest ribozyme and one of the most studied ones, is composed of ~30 nt and is capable of self-cleaving a phosphodiester bond (Symons 1989). However, the hammerhead ribozyme can be divided into a substrate and a catalytic strand (ribozyme), thus providing its possible application as a trans-acting ribozyme by constructing a catalytic core flanked by two sequences that are complementary to the RNA target sequence (Haseloff & Gerlach 1988). Every RNA molecule can be targeted by the hammerhead ribozyme since its putative cleavage site is "XUY", where "X" is any base and "Y" is any base except "G" (Shimayama *et al.* 1995) (Figure 5).
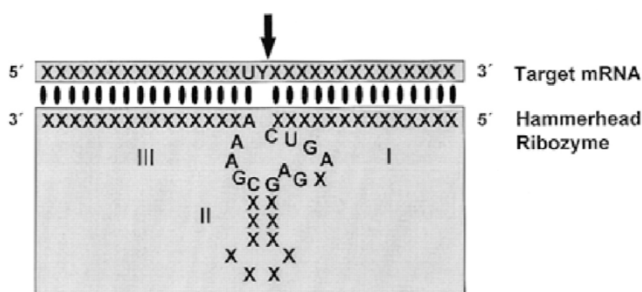
Figure 5. Cleavage of a target mRNA molecule by a hammerhead ribozyme. The hammerhead ribozyme binds to its target mRNA sequence forming a typical three-stem structure (I-III) which leads to the cleavage of the target mRNA at the site (indicated with an arrow). The only sequence requirement is the presence of an XUY cleavage site, where X is any base and Y is any base but G. Obtained from (Phylactou *et al.* 1998).

Ribozymes have been developed to knockdown genes involved in cancer progression such as *Erb-B2 receptor tyrosine kinase 2 (HER-2)* (He *et al.* 2010) and *survivin* (Fei *et al.* 2008). Additionally, ribozymes have also been used as antiviral agents against the human immunodeficiency virus 1 (HIV-1) (Nazari *et al.* 2008) and hepatitis B (Weinberg *et al.* 2000) and C viruses (Sakamoto *et al.* 1996).

1.1.6 Decoys

Decoys typically comprise dsDNA oligonucleotides that contain either one copy or a tandem repeat sequence representative of the consensus binding sequence recognized by a targeted TF (Mann 2005) (Figure 6). Therefore, these molecules are used to draw proteins away from their binding sites present in promoters or enhancer regions of a target gene. The usage of decoys for modulation of gene expression was first described in 1995. Dzau and coworkers reported the usage *in vivo* of a decoy oligonucleotide with high affinity for the transcription factor E2F to block the activation of genes related to cell cycle progression and intimal hyperplasia after vascular injury such as *C-MYC*, *cyclin dependent kinase 1* (*CDC2*) and *proliferating cell nuclear antigen* (*PCNA*) (Morishita *et al.* 1995).
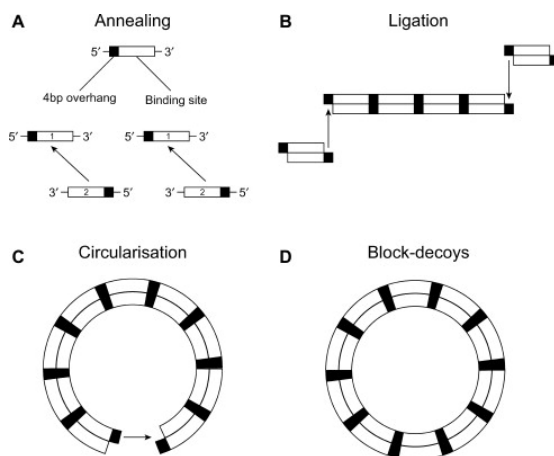
Figure 6. Block-decoys formation. (A) ssDNA molecules are annealed to form regulatory element block containing a transcription factor binding site and a 4-bp single-stranded overhang at 5' terminus. (B) Regulatory element blocks are ligated together, (C) which circularize, allowing intramolecular ligation of cohesive termini, forming (D) a covalently closed circular block decoy containing multiple copies of the target binding site. Obtained from (Brown *et al.* 2013)**.**

Decoys have also been used in models of inflammation targeting nuclear factor kappa β (NF-Kβ) (D'Acquisto *et al.* 2000), E2F (Tomita *et al.* 2004) and AP-1 (Ahn *et al.* 2004). Moreover, anticancer approaches targeting cAMP-responsive element-binding protein 1 (CREB-1) (Liu *et al.* 2004), signal transducer and activator of transcription 3 (STAT3) (Leong *et al.* 2003) and SP1 (Novak *et al.* 2003) have also been performed.

1.2 PPRHs as gene silencing tool

PolyPurine Reverse Hoogsteen (PPRH) hairpins are nonmodified single-stranded DNA molecules formed by two antiparallel polypurine mirror repeat domains linked by a five-thymidine loop. The two polypurine domains are bound through intramolecular reverse Hoogsteen bonds, thus allowing the formation of the hairpin structure. PPRHs can bind in a sequence specific manner to their polypyrimidine target sequence in the dsDNA by WC bonds, producing a triplex structure and displacing the polypurine strand of the dsDNA (Coma *et al.* 2005; Ciudad *et al.* 2017) (Figure 7). Both strands of the genomic DNA (gDNA) can be targeted by PPRHs since the only requirement for their design is the presence of a polypyrimidine domain located in one strand or the other. PPRHs directed against the template strand of the target gene are called template-PPRHs whereas the ones targeting the coding strand of the DNA are called coding-PPRHs, which are also able to bind to the transcribed mRNA, since it has the same sequence and orientation than the coding strand of the target gene. Therefore, PPRHs can act as antigene and antisense oligonucleotides depending on the strand and nucleic acid they target.

5'- GAGTTCCCCTCCCTACCTCACGTCATTA -3'
||||||||||||||||||||||||
3'- AGGGGAGGGA**T**GGAG**T**GCAG T T
● ● ● ● ● ● ● ● ● ● ● ● ● ● ● ● ● ● ● T
5'- AGGGGAGGGA**T**GGAG**T**GCAG T T
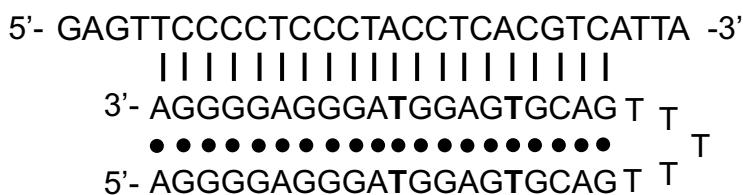
Figure 7. PPRH binding to its target sequence. The PPRH could contain up to 3 pyrimidine interruptions without losing binding affinity. Pyrimidine interruptions are indicated in bold. (I) indicate Watson-Crick bonds. (·) indicate reverse-Hoogsteen bonds.

Our seminal paper demonstrated that template-PPRHs directed against either the *dihydrofolate reductase* (*DHFR)*, *telomerase* or *survivin* genes were able to inhibit their transcription. The incubation of these PPRHs in MCF7 and SKBR3 human breast cancer cell lines led to a 90% of cell mortality (de Almagro *et al.* 2009). On the other hand, a coding-PPRH targeting a polypyrimidine region located in intron 3 of the *DHFR* gene led to a splicing alteration by avoiding the binding of the U2AF65 splicing factor. Therefore, in the latter case, DHFR protein levels were reduced due to the accumulation of the immature mRNA and cell viability was significantly reduced (80-90%) (de Almagro *et al.* 2011).

In another work, a template-PPRH (HpsPr-T) and a coding-PPRH (HpsPr-C) targeting the *survivin* promoter reduced the binding of transcription factors GATA binding protein 3 (GATA-3) and SP1, respectively, thus decreasing *survivin* mRNA and protein levels. (Rodríguez *et al.* 2013). Additionally, two PPRHs were designed against either intron 1 or exon 4 of the *survivin* gene and their effect was compared in terms of cell viability and apoptosis. The four PPRHs were able to decrease cell viability and increase apoptosis at concentrations of 30-100 nM in PC3 prostate cancer cells. On the contrary, these PPRHs did not produce any cytotoxic effect when transfected either in human umbilical vein endothelial cells (HUVEC) or CT26 and 4T1 murine cancer cell lines. Finally, two *in vivo* efficacy assays were conducted using two different routes of administration (intratumoral and intravenous) in a subcutaneous xenograft tumor model of PC3 prostate cancer cells. We compared the tumor growth throughout the administration of either the specific HpsPr-C PPRH or the Hps-Sc scrambled PPRH as negative control. The results showed that regardless of the route of administration, the specific PPRH caused a decrease in tumor volume and blood vessel formation, in parallel with a decrease in survivin protein levels (Rodríguez *et al.* 2013). Overall, this work established the proof of principle of PPRHs as therapeutic tools in cancer.

Recently, to further study the usage of PPRHs as gene silencing tools in cancer and prove their general applicability, we selected a collection of therapeutic genes involved in apoptosis (*B-cell CLL/lymphoma 2, BCL2*), cellular proliferation (*mechanistic target of rapamycin kinase*, *mTOR*), DNA topology (*DNA topoisomerase 1, TOP1*), transcription factors (*C-MYC*) and proto-oncogenes (*MDM2*). We designed a total of 11 PPRHs directed against different polypyrimidine domains of each target gene: two of these stretches were located in the promoter region (*BCL2* and *mTOR*), two in exonic sequences (*BCL2* and *mTOR*) and seven in introns (*BCL2*, *mTOR*, *TOP1, C-MYC* and *MDM2*). All PPRHs were tested in Pancreatic cancer MIA PaCa-2, prostate cancer PC-3, colon cancer HCT116, and breast cancer SKBR3, MCF7, and MDA-MB-468 cell lines (Villalobos *et al.* 2015).

All PPRHs were effective in their corresponding target genes. Nevertheless, the best results in decreasing mRNA levels and cell viability and increasing apoptosis were obtained with PPRHs against *BCL2* in PC3, MIA PaCa-2 and HCT116 cancer cell lines. Also, 3 out of 4 PPRHs designed against *mTOR* were very effective in HCT116 cells. PPRHs against *TOP1*, *MDM2* and

C-MYC genes showed a strong effect in reducing mRNA levels and cell viability and increasing apoptosis in the three breast cancer cell lines used. We determined that PPRHs produced a 40-70% decrease in the target mRNA levels, which was enough to reduce cell survival significantly (Villalobos *et al.* 2015). In our original PPRH design, we used to substitute with an adenine the pyrimidine base complementary to the purine interruption in the target sequence. Later work demonstrated that wild-type PPRHs, which maintain the pyrimidine interruption in the PPRH sequence, presented higher affinity to the target sequence and stability of binding (Rodríguez *et al.* 2015). The collection of PPRHs designed in our laboratory against different cancer target genes is shown in Table 1.

Table 1. Compendium of PPRHs against different target genes involved in cancer progression.

Targeted gene	Cell line	PPRH	Cytotoxicity (relative to control)	mRNA levels (relative to control)	Protein levels (relative to control)	Apoptosis (Fold-change relative to control)
DHFR	SKBR3	HpdI3-A-TA	86%	50%	60%	ND
	MCF7-R	HpdI3-B	71%	58%	60%	ND
telomerase	SKBR3	HptI8-B	90%	45%	ND	ND
survivin	PC3	HpsPr-T and HpsPr-C	90%	40%	20%	1.65
	HeLa		90%	ND	ND	ND
BCL2	MIA PaCa-2	HpBcl2E1-C	95%	55%	ND	2.2
	PC3		90%	55%	ND	2.0
	HCT 116		95%	60%	ND	7.8
TOP1	SKBR3	HpTopI2-T	95%	58%	ND	2.0
	MCF7		60%	55%	ND	2.5
	MDA-MB-468		85%	68%	ND	4.2
MDM2	SKBR3	HpMdmI7-T	50%	42%	ND	4.5
	MCF7		60%	65%	ND	4
	MDA-MB-468		85%	38%	ND	13.5
MYC	SKBR3	HpMycI1-T	85%	40%	ND	4.4
	MCF7		80%	43%	ND	3.5
	MDA-MB-468		95%	72%	ND	12.5
mTOR	HCT 116	HpTorPr-C	90%	59%	ND	4.0
MCL1	HeLa	HpMcl1Pr-C, HpMcl1-I2-C and HpMcl1-E1-C	95%	ND	ND	1.9
	PC3		95%			20.0
	MCF7		95%			ND
	HepG2		95%			ND

For each targeted gene, cytotoxicity, apoptosis fold-change and mRNA and protein levels upon incubation with the corresponding PPRH is shown.

1.3 Cancer immunotherapy

The dysfunction of the immune system of the host represents one of the major mechanisms by which cancer cells evade immunosurveillance. In cancer immunotherapy, pharmacological agents are designed to stimulate host's immune system, thus recognizing and eliminating cancer cells by natural mechanisms (Seliger 2005). In recent years, immunotherapy approaches have become a crucial component of cancer treatment. In fact, the importance of cancer immunotherapy was reflected in the 2018 Nobel prize for physiology or medicine awarded to James P. Allison and Tasuku Honjo for their studies on the inhibition of negative immune regulation. Their pioneering work on cytotoxic T lymphocyte antigen 4 (CTLA4), programmed cell death protein 1 (PD-1) and programmed cell death protein ligand 1 (PD-L1) showed that inhibition of these checkpoint pathways allowed T cells to eradicate tumor cells more effectively (Altmann 2018). Nevertheless, different immunotherapies have also been developed during the last decades including lymphocyte-promoting cytokines, engineered T cells, cancer vaccines and other checkpoint inhibitors.

1.3.1 Lymphocyte-promoting cytokines

Interferons (IFNs), interleukins (ILs) and granulocyte-macrophage colony-stimulating factor (GM-CSF) are the most used cytokines in immunotherapy. Briefly, interferons induce the maturation of macrophages, natural killer (NK) cells, lymphocytes and dendritic cells (He et $al.$ 2007; Müller et $al.$ 2017) whereas interleukins can promote growth and activity of CD4$^+$ and CD8$^+$ T cells (Ben-Sasson et $al.$ 2009; Cox et $al.$ 2011). Finally, GM-CSF promotes T cell homeostasis and supports dendritic cell differentiation so that these cells express tumor specific antigens (Yan et $al.$ 2017).

Cytokines were the first type of immunotherapy implemented into the clinic with the approval of recombinant IFNα therapies for hairy cell leukaemia in 1986 (Ahmed & Rai 2003). Later, recombinant interleukin-2 (IL-2) was also approved by the FDA for metastatic renal cancer in 1992 (Rosenberg 2014).

1.3.2 Engineered T cells

Chimeric antigen receptors (CARs) are fusion proteins composed of an extracellular portion that is usually derived from an antibody and intracellular signaling modules derived from T cell signaling proteins (Figure 8). In the CAR T cell approach, T cells are collected from the patient and are then genetically modified to express CARs that recognize a specific antigen present on tumor cells. Therefore, once these modified T cells are re-administered to the patient, they recognize the targeted antigen on cancer cells and induce their elimination (Lim & June 2017). Tisagenlecleucel and axicabtagene ciloleucel are two CD19-specific CAR T cell therapies against B cell acute lymphocytic leukemia that were approved by FDA in 2017 (Grupp *et al.* 2013).
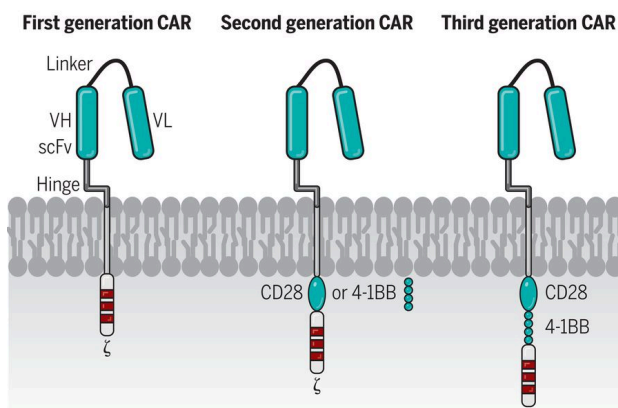
Figure 8. Engineered T cells. T cells can be reconfigured to present specificity for tumors by the introduction of CAR proteins. First-generation CARs contain CD3z, whereas second-generation CARs possess a costimulatory endodomain (e.g. CD28 or 4-1BB) fused to CD3z. Third-generation CARs consist of two costimulatory domains linked to CD3z. scFv, single-chain variable fragment; VH, variable heavy chain; VL, variable light chain. Adapted from (June *et al.* 2018).

1.3.3 Cancer vaccines

There are different types of cancer vaccines depending on their composition. Dendritic cell vaccines are made of dendritic cells collected from patients that are genetically engineered to express tumor-associated antigens, thus activating T cells to attack the tumor (Garg *et al.* 2017). In 2010, sipuleucel-T was approved to treat metastatic castration-resistant prostate cancer due to its ability to prolong overall survival (Kantoff *et al.* 2010). Furthermore, RNA-

based or DNA-based vaccines have emerged as promising alternatives to traditional vaccines and rely on the delivery of exogenous nucleic acids into target cells. Basically, DNA or mRNA is uptaken by antigen presenting cells (APCs) and translated to produce antigen expression. Then, the targeted antigens are presented to T cells leading to their activation against tumor cells that express that specific antigen (Pardi *et al.* 2018). DNA and mRNA vaccines have been tested in a number of clinical trials, however, they are often unsuccessful due to degradation by nucleases, delivery difficulties and immunogenicity (Yang *et al.* 2014; McNamara *et al.* 2015).

1.3.4 Checkpoint inhibitors

The two main checkpoint inhibition approaches are CTLA4 inhibition and PD-1/PD-L1 blockade. In normal circumstances, these immune checkpoints protect healthy tissues from immune attack (Pardoll 2012). However, tumor cells present different mechanisms by which they can evade the host's immune system. When CTLA4, which is located in the membrane of T cells and regulates their activation, interacts with its ligands CD80 and CD86 presented by tumor cells, T cell activity is inhibited leading to the progression of the tumor (Webb *et al.* 2018). In a similar way, cancer cells express PD-L1 which binds to the PD-1 protein that is expressed on T cells, thus avoiding their activation (Alsaab *et al.* 2017). It has also been demonstrated that PD-1 expression in tumor-associated macrophages (TAMs) impairs phagocytosis against tumor cells (Gordon *et al.* 2017). Therefore, blocking the interaction between either CTLA4 and its ligands or PD-1 and PD-L1 using monoclonal antibodies has become one of the strategies with higher clinical impact.

So far, one CTLA4 inhibitor and five PD-1/PD-L1 inhibitors have been approved to treat different types of cancer, showing improvement in overall survival (Ellis *et al.* 2017). The first drug to be approved was an anti-CTLA4 monoclonal antibody named ipilimumab in 2011 for the treatment of melanoma. Three years later, two antibodies directed against PD-1 (pembrolizumab and nivolumab) were approved for the treatment of melanoma, bladder cancer and Hodgkin lymphoma, among others. Finally, in 2016 and 2017 three different antibodies against PD-L1 (atezolizumab, avelumab and durvalumab) were approved for the treatment of urothelial cancer, merkel cell carcinoma and non-small-cell lung cancer (Riley *et al.* 2019).

The promising results obtained with CTLA4 and PD-1/PD-L1 checkpoint inhibitors has led to the exploration of additional immune checkpoints that could be used to be targeted for cancer immunotherapy such as the CD47/SIRPα tandem (Sharpe 2017). The signal-regulatory protein (SIRPα) is an inhibitory receptor expressed on macrophages, neutrophils and dendritic cells that recognizes its ligand CD47, which is a receptor broadly expressed on the membrane of normal cells but often overexpressed on tumor cells. It is known that the binding of CD47 and SIRPα disables the phagocytic capacity of the macrophage against the cancer cell. Therefore, the blockade of CD47/SIRPα interaction could be used to promote the ability of macrophages to kill tumor cells (Matlung *et al.* 2017) (Figure 9). In this regard, different studies have demonstrated that inhibition of this pathway using either anti-CD47 or anti-SIRPα antibodies led to the regression of tumors both *in vitro* and *in vivo* (Chao *et al.* 2010a; Alvey *et al.* 2017). Several blocking antibodies are currently being tested in clinical trials (Cabrales 2019; Sikic *et al.* 2019).
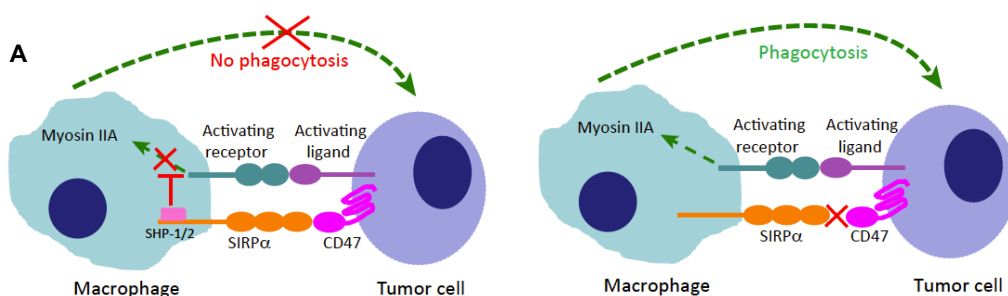
Figure 9. Regulation of phagocytosis by the CD47/SIRPα immune checkpoint. Obtained from (Veillette & Chen 2018).

1.4 DNA repair pathways

Since the discovery of DNA structure, the mechanisms by which the genetic information is preserved have been deeply studied. Mutations are alterations in the DNA sequence of a genome that can be produced by either endogenous or exogenous sources (Ciccia & Elledge 2010). Endogenous sources of DNA damage include replication errors, DNA base mismatches, spontaneous base deaminations, abasic sites and oxidative DNA damage from

reactive oxygen species. Sources for exogenous DNA damage include ionizing radiation, ultraviolet radiation, alkylating agents, aromatic amines, toxins and environmental stress such as extreme temperatures or hypoxic conditions (Chatterjee & Walker 2017). Altogether, it has been estimated that every cell in the human body could experience up to 10^5 DNA lesions per day (Hoeijmakers 2009). Although not all the mutations result in functional impairment, sometimes small changes in the DNA sequence can cause a massive impact on an entire organism. Therefore, living beings have developed several DNA repair pathways to physically remove the damage in a substrate-dependent manner. The main repair pathway for single-strand DNA damage is the nucleotide excision repair (NER) pathway, whereas the non-homologous end joining (NHEJ) and the homology directed repair (HDR) pathways are involved in the repair of double-strand DNA breaks (DSBs) (Hakem 2008).

1.4.1 NER

NER is a flexible and versatile pathway that acts on many types of structurally unrelated types of damage (Costa *et al.* 2003). NER repairs helix-distorting, bulky lesions when only one of the two DNA strands is affected and involves more than 30 proteins in a multistep "cut-and-patch" processing. The DNA repair is restricted to the damaged strand so that the complementary undamaged strand can serve as a template for the "patch" process (Dip *et al.* 2004).

Briefly, a nine-unit complex called transcription factor IIH (TFIIH) is recruited to the DNA damage site, including its component helicases, XPB and XPD (*xeroderma pigmentosum* complementary group B and D proteins) that unwind the DNA strand on either side of the DNA damage. XPA and RPA (replication protein A) stabilize the exposed single-strand DNA, followed by the cleavage of the ~30 nt fragment at 3' and 5' of the lesion by endonucleases XPG and the ERCC1/XPF1/XPF complex. The resulting gap is filled in by the DNA polymerases δ or ε, along with PCNA, RPA, and replication factor C (RFC) by using the undamaged strand as a template (Luo *et al.* 2010; Kelley & Fishel 2016). A scheme representing the NER pathway is shown in Figure 10.
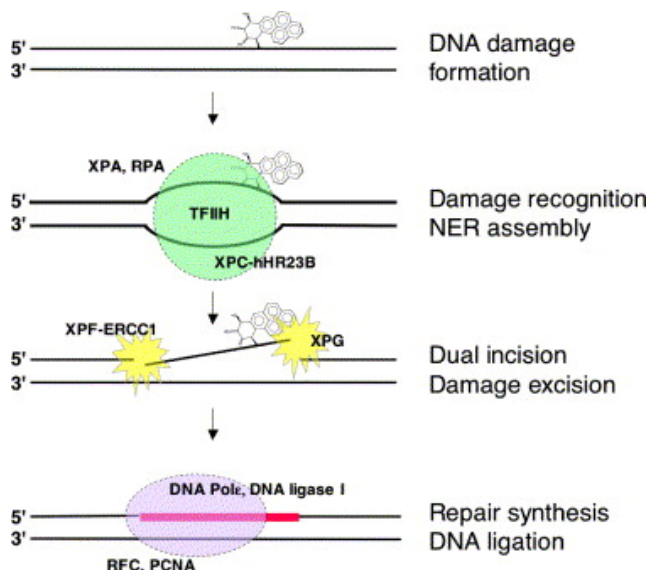
Figure 10. Scheme of the NER pathway. Obtained from (Dip *et al.* 2004).

1.4.2 NHEJ

The NHEJ is the main DNA repair pathway found in eukaryotes and repairs DSBs without using a homologous DNA template by (i) direct ligation of the two ends of the targeted DNA or (ii) via insertion or deletion of nucleotides (Hefferin & Tomkinson 2005). Therefore, NHEJ can generate small insertions and deletions at high frequencies in the targeted site (Haber & Moore 1996). All NHEJ reactions require the core NHEJ machinery that is composed of the Ku, MRX and DNA ligase complexes. It is thought that Ku and MRX complexes bind DSB ends, bridging them together and inhibiting their degradation. Ku and MRX also play essential roles in recruiting, stabilizing and stimulating the ligase complex at DSBs sites (Daley *et al.* 2005).

1.4.3 HDR

HDR occurs at a lower frequency in comparison to NHEJ and corresponds to an exchange or a transfer of an identical or quasi-identical sequence between the targeted site that contains the DSB and another intact DNA molecule. This pathway involves proteins of the RAD52 group composed

of RAD50, RAD51, RAD52, RAD54, RAD55, RAD57, RAD59, RDH54, MRE11 and XRS2. In addition to these proteins, helicases (SGS1, SRS2), topoisomerase 3 (TOP3), DNA nucleases (EXO1, SAE2, RAD1-RAD10), polymerases (POL32) and ligases may also be necessary to produce homologous recombination (Pardo *et al.* 2009). A scheme depicting both the NHEJ and HDR pathways is shown in Figure 11.
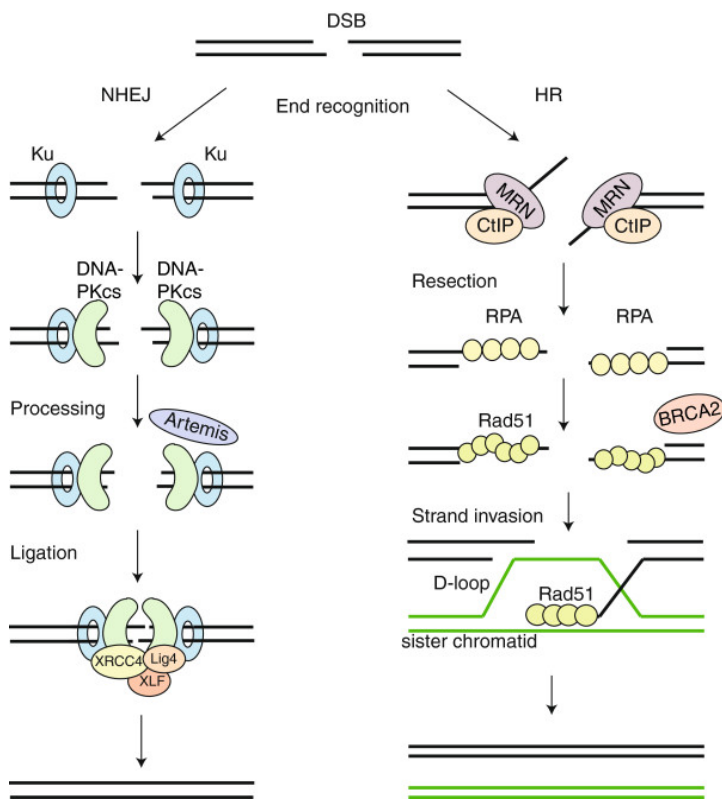
Figure 11. Scheme of HDR and NHEJ pathways. Obtained from (Brandsma & Gent 2012).

1.5 Nuclease-based gene editing tools

Monogenic diseases present a global prevalence at birth of 10 out of 1000 cases, thus affecting millions of people worldwide ("Control of hereditary diseases. Report of a WHO Scientific Group." 1996). These disorders are caused by the presence of single-point mutations in the DNA sequence of a

specific gene that lead to the production of nonfunctional versions of the protein. In modern research, different molecular tools have been developed to correct point mutations in the dsDNA. Site-specific nucleases such as zinc-finger nucleases (ZFNs), transcription activator-like effector nucleases (TALENs) and clustered regularly interspaced short palindromic repeats Cas RNA-guided nucleases (CRISPR/Cas) have been programmed to generate specific DSBs in the mutation site, thus stimulating the NHEJ and HDR pathways to produce the editing (Figure 12).
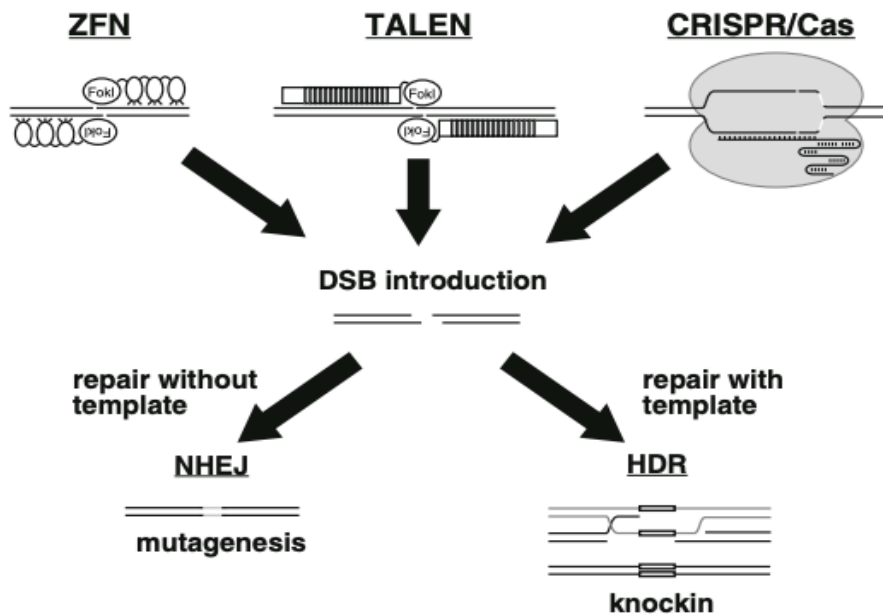
Figure 12. ZFNs, TALENs and CRISPR/Cas introduce DSBs at target sites that are mainly repaired by NHEJ or HDR. When DSBs are repaired through NHEJ, small insertion or deletion mutations are frequently introduced at the sites. However, co-introduction of site-specific nucleases and exogenous DNA donors facilitates transgene integration through HDR repair. Obtained from (Yamamoto 2015).

1.5.1 ZFNs

Zinc-finger (ZF) motifs were first described in 1985 as zinc-binding domains in transcription factor IIIA in *Xenopus* oocytes (Miller *et al.* 1985). ZFs are composed of approximately 30 amino acids where the zinc atom is attached to two pairs of cysteine and histidine residues (C_2H_2). Since each ZF can

recognize 3–4 base pairs of DNA (Pavletich & Pabo 1991), several ZFs can be linked in tandem to recognize a wide range of DNA sequences with high specificity (Choo & Isalan 2000). In 1996, the Chandrasegaran laboratory showed that two different ZFs could be coupled to the nonspecific DNA cleavage domain of the Type IIS restriction enzyme FokI to cut a specific DNA sequence (Kim *et al.* 1996). Today, these hybrid restriction enzymes are known as ZFNs.

ZFNs have been extensively used to disrupt (knockout) relevant genes such as *DHFR* (Santiago *et al.* 2008), *C-C motif chemokine receptor 5* (*CCR5*) (Perez *et al.* 2008; Holt *et al.* 2010), *C-X-C motif chemokine receptor 4* (*CXCR4*) (Del Prete *et al.* 2009) and *VEGF* (Maeder *et al.* 2008). Moreover, ZFNs have also been applied to correct different genes responsible for human diseases such as the *interleukin 2 receptor subunit gamma* (*IL2RG)* for severe combined immune deficiency (Urnov *et al.* 2005) and the *cystic fibrosis transmembrane conductance regulator* (*CFTR)* for cystic fibrosis (Lee *et al.* 2012).

1.5.2 TALENs

TALENs emerged as an alternative to ZFNs for genome editing. TALENs also comprise a non-specific FokI nuclease domain fused to a customizable DNA-binding domain (Joung & Sander 2013). In this case, the DNA-binding domain is composed of highly conserved repeats derived from transcription activator-like effectors (TALEs), which are proteins secreted by *Xanthomonas* bacteria into host plant cells to alter gene expression, thus promoting bacterial virulence, proliferation and dissemination (Boch & Bonas 2010). A TALE consists of a repeating unit composed of approximately 33-35 amino acids where each unit recognizes a single base pair. TALE specificity is determined by two hypervariable amino acids at positions 12 and 13 that are known as the repeat-variable di-residues (RVDs) (Deng *et al.* 2012). Four different RVDs i.e. NI, HD, NG/HG and NN are mainly used to identify adenine, cytosine, thymine and guanine/adenine, respectively. The presence of this DNA recognition code can provide specific interaction between the array of amino acid repeats and the target nucleotide sequence of the genome. Therefore, similarly to ZFNs, TALENs can also be used to provoke DSBs in a specific *locus* in order to disrupt or correct a desired gene.

TALENs have been used to knockout clinically relevant genes such as the *low-density lipoprotein receptor (LDLR*) for hypercholesterolemia (Carlson *et al.* 2012) and *CCR5* for HIV infection (Mussolino *et al.* 2011). Mitochondrial DNA mutations have also been targeted to change the heteroplasmy level in a model of myopathy, encephalopathy, lactic acidosis and stroke-like episodes disease (Yahata *et al.* 2017). Additionally, trinucleotide repeat expansions involving CTG/CAG triplets that are responsible for several neurodegenerative disorders, such as myotonic dystrophy and Huntington's disease, have also been targeted (Mosbach *et al.* 2018).

Correction of mutations in a specific gene using TALENs and a donor DNA sequence to produce the homologous recombination event have also been performed. TALENs were able to repair the IVS2–654 (C > T) mutation present in the *β-globin* gene in induced-pluripotent stem cells (Xu *et al.* 2015), the *type VII collagen* (*COL7A1*) gene for recessive dystrophic epidermolysis bullosa (Osborn *et al.* 2013) and the *pyruvate kinase 1* (*PKLR)* gene for pyruvate kinase deficiency (Quintana-Bustamante *et al.* 2019). Finally, TALEN systems were also able to correct *in vivo* the *Crb1rd8* gene involved in retinal pathology in mice (Low *et al.* 2013) and the *tyrosine hydroxylase* (*th*) gene in zebrafish by homologous recombination (Zu *et al.* 2013).

1.5.3 CRISPR/Cas

CRISPR/Cas systems provide microorganisms with an RNA-guided adaptive immunity to foreign genetic elements (e.g. bacteriophages or conjugative plasmids) by directing nucleases to bind and cut specific nucleotide sequences (Mojica et al. 2005; Mojica et al. 2009). By a process named adaptation, bacteria capture small pieces of foreign genetic elements and incorporate them into their genomic CRISPR array. Transcription of these CRISPR arrays creates CRISPR RNAs (crRNAs) that bind to Cas nucleases, thus providing specificity by base-pairing and cleaving target nucleic acids (Barrangou *et al.* 2007; Brouns *et al.* 2008).

The first effector to be harnessed for genome editing was the Cas9 protein derived from *Streptococcus pyogenes*. Cas9 specifically binds the guide RNA through recognition of the crRNA and its interaction with a transactivating crRNA (tracrRNA). The crRNA-tracrRNA can be fused into a chimeric single-guide RNA (sgRNA), thus creating a system composed of Cas9 and its sgRNA directed against the desired target gene. Finally, it is also necessary that the

target DNA sequence is adjacent to a specific protospacer adjacent motif (PAM) with the correct nucleotide sequence (NGG where N can be any nucleotide) to activate Cas9 and generate the DSB (Jinek *et al.* 2012).

Nowadays, CRISPR/Cas systems are extensively used for different gene therapy applications: to protect against viral infections such as HIV-1 by disrupting the *CCR5* gene (Ye *et al.* 2014; Kang *et al.* 2015); to produce exon skipping by alternative splicing or exon deletion in the *dystrophin* gene for the treatment of DMD (Tremblay *et al.* 2016; Mou *et al.* 2017; Min *et al.* 2019b, 2019a); in blood diseases, to correct different genes of the Fanconi anemia (FA) pathway such as *FANCA*, *FANCC, FANCD* or *FANCF* (Osborn *et al.* 2015; Román-Rodríguez *et al.* 2019; van de Vrugt *et al.* 2019) or the *ß-globin* gene to treat either ß-thalassemia or sickle cell disease (Dever *et al.* 2016; Park *et al.* 2019; Xiong *et al.* 2019); to treat metabolic disorders like hereditary tyrosinemia type 1 by correcting the *fumarylacetoacetate hydrolase* (*FAH*) gene (Rossidis *et al.* 2018; Shao *et al.* 2018; Vanlith *et al.* 2018) or familial hypercholesterolemia through correction of the *LDLR* (Omer *et al.* 2017; Zhao *et al.* 2019).

Furthermore, CRISPR/Cas systems have also been used to correct neurological disorders including spinal muscular atrophy by correcting the *SMN2* gene (Zhou *et al.* 2018; Valetdinova *et al.* 2019), Huntington's disease by disrupting the expression of the mutant *huntingtin* gene (*HTT*) (Ekman *et al.* 2019), spinocerebellar ataxia type 3 by deleting the expanded polyglutamine-encoding region of the *ataxin 3* (*ATXN3)* gene (Ouyang *et al.* 2018), amyotrophic lateral sclerosis by targeting the *superoxide dismutase 1* (*SOD1*) gene (Duan *et al.* 2019) and fragile X syndrome by targeted demethylation of CGG repeats in the *fragile X mental retardation 1* (*FMR1)* gene (Liu *et al.* 2018).

In recent years, new CRISPR/Cas-based approaches such as base editing and prime editing that do not rely on DSBs to produce the correction have also been developed. On the one hand, base editing is based on the deamination of the purine or pyrimidine base to eventually convert one base pair to another in the dsDNA. This process is achieved by fusing the CRISPR/Cas9 system to either a cytidine deaminase (Komor *et al.* 2016) or an adenosine deaminase (Gaudelli *et al.* 2017) to convert the base-pairs G·C to A·T or A·T to G·C, respectively. On the other hand, prime editing technology can directly write new genetic information into a specific DNA site by a Cas9 endonuclease fused to a reverse transcriptase programmed with a guide RNA that both specifies the target and encodes the desired editing. In this case, it is necessary to generate

a nick in one of the strands (PAM strand) (Anzalone *et al.* 2019). Nevertheless, these are not the only emerging tools available within the CRISPR platform since new modifications of this technology are currently under development to provide different genome modifications (Figure 13).
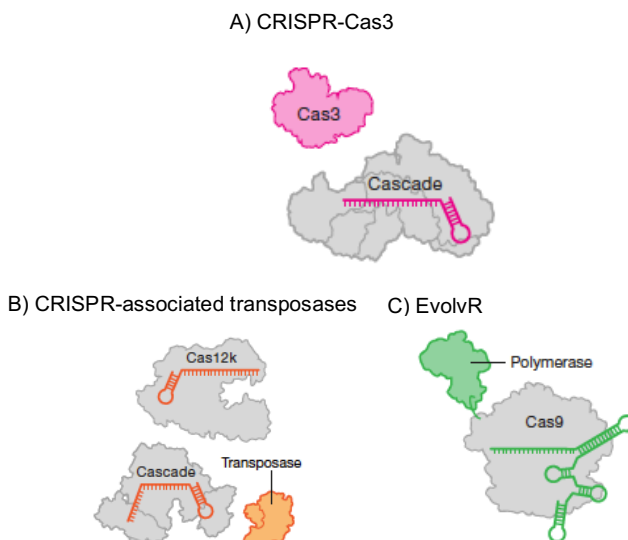
Figure 13. Emerging CRISPR tools. A) Cascade binds to a genomic target, inducing processive cleavage by Cas3 and generating large deletions. B) Cascade or Cas12k binds to the genomic target and directs donor DNA insertion by the Tn7- like transposase. C) Cas9 binds to and nicks the genomic target, after which the error-prone polymerase generates diversity in an adjacent window, thus enabling directed evolution. Adapted from (Doudna 2020).

1.6 Nuclease-free gene editing tools

Different approaches using both modified and non-modified oligonucleotides including chimeric RNA-DNA oligonucleotides, single-stranded oligonucleotides and TFOs have also been developed to correct single-point mutations in the DNA.

1.6.1 Chimeric RNA-DNA oligonucleotides

Chimeric RNA/DNA oligonucleotides (chimeraplasts) contain one DNA strand that aligns to 25 nucleotides of gDNA flanking the mutation site with the exception of the corrected nucleotide located in the center, and one

complementary RNA/DNA hybrid strand composed of two blocks of 10 2'-O-methylated RNA residues flanking both sides of a five-residue stretch of DNA. This folded double-hairpin structure, containing four T residues in each loop, a 5 bp GC clamp and the modified RNA residues, was designed to avoid degradation by nucleases (Lai & Lien 2002). The binding of the chimeric oligonucleotide to the target site triggered an endogenous repair pathway, thus facilitating the correction. This mechanism involved homologous recombination and mismatch repair activities (Cole-Strauss *et al.* 1999) (Figure 14).

In 1996, Eric Kmiec and coworkers first described the use of chimeraplasts to induce and correct point mutations in the DNA (Yoon *et al.* 1996). In their seminal paper, a human *alkaline phosphatase* gene contained in an expression plasmid in CHO cells was corrected using this strategy. The first gene correction in a genomic context was demonstrated in a second work performed by the same laboratory. In that case, chimeraplasts were designed to correct the sickle cell anemia mutation in the *ß-globin* gene (Cole-Strauss *et al.* 1996). The following year, it was demonstrated the *in vivo* application of chimeraplasts to induce a mutation in the *clotting factor IX* (*F9*) gene, which causes haemophilia-B (Kren *et al.* 1998).

Chimeraplasts have been applied to correct mutations in the *UDP-glucuronosyltransferase (UGT1A1)* gene for the treatment of Crigler-Najjar syndrome type I (Kren *et al.* 1999), the *tyrosinase* (*TYR*) gene for albinism (Alexeev *et al.* 2000), the *dystrophin* gene in DMD mice (Rando *et al.* 2000) and canine (Bartlett *et al.* 2000) models, and the *apolipoprotein E* (*APOE*) gene, which can be linked to several neurodegenerative diseases (Tagalakis *et al.* 2005).
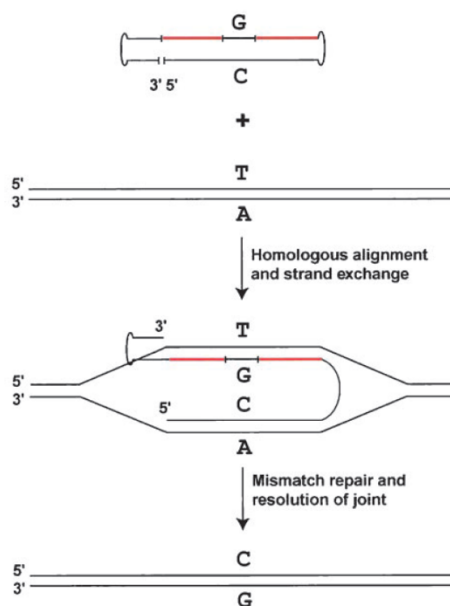
Figure 14. Proposed mechanism for chimeraplast gene repair. The chimeraplast interacts with the target DNA by homologous base pairing, forming a double D-loop juncture that is recognized by the cell's DNA repair machinery. Obtained from (Rice *et al.* 2000).

1.6.2 Single-stranded oligonucleotides

Since chimeraplasts lacked robustness and reproducibility in their targeting activity (Graham & Dickson 2002), the original chimeraplast molecule was broken down into its functional parts to identify the active component that actually produced gene correction. The analyses of these structures showed that the DNA strand was the element that initialized and directed the repair event, thus demonstrating that the RNA segment of the chimeraplast was nonfunctional. As a result, modified single-stranded oligonucleotides (ssODNs) containing three or six phosphorothioate linkages at each end of the molecule, became the next generation tool for gene correction, showing more repair activity than chimeraplasts (Gamper *et al.* 2000). Sherman and coworkers first described the usage of ssODNs to mutate the *cytochrome c1 (cyc1)* gene from *Saccharomyces cerevisiae* (Moerschell *et al.* 1988; Yamamoto *et al.* 1992b, 1992a). In that time, ssODNs were also used to correct a plasmid that contained a mutant *neomycin phosphotransferase* gene in human cells (Campbell *et al.* 1989). The different mechanisms by which ssODNs lead to gene repair involve

replication (Huen *et al.* 2006), physical incorporation of the ssODN into the target *locus* (Radecke *et al.* 2006) and homologous recombination (Mclachlan *et al.* 2009).

ssODNs have been used to correct mutations in the *cyc1* gene from *S.cerevisiae* (Brachman & Kmiec 2003), the *β-galactosidase (glb1)* gene (Igoucheva *et al.* 2001) and the *hypoxanthine phosphoribosyltransferase* (*hprt*) gene (Mclachlan *et al.* 2009) in CHO cells, and to disrupt the *Fancf* gene in mouse embryonic stem cells (Dekker *et al.* 2006). In addition, ssODNs have shown their activity in mouse retinal cells (Ciavatta *et al.* 2005) and bone marrow-derived mesenchymal stem cells (Flagler *et al.* 2008). Finally, modified oligonucleotides such as locked nucleic acids (LNA) have also demonstrated their ability to produce gene modifications in the targeted DNA (Andrieu-Soler *et al.* 2005; van Ravesteyn *et al.* 2016).

1.6.3 TFOs for gene editing

TFOs have been shown to inhibit transcription, replication and binding of proteins to DNA, as stated in section 1.1.1. However, different TFOs have also been developed to produce site-specific mutagenesis (Wang *et al.* 1995, 1996; Vasquez *et al.* 1999, 2000) and site-specific recombination (Faruqi *et al.* 1996) in the dsDNA by linking the TFO to a psoralen molecule. Therefore, TFOs can also be used to create permanent changes in the genome. The mechanism by which the recombination takes place relies on the recognition of the triplex structure by the cell's own DNA repair machinery, sensitizing the surrounding DNA for homologous recombination (Rogers *et al.* 2002a). Moreover, it has been demonstrated that NER pathway factors XPA and RPA also play a role in recognizing and repairing triplex structures (Rogers *et al.* 2002b; Vasquez *et al.* 2002). For that reason, the most frequent approach to produce the gene correction event is to provide (i) the TFO molecule to generate a triplex structure in the target sequence and (ii) a donor DNA molecule that is homologous to the mutation site but contains the correct nucleotide instead of the mutation (Figure 15).

Additionally, different backbone modifications such as peptide nucleic acids (PNAs) can be used for TFO synthesis in order to increase the stability of

the molecule and its binding affinity towards the target sequence, thus producing a greater effect (Ricciardi *et al.* 2014).
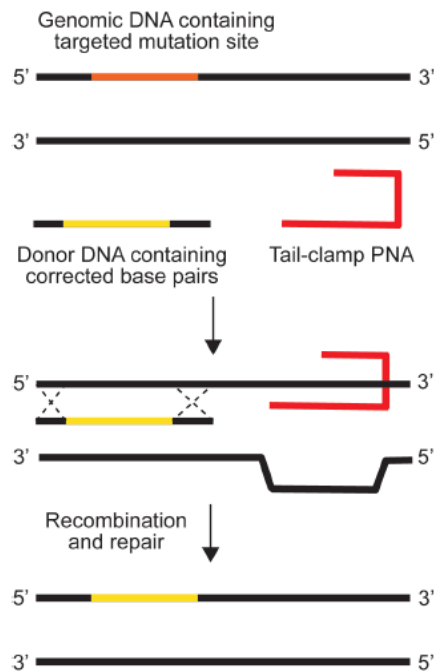
Figure 15. PNAs for gene-editing. PNAs stimulate recombination of short DNA fragments into genomic DNA. The binding of the PNA produces a local helical distortion that activates cellular repair mechanisms, including NER. Obtained from (Quijano *et al.* 2017).

PNAs were first used to correct a splice-site mutation in the *ß-globin* gene responsible for ß-thalassemia in CHO cells (Chin *et al.* 2008). Since then, different PNAs have been developed to correct mutations responsible for different monogenic diseases in human cells. PNAs delivered by polymeric nanoparticles have been used to correct the *ß-globin* gene in ß-thalassemic mice (Bahal *et al.* 2016; Ricciardi *et al.* 2018). Moreover, intranasal delivery of polymeric nanoparticles containing PNAs directed against the *CFTR* gene in cystic fibrosis mice led to the correction of the mutation *in vivo* (McNeer *et al.* 2015). Finally, the disruption of the *CCR5* gene to obtain HIV-resistant human cells using PNAs has also been reported (Schleifman *et al.* 2011; McNeer *et al.* 2013).

1.7 Repair-PPRHs as gene editing tool

To apply the PPRHs technology to correct point mutations in the DNA, we devised an advanced design of the PPRH molecule that we called repair-PPRH. Repair-PPRHs are hairpins that bear an extension sequence at one end of the molecule which is homologous to the DNA sequence to be repaired but containing the wild-type nucleotide instead of the mutated one (Figure 16). Previous studies performed in our laboratory demonstrated that repair-PPRHs were able to correct *in vitro* a single-point mutation in a plasmid containing a mutated version of the *dhfr* minigene. The correction was also achieved in cells when the plasmid was stably transfected into a *dhfr*-deficient CHO cell line. Finally, this methodology was successfully applied to repair a single deletion located in the endogenous *locus* of the *dhfr* gene in the DA5 mutant CHO cell line (Solé *et al.* 2014).

More recently, in our laboratory we expanded the usage of repair-PPRHs to correct a representative collection of point mutations (substitutions, double substitutions, deletions and insertions). We again selected the *dhfr* gene as a model because it is a selectable marker that readily allows for the identification of repaired clones since they are able to grow in a DHFR selective culture medium without glycine, hypoxanthine and thymidine (-GHT). It was used a collection of various mutant CHO cell lines bearing different point mutations in the endogenous *locus* of the *dhfr* gene, all derived from the parental cell line UA21 (Urlaub *et al.* 1983) which carries only one copy of the *dhfr* gene (hemizygous). All mutants contained premature termination codons either by a direct base substitution or indirectly due to frameshift by single insertions, deletions or by exon skipping, thus producing a nonfunctional DHFR enzyme. Different repair-PPRHs targeting the different mutations were transfected in their corresponding mutant cell lines. After selection of the repaired clones, cells were expanded and analyzed by DNA sequencing of the targeted site, thus demonstrating the correction of the mutation. Additionally, DHFR mRNA and protein levels, and enzyme activity levels were also determined to corroborate the functionality of the DHFR enzyme at the phenotype level (Solé *et al.* 2016).

Figure 16. Example of a repair-PPRH. The hairpin core binds to its polypyrimidine target sequence in the dsDNA. The repair domain is a sequence homologous to the DNA sequence to be repaired but containing the corrected nucleotide instead of the mutation. Mutation in the dsDNA is represented in red, whereas the correct nucleotide contained in the repair-PPRH is shown in green.

1.8 APRT deficiency

The *adenine phosphoribosyltransferase* (*APRT*) gene encodes for an enzyme that is involved in the biosynthesis of purines and belongs to the nucleotide salvage pathway, which provides an alternative to the *de novo* nucleotide biosynthesis pathway. APRT catalyzes the conversion of adenine to adenosine monophosphate (AMP) using phosphoribosyl pyrophosphate (PRPP). A lack of functional APRT impairs the conversion of adenine to AMP, thus accumulating an excess of adenine. As a result, adenine is converted to 2,8-dihydroxyadenine (2,8-DHA), which crystallizes in urine, forming stones in the kidneys and urinary tract (Valaperta *et al.* 2014).

Individuals affected by APRT deficiency can develop features of this condition anytime from infancy to late adulthood. Since 2,8-DHA is toxic to kidneys, it may explain the possible decline in kidney function and the progression to end-stage renal disease (ESRD). ESRD is a life-threatening failure of kidney function that occurs when the kidneys are no longer able to filter fluids and waste products effectively from the body. (Bollée *et al.* 2012).

1.9 Fanconi anemia

FA is a rare genetic disorder, in the category of inherited bone marrow failure syndromes. The disease is often associated with a progressive deficiency of all bone marrow production of blood cells, red blood cells, white blood cells, and platelets but also linked to cancer predisposition (primarily acute myeloid leukaemia and squoamous cell carcinoma) (Joenje & Patel 2001). Moreover, renal, cardiac, gastrointestinal and reproductive systems can also be affected. This wide range of symptoms can be explained by the fact that FA is a genomic instability disorder, thus the patients accumulate DNA mutations at an increased rate (Moldovan & D'Andrea 2009). Half the FA patients are diagnosed prior to age 10, while about 10% are diagnosed as adults and their life expectancy is reduced to an average of 20 years. The cause of FA is the appearance of mutations in one of the 21 *FANC* genes that have been described so far (Palovcak *et al.* 2017) that are involved in the FA pathway (Taniguchi & D'Andrea 2006). The FA pathway is responsible for triggering DNA repair when DNA replication is blocked due to DNA damage, especially with interstrand cross-links (ICLs), which occur when two DNA nucleotides on opposite strands of DNA are abnormally attached or linked together. In 80-90% of the FA cases, these mutations are located in either the *FANCA*, *FANCC* or *FANCG* genes. As a result, DNA damage is not repaired efficiently and ICLs build up over time, thus stalling DNA replication and resulting in either abnormal cell death or uncontrolled cell growth. Cells that divide quickly, such as bone marrow cells and cells of the developing fetus, are particularly affected. For that reason, cells derived from FA patients are highly susceptible to apoptosis after exposure to DNA cross-linking agents such as mitomycin C (MMC) or diepoxybutane (DEB) (Ishida & Buchwald 1982).

2. OBJECTIVES

48

This work is divided in two main parts, one studying the pharmacogenomics and toxicity of PPRHs as gene silencing tools and expanding their usage in immunotherapy approaches, and a second part focused on the application of repair-PPRHs as gene editing tools to correct point mutations in the DNA.

Therefore, the major goals of this work were the following:

1. To determine the functional pharmacogenomic effects of a PPRH directed against the *survivin* gene and the hepatotoxicity and nephorotoxicity profiles of PPRH molecules.

2. To apply the PPRHs technology in immunotherapy approaches by targeting both the CD47/SIRPα and PD-1/PD-L1 pathways.

3. To demonstrate the generality of action of repair-PPRHs by correcting different single-point mutations in the endogenous locus of the *aprt* gene in mammalian cells and evaluating the off-target effects of this technology.

4. To get insight into the molecular mechanism responsible for the gene repair event triggered by repair-PPRHs.

5. To develop repair-PPRHs to correct a mutation responsible for a monogenic disease in human cells.

3. MATERIALS AND METHODS

Materials and Methods are already described within the articles presented in the "Results" section of this thesis. However, additional materials or methodologies that are not included in the manuscripts are described within this section.

3.1 Functional pharmacogenomics and toxicity of PPRHs (Article I)

3.1.1 Hepatotoxicity and nephrotoxicity RT-qPCR determinations

Hepatic HepG2 and renal 786-O cancer cell lines were selected to evaluate hepatotoxicity and nephrotoxicity *in vitro*, respectively. Cell toxicity was analyzed by determining the changes in gene expression of selected genes present in RT-qPCR arrays specifically developed for hepatic and renal toxicity screening.

To perform the toxicity analyses, RNA was extracted from triplicate points of two different conditions for both cell lines: (i) untreated cells and (ii) cells treated with 100 nM of Watson-Crick negative control hairpin (Hp-WC). For each sample, 1 µg of cDNA was synthesized using the High Capacity cDNA Reverse Transcription Kit (Applied Biosystems) following the instructions of the manufacturer. Then, the cDNA product was diluted 1/12 with nuclease-free H_2O mQ. Human Drug Hepatotoxicity SignArrays and Human Drug Nephrotoxicity SignArrays (purchased from AnyGenes) were used to determine gene expression in HepG2 and 786-O cell lines, respectively. The full list of genes contained in the hepatotoxicity and nephrotocixity arrays are shown in Table 2 and Table 3, respectively. RT-qPCR was performed following the manufacturer's recommendations. Finally, mRNA expression data was analyzed using the Analysis Tool Software provided by AnyGenes.

Table 2. List of genes contained in the RT-qPCR array for hepatotoxicity screening. It is shown the symbol and name of the gene, as well as the RefSeq number.

Gene name	RefSeq	Symbol
v-akt murine thymoma viral oncogene homolog 1	NM_005163.2	AKT1
BCL2-associated agonist of cell death	NM_004322.3	BAD
BCL2 binding component 3	NM_001127240.2	BBC3
B-cell CLL/lymphoma 2	NM_000633.2	BCL2
BCL2-like 1	NM_138578.1	BCL2L1
BCL2-like 11 (apoptosis facilitator)	NM_138621.4	BCL2L11
BH3 interacting domain death agonist	NM_197966.1	BID
caspase 10, apoptosis-related cysteine peptidase	NM_032977.3	CASP10
caspase 3, apoptosis-related cysteine peptidase	NM_032991.2	CASP3
caspase 4, apoptosis-related cysteine peptidase	NM_001225.3	CASP4
caspase 9, apoptosis-related cysteine peptidase	NM_001229.3	CASP9
CD14 molecule	NM_001040021.2	CD14
crystallin, alpha A	NM_000394.3	CRYAA
catenin (cadherin-associated protein), beta 1, 88kDa	NM_001904.3	CTNNB1
dual specificity phosphatase 1	NM_004417.3	DUSP1
eukaryotic translation initiation factor 4 gamma, 3	NM_001198801.1	EIF4G3
Fas ligand (TNF superfamily, member 6)	NM_000639.1	FASLG
high mobility group box 1	NM_002128.4	HMGB1
heat shock 70kDa protein 1A	NM_005345.5	HSPA1A
heat shock 70kDa protein 1B	NM_005346.4	HSPA1B
interferon, gamma	NM_000619.2	IFNG
interleukin 17A	NM_002190.2	IL17A
myeloid cell leukemia sequence 1 (BCL2-related)	NM_021960.4	MCL1
serpin peptidase inhibitor, clade E (nexin, plasminogen activator inhibitor type 1), member 1	NM_000602.4	SERPINE1
superoxide dismutase 2, mitochondrial	NM_000636.2	SOD2
sequestosome 1	NM_003900.4	SQSTM1
tumor necrosis factor	NM_000594.2	TNF
X-linked inhibitor of apoptosis	NM_001167.3	XIAP
BTB and CNC homology 1, basic leucine zipper transcription factor 1	NM_206866.1	BACH1
cullin 1	NM_003592.2	CUL1
DNA-damage-inducible transcript 3	NM_001195053.1	DDIT3
endoplasmic reticulum to nucleus signaling 1	NM_001433.3	ERN1
heat shock 70kDa protein 8	NM_006597.4	HSPA8
interleukin 12A (natural killer cell stimulatory factor 1, cytotoxic lymphocyte maturation factor 1, p35)	NM_000882.2	IL12A
keratin 18	NM_000224.2	KRT18
mitogen-activated protein kinase kinase kinase 8	NM_005204.3	MAP3K8
mitogen-activated protein kinase 1	NM_002745.4	MAPK1
mitogen-activated protein kinase 3	NM_002746.2	MAPK3
activating transcription factor 4 (tax-responsive enhancer element B67)	NM_001675.2	ATF4
activating transcription factor 6	NM_007348.3	ATF6
eukaryotic translation initiation factor 2A, 65kDa	NM_032025.3	EIF2A
eukaryotic translation initiation factor 2, subunit 1 alpha, 35kDa	NM_004094.4	EIF2S1
eukaryotic translation initiation factor 2, subunit 2 beta, 38kDa	NM_003908.3	EIF2S2
eukaryotic translation initiation factor 2, subunit 3 gamma, 52kDa	NM_001415.3	EIF2S3
eukaryotic translation initiation factor 4A1	NM_001416.3	EIF4A1

eukaryotic translation initiation factor 4A2	NM_001967.3	EIF4A2
homocysteine-inducible, endoplasmic reticulum stress-inducible, ubiquitin-like domain member 1	NM_014685.3	HERPUD1
heat shock 70kDa protein 5 (glucose-regulated protein, 78kDa)	NM_005347.4	HSPA5
X-box binding protein 1	NM_005080.3	XBP1
DnaJ (Hsp40) homolog, subfamily B, member 1	NM_006145.2	DNAJB1
DnaJ (Hsp40) homolog, subfamily B, member 6	NM_058246.3	DNAJB6
heat shock 70kDa protein 6 (HSP70B')	NM_002155.4	HSPA6
jun proto-oncogene	NM_002228.3	JUN
mitogen-activated protein kinase 8 interacting protein 3	NM_015133.3	MAPK8IP3
Fanconi anemia, complementation group F	NM_022725.3	FANCF
growth arrest and DNA-damage-inducible, alpha	NM_001924.3	GADD45A
activating transcription factor 2	NM_001880.3	ATF2
chemokine (C-X-C motif) ligand 10	NM_001565.3	CXCL10
C-X-C motif chemokine ligand 8	NM_000584.2	CXCL8
FBJ murine osteosarcoma viral oncogene homolog	NM_005252.3	FOS
interleukin 23, alpha subunit p19	NM_016584.2	IL23A
v-Ki-ras2 Kirsten rat sarcoma viral oncogene homolog	NM_004985.3	KRAS
mechanistic target of rapamycin (serine/threonine kinase)	NM_004958.3	MTOR
nuclear factor of kappa light polypeptide gene enhancer in B-cells 2 (p49/p100)	NM_001077493.1	NFKB2
pentraxin 3, long	NM_002852.3	PTX3
dual specificity phosphatase 10	NM_007207.4	DUSP10
sulfiredoxin 1	NM_080725.1	SRXN1
VCP-interacting membrane protein	NM_203472.1	VIMP
cytochrome P450, family 2, subfamily B, polypeptide 6	NM_000767.4	CYP2B6
phosphatidylinositol-4-phosphate 3-kinase, catalytic subunit type 2 alpha	NM_002645.2	PIK3C2A
c-ros oncogene 1 , receptor tyrosine kinase	NM_002944.2	ROS1
v-raf murine sarcoma 3611 viral oncogene homolog	NM_001654.3	ARAF
chemokine (C-X-C motif) ligand 2	NM_002089.3	CXCL2
epidermal growth factor receptor	NM_005228.3	EGFR
interleukin 6 (interferon, beta 2)	NM_000600.3	IL6
mitogen-activated protein kinase kinase kinase kinase 4	NM_145686.3	MAP4K4
son of sevenless homolog 1 (Drosophila)	NM_005633.3	SOS1
tumor necrosis factor receptor superfamily, member 10b	NM_003842.4	TNFRSF10B
early growth response 1	NM_001964.2	EGR1
jun D proto-oncogene	NM_005354.4	JUND
nuclear factor, erythroid 2-like 2	NM_006164.4	NFE2L2
ATP-binding cassette, sub-family C (CFTR/MRP), member 2	NM_000392.4	ABCC2
ATP-binding cassette, sub-family C (CFTR/MRP), member 4	NM_005845.3	ABCC4
cytochrome P450, family 7, subfamily A, polypeptide 1	NM_000780.3	CYP7A1
peptidylprolyl isomerase A (cyclophilin A)	NM_021130	PPIA
actin, beta	NM_001101	ACTB
TATA box binding protein	NM_003194.4	TBP
beta-2-microglobulin	NM_004048	B2M
ribosomal protein, large, P0	NM_053275	RPLP0
Hypoxanthine guanine phosphoribosyl transferase I	NM_000194	HPRT1
Transferrin receptor (p90, CD71)	NM_003234.2	TFRC
Glucuronidase, beta	NM_000181.3	GUSB

Table 3. List of genes contained in the RT-qPCR array for nephrotoxicity screening. It is shown the symbol and name of the gene, as well as the RefSeq number.

Gene name	RefSeq	Symbol
apoptosis-inducing factor, mitochondrion-associated, 1	NM_004208.3	AIFM1
Rho guanine nucleotide exchange factor (GEF) 26	NM_001251962.1	ARHGEF26
BCL2-antagonist/killer 1	NM_001188.3	BAK1
BCL2-associated X protein	NM_004324.3	BAX
caspase 1, apoptosis-related cysteine peptidase (interleukin 1, beta, convertase)	NM_033292.2	CASP1
caspase 8, apoptosis-related cysteine peptidase	NM_001080125.1	CASP8
CD40 molecule, TNF receptor superfamily member 5	NM_001250.4	CD40
E2F transcription factor 1	NM_005225.2	E2F1
Fas (TNF receptor superfamily, member 6)	NM_000043.4	FAS
heme oxygenase (decycling) 1	NM_002133.2	HMOX1
interleukin 1, beta	NM_000576.2	IL1B
interleukin 6 (interferon, beta 2)	NM_000600.3	IL6
mitogen-activated protein kinase 14	NM_001315.2	MAPK14
nuclear factor of kappa light polypeptide gene enhancer in B-cells 1	NM_003998.3	NFKB1
tumor necrosis factor	NM_000594.2	TNF
tumor necrosis factor receptor superfamily, member 1A	NM_001065.3	TNFRSF1A
tumor protein p53	NM_000546.4	TP53
glyoxalase domain containing 4	NM_016080.3	GLOD4
alpha-1-microglobulin/bikunin precursor	NM_001633.3	AMBP
intercellular adhesion molecule 1	NM_000201.2	ICAM1
vascular cell adhesion molecule 1	NM_001078.3	VCAM1
cyclin-dependent kinase 2	NM_001798.3	CDK2
hepatocyte growth factor (hepapoietin A; scatter factor)	NM_000601.4	HGF
mitogen-activated protein kinase 1	NM_002745.4	MAPK1
mitogen-activated protein kinase 3	NM_002746.2	MAPK3
poly(A) binding protein interacting protein 1	NM_006451.4	PAIP1
par-3 family cell polarity regulator	NM_019619.3	PARD3
polymerase (DNA directed), mu	NM_013284.3	POLM
slit homolog 1 (Drosophila)	NM_003061.2	SLIT1
transforming growth factor, beta 1	NM_000660.4	TGFB1
CD27 molecule	NM_001242.4	CD27
clusterin	NM_001831.3	CLU
chemokine (C-X3-C motif) ligand 1	NM_002996.3	CX3CL1
interleukin 18 (interferon-gamma-inducing factor)	NM_001562.3	IL18
interleukin 4	NM_000589.3	IL4
selectin E	NM_000450.2	SELE
toll-like receptor 2	NM_003264.3	TLR2
toll-like receptor 4	NM_138554.4	TLR4
toll-like receptor 9	NM_017442.3	TLR9
tumor necrosis factor receptor superfamily, member 1B	NM_001066.2	TNFRSF1B
calpain 1, (mu/l) large subunit	NM_001198868.1	CAPN1
fatty acid binding protein 1, liver	NM_001443.2	FABP1
microsomal glutathione S-transferase 3	NM_004528.3	MGST3
nitric oxide synthase 3 (endothelial cell)	NM_000603.4	NOS3
platelet-activating factor acetylhydrolase 1b, regulatory subunit 1 (45kDa)	NM_000430.3	PAFAH1B1
platelet-activating factor acetylhydrolase 1b, catalytic subunit 2 (30kDa)	NM_002572.3	PAFAH1B2
platelet-activating factor acetylhydrolase 1b, catalytic subunit 3 (29kDa)	NM_001145939.1	PAFAH1B3
chemokine (C-C motif) ligand 2	NM_002982.3	CCL2
interleukin 10	NM_000572.2	IL10
phosphatase and tensin homolog	NM_000314.4	PTEN

v-rel reticuloendotheliosis viral oncogene homolog A (avian)	NM_021975.3	RELA
cystatin C	NM_001288614.1	CST3
G protein-coupled receptor 20	NM_005293.2	GPR20
albumin	NM_000477.5	ALB
annexin A5	NM_001154.3	ANXA5
ATG3 autophagy related 3 homolog (S. cerevisiae)	NM_022488.3	ATG3
bradykinin receptor B2	NM_000623.3	BDKRB2
chemokine (C-C motif) ligand 1	NM_002981.1	CCL1
chemokine (C-C motif) ligand 5	NM_002985.2	CCL5
cAMP responsive element binding protein 1	NM_134442.3	CREB1
colony stimulating factor 2 (granulocyte-macrophage)	NM_000758.3	CSF2
chemokine (C-X-C motif) ligand 10	NM_001565.3	CXCL10
chemokine (C-X-C motif) ligand 11	NM_005409.4	CXCL11
estrogen receptor 1	NM_000125.3	ESR1
insulin-like growth factor binding protein 5	NM_000599.3	IGFBP5
mechanistic target of rapamycin (serine/threonine kinase)	NM_004958.3	MTOR
plasminogen activator, urokinase receptor	NM_002659.3	PLAUR
secreted phosphoprotein 1	NM_001251830.1	SPP1
vitamin D (1,25- dihydroxyvitamin D3) receptor	NM_001017536.1	VDR
colony stimulating factor 3 (granulocyte)	NM_000759.3	CSF3
nitrogen permease regulator-like 2 (S. cerevisiae)	NM_006545.4	NPRL2
runt-related transcription factor 3	NM_001031680.2	RUNX3
zinc finger protein 671	NM_024833.2	ZNF671
ATP-binding cassette, sub-family B (MDR/TAP), member 1	NM_000927.4	ABCB1
ATP-binding cassette, sub-family C (CFTR/MRP), member 1	NM_004996.3	ABCC1
potassium channel, voltage gated KQT-like subfamily Q, member 4	NM_004700.3	KCNQ4
lipocalin 2	NM_005564.3	LCN2
large 60S subunit nuclear export GTPase 1	NM_018385.2	LSG1
solute carrier family 22 (organic cation transporter), member 1	NM_003057.2	SLC22A1
solute carrier family 22 (organic cation transporter), member 2	NM_003058.3	SLC22A2
solute carrier family 22 (organic cation transporter), member 3	NM_021977.3	SLC22A3
solute carrier family 22 (organic anion transporter), member 8	NM_004254.3	SLC22A8
solute carrier family 31 (copper transporter), member 1	NM_001859.3	SLC31A1
solute carrier family 47 (multidrug and toxin extrusion), member 1	NM_018242.2	SLC47A1
peptidylprolyl isomerase A (cyclophilin A)	NM_021130	PPIA
actin, beta	NM_001101	ACTB
TATA box binding protein	NM_003194.4	TBP
beta-2-microglobulin	NM_004048	B2M
ribosomal protein, large, P0	NM_053275	RPLP0
Hypoxanthine guanine phosphoribosyl transferase I	NM_000194	HPRT1
Transferrin receptor (p90, CD71)	NM_003234.2	TFRC
Glucuronidase, beta	NM_000181.3	GUSB

3.2 Correction of the *aprt* gene using repair-PPRHs (Article V)

3.2.1 Cell culture

Different *aprt*-deficient CHO cell lines were used for gene correction. All cell lines contained a single nucleotide substitution within the coding sequence of the *aprt* gene that produced a premature stop codon (nonsense mutation), thus generating a truncated protein. The mutant cell lines were isolated using different mutagens from the parental cell line D422 (Phear *et al.* 1989) which is a CHO cell line hemizygous for the *aprt* gene (Simon *et al.* 1982). The different cell lines and their corresponding mutations are described in Table 4. Cells were grown in Ham's F12 medium containing 10% fetal bovine serum (FBS) (Gibco) at 37°C in a 5% CO_2–controlled humidified atmosphere. Trypsinization of the cells was performed using 0,05% Trypsin (Sigma-Aldrich).

Table 4. *aprt*-deficient CHO mutant cell lines subjected to correction with repair-PPRHs.

Cell line	Position	Mutation (5'-3')	Codon change
S23	+93 (exon 1)	GAA > TAA	Glutamic acid > Ochre in place
S62	+1968 (exon 5)	GGA > TGA	Glycine > Opal in place
S1	+397 (exon 2)	TAC > TAG	Tyrosine > Amber in place

Position numbers refer to the transcription start site. Point mutations are underlined in their position within the codon.

3.2.2 Repair-PPRHs against the *aprt* gene

Repair-PPRHs were designed according to the rules of Hoogsteen and Watson-Crick pairing. We also designed a long-distance repair-PPRH (LD-HpS1E2rep) in which the hairpin core was located 24 nt away from the repair domain. In this case, an additional pentathymidine loop between the hairpin core and the repair domain was included to provide flexibility to the repair domain. All oligodeoxynucleotides were synthesized by Sigma-Aldrich, dissolved at 10 µg/µL (stock solution) in a sterile RNAse-free Tris-EDTA buffer (1 mM EDTA and 10 mM Tris, pH 8.0; both from Sigma-Aldrich) and stored at -20°C until use. The names and sequences of repair-PPRHs and other oligonucleotides used in this work are shown in Table 5.

As negative controls, different oligodeoxynucleotides that contained only the repair domain for each mutant, without the hairpin core, were used. In addition, a scrambled polypurine hairpin core attached to the repair domain of the S23 mutant was transfected into S23 mutant cells as an additional negative control. Negative control oligonucleotides are shown in Table 6.

Table 5. Oligodeoxynucleotides used in this work.

Name	Length (nt)	Sequence
HpS23E1rep	100	5' CGCGGCTATGGCG**G**AATCTGAGTTGCAGCTGGTGGCGCAGCGCATCCGCAGAAAGGGGCTGAAGGGGTAGGGG • • • • • • • •)5T 3' AAAGGGGCTGAAGGGGTAGGGG
HpS62E5rep	100	5' TGTGTGAGCCTGGTGGAGCTGACCTCACTTAAGGGCAGAGAGAAGCTA**G**GATCAGTAGGTAAGAAGAGAGAGGACG • • • • • • • •)5T 3' GGTAAGAAGAGAGAGGACG
HpS1E2rep	100	5' CGACTA**C**ATCGCAGGCGAGTGGCCATGCCAGGCCGTGCTGGTCCCCCACTGTGCAGGGAGGGGAGGGAAGGGAATA • • • • • • • •)5T 3' GAGGGGAGGGAAGGGAATA
LD-HpS1E2rep	100	5' CCACGCATGGCGGCAAGATCGACTA**C**ATCGCAGGCGAGTGGCCATGCCAGGC 5T GAGGGGAGGGAAGGGAATA • • • • • • • •)5T 3' GAGGGGAGGGAAGGGAATA
HpS23E1-core	49	5' AAAGGGGCTGAAGGGGTAGGGG • • • • • • • •)5T 3' AAAGGGGCTGAAGGGGTAGGGG
O-16	16	5' CCCCGACTTCCCCATC 3'
O-40	40	5' GCAGCGCATCCGCAGTTTCCCCGACTTCCCCATCCCCGGC 3'
O-60	60	5' TCTGAGTTGCAGCTGGTGGCGCAGCGCATCCGCAGTTTCCCCGACTTCCCCATCCCCGGC 3'

The corrected nucleotides in the repair-PPRHs are represented in green.

Table 6. Oligodeoxynucleotides used as negative controls in this study.

Name	Length (nt)	Sequence
RD-S23E1rep	51	5' CGCGGCTATGGCGGAATCTGAGTTGCAGCTGGTGGCGCAGCGCATCCGCAG 3'
RD-S62E5rep	57	5' TGTGTGAGCCTGGTGGAGCTGACCTCACTTAAGGGCAGAGAGAAGCTAGGATCAGTA 3'
RD-S1E2rep	57	5' CGACTACATCGCAGGCGAGTGGCCATGCCAGGCCGTGCTGGTCCCCCACTGTGCAGG 3'
Hp-core-Sc	53	5' AAGGAAGGAAGGAAGGAAGGAAGG • • • • • • • • ⟩5T 3' AAGGAAGGAAGGAAGGAAGGAAGG
RD-Sc	46	5' TAGTTAATAATTGTAGTACTTACTCTGGGAGAAGTTTATATTTCTC 3'
Hp-rep-Sc	95	5' CTGCGGATGCGCTGCGCCACCAGCTGCAACTCAGATTCCGCCATAGCCGCGTGCACGAGAAAGGGCGGAGGGA • • • • • • • ⟩5T 3' GAGAAAGGGCGGAGGGA
HpS23E1rep-Sc	104	5' CGCGGCTATGGCG**G**AATCTGAGTTGCAGCTGGTGGCGCAGCGCATCCGCAGAAGGAAGGAAGGAAGGAAGGAAGG • • • • • • • • ⟩5T 3' AAGGAAGGAAGGAAGGAAGGAAGG

The corrected nucleotides in the repair-PPRHs are represented in green.

3.2.3 Gene correction frequency

Gene correction frequency was determined for the S23 mutant cell line using the HpS23E1rep repair-PPRH. On the one hand, transfection was performed either in asynchronous cells or in cells in the S phase of the cell cycle. Synchronization in S-phase was achieved following the protocol described by (Chin *et al.* 2008), which consisted basically in incubating the cells in medium supplemented with 0.1% serum for 72 hours followed by incubation with 1.5 mM Hydroxyurea for 15 hours. On the other hand, to study the possible implication of homologous recombination in the gene repair event, we transfected the HpS23E1rep either alone or in combination with 5 µg of a RAD51 expression vector.

After transfection and selection in +AAT medium (containing adenine, aminopterin and thymidine), surviving cell colonies were fixed with 6% Formaldehyde, stained with crystal violet (all from Sigma-Aldrich) and counted. Gene correction frequency values were calculated as the ratio between the number of surviving colonies and the total number of cells initially plated.

3.2.4 PCR reactions for replication theory

Total gDNA from S23 mutant cells was extracted using the Wizard genomic DNA purification kit (Promega) following the manufacturer's instructions. PCR was carried out using a forward primer with sequence 5'-TTACCCTTGTTCCCGGACTG-3' and a repair-PPRH containing the correct nucleotide for the S23 mutation as reverse primer. The sequence of the HpS23repli repair-PPRH (reverse primer) was 5'-AAAGGGGCTGAAGGGGTAGGGGTTTTTGGGGATGGGGAAGTCGGGGAA ACTGCGGATGCGCTGCGCCACCAGCTGCAACTCAGATTCCGCCATA-3'.

PCR cycling conditions were 3 min denaturation at 94ºC, followed by 35 cycles of 30 s at 94ºC, 1 min at 59ºC and 1 min at 68ºC, and a final extension step of 5 min at 68 ºC. The 137 bp PCR product was resolved in a 6% polyacrylamide gel electrophoresis, purified and sequenced by Macrogen. The experimental design to test whether a replication process could be involved in the repair event is depicted in Figure 17.

5-TTACCCTTGTTCCCGGACTGGTATGACCCCAGCCTGCTGACATCCCTCCGCCCTTTCTCGTGCACGCGGC

TATGGCGTAATCTGAGTTGCAGCTGGTGGCGCAGCGCATCCGCAGTTTCCCCGACTTCCCCATCCCCGGC-3'

Figure 17. DNA fragment of the *aprt* gene sequence corresponding to the S23 mutation site. It is represented the sequence where the forward primer hybridizes (blue) and the sequence where the repair-PPRH binds acting as reverse primer (green). The underlined green sequence represents the polypyrimidine target sequence where the hairpin core of the repair-PPRH binds. Red represents the mutated nucleotide.

3.3 Correction of the human *FANCA* gene using repair-PPRHs

3.3.1 Fanconi anemia cell lines

The FA-55 cell line, which is lymphoblastic and derived from a FA patient, was a gift from Paula Rio and Juan Bueren (CIEMAT). This cell line bears an homozygotic single-point mutation in the *FANCA* gene that consists in a C>T substitution in position c.295 (exon 4) that leads to a premature stop codon, thus truncating the FANCA protein. We also received the CP1 cell line, which is equivalent to the FA-55 cell line but derived from a healthy donor. Both cell lines were cultured in RPMI + 20% FBS medium supplemented with 1 mM sodium pyruvate (Sigma-Aldrich), 5 μM β-mercaptoethanol and 100 μM non-essential aminoacids (both from Gibco) at 37˚C in a 5% CO_2-controlled humidified atmosphere.

3.3.2 Enrichment of FANCA+ cells using MMC

The partial selection of repaired cells was based on the different sensitivity presented by FANCA$^-$ and FANCA$^+$ cells to the crosslinking agent MMC. To determine the appropriate concentration of MMC to enrich the repaired population, both FA-55 and CP1 cells (50,000) were plated and incubated with different concentrations of MMC. Six days after incubation, 500 μg/mL of 3-(4,5-Dimethylthiazol-2-yl)-2,5-Diphenyltetrazolium Bromide (MTT) and 100 μM of sodium succinate (both from Sigma-Aldrich) were added to the culture medium and incubated for 2.5 h at 37˚C. After incubation, cells were centrifuged at 5,000 x g, medium was removed and the solubilization reagent (0.57% acetic acid and 10% sodium dodecyl sulfate in DMSO) (Sigma-Aldrich) was added. Cell survival was measured at 570 nm in a Modulus Microplate luminometer (Turner BioSystems; Promega).

3.3.3 Repair-PPRHs against the *FANCA* gene

A total of three different repair-PPRHs directed against the c.295 (C>T) mutation were designed. In two cases, the mutation was located far away from the polypyrimidine target sequence of the hairpin, so we followed the long-distance approach to design those repair-PPRHs (LD-HpFANCA-1 and LD-HpFANCA-2). On the other hand, we also designed a short repair-PPRH whose

polypyrimidine target sequence was located near to the mutation (HpFANCA-short). Repair-PPRHs are shown in Table 7.

Table 7. Repair-PPRHs used for *FANCA* gene correction.

Name	Length (nt)	Sequence
LD-HpFANCA-1	99	5'-GCCTTGAGGCTTGATCCTGCAAAGCAGAGCCTTAAAC—5T / GGGGAGAATAGATGCAAAGGGAAAAA—5T / 3'- GGGGAGAATAGATGCAAAGGGAAAAA
LD-HpFANCA-2	110	5'-TTGTTTTGTGTTTAAGGCTCTGCTTTGCAGGATCAAGCCTCAAGGCTGGGGGTTCC—5T / AAGAGGGCAGAAAGGAAGACAG—5T / 3'- AAGAGGGCAGAAAGGAAGACAG
HpFANCA-short	73	5'- CCCCAGCCTTGAGGCTTGATCCTGCAAAGCAGAGCCTTAAACACAAAACAAAA—5T / 3'- AAACACAAAACAAAA

The corrected nucleotides in the repair-PPRHs are represented in green.

3.3.4 DNA binding assays

The ssDNA-FANCA-Fw and ssDNA-FANCA-Rv oligodeoxynucleotides corresponding to the *FANCA* target sequence (Table 8) were synthesized by Sigma-Aldrich and the ssDNA-FANCA-Fw was 5'-end-labeled with 6-FAM fluorophore. The dsDNA-FANCA probe was formed by mixing 20 µg of each single-stranded oligodeoxynucleotide in a 150 mM NaCl solution. After incubation at 90°C for 5 min, solutions were allowed to cool down slowly to room temperature. Duplexes were purified by nondenaturing 20% polyacrylamide gel electrophoresis and DNA concentration was determined by measuring its absorbance (260 nm) in a Nanodrop ND-1000 spectrophotometer (Thermo Fisher Scientific).

Binding experiments were carried out by incubating the 6-FAM-labeled dsDNA-FANCA probe (65 bp) with the HpFANCA-short repair-PPRH in a buffer containing 10 mM $MgCl_2$, 100 mM NaCl, and 50 mM HEPES (pH 7.2). Binding reactions (20 µL) were incubated for 5 min at 92ºC followed by 25 min of cooling down until reaching room temperature. Unspecific poly(dI:dC) DNA was included

in each reaction at a 1:1 unspecific DNA/specific DNA ratio. In the case of the bindings between the ssDNA-FANCA-Fw probe and the HpFANCA-short, reaction mixes were incubated for 30 min at 37ºC and tRNA was used as unspecific competitor. The scrambled Hp-Sc6 PPRH was used as negative control (Table 8). Electrophoresis were performed on nondenaturing 8% polyacrylamide gels containing 10 mM $MgCl_2$, 5% glycerol, and 50 mM HEPES (pH 7.2). Gels were run at a fixed voltage of 190 V (4ºC) using a running buffer containing 10 mM $MgCl_2$ and 50 mM HEPES (pH 7.2). Finally, bands were visualized using the Gel Doc™ EZ with the Image Lab Software, Version 6.0 (Bio-Rad). All reagents were obtained from Sigma-Aldrich.

Table 8. Oligodeoxynucleotides used in the DNA binding assays.

Name	Length (nt)	Sequence (5'-3')
ssDNA-FANCA-Fw	65	CTATGGTTTTGTTTTGTGTTTAAGGCTCTGCTTTGCAGG ATCAAGCCTCAAGGCTGGGGGTTCCC
ssDNA-FANCA-Rv	65	GGGAACCCCCAGCCTTGAGGCTTGATCCTGCAAAGCA GAGCCTTAAACACAAAACAAAACCATAG
Hp-Sc6	53	AAGGAAGGAAGGAAGGAAGGAAGGTTTTTGGAAGGAA GGAAGGAAGGAAGGAA

3.3.5 Transfection of FA-55 cells

FA-55 cells (100,000-300,000) were plated in 6-well dishes in 800 µL of RPMI + 20% FBS medium. Cell transfection consisted in mixing 10 µg of the repair-PPRH with 10 µM of the cationic liposome N-[1-(2,3-dioleoyloxy)propil]-N,N,N-trimethylammonium methylsufate (DOTAP) (Biontex) in a final volume of 200 µL of free-serum medium. The mixture was incubated for 20 min at room temperature. Finally, the repair-PPRH/liposome complex was added to the cells to attain a final volume of 1 mL. After 72h of incubation with the complex, 33 nM MMC were added to the pool of cells to enrich the repaired population.

3.3.6 Next Generation Sequencing

After at least one week of treatment with MMC, total genomic DNA was extracted using the Wizard genomic DNA purification kit (Promega), following the manufacturer's instructions.

To evaluate the percentage of gene correction, we performed Next Generation Sequencing (NGS) at high coverage (deep sequencing). Specific primers were designed to amplify the target site (334 bp) in the *FANCA* gene. The sequences of the forward and reverse primer were 5'-GTGAGCTGCTTGGATCATCA-3' and 5'-TACTCTCTGCTCCACAGTCA-3', respectively. A fusion PCR with the GeneRead HotStarTaq polymerase (Qiagen) for indexing and adding the adaptors was performed. Finally, the library was sequenced on a MiSeq system with a 500-cycle MiSeq Reagent Kit v2 (Illumina). The resulting sequences were aligned against the wild-type reference sequence and the percentage of mutation correction assessed with the Low Frequency Variant Detection algorithm. Analyses were performed with the CLCBio Genomic Workbench 20 program (Qiagen). The number of reads aligned to the target were between 30.000 and 50.000 reads.

As positive control of the repair capacity of PPRHs, we sequenced *dhfr* DF42 mutant cells before and after transfection with the HpDE6rep repair-PPRH at different times of selection in -GHT medium. The description of the DF42 mutant cell line, the design of the repair-PPRH and the entire gene correction procedure can be found in (Solé *et al.* 2016). The sequences of the forward and reverse primer to amplify the target site (227 bp) in the *dhfr* gene were 5'-GTCATGTGTCTTCAATGGGTG-3' and 5'- TCTAAAGCCAACACAAGTCCC-3', respectively. Deep-sequencing analyses were performed as previously described for the *FANCA* gene.

4. RESULTS

Informe dels directors

Els Drs. Carlos J. Ciudad Gómez i Verónica Noé Mata, directors de la tesi doctoral titulada "*Biomedical applications of PolyPurine Reverse Hoogsteen hairpins: immunotherapy and gene repair*"

INFORMEN:

Del factor d'impacte de les revistes de publicació dels articles inclosos en aquesta tesi doctoral.

Que els articles II i III es tracten de treballs de coautoria en que ambdós coautors han compartit el projecte i han realitzat els experiments per igual.

Que els articles II i III no s'han utilitzat per la realització de cap tesi doctoral prèvia.

Llistat de publicacions

- Article I. Functional pharmacogenomics and toxicity of PolyPurine Reverse Hoogsteen hairpins directed against survivin in human cells

Alex J. Félix, Carlos J. Ciudad and Véronique Noé

Biochemical Pharmacology (2018) (Impact factor: 4.825)

- Article II. Silencing of CD47 and SIRPα by PolyPurine Reverse Hoogsteen hairpins to promote MCF7 breast cancer cells death by PMA-differentiated THP-1 cells

Gizem Bener*, Alex J. Félix*, Cristina Sánchez de Diego, Isabel Pascual Fabregat, Carlos J. Ciudad and Véronique Noé

*These authors contributed equally to this work

BMC immunology (2016) (Impact factor: 2.615)

- **Article III.** Cancer immunotherapy using PolyPurine Reverse Hoogsteen hairpins targeting the PD-1/PD-L1 pathway in human tumor cells

Miriam Marlene Medina Enríquez*, Alex J. Félix*, Carlos J. Ciudad and Véronique Noé

*These authors contributed equally to this work

PLOS ONE (2018) (Impact factor: 2.776)

- **Article IV.** Silencing PD-1 and PD-L1: the potential of PolyPurine Reverse Hoogsteen hairpins for the elimination of tumor cells

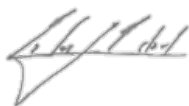Carlos J. Ciudad, Miriam Marlene Medina Enriquez, Alex J. Félix, Gizem Bener and Véronique Noé.

Immunotherapy (2019) (Impact factor: 3.028)

- **Article V.** Correction of the aprt gene using Repair-PolyPurine Reverse Hoogsteen hairpins in mammalian cells

Alex J. Félix, Carlos J. Ciudad and Véronique Noé

Molecular Therapy-Nucleic Acids (2020) (Impact factor: 7.032)

Dr. Carlos J. Ciudad Gómez   Dra. Verónica Noé Mata

4.1 Article I:

Functional pharmacogenomics and toxicity of PolyPurine Reverse Hoogsteen hairpins directed against *survivin* in human cells

Alex J. Félix, Carlos J. Ciudad and Véronique Noé

Background: During the last decade, PolyPurine Reverse Hoogsteen hairpins (PPRHs) have been applied in our group for silencing different target genes involved in cancer progression. Previously, we reported that specific PPRHs against the antiapoptotic gene *survivin* were able to effectively decrease cell viability in PC3 prostate cancer cells by increasing apoptosis *in vitro*. In addition, the most effective PPRH directed against survivin (HpsPr-C-WT) was also tested in a subcutaneous xenograft tumor mice model of PC3 prostate cancer cells, showing either a 40% or 60% decrease in tumor volume after intratumoral or intravenous administration, respectively, compared to the negative control PPRH.

Objectives: The aim of this work was to study the functional genomic response in PC3 cells upon treatment with the HpsPr-C-WT PPRH directed against the *survivin* gene. Additionally, we tested the possible off-target effects and the *in vitro* toxicity of a negative control hairpin in both hepatic and renal human cell lines.

Results: We performed microarray experiments for three different conditions: untreated cells, cells treated with the negative hairpin (Hp-WC) and cells treated with the HpsPr-C-WT. On the one hand, we observed that the incubation with the Hp-WC negative hairpin did not show any differentially expressed genes when compared with untreated cells. On the other hand, incubation with the HpsPr-C-WT showed 244 differentially expressed genes when compared with cells treated with the Hp-WC negative hairpin. We analyzed the 244 differentially expressed genes to find functional relationships among the gene products using different softwares. Gene Ontology (GO) analyses were carried out to classify the differentially expressed genes according to the categories of biological process, molecular function and cellular component. In

addition, Gene Set Enrichment Analysis (GSEA) revealed that the differentially expressed genes clustered very significantly within the gene sets of Regulation of cell proliferation, Cellular response to stress, Apoptosis and Prostate cancer. Finally, the STRING software identified important interacting gene-nodes such as *POLR2G*, *PAK1IP1*, *SMC3*, *SF3A1*, *PPARGC1A* and NCOA6 that were involved in genomic maintenance and regulation of transcriptional or splicing processes, thus demonstrating that inhibition of *survivin* led to an apoptotic response with the subsequent deregulation of vital cellular processes.

A series of RT-qPCR arrays specifically designed for hepatotoxicity and nephrotoxicity screening were used to study the possible cytotoxicity of PPRHs in hepatic (HepG2) and renal (786-O) human cells, respectively. We showed that less than 6% of the genes were differentially expressed in the hepatic screening and less than 14% in the renal screening. However, these changes in gene expression did not cause any harmful effect in the viability of HepG2 and 786-O human cells.

Conclusions: We performed a functional pharmacogenomics study including GO, GSEA and STRING analyses of the effect of the HpsPr-C-WT PPRH against the antiapoptotic gene *survivin*, previously validated both *in vitro* and *in vivo*. The negative control counterpart did not cause any effect on cell viability nor significant changes in gene expression. In addition, we determined the absence of cytotoxicity upon incubation with a negative hairpin in HepG2 and 786-O cells and observed minor changes in gene expression using RT-qPCR arrays specifically developed for hepatotoxicity and nephrotoxicity screening.

Functional pharmacogenomics and toxicity of PolyPurine Reverse Hoogsteen hairpins directed against *survivin* in human cells

Alex J. Félix, Carlos J. Ciudad*[,1], Véronique Noé[1]

Department of Biochemistry and Physiology, School of Pharmacy, and IN2UB, University of Barcelona, 08028 Barcelona, Spain

ARTICLE INFO

ABSTRACT

PolyPurine Reverse Hoogsteen (PPRH) hairpins constitute a relatively new pharmacological agent for gene silencing that has been applied for a growing number of gene targets. Previously we reported that specific PPRHs against the antiapoptotic gene *survivin* were able to decrease viability of PC3 prostate cancer cells by increasing apoptosis, while not acting on HUVEC non-tumoral cells. These PPRHs were efficient both *in vitro* and *in vivo*. In the present work, we performed a functional pharmacogenomics study on the effects of specific and unspecific hairpins against *survivin*. Incubation of PC3 cells with the specific HpsPr-C-WT led to 244 differentially expressed genes when applying the p < 0.05, FC > 2, Benjamini-Hochberg filtering. Importantly, the unspecific or control Hp-WC did not originate differentially expressed genes using the same settings. Gene Set Enrichment Analysis (GSEA) revealed that the differentially expressed genes clustered very significantly within the gene sets of Regulation of cell proliferation, Cellular response to stress, Apoptosis and Prostate cancer. Network analyses using STRING identified important interacting gene-nodes within the response of PC3 cells to treatment with the PPRH against *survivin*, mainly POLR2G, PAK1IP1, SMC3, SF3A1, PPARGC1A, NCOA6, UGT2B7, ALG5, VAMP7 and HIST1H2BE, the former six present in the Gene Sets detected in the GSEA. Additionally, HepG2 and 786-O cell lines were used to carry out *in vitro* experiments of hepatotoxicity and nephrotoxicity, respectively. The unspecific hairpin did not cause toxicity in cell survival assays (MTT) and produced minor changes in gene expression for selected genes in RT-qPCR arrays specifically developed for hepatic and renal toxicity screening.

1. Introduction

In the last decades, new pharmacological agents composed of DNA such as Triplex-Forming Oligonucleotides (TFOs) and Antisense Oligonucleotides (ASOs) have been widely used as gene silencing tools to inhibit specific genes involved in a particular disease or condition. In the same way, RNA-based drugs such as small interfering RNAs (siRNAs) and short hairpin RNAs (shRNAs) are also commonly used. Nowadays, the spectrum of diseases that can potentially be addressed by nucleic acids is broad and ranges from infectious diseases to diabetes and cancer [1]. DNA and RNA-based agents have demonstrated their pharmacological effect both *in vitro* and *in vivo*, and according to the database of clinical trials (https://clinicaltrials.gov), a total of 156 antisense oligonucleotides, 33 aptamers, 2 TFOs and 53 siRNAs are in various stages of development.

In our laboratory, we developed a new gene silencing tool called PolyPurine Reverse Hoogsteen (PPRHs) hairpins, which are non-modified single-stranded oligonucleotides composed of two antiparallel polypurine domains linked by a pentathymidine loop. The intramolecular linkage consists of reverse-Hoogsteen bonds between adenines and guanines allowing the formation of the hairpin structure. PPRHs can bind to polypyrimidine stretches in the double-stranded DNA (dsDNA) via Watson-Crick bonds producing a triplex structure and displacing the fourth strand of the dsDNA, thus leading to the gene silencing effect [2,3]. It is therefore essential, for PPRH design, to find polypurine/polypirimidine tracts within the sequence of the target gene which are commonly present in promoter or intronic regions [4].

PPRHs have been used as therapeutic tools to target genes related to resistance to drugs [5], immunotherapy approaches [6] and cancer progression [7–11].

The gene *survivin* (*BIRC5*) is a member of the inhibitor of apoptosis (IAP) family and it is involved in cancer proliferation. The expression of *survivin* is developmentally controlled, with prominent mRNA and protein distribution in fetal tissues and complete down-regulation in adult cells, with the exception of thymus [12], the basal crypt epithelial cells of normal mucosa [13] and CD34^{+} cells and normal peripheral blood mononuclear cells [14]. Furthermore, this gene is overexpressed in different types of tumors, such as bladder [15], prostate [12], lung

Results

[16,17], colon [18,19], pancreas [20,21], ovary [22], hepatic [23], glioma [24], gastric [25], melanoma [26,27], leukemia [28] and squamous cell carcinoma [29]. *Survivin* overexpression has also been associated with an increased risk of distant metastasis in patients with prostate cancer [30] and osteosarcoma [31].

In addition, it has been reported that targeted inhibition of *survivin* appears to enhance the therapeutic effects of Flutamide (a non-steroidal antiandrogen) both *in vitro* and *in vivo*, revealing a novel strategy to enhance sensitivity to androgen deprivation therapy [32]. Moreover, the inhibition of *survivin* also sensitizes prostate cancer cells to paclitaxel-induced apoptosis [33].

As a new therapeutic approach, we reported the effects of different PPRHs against *survivin* both *in vitro* and *in vivo*. On the one hand, human prostate cancer cells (PC3) treated with 100 nM of a Coding-PPRH (HpsPr-C) against the promoter of *survivin* showed more than 90% decrease in cell viability *in vitro*. The specific effect of the PPRH against *survivin* was demonstrated by mRNA and protein analyses. *Survivin* mRNA expression levels after 24 h of incubation with 100 nM of HpsPr-C were 2-fold decrease compared to that of the control cells. Furthermore, we found out that there were no off-target effects by determining mRNA levels of a set of 5 non-related genes (*APOA1*, *BCL2*, *DHFR*, *PDK1* and *S100A4*). The protein levels of *survivin* after 6 h of incubation with 100 nM of HpsPr-C were also 50% decreased compared to the control [7].

On the other hand, the *in vivo* intratumoral administration of HpsPr-C in subcutaneous xenograft tumor mice models of PC3 prostate cancer cells produced a reduction of 40% in tumor volume and 30% in tumor weight when compared to mice treated with a negative-control PPRH. In addition, when injecting the HpsPr-C through the tail vein (intravenous administration) the relative tumor volume was reduced by a half compared to the negative-control group. In both types of *in vivo* PPRH-administration, the mice body weight loss was approximately 2%, indicating lack of toxicity [7].

The aims of this work were to study the functional pharmacogenomics response in prostate cancer cells upon treatment with a specific PPRH against the *survivin* gene. In addition, we also analyzed the possible off-target effects and the preliminary *in vitro* toxicity of a negative control hairpin in hepatic and renal cell lines.

2. Materials and methods

2.1. Design and usage of PPRH

To design the PPRH used in this study we used the Triplex-Forming Oligonucleotide Target Sequence Search software (http://utw10685.utweb.utexas.edu/tfo/, Austin, TX), which searches stretches of polypurines within the DNA; therefore, the polypyrimidine tracks in the complementary strand are the target of the PPRHs. The candidate sequences were subjected to BLAST analyses to confirm the specificity of the PPRHs selecting the ones without unintended targets.

All hairpins were synthesized as non-modified oligodeoxynucleotides by Sigma-Aldrich (Haverhill, United Kingdom). They were dissolved at 1 mM (stock solution) in a sterile RNase-free Tris-EDTA buffer (1 mM EDTA and 10 mM Tris, pH 8.0; both from Sigma-Aldrich, Madrid, Spain) and stored at −20 °C until use.

As negative control we used a Watson-Crick (WC) hairpin (Hp-WC). This hairpin forms intramolecular WC bonds instead of reverse Hoogsteen bonds, thus preventing additional WC bonding to the target DNA and, consequently, triplex formation. The sequences of the hairpins and their abbreviations are described in Table 1.

2.2. Cell culture

Prostate cancer PC3, hepatocellular carcinoma HepG2 and renal adenocarcinoma 786-O human cell lines were used in this study. Cells were cultured in Ham's F-12 medium supplemented with 7% fetal bovine serum (both from Gibco, Madrid, Spain) at 37 °C in a 5% CO$_2$ – controlled humidified atmosphere. Trypsinization of the cells was performed using 0,05% Trypsin (Sigma-Aldrich, Madrid, Spain) in PBS 1X (154 mM NaCl, 3.88 mM H$_2$NaPO$_4$, 6.1 mM HNaPO$_4$, pH 7.4; all from Sigma-Aldrich, Madrid, Spain).

2.3. Transfection of PPRHs

Cells (30,000) were plated in 6-well dishes one day before transfection. Transfection consisted in mixing the appropriate amount of hairpin and N-[1-(2,3-dioleoyloxy)propyl]-N,N,N-trimethylammonium methylsulfate (DOTAP) (Biontex, Munich, Germany) for 20 min in 200 μL of medium at room temperature, followed by the addition of this mixture to the cells to attain a final volume of 1 mL. Hairpins were incubated at 100 nM transfected with the cationic liposome DOTAP at 10 μM, final concentrations in the incubation medium.

2.4. Cell survival assay (MTT)

Three days after transfection, 500 μg/mL of 3-(4,5-Dimethylthiazol-2-yl)-2,5-Diphenyltetrazolium Bromide (MTT) and 100 μM of sodium succinate (both from Sigma-Aldrich, Madrid, Spain) were added to the culture medium and incubated for 2.5 h at 37 °C. Then medium was discarded and the lysis reagent (0.57% acetic acid and 10% sodium dodecyl sulfate in DMSO, all from Sigma-Aldrich, Madrid, Spain) was added. Cell survival was measured at 570 nm in a Modulus™ Microplate luminometer (Turner BioSystems; Promega, Madrid, Spain).

2.5. RNA isolation

Total RNA was extracted using TRI Reagent™ (Life technologies, Barcelona, Spain) following the instructions provided by the manufacturer. RNA concentration was determined by measuring its absorbance (260 nm) at 25 °C using a Nanodrop ND-1000 spectrophotometer (Thermo Fisher Scientific, Barcelona, Spain).

2.6. Retrotranscription

cDNA was synthesized in a 20 μL reaction mixture containing 1 μg of total RNA, 125 ng of random hexamers (Roche, Barcelona, Spain), 0.5 mM of each dNTP (Ecogen, Barcelona, Spain), 2 μL of Buffer (10×), 20 units of RNAse inhibitor and 200 units of Moloney murine leukemia virus reverse transcriptase (Last three from Lucigen, Wisconsin, USA). The reaction was incubated at 42 °C for 1 h. 3 μL of the cDNA mixture was used for Real-Time qPCR amplification.

2.7. Real-Time PCR

A StepOnePlus™ Real-Time PCR System (Applied Biosystems, Barcelona, Spain) was used to perform these experiments. PCR cycling conditions were 10 min denaturation at 95 °C, followed by 40 cycles of 15 s at 95 °C and 1 min at 60 °C. *Survivin* (*BIRC5*) mRNA Taqman probe (Assay ID: Hs04194392_s1; Life Technologies, Barcelona, Spain) was used to determine the mRNA expression of *survivin*. The relative mRNA amount of the target gene was calculated using the $\Delta\Delta C_T$ method, where C_T is the threshold cycle that corresponds to the cycle where the amount of amplified mRNA reaches the threshold of fluorescence. Peptidylprolyl isomerase A (*PPIA*) mRNA Taqman probe (Assay ID: Hs04194521_s1; Life Technologies, Barcelona, Spain) was used as endogenous control. The final volume of the reaction was 20 μL containing 1x Taqman Universal PCR Mastermix II, 1x Taqman probe (Both from Life technologies, Barcelona, Spain), 3 μL of cDNA and nuclease-free H$_2$0 mQ.

9

Table 1
DNA hairpins used in this study.

Specific PPRH		
Name	**Target gene**	**Sequence (5'-3')**
HpsPr-C-WT	*Survivin (BIRC5)*	AGGGGAGGGA**T**GGAG**T**GCAG**G** T T T AGGGGAGGGA**T**GGAG**T**GCAG T T T

Negative control		
Name	**Target gene**	**Sequence (5'-3')**
Hp-WC	-	AGGGGAGGGATGGAGTGCAG**G** T T T TCCCCTCCCTACCTCACGTC T T T

The PPRH was designed using the Triplex-Forming Oligonucleotide Target Sequence Search software (http://utw10685.utweb.utexas.edu/tfo/). The abbreviations used for the nomenclature of the PPRH are: Hp, hairpin; Pr, promoter; -C, Coding-PPRH. Pyrimidine interruptions in the PPRH sequence are indicated in orange. The target sequence of the PPRH within the promoter region is located between nucleotides -525 and -506 relative to the transcription initiation site.
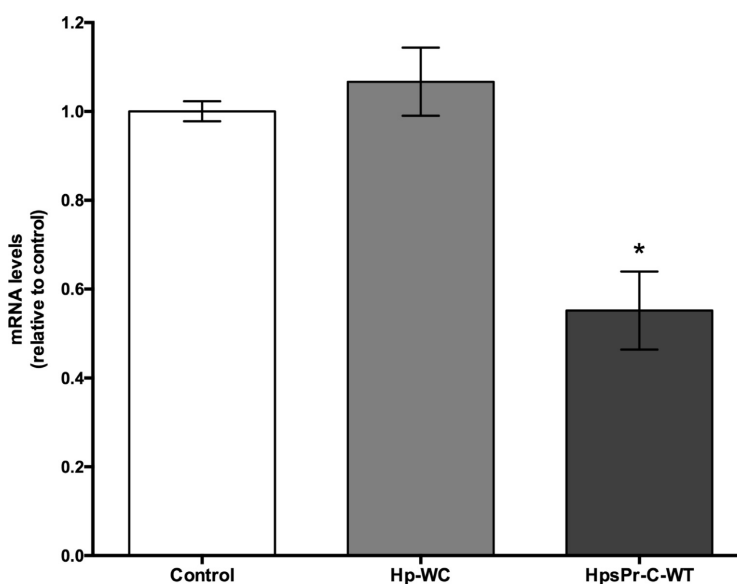

Fig. 1. *Survivin* mRNA levels after hairpin incubation. The expression levels of *survivin* in PC3 cells after treatment with 100 nM of either HpsPr-C-WT or Hp-WC at 24 h were determined by qRT-PCR using a specific TaqMan® probe. Experiments were performed in triplicate. Data represent the mean ± SEM. $p < 0.05$ (*).

2.8. Microarrays

The PC3 cell line was selected for microarray analyses. Total RNA was prepared from triplicate of three different conditions: i) control cells; ii) cells treated with the specific PPRH against survivin (HpsPr-C-WT) for 24 h and iii) cells incubated 24 h with Hp-WC, the WC negative control hairpin. For gene expression analyses, Clariom™ S human array from Affymetrix covering 20,800 genes and 337,100 transcripts was used. Labeling, hybridization and detection were carried out in each case following the recommendations of the manufacturer. Data was submitted to the Gene Expression Omnibus database (GEO) with the

reference number GSE107106.

2.9. Microarray analyses

Data files from mRNA microarrays were analyzed with GeneSpring GX14.9 software (Agilent Technologies, Madrid, Spain) to find differentially expressed mRNAs. Triplicate samples for each condition were imported into one single experiment. Average values of the replicate spots of each mRNA were subjected to RMA (Robust Multi-array Average), a method for normalizing and summarizing probe-level intensity and referred against the median of the control samples. Gene
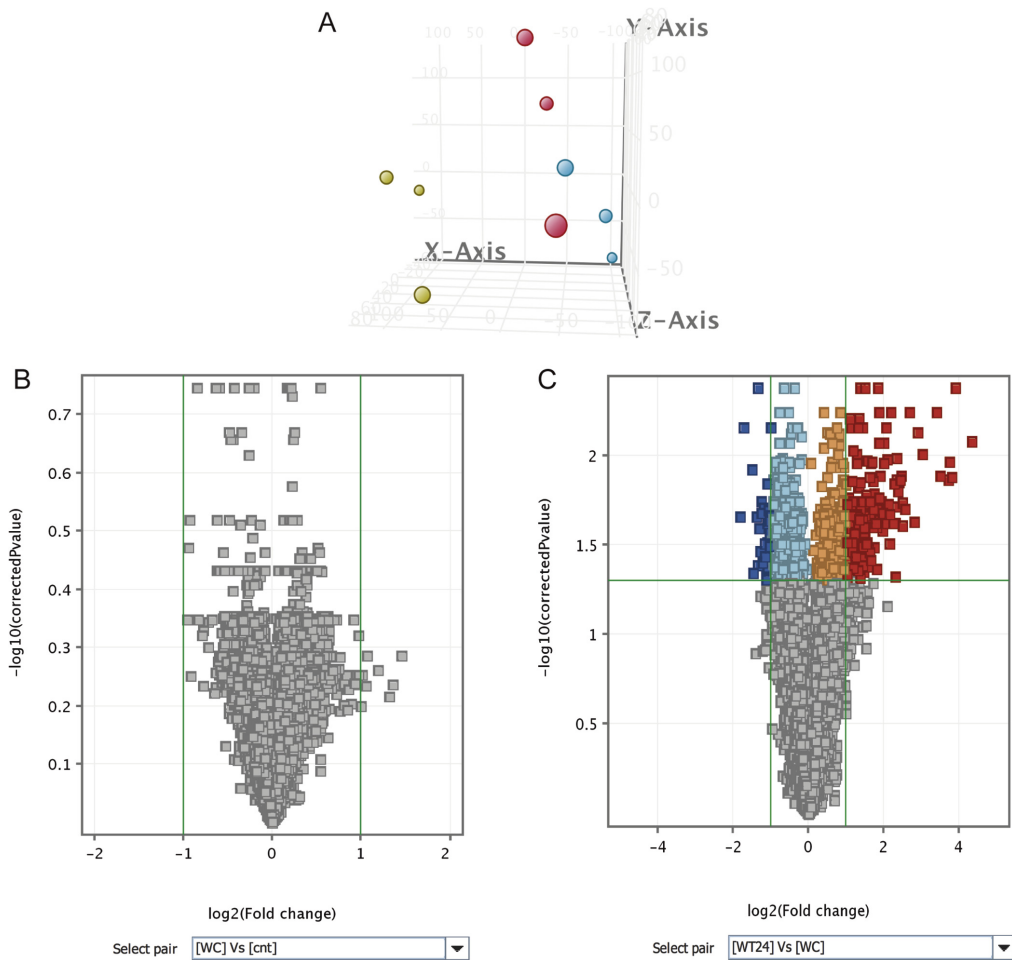
Results

Fig. 2. Microarray analyses. Raw data (.CEL files) were imported into the GeneSpring-GX software, normalized using RMA and referred against the median of the control samples. (A) Principal Component Analysis (PCA) showing the triplicate samples of the 3 different groups (blue, control cells; red, negative control hairpin; yellow, specific PPRH). Volcano plot representation of differentially expressed genes ($p < 0.05$, FC > 2.0, Benjamini-Hochberg) when comparing cells treated with the negative control hairpin (Hp-WC) vs Control cells (B) or when comparing cells incubated with the specific PPRH (HpsPr-C-WT) vs cells treated with the negative control hairpin (C). Dark blue and red squares represent underexpressed or overexpressed genes, respectively. (For interpretation of the references to colour in this figure legend, the reader is referred to the web version of this article.)

Table 2
Differentially expressed genes.

	P all	P < 0.05	P < 0.02	P < 0.01	P < 0.005	P < 0.001
FC all	21,448	1293	198	48	7	0
Fc > 1.1	11,060	1288	197	48	7	0
Fc > 1.5	1500	720	153	36	6	0
Fc > 2.0	319	244	85	25	5	0
Fc > 3.0	76	74	44	13	2	0

Number of differentially expressed genes depending on the p-value and the absolute fold change (FC) selection. Analyses of data from PC3 cells incubated with the negative control (Hp-WC) compared with cells treated for 24 h with HpsPr-C-WT both in triplicate, were performed using unpaired T-test, the multiple testing correction of Benjamini-Hochberg and asymptotic p-value (adjusted) computation.

Table 3
Underexpressed genes.

Genbank	Symbol	Gene name	Fold-change	Control	Treated
					Raw expression
–	*WDR45B*	WD Repeat Domain 45B	−3.47	404.26	116.39
BC112254	*HIST1H2AI*	Histone Cluster 1 H2A Family Member I	−3.27	560.62	171.21
BC020221	*STAC*	SH3 And Cysteine Rich Domain	−2.85	496.76	174.60
BC069306	*HIST1H2AL*	histone cluster 1, H2al	−2.74	562.79	205.31
BC075082	*PDE7B*	Phosphodiesterase 7B	−2.58	169.77	65.85
BC021161	*PHAX*	Phosphorylated Adaptor for RNA Export	−2.52	1537.94	609.41
BC010907	*PAK1IP1*	PAK1 Interacting Protein 1	−2.50	1338.60	534.55
–	*TOPORS-AS1*	TOPORS antisense RNA1	−2.48	491.66	198.42
BC012916	*FRK*	Fyn Related Src Family Tyrosine Kinase	−2.40	422.27	175.80
BC157068	*PPARGC1A*	peroxisome proliferator-activated receptor gamma, coactivator 1 alpha	−2.37	187.57	79.21
BC042547	*TEX13A*	Testis Expressed 13A	−2.36	364.99	154.64
BC104041	*FAM167A*	family with sequence similarity 167, member A	−2.32	287.25	123.62
BC001483	*TFG*	TRK-Fused Gene	−2.30	591.07	256.55
BC001025	*RCL1*	RNA terminal phosphate cyclase-like 1	−2.25	2484.07	1102.48
–	*COL4A2*	Collagen Type IV Alpha 2 Chain	−2.23	2181.99	977.83
BC001976	*SF3A1*	splicing factor 3a, subunit 1	−2.22	188.63	84.83
BC021285	*MSX1*	Msh Homeobox 1	−2.19	363.85	166.22
BC004954	*RPL13*	ribosomal protein L13	−2.17	215.67	99.35
BC053600	*TMCO4*	Transmembrane and Coiled-Coil Domains 4	−2.15	983.41	457.26
–	*MGAM2*	maltase-glucoamylase 2 (putative)	−2.15	749.33	348.68
BC141619	*PLA2G2E*	Phospholipase A2 Group IIE	−2.12	2280.79	1073.78
BC151244	*FRMD4A*	FERM domain containing 4A	−2.12	174.49	82.19
BC000506	*HNRNPA2B1*	heterogeneous nuclear ribonucleoprotein A2/B1	−2.11	1327.71	630.26
BC066282	*IL5*	interleukin 5	−2.09	233.29	111.85
–	*CT45A9*	Cancer/Testis Antigen Family 45 Member A9	−2.08	340.70	163.81
BC136409	*CACNB2*	Calcium Voltage-Gated Channel Auxiliary Subunit Beta 2	−2.08	119.25	57.37
BC014659	*SLC44A4*	solute carrier family 44, member 4	−2.05	890.01	433.40
–	*FBXL21*	F-Box And Leucine Rich Repeat Protein 21 (Gene/Pseudogene)	−2.04	495.78	242.58
–	*ZNF442*	zinc finger protein 442	−2.04	440.38	215.83
–	*CUL2*	Cullin 2	−2.04	370.70	182.16
BC101643	*SEMA7A*	Semaphorin 7A (John Milton Hagen Blood Group)	−2.03	163.48	80.41
BC069360	*XCL2*	Chemokine (Cmotif) ligand 2	−2.03	1426.09	701.69
BC130299	*C5orf56*	chromosome 5 open reading frame 56	−2.02	183.14	90.66
BC069554	*CSN2*	casein beta	−2.02	273.20	135.32
BC000053	*LITAF*	lipopolysaccharide-induced TNF factor	−2.02	1396.61	692.55
BC014416	*SLC33A1*	solute carrier family 33 (acetyl-CoA transporter), member 1	−2.02	215.59	106.95
–	*HIST2H3D*	histone cluster 2, H3d	−2.01	533.28	264.95
BC030572	*GTF2E2*	general transcription factor IIE subunit 2	−2.00	326.00	162.69
BC042864	*SH3GL3*	SH3 Domain Containing GRB2 Like 3, Endophilin A3	−2.00	140.25	70.08

The table shows the 50 top underexpressed genes filtered by 2.0-fold with a p-value < 0.05 obtained after comparing cells incubated with HpsPr-C-WT vs Hp-WC. It is shown the GenBank accesion number, the Gene Symbol and Gene Name for each gene including the fold change and the differences in raw expression data between the control and treated conditions.

expression was calculated as the ratio of the normalized values obtained for all conditions after normalization of the data. Differentially expressed mRNAs with a p-value (p) of less than 0.05 and a fold change (FC) > 2 were selected (Volcano plot). Multiple testing correction was applied (Benjamini–Hochberg false discovery rate, FDR).

2.10. Gene ontology

Gene Ontology (GO) was determined and represented as bar charts based on three different criteria: biological process, cellular component and molecular function. GO bar charts were plotted with the online available tool PANTHER (Protein Analysis Through Evolutionary Relationships; http://www.pantherdb.org) [34].

2.11. Gene Set Enrichment Analysis

Gene Set Enrichment Analysis (GSEA) [35], a computational method that determines whether an a priori defined set of genes shows statistically significant differences between two biological states, was performed by computing overlaps among the differentially expressed gene list and the different gene sets using the platform in http://software.broadinstitute.org/gsea/index.jsp.

2.12. Network analyses

Functional protein association networks was conducted by using STRING [36] (Search Tool for the Retrieval of Interacting Genes; https://string-db.org/), a database of known and predicted protein-protein interactions. The interactions include direct (physical) and indirect (functional) associations; they stem from computational prediction, from knowledge transfer between organisms, and from interactions aggregated from other (primary) databases. These are provided with confidence scores and this tool also offers accessory information such as protein domains and 3D structures (with link to databases) if available.

2.13. RT-qPCR arrays

HepG2 and 786-O cell lines were selected to evaluate hepatotoxicity and nephrotoxicity *in vitro*, respectively. Cell toxicity was determined both by cell survival assays (MTT) and by determining the changes in gene expression of selected genes present in RT-qPCR arrays specifically developed for hepatic and renal toxicity screening. RNA was extracted from triplicate points of two different conditions for both cell lines: (i) untreated cells and (ii) cells treated with 100 nM of Watson-Crick negative control hairpin (Hp-WC). For each sample, 1 μg of cDNA was synthesized using the High Capacity cDNA Reverse Transcription Kit

Results

Table 4
Overexpressed genes.

Genbank	Symbol	Gene name	Fold-change	Control	Treated
				Raw expression	
BC021104	*APLN*	apelin	19.90	175.44	3491.24
BC000635	*ACAA1*	acetyl-CoA acyltransferase1	14.76	222.68	3286.70
BC038585	*TRIM15*	tripartite motif-containing 15	13.94	129.39	1804.28
BC012145	*NKIRAS1*	NFKB inhibitor interacting Ras-like1	13.42	128.76	1728.12
BC110412	*RASSF1*	Ras-association (RalGDS/AF-6) domain family member 1	13.20	154.12	2034.43
BC172406	*ITPR3*	inositol 1,4,5-trisphosphatereceptor, type3	11.32	96.68	1093.98
BC000283	*DBN1*	drebrin 1	10.63	38.98	414.51
BC152456	*DCLK1*	doublecortin-like kinase1	8.15	362.67	2956.43
BC047085	*IL33*	interleukin 33	7.52	435.90	3277.13
BC152469	*CNOT6*	CCR4-NOT transcription complex subunit 6	6.99	133.02	930.29
BC157052	*TRIM71*	tripartite motif containing 71, E3 ubiquitin protein ligase	6.44	864.38	5569.96
BC047083	*SPG20*	spastic paraplegia 20 (Troyer syndrome)	5.82	185.76	1080.19
BC167147	*ERBB2*	erb-b2 receptor tyrosine kinase 2	5.59	119.76	669.58
BC068995	*EED*	embryonic ectoderm development	5.58	153.07	853.96
BC018070	*DPPA2*	developmental pluripotency associated 2	5.53	137.76	761.26
–	*LINC00521*	long intergenic non-protein coding RNA 521	5.42	438.89	2377.78
BC012605	*RHAG*	Rh-associated glycoprotein	5.29	33.28	176.08
–	*PGA4*	pepsinogen 4, group I (pepsinogenA)	5.19	90.67	470.83
BC066552	*LAMA4*	laminin, alpha 4	5.11	345.16	1762.54
BC019221	*FAM122B*	family with sequence similarity 122B	5.09	433.38	2207.32
BC058000	*TTPA*	tocopherol (alpha) transfer protein	5.09	46.09	234.52
BC063801	*DGKQ*	diacylglycerol kinase theta	5.07	150.43	762.77
BC036062	*PCDHB16*	protocadherin beta 16	4.99	114.30	570.40
BC117444	*LINC01587*	long intergenic non-protein coding RNA 1587	4.96	289.78	1438.27
BC136272	*NCOA6*	nuclear receptor coactivator 6	4.88	384.59	1878.03
BC111497	*SLAIN1*	SLAIN motif family member 1	4.81	752.18	3618.32
BC094779	*MORC3*	MORC family CW-type zinc finger 3	4.78	68.63	328.10
–	*C9orf172*	chromosome 9 open reading frame 172	4.58	1096.36	5021.05
BC000751	*EIF5A*	eukaryotic translation initiation factor 5A	4.42	143.01	631.44
–	*ZNF546*	zinc finger protein 546	4.41	157.34	694.07
BC042452	*SLCO1A2*	solute carrier organic anion transporter family, member 1A2	4.31	281.43	1211.92
BC001435	*DDAH2*	dimethylarginine dimethylaminohydrolase 2	4.28	275.12	1177.81
BC032583	*TROAP*	trophinin associated protein	4.17	550.97	2298.85
BC172220	*THOC2*	THO complex 2	4.17	51.93	216.68
BC069353	*HAS2*	hyaluronan synthase 2	4.13	179.17	740.61
–	*FLNA*	Filamin A	4.13	100.39	414.35
BC113544	*MYO1G*	myosin IG	3.96	1827.16	7230.45
BC130404	*C9orf57*	chromosome 9 open reading frame 57	3.95	82.26	325.10
BC055089	*CAMP*	cathelicidin antimicrobial peptide	3.94	113.95	448.57
BC012531	*ALG5*	Dolichyl-Phosphate Beta-Glucosyltransferase	3.93	224.25	881.19
BC036653	*PAPOLB*	poly(A) polymerase beta	3.88	122.57	475.27
BC013188	*TPST1*	tyrosyl protein sulfotransferase 1	3.82	214.69	821.13
BC017867	*SGOL1*	shugoshin-like1	3.70	69.60	257.73
BC146979	*SMIM24*	small integral membrane protein 24	3.68	72.26	265.89
BC001936	*BAG1*	BCL2-associated athanogene	3.67	279.99	1028.83
BC016282	*MUT*	methylmalonyl-CoA mutase	3.67	586.22	2153.23
BC050547	*PILRB*	paired immunoglobin-like type 2 receptor beta	3.65	295.51	1079.04
–	*OR5K3*	olfactory receptor, family 5, subfamily K, member 3	3.62	361.32	1309.80
BC010618	*DTD2*	D-tyrosyl-tRNA deacylase2 (putative)	3.61	225.21	812.71
BC063283	*ADAMTS18*	ADAM Metallopeptidase with Thrombospondin Type 1 Motif 18	3.52	131.30	462.60

The table shows the 50 top overexpressed genes filtered by 2.0-fold with a p-value < 0.05 obtained after comparing cells incubated with HpsPr-C-WT vs Hp-WC. It is shown the GenBank accesion number, the Gene Symbol and Gene Name for each gene including the fold change and the differences in raw expression data between the control and treated conditions.

(Applied Biosystems, Barcelona, Spain) following the instructions of the manufacturer. Then, the cDNA product was diluted 1/12 with nuclease-free H_2O mQ. Human Drug Hepatotoxicity SignArrays® and Human Drug Nephrotoxicity SignArrays® (both from AnyGenes, Paris, France) were used to determine gene expression in HepG2 and 786-O cell lines, respectively. RT-qPCR was performed following the manufacturer's recommendations. The mRNA expression data was analyzed using the Analysis Tool Software provided by AnyGenes®.

2.14. Statistical analyses

All data is presented as the mean ± SEM values of three independent experiments. Statistical analyses were performed using Unpaired Student's T Test. GraphPad Prism version 6.0 software (GraphPad Software, California, USA) was used to analyze and

represent the data. Results were considered statistically significant if $p < 0.05$ (*), $p < 0.01$ (**), $p < 0.001$ (***), or $p < 0.0001$ (****).

3. Results

3.1. The specific PPRH against survivin decreases its mRNA levels

We performed a Functional Genomics study using full genome microarrays of the effects of a previously tested PPRH against the anti-apoptotic gene *survivin*. This refers to HpsPr-C-WT, a coding-PPRH that binds without mismatches to a polypririmidine target in the *survivin* promoter. The sequence and structure of this PPRH is shown in Table 1 as well as the negative control that forms a WC intramolecular hairpin and thus is unable to bind to the *survivin* target. The effect of the specific PPRH was compared with the effect caused by the negative control.
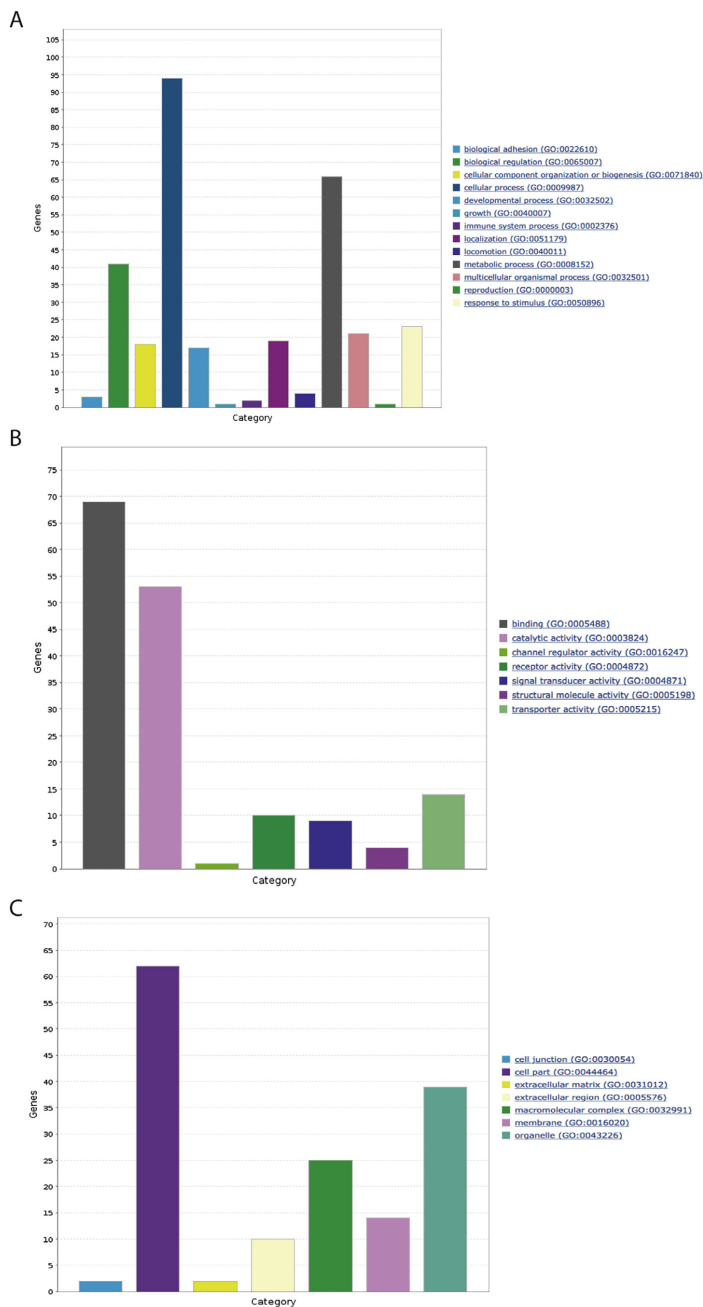
Fig. 3. Gene Ontology represented by PANTHER. Gene Ontology analyses of differentially expressed genes were classified by Gene Ontology divided into three different criteria: Biological process (A), Molecular function (B), and Cellular component (C). Data were plotted as bar charts using PANTHER (http://www.pantherdb.org/).

14

Table 5
Gene Set Enrichment Analysis (GSEA).

Gene set name	Gene set description	Number of genes in overlap	Gene list	p-value
Regulation of cell proliferation	Any process that modulates the frequency, rate or extent of cell proliferation	20	TRPV2, ADAMTS8, HAS2, PPARGC1A, IL5, MSX1, CREB3, TRIM71, APLN, SCGB1A1, FRK, CNOT6, PKHD1, MORC3, EIF5A, RXFP2, SERPINB5, GAS8 and PBRM1	$1.58\ e^{-30}$
Cellular response to stress	Any process that results in a change in state or activity of a cell as a result of a stimulus indicating the organism is under stress.	18	PLK2, RASSF1, SMC3, MYOF, SLCO1A2, HAS2, CREB3, NCOA6, VKORC1L1, GPS2, WNT9B, POLR2G, PPARGC1A, RFC2, RNF169, STAC, UBE2V2 and TMX3	$3.45\ e^{-27}$
Apoptosis	Genes up-regulated in ME-A cells (breast cancer) undergoing apoptosis in response to doxorubicin	18	PLK2, LLGL2, DGKQ, LITAF, SLC33A1, HAS2, SERPINB5, CIRBP, SF3A1, BAG1, GTPBP1, SLAIN1, PAK1IP1, SPON2, UBE2V2, METTL16, NAA35 and CAMP	$1.14\ e^{-29}$
Prostate cancer	Genes down-regulated in prostate cancer samples.	10	FLNA, FERMT2, MYOF, IL33, TPST1, PCDH9, SERPINB5, SC6B1A1, LAMA4 and COL4A2	$1.4\ e^{-18}$

GSEA of all differentially expressed genes after 24 h of incubation with HpsPr-C-WT in PC3 cells compared to cells treated with Hp-WC.

Before performing the microarray experiments, we verified the underexpression of *survivin* by RT-qPCR upon incubation with 100 nM of the specific PPRH HpsPr-C-WT at 24 h. *Survivin* mRNA levels were 55% when compared to the untreated control (Fig. 1). Moreover, the incubation with 100 nM of the negative control hairpin (Hp-WC) did not provoke any silencing effect on *survivin* mRNA levels.

3.2. The specific PPRH against survivin modulates gene expression

Microarrays were performed using Clariom-S Affymetrix chips corresponding to platform GPL23159. After scanning, the CEL files were analyzed with the software package included in GeneSpring GX v.14.9. Determination of differentially expressed genes was calculated after normalization as specified in M&M. The Principal Component Analysis (PCA) of the microarray results are shown in Fig. 2A.

First, the effect of the WC negative control hairpin (Hp-WC) was compared to the untreated control cells; and then the samples incubated with the specific PPRH against *survivin* (HpsPr-C-WT) for 24 h were compared to the WC negative control. The Volcano Plots of these analyses (Fig. 2B and C) revealed that Hp-WC did not provoke differentially expressed genes satisfying the $p < 0.05$ FC > 2, Benjamini-Hochberg filtering. On the other hand, HpsPr-C-WT brought about a number of differentially expressed genes shown in Table 2, depending of the cut-off used. In the case of FC > 2 and $p < 0.05$ this number was 244.

The 50 top underexpressed and overexpressed genes are listed separately in Tables 3 and 4, respectively.

3.3. The differentially expressed genes belong to the categories of cell proliferation, response to stress, apoptosis and prostate cancer

We analyzed, using different softwares, the list of the two-fold differentially expressed genes in PC3 cells treated for 24 h with HpsPr-C-WT to find functional relationships among the gene products. First, we carried out Gene Ontology analyses using the PANTHER classification system; results were presented according to Biological process, Molecular function, and Cellular component as shown, respectively, in Fig. 3, A, B, and C. Additionally, GSEA of all the differentially expressed genes ($p < 0.05$, FC > 2) after 24 h of incubation with HpsPr-C-WT was performed using the on line tool at the Broad Institute, obtaining as a result, with high statistical significance, the gene sets corresponding to Regulation of cell proliferation, Cellular response to stress, Apoptosis and Prostate cancer (Table 5).

The differentially expressed genes establish a network with interconnected gene nodes.

Additionally, STRING analyses of the differentially expressed genes were performed to reveal the genes that were the most interconnected using all known interactions (Fig. 4). A list of the gene-nodes that were highly statistically significant was obtained and the top 10 interrelated nodes are shown in Table 6. Interestingly, six gene-nodes (POLR2G, PAK1IP1, SMC3, SF3A1, PPARGC1A, NCOA6) were also present in the list identified in the GSEA.

3.4. PPRHs do not cause hepatotoxicity nor nephrotoxicity in vitro

Cell lines are a valuable tool to screen for cell toxicity mechanisms [37]. They have the potential to serve as the primary choice for toxicity screening of drugs since are convenient, cost and time efficient and involve no ethical issues [38]. Regarding oligonucleotides, there are clinical and preclinical adverse effects reported, including injury to the liver and kidneys, two primary organs of oligonucleotide accumulation [39]. For these reasons, aside from investigating the absence of off-target effects of an unspecific WC-hairpin, we also wanted to explore the possible effects on toxicity *in vitro* at the hepatic and renal levels. Therefore, a series of RT-qPCR arrays, profiling the expression of 84 key genes implicated as potential biomarkers of liver and renal toxicity,
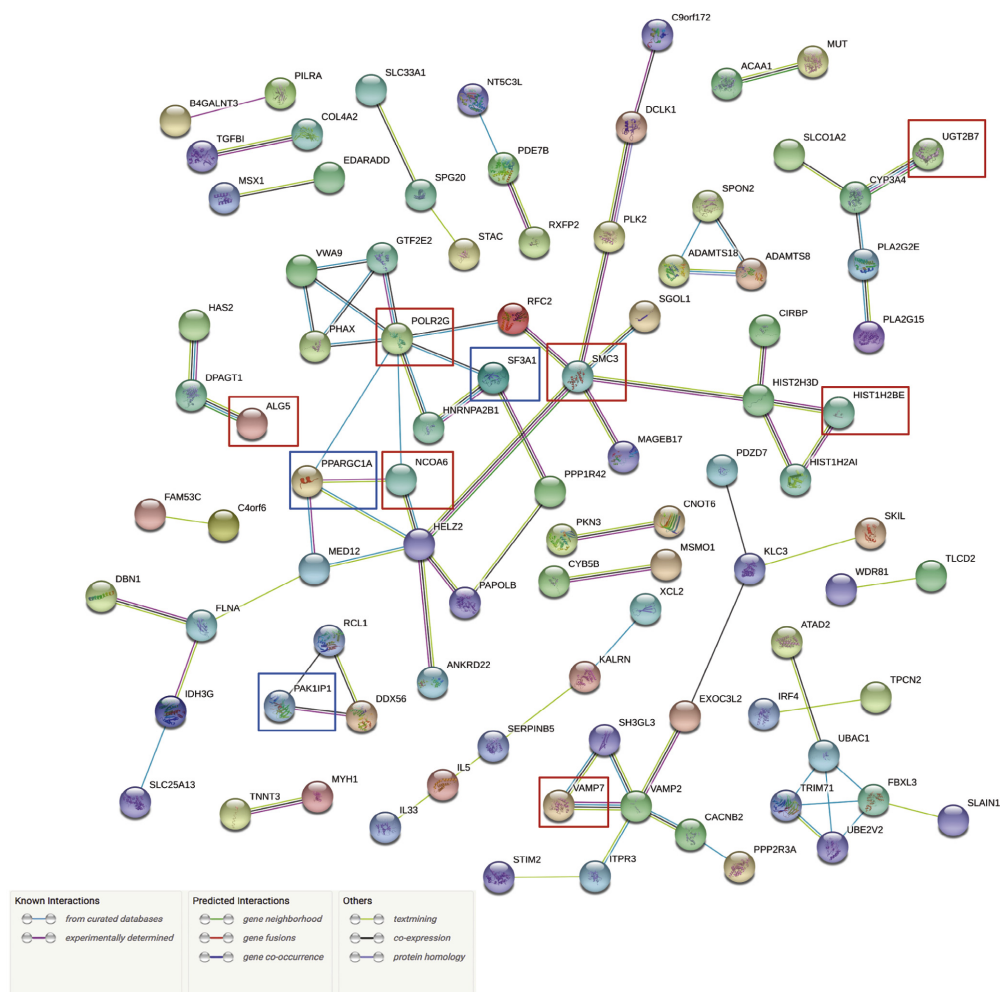
Fig. 4. Functional Protein Association Network. The list of differentially expressed genes after 24 h of incubation with HpsPr-C-WT (100 nM) in PC3 cells was subjected to network analyses using the STRING software. Overexpressed gene nodes are labeled with red frames and underexpressed gene nodes with blue. The minimum required interaction score was set at medium confidence (0.4). Other selected parameters were: average node degree: 0.771, average local clustering coefficient: 0.284 and active interaction sources including: neighborhood, gene fusion, co-occurrence, textmining, experiments, databases, co-expression and protein homology. Disconnected nodes in the network were not included. (For interpretation of the references to colour in this figure legend, the reader is referred to the web version of this article.)

were carried out using hepatic HepG2 and 786-O renal cells.

Cell viability was not affected when both cell lines were treated with 100 nM of the negative control hairpin Hp-WC up to 72 h (data not shown).

When determining gene expression by RT-qPCR arrays upon incubation with the negative control hairpin, Hp-WC, we observed that less than 6% of the genes were differentially expressed in the hepatic screening (Table 7) and less than 14% in the renal screening (Table 8), respectively. In the case of the hepatic screening less than 4% of the genes were overexpressed: EGR1, DUSP10 and XIAP. With regard to

renal 786-O cells, 7% of the genes represented in the RT-qPCR array were overexpressed: HMOX1, CD27, IL4, TLR9, GPR20 and SLC22A3.

4. Discussion

PolyPurine Reverse Hoogsteen hairpins represent a recent tool for gene silencing in gene therapy. PPRHs offer advantages since they show gene expression inhibition at lower concentration than that needed for aODNs or TFOs [40]. In addition, while working at a similar range of concentration [2] PPRHs have advantages over siRNAs taking into

16

Results

Table 6
Top 10 most interrelated nodes after STRING analysis.

Interrelated nodes		Combined score
GTF2E2 (−)	POLR2G (+)	0.993
CYP3A4 (+)	UGT2B7 (+)	0.988
DPAGT1 (+)	ALG5 (+)	0.986
VAMP2 (+)	VAMP7 (+)	0.979
HIST1H2AI (−)	HIST1H2BE (+)	0.973
PAK1IP1 (−)	DDX56 (+)	0.954
SMC3 (+)	SGOL1 (+)	0.941
HNRNPA2B1 (−)	SF3A1 (−)	0.936
MED12 (+)	PPARGC1A (−)	0.93
HELZ2 (+)	NCOA6 (+)	0.92

It is shown the top 10 nodes sorted by the highest combined scores for interaction sources (neighborhood, gene fusion, co-occurrence, textmining, experiments, databases, co-expression and protein homology) found in the Network represented in Fig. 4. (+) overexpressed genes; (−) underexpressed genes.

Table 7
RT-qPCR arrays in HepG2 cells.

RefSeq	Gene symbol	Gene name	Fold-change	p-value
NM_001167.3	XIAP	X-linked inhibitor of apoptosis	2.06	0.0140
NM_007207.4	DUSP10	dual specificity phosphatase 10	2.08	0.0230
NM_005633.3	SOS1	son of sevenless homolog 1 (Drosophila)	−2.05	0.0004
NM_001964.2	EGR1	early growth response 1	2.20	0.0050
NM_000392.4	ABCC2	ATP-binding cassette, sub-family C (CFTR/MRP), member 2	−2.37	0.0030

The genes with changes in mRNA expression satisfying FC > 2.0 and p < 0.05 out of the 84 genes present in the Hepatotoxicity RT-qPCR panel after 24 h of incubation of HepG2 cells with Hp-WC compared to the Control are shown.

Table 8
RT-qPCR arrays in 786-O cells.

RefSeq	Gene symbol	Gene name	Fold-change	p-value
NM_002133.2	HMOX1	heme oxygenase (decycling) 1	2.03	0.0020
NM_000576.2	IL1B	interleukin 1, beta	−5.43	0.0020
NM_000601.4	HGF	hepatocyte growth factor (hepapoietin A; scatter factor)	−4.21	0.0020
NM_001242.4	CD27	CD27 molecule	3.24	0.0400
NM_000589.3	IL4	interleukin 4	2.1	0.0450
NM_017442.3	TLR9	toll-like receptor 9	2.64	0.0450
NM_005293.2	GPR20	G protein-coupled receptor 20	4.17	0.0410
NM_000125.3	ESR1	estrogen receptor 1	−2.84	0.0020
NM_001031680.2	RUNX3	runt-related transcription factor 3	−4.42	0.0002
NM_024833.2	ZNF671	zinc finger protein 671	−2.9	0.0010
NM_021977.3	SLC22A3	solute carrier family 22 (organic cation transporter), member 3	2.64	0.0002

The genes with changes in mRNA expression satisfying FC > 2.0 and p < 0.05 out of the 84 genes present in the Nephrotoxicity RT-qPCR panel after 24 h of incubation of 786-O cells with Hp-WC compared to the Control are shown.

account their stability, economy and lack of immunogenicity [41].

We tested its efficiency in a growing number of genes in different cell lines *in vitro* [3,8] and also *in vivo* for the case of PPRHs against the antiapoptotic gene *survivin* [7]. However, their effect at the transcriptomic level had not been explored and the possible off-target effects had been studied only in a limited amount of genes [7].

Therefore, in this work we performed Functional Pharmacogenomics analyses to address the gene expression response to cellular incubation with either a specific PPRH against the *survivin* promoter or with its negative control counterpart. PC3 cells were selected because prostate cancer is the most frequent incident cancer in men and the second cause of cancer death [42]. In addition, the degree of *survivin* expression is related to the progression and aggressiveness of prostate cancer [43] and it mediates resistance to antiandrogen therapy [32], thus making *survivin* a good target for prostate cancer therapy. A first conclusion of our work is that the negative control hairpin Hp-WC did not originate differentially expressed genes when applying the p < 0.05, FC > 2, Benjamini-Hochberg filtering compared to control cells. This observation supports the idea that PPRHs do not promote significant off-target effects extending previous results obtained after analyzing five non-related genes chosen randomly [7]. On the other hand, when using the specific PPRH HpsPr-C-WT against survivin, 244 genes were differentially expressed vs the negative control hairpin when using the same filtering settings. These genes represent the transcriptomic response provoked by the silencing effect of the specific PPRH for *survivin*, which was confirmed by a TaqMan probe specifically devised for this gene.

The differentially expressed genes were classified by GO mainly into the categories of cellular and metabolic within biological processes; binding and catalytic activities within molecular function; and cell part and organelle within cellular component. The proapoptotic wave, among others, produced by *survivin* underexpression resulted in the alteration of gene sets belonging to regulation of cell proliferation, cellular response to stress, apoptosis and prostate cancer according to GSEA.

To investigate the possible relationships among the differentially expressed genes upon *survivin* underexpression, network analyses using STRING were performed identifying the top-ten pairs of gene-nodes. Among them, it is worth mentioning some important relationships: i) Regarding the gene-node *GTF2E2-POLR2G*, the general transcription factor GTF2E2 is essential for the formation and stabilization of the pre-initiation complex during transcription [44], thus it is directly related with the subunit G of the RNA polymerase II (*POLR2G*). ii) Histones (represented by the gene-node *HIST1H2AI-HIST1H2BE*) play also a vital role in chromosomal stability and transcription regulation. iii) In the case of the *PAK1IP1-DDX56* gene-node, PAK1IP1 negatively regulates PAK1 kinase which is involved in gene expression, cytoskeletal architecture, cellular apoptosis and neuronal cell growth [45] and *DDX56* encodes for a putative RNA helicase that participates in different cellular processes such as spliceosome assembly, nuclear and mitochondrial splicing and translation initiation [46]. iv) In the *SGOL1-SMC3* gene-node, SGOL1 prevents premature dissociation of the cohesin complex from centromeres after prophase [47] whereas SMC3 along with SMC1 prevents the premature separation of sister chromatids at the end of mitosis [48,49]. v) With regard to the *HNRNPA2B1-SF3A1* gene-node, *HNRNPA2B1* encodes for a heterogeneous nuclear ribonucleoprotein that associates with nascent pre-mRNAs [50] and SF3A1 is a subunit of the splicing factor SF3A required for the assembly of the A complex [51,52]. vi) When analyzing the *MED12-PPARGC1A* gene-node, it was found that MED12 is a component of the Mediator complex, which is recruited to promoters and serves as a scaffold for the assembly of a functional preinitiation complex with RNA polymerase II and the general transcription factors [53], and PPARGC1A acts as a transcriptional coactivator for steroid receptors and nuclear receptors [54]. vii) Finally, HELZ2 in the *HELZ2-NCOA6* gene-node is an helicase that acts as a transcriptional coactivator for a number of nuclear receptors including THRA, THRB, PPARA, PPARG, and RXRA [55,56] while NCOA6 is a nuclear receptor coactivator that directly binds to nuclear receptors such those for steroids, retinoids, thyroid hormone, vitamin D3 and prostanoids and stimulates the transcriptional activities in a hormone-dependent fashion [57,58]. In summary, all genes included in these gene-nodes are involved in genomic maintenance and

the regulation of transcriptional and splicing processes. Therefore, gene expression deregulation of this group of genes caused by the silencing of the antiapoptotic gene *survivin* with HpsPr-C-WT severely affect cell viability.

Cell culture based-methods offer a first option useful approach to evaluate the toxicological effects of a given compound, in well controllable conditions and lack of ethical limitations. Since liver and kidney are the two major sites for oligonucleotide accumulation, we explored the possible effects of PPRHs on toxicity *in vitro* at the hepatic and renal levels, using RT-qPCR arrays and hepatic HepG2 and 786-O renal cells. Our results indicate the absence of relevant toxicity in liver and kidney since 94 and 86%, respectively, of the genes present in the PCR arrays were not significantly affected at their expression levels upon cell incubation with Hp-WC.

In the case of the hepatic screening less than 4% of the genes were overexpressed, namely the EGR1 transcription factor which is induced in response to cytokines and growth factors, as well as environmental stress and tissue damage [59]. EGR1 contributes to the overexpression of TNFα and other proinflammatory genes during injury, but it also participates in the expression of genes involved in tissue repair [60]. Therefore, its expression could be either beneficial or damaging depending on the context. DUSP10 is a MAP kinase phosphatase that inactivates JNK/SAPK MAP kinases and p38 [61] and it is involved in the immune response during injuries [62]. DUSP10 expression protects against sepsis-induced acute lung injury [63]. SOS1 contributes to the exchange of Ras-bound GDP by GTP [64], probably by promoting Ras activation, and regulates phosphorylation of MAPK3 in response to EGF [65]. Finally, XIAP is also slightly overexpressed and it is a member of the IAP family that suppresses the proteolytic activity of caspase-3 and caspase-7, thus avoiding the apoptotic activity of these proteins [66].

With regard to renal 786-O cells, 7% of the genes represented in the RT-qPCR array were overexpressed. HMOX1 is a stress-responsive enzyme that degrades free heme, thus preventing its accumulation and the formation of free radicals [67]. In fact, the induction of HMOX1 promotes a cytoprotective response to oxidative stress in human fibroblasts [68] and human endothelial cells [69]. CD27 is a membrane receptor of the tumor necrosis factor receptor superfamily and promotes apoptosis when binding to the CD27-binding protein [70]. IL4 mainly participates in several B-cell activation processes [71] and it exerts as a co-stimulator of DNA synthesis [72]. However, IL1B, IL6, IL18 and IL10 were not differentially expressed in the RT-qPCR array. TLR9 belongs to the Toll-like receptors family that recognizes molecular DNA or RNA patterns specific to microorganisms and promotes the activation of the innate immunity. TLR9 recognizes CpG DNA and enhances its vesicular uptake [73]. Nonetheless, TLR2 and TLR4 expression was unaffected. GPR20 is a receptor that activates Gi proteins and it regulates cell proliferation by controlling intracellular cAMP levels [74]. Finally, SLC22A3 which is an organic cation transporter that plays an important role in the renal secretion of different cationic drugs and endogenous substances such as histamine, norepinephrine and dopamine [75] was overexpressed although SLC22A1, SLC22A2, SLC22A8, SLC31A1 and SLC47A1, also present in the RT-qPCR arrays, were not. It is important to emphasize that only a low percentage of genes were overexpressed in both hepatic and renal cell line models. However, those changes in gene expression did not cause any harmful effect in the viability of HepG2 and 786-O human cells.

In conclusion, we performed a functional pharmacogenomics analysis including GO, GSEA and Networking of the effect of a specific PPRH against the antiapoptotic gene *survivin*, previously validated both *in vitro* and *in vivo*. The negative control counterpart did not cause any effect on cell viability nor significant changes in gene expression. In addition, we determined the absence of cytotoxicity of hairpin incubation in HepG2 and 786-O cells and observed minor changes in gene expression using RT-qPCR arrays specifically developed for hepatotoxicity and nephrotoxicity screening. Therefore, this work set the basis for the development of PPRHs as innovative, target-specific and safe

drugs in pharmacology for cancer therapeutics.

Conflict of interest statement

The authors declare that they do not have any competing interests.

References

[1] K. Sridharan, N.J. Gogtay, Therapeutic nucleic acids: current clinical status, Br. J. Clin. Pharmacol. (2016) 659–672, http://dx.doi.org/10.1111/bcp.12987.

[2] M.C. de Almagro, S. Coma, V. Noé, C.J. Ciudad, Polypurine hairpins directed against the template strand of DNA knock down the expression of mammalian genes, J. Biol. Chem. 284 (2009) 11579–11589, http://dx.doi.org/10.1074/jbc.M900981200.

[3] C.J. Ciudad, L. Rodríguez, X. Villalobos, A.J. Félix, V. Noé, Polypurine reverse hoogsteen hairpins as a gene silencing tool for cancer, Curr. Med. Chem. 24 (2017) 2809–2826, http://dx.doi.org/10.2174/0929867324666170301114127.

[4] J.R. Goñi, X. de la Cruz, M. Orozco, Triplex-forming oligonucleotide target sequences in the human genome, Nucleic Acids Res. 32 (2004) 354–360, http://dx.doi.org/10.1093/nar/gkh188.

[5] N. Mencia, E. Selga, V. Noé, C.J. Ciudad, Underexpression of miR-224 in methotrexate resistant human colon cancer cells, Biochem. Pharmacol. 82 (2011) 1572–1582, http://dx.doi.org/10.1016/j.bcp.2011.08.009.

[6] G. Bener, A.J. Félix, C. Sánchez de Diego, I. Pascual Fabregat, C.J. Ciudad, V. Noé, Silencing of CD47 and SIRPα by Polypurine reverse Hoogsteen hairpins to promote MCF-7 breast cancer cells death by PMA-differentiated THP-1 cells, BMC Immunol. 17 (2016) 32, http://dx.doi.org/10.1186/s12865-016-0170-z.

[7] L. Rodríguez, X. Villalobos, S. Dakhel, L. Padilla, R. Hervas, J.L. Hernández, C.J. Ciudad, V. Noé, Polypurine reverse Hoogsteen hairpins as a gene therapy tool against survivin in human prostate cancer PC3 cells in vitro and in vivo, Biochem. Pharmacol. 86 (2013) 1541–1554, http://dx.doi.org/10.1016/j.bcp.2013.09.013.

[8] X. Villalobos, L. Rodríguez, A. Solé, C. Lliberós, N. Mencia, C.J. Ciudad, V. Noé, Effect of polypurine reverse hoogsteen hairpins on relevant cancer target genes in different human cell lines, Nucleic Acid Ther. 25 (2015) 198–208, http://dx.doi.org/10.1089/nat.2015.0531.

[9] M.C. de Almagro, N. Mencia, V. Noé, C.J. Ciudad, Coding polypurine hairpins cause target-induced cell death in breast cancer cells, Hum. Gene Ther. 22 (2011) 451–463, http://dx.doi.org/10.1089/hum.2010.102.

[10] C. Oleaga, S. Welten, A. Belloc, A. Solé, L. Rodriguez, N. Mencia, E. Selga, A. Tapias, V. Noé, C.J. Ciudad, Identification of novel Sp1 targets involved in proliferation and cancer by functional genomics, Biochem. Pharmacol. 84 (2012) 1581–1591, http://dx.doi.org/10.1016/j.bcp.2012.09.014.

[11] M.C. de Almagro, S. Coma, V. Noe, C.J. Ciudad, Polypurine hairpins directed against the template strand of DNA knock down the expression of mammalian genes, J. Biol. Chem. 284 (2009) 11579–11589, http://dx.doi.org/10.1074/jbc.M900981200.

[12] G. Ambrosini, C. Adida, D.C. Altieri, A novel anti-apoptosis gene, survivin, expressed in cancer and lymphoma, Nat. Med. 4 (1996) 303–308, http://dx.doi.org/10.1038/nm0798-822.

[13] R. Gianani, E. Jarboe, D. Orlicky, M. Frost, J. Bobak, R. Lehner, K.R. Shroyer, Expression of survivin in normal, hyperplastic, and neoplastic colonic mucosa, Hum. Pathol. 32 (2001) 119–125, http://dx.doi.org/10.1053/hupa.2001.21897.

[14] B.Z. Carter, M. Milella, D.C. Altieri, M. Andreeff, Cytokine-regulated expression of survivin in myeloid leukemia cytokine-regulated expression of survivin in myeloid leukemia, Neoplasia 97 (2009) 2784–2790, http://dx.doi.org/10.1182/blood.V97.9.2784.

[15] K.-T. Kiu, T.I.S. Hwang, H.-Y. Hsieh, C.-H. Shen, Y.-H. Wang, G.-D. Juang, Expression of survivin in bladder cancer cell lines using quantitative real-time polymerase chain reaction, Urol. Sci. 25 (2014) 19–21, http://dx.doi.org/10.1016/j.urols.2013.11.002.

[16] G. Kapellos, K. Polonifi, D. Farmakis, E. Spartalis, P. Tomos, A. Aessopos, A. Polizos, M. Mantzourani, Overexpression of survivin levels in circulation and tissue samples of lung cancer patients, Anticancer Res. 3480 (2013) 3475–3480.

[17] M. Falleni, C. Pellegrini, A. Marchetti, B. Oprandi, F. Buttitta, F. Barassi, L. Santambrogio, G. Coggi, S. Bosari, Survivin gene expression in early-stage non-small cell lung cancer, J. Pathol. 200 (2003) 620–626, http://dx.doi.org/10.1002/path.1388.

[18] J.M. Hernandez, J.M. Farma, D. Coppola, A. Hakam, W.J. Fulp, D.T. Chen, E.M. Siegel, T.J. Yeatman, D. Shibata, Expression of the antiapoptotic protein survivin in colon cancer, Clin. Colorectal Cancer 10 (2011) 188–193, http://dx.doi.org/10.1016/j.clcc.2011.03.014.

[19] A. Krieg, T.A. Werner, P.E. Verde, N.H. Stoecklein, W.T. Knoefel, Prognostic and clinicopathological significance of survivin in colorectal cancer: a meta-analysis,

PLoS One 8 (2013) 1–8, http://dx.doi.org/10.1371/journal.pone.0065338.

[20] J.-G. Qiao, Y.-Q. Zhang, Y.-C. Yin, Z. Tan, Expression of Survivin in pancreatic cancer and its correlation to expression of Bcl-2, World J. Gastroenterol. 10 (2004) 2759–2761 http://www.ncbi.nlm.nih.gov/pubmed/15309737.

[21] H. Dong, D. Qian, Y. Wang, L. Meng, D. Chen, X. Ji, W. Feng, Survivin expression and serum levels in pancreatic cancer, World J. Surg. Oncol. 13 (2015) 189, http://dx.doi.org/10.1186/s12957-015-0605-7.

[22] C. Cohen, C.M. Lohmann, G. Cotsonis, D. Lawson, R. Santoianni, Survivin expression in ovarian carcinoma: correlation with apoptotic markers and prognosis, Mod. Pathol. 16 (2003) 574–583, http://dx.doi.org/10.1097/01.MP.0000073868.31297.B0.

[23] S. Peroukides, V. Bravou, A. Alexopoulos, J. Varakis, H. Kalofonos, H. Papadaki, Survivin overexpression in HCC and liver cirrhosis differentially correlates with p-STAT3 and E-cadherin, Histol. Histopathol. 25 (2010) 299–307.

[24] M. Katoh, R. Wilmotte, M.C. Belkouch, N. De Tribolet, G. Pizzolato, P.Y. Dietrich, Survivin in brain tumors: an attractive target for immunotherapy, J. Neurooncol. 64 (2003) 71–76, http://dx.doi.org/10.1023/A:1024942127462.

[25] X.-D. Zhu, G.-J. Lin, L.-P. Qian, Z.-Q. Chen, Expression of survivin in human gastric carcinoma and gastric carcinoma model of rats, World J. Gastroenterol. 9 (2003) 1435–1438 http://www.ncbi.nlm.nih.gov/pubmed/12854136.

[26] M. Adamkov, L. Lauko, J. Rajčáni, S. Bálentová, S. Rybárová, D. Mištuna, D. Statelová, Expression of antiapoptotic protein survivin in malignant melanoma, Biologia (Bratisl.) 64 (2009) 840–844, http://dx.doi.org/10.2478/s11756-009-0134-3.

[27] J.A. Mckenzie, D. Grossman, Role of the apoptotic and mitotic regulator survivin in melanoma, Anticancer Res. 32 (2012) 397–404.

[28] A. Mori, H. Wada, Y. Nishimura, T. Okamoto, Y. Takemoto, E. Kakishita, Expression of the antiapoptosis gene survivin in human leukemia, Int. J. Hematol. 75 (2002) 161–165, http://dx.doi.org/10.1007/s00737-002-0148-0.

[29] Z. Khan, A.A. Khan, H. Yadav, G.B.K.S. Prasad, P.S. Bisen, Survivin, a molecular target for therapeutic interventions in squamous, cell carcinoma (2017) 1–32, http://dx.doi.org/10.1186/s11658-017-0038-0.

[30] M. Zhang, J.J. Coen, Y. Suzuki, M.R. Siedow, A. Niemierko, L.-Y. Khor, A. Pollack, Y. Zhang, A.L. Zietman, W.U. Shipley, A. Chakravarti, Survivin is a potential mediator of prostate cancer metastasis, Int. J. Radiat. Oncol. Biol. Phys. 78 (2010) 1095–1103, http://dx.doi.org/10.1016/j.ijrobp.2009.09.007.

[31] L. Zhang, Y. Ye, D. Yang, J. Lin, Survivin and vascular endothelial growth factor are associated with spontaneous pulmonary metastasis of osteosarcoma: development of an orthotopic mouse model, Oncol. Lett. 8 (2014) 2577–2580, http://dx.doi.org/10.3892/ol.2014.2556.

[32] M. Zhang, D.E. Latham, M.A. Delaney, A. Chakravarti, Survivin mediates resistance to antiandrogen therapy in prostate cancer, Oncogene 24 (2005) 2474–2482, http://dx.doi.org/10.1038/sj.onc.1208490.

[33] M. Zhang, N. Mukherjee, R.S. Bermudez, D.E. Latham, M.A. Delaney, A.L. Zietman, W.U. Shipley, A. Chakravarti, Adenovirus-mediated inhibition of survivin expression sensitizes human prostate cancer cells to paclitaxel in vitro and in vivo, Prostate 64 (2005) 293–302, http://dx.doi.org/10.1002/pros.20263.

[34] H. Mi, X. Huang, A. Muruganujan, H. Tang, C. Mills, D. Kang, P.D. Thomas, PANTHER version 11: expanded annotation data from gene ontology and reactome pathways and data analysis tool enhancements, Nucleic Acids Res. 45 (2017) 183–189, http://dx.doi.org/10.1093/nar/gkw1138.

[35] A. Subramanian, P. Tamayo, V.K. Mootha, S. Mukherjee, B.L. Ebert, M.A. Gillette, A. Paulovich, S.L. Pomeroy, T.R. Golub, E.S. Lander, J.P. Mesirov, Gene set enrichment analysis: A knowledge-based approach for interpreting genome-wide expression profiles, Proc. Natl. Acad. Sci. 102 (2005) 15545–15550, http://dx.doi.org/10.1073/pnas.0506580102.

[36] D. Szklarczyk, J.H. Morris, H. Cook, M. Kuhn, S. Wyder, M. Simonovic, A. Santos, N.T. Doncheva, A. Roth, P. Bork, L.J. Jensen, C. von Mering, The STRING database in, quality-controlled protein-protein association networks, made broadly accessible, Nucleic Acids Res. 45 (2017) (2017) D362–D368, http://dx.doi.org/10.1093/nar/gkw937.

[37] D.D. Allen, R. Caviedes, A.M. Cárdenas, T. Shimahara, J. Segura-Aguilar, P.A. Caviedes, Cell lines as in vitro models for drug screening and toxicity studies, Drug Dev. Ind. Pharm. 31 (2005) 757–768, http://dx.doi.org/10.1080/03639040500216246.

[38] R. Zang, D. Li, I.-C. Tang, J. Wang, S.-T. Yang, Cell-based assays in high-throughput screening for drug discovery, Int. J. Biotechnol. Wellness Ind. 1 (2012) 31–51, http://dx.doi.org/10.6000/1927-3037.2012.01.01.02.

[39] K.S. Frazier, Antisense oligonucleotide therapies: the promise and the challenges from a toxicologic pathologist's perspective, Toxicol. Pathol. 43 (2015) 78–89, http://dx.doi.org/10.1177/0192623314551840.

[40] L. Rodríguez, X. Villalobos, A. Solé, C. Lliberós, C.J. Ciudad, V. Noé, Improved design of PPRHs for gene silencing, Mol. Pharm. 12 (2015) 867–877, http://dx.doi.org/10.1021/mp5007008.

[41] X. Villalobos, L. Rodríguez, J. Prévot, C. Oleaga, C.J. Ciudad, V. Noé, Stability and immunogenicity properties of the gene-silencing polypurine reverse hoogsteen hairpins, Mol. Pharm. 11 (2014) 254–264, http://dx.doi.org/10.1021/mp400431f.

[42] A. Jemal, E.M. Ward, C.J. Johnson, K.A. Cronin, J. Ma, A.B. Ryerson, A. Mariotto, A.J. Lake, R. Wilson, R.L. Sherman, R.N. Anderson, S.J. Henley, B.A. Kohler, L. Penberthy, E.J. Feuer, H.K. Weir, Annual report to the nation on the status of cancer, 1975–2014, featuring survival, J. Natl. Cancer Inst. 109 (2017) 1–22, http://dx.doi.org/10.1093/jnci/djx030.

[43] H. Kishi, M. Igawa, N. Kikuno, T. Yoshino, S. Urakami, H. Shiina, Expression of the survivin gene in prostate cancer: correlation with clinicopathological characteristics, proliferative activity and apoptosis, J. Urol. 171 (2004) 1855–1860, http://dx.doi.org/10.1097/01.ju.0000120317.88372.03.

[44] Y. He, J. Fang, T.J. Dylan, E. Nogales, Structural visualization of key steps in human transcription initiation, Nature 495 (2013) 481–486, http://dx.doi.org/10.1038/nature11991.Structural.

[45] C. Xia, W. Ma, L.J. Stafford, S. Marcus, W.C. Xiong, M. Liu, Regulation of the p21-activated kinase (PAK) by a human Gbeta-like WD-repeat protein, hPIP1, Proc. Natl. Acad. Sci. U.S.A. 98 (2001) 6174–6179, http://dx.doi.org/10.1073/pnas.101137298.

[46] R.F. Zirwes, J. Eilbracht, S. Kneissel, M.S. Schmidt-Zachmann, A novel helicase-type protein in the nucleolus: protein NOH61, Mol. Biol. Cell. 11 (2000) 1153–1167, http://dx.doi.org/10.1091/MBC.11.4.1153.

[47] B.E. McGuinness, T. Hirota, N.R. Kudo, J.M. Peters, K. Nasmyth, Shugoshin prevents dissociation of cohesin from centromeres during mitosis in vertebrate cells, PLoS Biol. 3 (2005) 0433–0449, http://dx.doi.org/10.1371/journal.pbio.0030086.

[48] D.E. Koshland, V. Guacci, Sister chromatid cohesion: the beginning of a long and beautiful relationship, Curr. Opin. Cell Biol. 12 (2000) 297–301, http://dx.doi.org/10.1016/S0955-0674(00)00092-2.

[49] F. Uhlmann, Chromosome cohesion in mitosis and meiosis, Curr. Opin. Cell Biol. 13 (2001) 754–761, http://dx.doi.org/10.1242/jcs.03324.

[50] Y. He, R. Smith, Nuclear functions of heterogeneous nuclear ribonucleoproteins A/B, Cell. Mol. Life Sci. 66 (2009) 1239–1256, http://dx.doi.org/10.1007/s00018-008-8532-1.

[51] O. Gozani, R. Feld, R. Reed, Evidence that sequence-independent binding of highly conserved U2 snRNP proteins upstream of the branch site is required for assembly of spliceosomal complex A, Genes Dev. 10 (1996) 233–243, http://dx.doi.org/10.1101/gad.10.2.233.

[52] S. Bessonov, M. Anokhina, C.L. Will, H. Urlaub, R. Lührmann, Isolation of an active step I spliceosome and composition of its RNP core, Nature 452 (2008) 846–850, http://dx.doi.org/10.1038/nature06842.

[53] R.A. Philiber, A. Madan, Role of MED12 in transcription and human behavior, Pharmacogenomics 8 (2007) 909, http://dx.doi.org/10.2217/14622416.8.8.909.

[54] J. Lin, C. Handschin, B.M. Spiegelman, Metabolic control through the PGC-1 family of transcription coactivators, Cell Metab. 1 (2005) 361–370, http://dx.doi.org/10.1016/j.cmet.2005.05.004.

[55] S. Surapureddi, S. Yu, H. Bu, T. Hashimoto, A.V. Yeldandi, P. Kashireddy, M. Cherkaoui-Malki, C. Qi, Y.-J. Zhu, M.S. Rao, J.K. Reddy, Identification of a transcriptionally active peroxisome proliferator-activated receptor-interacting cofactor complex in rat liver and characterization of PRIC285 as a coactivator, Proc. Natl. Acad. Sci. 99 (2002) 11836–11841, http://dx.doi.org/10.1073/pnas.182426699.

[56] T. Tomaru, T. Satoh, S. Yoshino, T. Ishizuka, K. Hashimoto, T. Monden, M. Yamada, M. Mori, Isolation and characterization of a transcriptional cofactor and its novel isoform that bind the deoxyribonucleic acid-binding domain of peroxisome proliferator-activated receptor-γ, Endocrinology 147 (2006) 377–388, http://dx.doi.org/10.1210/en.2005-0450.

[57] S.K. Lee, S.L. Anzick, J.E. Choi, L. Bubendorf, X.Y. Guan, Y.K. Jung, O.P. Kallioniemi, J. Kononen, J.M. Trent, D. Azorsa, B.H. Jhun, J.H. Cheong, Y.C. Lee, P.S. Meltzer, J.W. Lee, A nuclear factor, ASC-2, as a cancer-amplified transcriptional coactivator essential for ligand-dependent transactivation by nuclear receptors in vivo, J. Biol. Chem. 274 (1999) 34283–34293, http://dx.doi.org/10.1074/jbc.274.48.34283.

[58] M.A. Mahajan, H.H. Samuels, A new family of nuclear receptor coregulators that integrate nuclear receptor signaling through CREB-binding protein, Mol. Cell. Biol. 20 (2000) 5048–5063, http://dx.doi.org/10.1128/MCB.20.14.5048-5063.2000.

[59] M.R. McMullen, M.T. Pritchard, Q. Wang, C.A. Millward, C.M. Croniger, L.E. Nagy, Early growth response-1 transcription factor is essential for ethanol-induced fatty liver injury in mice, Gastroenterology 128 (2005) 2066–2076, http://dx.doi.org/10.1037/a0015862.Trajectories.

[60] M.T. Pritchard, J.I. Cohen, S. Roychowdhury, B.T. Pratt, L.E. Nagy, Early growth response-1 attenuates liver injury and promotes hepatoprotection after carbon tetrachloride exposure in mice Michele, J. Hepatol. 53 (2010) 655–662, http://dx.doi.org/10.1038/nature10188.De.

[61] A. Theodosiou, A. Smith, C. Gillieron, S. Arkinstall, A. Ashworth, MKP5, a new member of the MAP kinase phosphatase family, which selectively dephosphorylates stress-activated kinases, Oncogene 18 (1999) 6981–6988, http://dx.doi.org/10.1038/sj.onc.1203185.

[62] Y. Zhang, J.N. Blattman, N.J. Kennedy, J. Duong, T. Nguyen, Y. Wang, R.J. Davis, P.D. Greenberg, R.A. Flavell, C. Dong, Regulation of innate and adaptive immune responses by MAP kinase, Nature 430 (2004) 793–797, http://dx.doi.org/10.1038/nature02775.1.

[63] F. Qian, J. Deng, B.N. Gantner, R.A. Flavell, C. Dong, J.W. Christman, R.D. Ye, Map kinase phosphatase 5 protects against sepsis-induced acute lung injury, Am. J. Physiol. Lung Cell Mol. Physiol. 302 (2012) L866–74, http://dx.doi.org/10.1152/ajplung.00277.2011.

[64] P. Chardin, J.H. Camonis, N.W. Gale, L. van Aelst, J. Schlessinger, M.H. Wigler, D. Bar-Sagi, Human Sos1: a guanine nucleotide exchange factor for Ras that binds to GRB2, Science. 260 (1993) 1338–1343, http://dx.doi.org/10.1126/science.8493579.

[65] K. Modzelewska, M.G. Elgort, J. Huang, G. Jongeward, A. Lauritzen, C.H. Yoon, P.W. Sternberg, N. Moghal, An activating mutation in sos-1 identifies its Dbl domain as a critical inhibitor of the epidermal growth factor receptor pathway during Caenorhabditis elegans vulval development, Mol. Cell. Biol. 27 (2007) 3695–3707, http://dx.doi.org/10.1128/MCB.01630-06.

[66] Q.L. Deveraux, R. Takahashi, G.S. Salvesen, J.C. Reed, X-linked IAP is a direct inhibitor of cell-death proteases, Nature 388 (1997) 300–304, http://dx.doi.org/10.1038/40901.

[67] M.P. Soares, F.H. Bach, Heme oxygenase-1: from biology to therapeutic potential,

19

84

Trends Mol. Med. 15 (2009) 50–58, http://dx.doi.org/10.1016/j.molmed.2008.12.004.

[68] G.F. Vile, S. Basu-Modak, C. Waltner, R.M. Tyrrell, Heme oxygenase 1 mediates an adaptive response to oxidative stress in human skin fibroblasts, Proc. Natl. Acad. Sci. 91 (1994) 2607–2610, http://dx.doi.org/10.1073/pnas.91.7.2607.

[69] G. Balla, H.S. Jacob, J. Balla, M. Rosenberg, K. Nath, F. Apple, J.W. Eaton, G.M. Vercellotti, Ferritin: a cytoprotective antioxidant strategem of endothelium, J. Biol. Chem. 267 (1992) 18148–18153.

[70] K.V.S. Prasad, Z. Ao, Y. Yoon, M.X. Wu, M. Rizk, S. Jacquot, S.F. Schlossman, CD27, a member of the tumor necrosis factor receptor family, induces apoptosis and binds to Siva, a proapoptotic protein, Immunology 94 (1997) 6346–6351, http://dx.doi.org/10.1073/pnas.94.12.6346.

[71] J.S. Rush, P.D. Hodgkin, B cells activated via CD40 and IL-4 undergo a division burst but require continued stimulation to maintain division, survival and differentiation, Eur. J. Immunol. 31 (2001) 1150–1159, http://dx.doi.org/10.1002/1521-4141(200104)31:4<1150::AID-IMMU1150>3.0.CO;2-V.

[72] M. Carlsson, C. Sundström, M. Bengtsson, T.H. Tütterman, A. Rosén, K. Nilsson, Interleukin 4 strongly augments or inhibits DNA synthesis and differentiation of B-type chronic lymphocytic leukemia cells depending on the costimulatory activation and progression signals, Eur. J. Immunol. 19 (1989) 913–921, http://dx.doi.org/10.1002/eji.1830190519.

[73] F. Takeshita, C.A. Leifer, I. Gursel, K.J. Ishii, S. Takeshita, M. Gursel, D.M. Klinman, Cutting edge: role of toll-like receptor 9 in CpG DNA-induced activation of human cells, J. Immunol. 167 (2001) 3555–3558, http://dx.doi.org/10.4049/jimmunol.167.7.3555.

[74] M. Hase, T. Yokomizo, T. Shimizu, M. Nakamura, Characterization of an orphan G protein-coupled receptor, GPR20, that constitutively activates Gi proteins, J. Biol. Chem. 283 (2008) 12747–12755, http://dx.doi.org/10.1074/jbc.M709487200.

[75] X. Wu, W. Huang, M.E. Ganapathy, H. Wang, R. Kekuda, S.J. Conway, F.H. Leibach, V. Ganapathy, Structure, function and regional distribution of the organic cation transporter OCT3 in the kidney, Am. J. Physiol. Physiol. 279 (2000) 449–458.

Results

4.2. Article II:

Silencing of CD47 and SIRPα by PolyPurine Reverse Hoogsteen hairpins to promote MCF7 breast cancer cells death by PMA-differentiated THP-1 cells

Gizem Bener*, Alex J. Félix*, Cristina Sánchez de Diego, Isabel Pascual Fabregat, Carlos J. Ciudad and Véronique Noé

*These authors contributed equally to this work

Background: It is known that cancer cells can overexpress CD47, an anti-phagocytic or "don't eat me" signal that interacts with the SIRPα receptor located in macrophages to escape from phagocytosis. Therefore, the blockade of CD47/SIRPα interaction has emerged as an alternative immunotherapy approach to stimulate the elimination of tumor cells by the host's immune system.

Objectives: To silence the expression of *CD47* in MCF7 breast cancer cells and SIRPα in macrophages using PPRHs to trigger the elimination of tumor cells by macrophages in co-culture experiments.

Results: We corroborated that THP-1 cells were differentiated to macrophages after treatment with PMA by analyzing at the mRNA level, using RT-qPCR, both macrophage surface markers (CD14 and MCL-1) and pro-inflammatory cytokines (IL-1β, IL-18, IL-6, IL-8 and TNF-α). The incubation of MCF7 cancer cells with two PPRHs designed against the *CD47* gene led to a 60% decrease in CD47 mRNA levels. Likewise, the incubation of THP-1 cells with two PPRHs designed against the *SIRPα* gene led to a 55% decrease in SIRPα mRNA levels. Moreover, both CD47 and SIRPα protein levels in MCF7 and THP-1 cells, respectively, were highly decreased after the treatment with their respective PPRHs. In the MCF7/macrophage co-culture experiments, the transfection of either MCF7 or THP-1 cells with a PPRH against *CD47* or *SIRPα*, respectively, led to a reduction on cell viability of 60%. However, the transfection of PPRHs against *CD47* and *SIRPα* in both MCF7 and THP-1 cells, respectively,

showed a 70% decrease on cell viability. Finally, we demonstrated that the detrimental effect on cell viability was obtained due to a 3-fold increase in the apoptosis level.

Conclusions: The usage of PPRHs to silence both the *CD47* and *SIRPα* genes to diminish the CD47/SIRPα interaction led to an enhanced killing of MCF7 cancer cells by macrophages in co-culture experiments, thus indicating that PPRHs could represent an alternative immunotherapy approach.

BMC Immunology

RESEARCH ARTICLE   **Open Access**

CrossMark

Silencing of CD47 and SIRPα by Polypurine reverse Hoogsteen hairpins to promote MCF-7 breast cancer cells death by PMA-differentiated THP-1 cells

Gizem Bener[†], Alex J. Félix[†], Cristina Sánchez de Diego, Isabel Pascual Fabregat, Carlos J. Ciudad and Véronique Noé[*]

Abstract

Background: In the context of tumor immunology, tumor cells have been shown to overexpress CD47, an anti-phagocytic signal directed to macrophages to escape from phagocytosis by interacting with Signal Regulatory Protein α SIRPα.
In the present work, we designed Polypurine reverse Hoogsteen hairpins, PPRHs, to silence the expression of CD47 in tumor cells and SIRPα in macrophages with the aim to eliminate tumor cells by macrophages in co-culture experiments.

Methods: THP-1 cells were differentiated to macrophages with PMA. The mRNA levels of differentiation markers CD14 and Mcl-1 mRNA and pro-inflammatory cytokines (IL-1β, IL-18, IL-6, IL-8 and TNF-α) were measured by qRT-PCR. The ability of PPRHs to silence *CD47* and *SIRPα* was evaluated at the mRNA level by qRT-PCR and at the protein level by Western Blot. Macrophages were co-cultured with tumor cells in the presence of PPRHs to silence CD47 and/or SIRPα. Cell viability was assessed by MTT assays.

Results: THP-1 cells differentiated to macrophages with PMA showed an increase in macrophage surface markers (CD14, Mcl-1) and pro-inflammatory cytokines (IL-1β, IL-18, IL-6, IL-8 and TNF-α). PPRHs were able to decrease both CD47 expression in MCF-7 cell line and SIRPα expression in macrophages at the mRNA and protein levels. In the presence of PPRHs, MCF-7 cells were eliminated by macrophages in co-culture experiments, whereas they survived in the absence of PPRHs.

Conclusions: Our data support the usage of PPRHs to diminish CD47/SIRPα interaction by decreasing the expression of both molecules thus resulting in an enhanced killing of MCF-7 cells by macrophages, which might translate into beneficial effects in cancer therapy. These results indicate that PPRHs could represent a new approach with immunotherapeutic applications.

Keywords: Immunotherapy, PPRH, CD47, SIRPα, Macrophage

* Correspondence: vnoe@ub.edu
[†]Equal contributors
Department of Biochemistry and Molecular Biology, School of Pharmacy,
University of Barcelona, IN2UB, Barcelona, Spain

BioMed Central

Background

The identification and elimination of tumor cells by the immune system on the basis of expression of tumor-specific antigens is the general concept of tumor immune surveillance which was first discussed over a century ago [1]. The critical components of the immune system involved in tumor elimination are macrophages.

Macrophage cytotoxicity in tumors can be mediated by cytokines such as tumor necrosis factor (TNF), by direct phagocytosis or combination of both [2], although primary elimination of tumor cells by macrophages occurs via phagocytosis [3]. The mechanism of tumor elimination by macrophage phagocytosis relies on distinguishing non-self molecules from self-molecules. There are several mechanisms to prevent macrophages from reacting to own tissues and there are also several mechanisms to trigger phagocytosis against tumor cells. These processes are achieved by many of the molecules and signaling pathways involved in macrophage recognition. When the specific identification of tumor cells by macrophages fails, cancer cells can evade elimination by the immune system, which has been shown as one of the hallmarks of cancer [4].

Recently, phagocytosis has been described as the result of balance between pro-phagocytic and anti-phagocytic ligands. In the last 10 years, studies have identified the large variety of pro-phagocytic molecules expressed by human tumors to induce phagocytosis and allow the immune system to eradicate them. However, a recent and promising anti-phagocytic molecule is CD47, which serves as a signal to avoid the macrophage phagocytosis when interacting its receptor Signal Regulatory Protein α (SIRPα) on macrophages [5–7].

CD47 or integrin associated protein, is an ubiquitously expressed cell surface protein in the immunoglobulin superfamily that binds many different proteins including integrins and thrombospondin-1, and it is associated with variable physiological processes including cell migration, neuronal development and T cell activation [8, 9]. CD47 consists of a highly glycosylated extracellular immunoglobulin variable (IgV) domain, a hydrophobic five transmembrane domain and an intracellular domain [10].

Poels et al. first identified CD47 as a tumor antigen on human ovarian cancer in 1986 [11]. Since then, many different human tumor types such as myeloid leukemia, non-Hodgkin's lymphoma, bladder cancer and other solid tumors have also been found to express CD47 [8]. CD47 is widely expressed on all cell types although tumor cells have increased levels of CD47 expression compared to normal cells, which turns into a mechanism by which tumor cells can evade phagocytosis.

CD47 functions as an inhibitor of phagocytosis, since its interaction with its receptor SIRPα in macrophages leads tumor cells to be recognized as self-molecules. The interaction of CD47 with SIRPα results in the phosphorylation of immune receptor tyrosine-based inhibition motifs on SIRPα cytoplasmic tail and leads to the accumulation of myosin-IIA at the phagocytic synapse by the recruitment of Src homology phosphatase-1 and 2, which inhibit phagocytosis function [12]. Cells that display lower levels of CD47 are primed for removal, whereas cells expressing elevated levels of CD47 are resistant to clearance.

Given the importance of SIRPα-CD47 interaction for tumor growth, CD47 has been used as a validated target for cancer therapies [8]. In this study, we used Polypurine reverse Hoogsteen hairpins (PPRHs) as a gene silencing tool to decrease CD47 in tumor cells and SIRPα in PMA-differentiated THP-1 cells with the aim to decrease their interaction and to eliminate tumor cells.

PPRHs are non-modified DNA molecules formed by two antiparallel polypurine stretches. These stretches are linked by a 5-thymidine loop and the intramolecular linkage consists of reverse Hoogsteen bonds between adenine and guanine of two antiparallel stretches. When PPRHs bind their polypyrimidine target sequence by Watson-Crick bonds, they form a triplex structure, which results in the displacement of the fourth strand of the dsDNA [13, 14]. Two types of PPRHs have been described depending on the location of their target in template or coding DNA strands [15]. PPRHs bound to the template DNA strand interfere and inhibit transcription, thus decrease the mRNA and protein levels of the target gene, whereas PPRHs against the coding DNA strand are able to bind both to the coding strand of DNA and to the mRNA, since they have the same sequence and orientation [15]. PPRHs, despite performing a similar function than siRNA, do not activate the innate inflammatory response and they have demonstrated a longer half-life in mouse, human and fetal calf serum as well as in in vitro cell lines compared to siRNAs [16].

Due to the lack of purity and the limited availability of primary tissue macrophages, the THP-1 cell line is commonly used as a model of macrophages, since it resembles primary monocytes in morphology and differentiation properties [17–20]. To differentiate monocytic cell lines to macrophages, THP-1 cells are treated with PMA, which is a well-studied differentiation-inducing chemical and acts as an analog of diacyl glycerol [21]. PMA activates protein kinase C, and triggers serine/threonine kinases involved in the regulation of cellular proliferation, survival and differentiation [22, 23].

The aims of this study were: to decrease the levels of CD47 in tumor cells and SIRPα level in PMA-differentiated THP-1 cells with PPRHs and ultimately to eliminate tumor cells by macrophages by diminishing the CD47/SIRPα interaction in co-culture experiments.

Methods

Cell culture and PMA induced differentiation

Human acute monocytic leukemia THP-1, breast adenocarcinoma MCF-7 cell lines were used throughout the experiments.

Cell lines were grown in Ham's F-12 medium supplemented with 7 % fetal bovine serum (FBS, both from GIBCO, Invitrogen) at 37 °C in a humidified 5 % CO2 atmosphere. Trypsinization of MCF-7 cells was performed using 0,05 % Trypsin in PBS 1× (154 mM NaCl, 3,88 mM H_2NaPO_4, 6,1 mM $HNaPO_4$, pH 7,4). Subculture of THP-1 was performed without trypsinization depending on cell density. For differentiation, THP-1 cells were plated in 6-well dishes and induced to differentiate into macrophages using 1–3 ng/ml (~5 nM) phorbol 12-myristate 13-acetate (PMA) dissolved in dimetyl sulfoxide (DMSO). After PMA induction, THP-1 cells changed morphology and adhered to the culture dish. To determine macrophage differentiation, non-adherent cells were removed and mRNA levels of pro-inflammatory cytokines (IL-1β, IL-18, IL-6, IL-8 and TNF-α) and macrophage surface markers (CD14 and Mcl-1) were measured by qRT-PCR at various time points.

Design of PPRHs

PPRHs were designed using the Triplex-Forming Oligonucleotide Target Sequence Search software (spi.mdanderson.org/tfo/, M.D. Anderson Cancer Center, Houston, TX). This software searches for polypurine sequences for the gene of interest. The output gives the location of the sequence within the gene, either the forward or the reverse strand, its exact starting point in the gene sequence and its location in the promoter, exon or intron. Only sequences with a minimum length of 20 nucleotides have been selected. After selecting proper candidates, BLAST analyses were preformed to confirm specificity of sequences and to avoid unintended targets. PPRHs were synthesized as non-modified, desalted oligodeoxynucleotides by Sigma-Aldrich (0.05 μmol scale). PPRHs were dissolved in sterile Tris-EDTA buffer (1 mM EDTA and 10 mM Tris, pH 8.0) and stored at −20 °C.

As negative controls scrambled sequences were used. Those PPRHs (Hp-Sc) do not bind to the target and have similar content in guanines than the specific PPRHs used. The sequences of the PPRHs used in this study and their abbreviations are described in Table 1.

Transfection of PPRHs

Cells were plated in 6-well dishes. 100 nM PPRHs lipofected with 10 μM N-[1- (2,3-dioleoyloxy)propyl]-N, N,N-trimethylammonium methylsulfate (DOTAP; Biontex) in a volume of 200 μl of medium was incubated for 20 min at room temperature before addition of the mixture to the cells in a final volume of 1 ml.

Table 1 PPRHs designed against the *CD47* and *SIRPα* gene, as well as the scrambled PPRH

PPRHs against *CD47* gene	
Name	Sequence (5'-3')
HpCD47I3-T	GAAAGGAAAAAAGGGGGAAGAAAGGGG T T T GAAAGGAAAAAAGGGGGAAGAAAGGGG T T
HpCd47Pr-T	GAGGAGAAAAG**T**AGAGAGAGAGGACAG T T T GAGGAGAAAAG**T**AGAGAGAGAGGACAG T T

PPRHs against *SIRPα* gene	
Name	Sequence (5'-3')
HpSIRPα-Pr-C	AGGGGGAAGGGGGAGAGGAAGAAGAGA T T T AGGGGGAAGGGGGAGAGGAAGAAGAGA T T
HpSIRPα-I7-T	GAGGGAAGGAGAGGAAGAAGATAAGG T T T GAGGGAAGGAGAGGAAGAAGATAAGG T T

Control PPRHs	
Name	Sequence (5'-3')
Hp-Sc	GAGAAGAGGAAGAGAGGAAGG T T T GAGAAGAGGAAGAGAGGAAGG T T

Abbreviations are
-*Hp* PPRH hairpin
-Location within the gene sequence: Pr for promoter; I for intron and number indicates which intron
- Type of PPRH: −T for Template-PPRHs, −C for Coding-PPRHs and −Sc for scrambled PPRHs
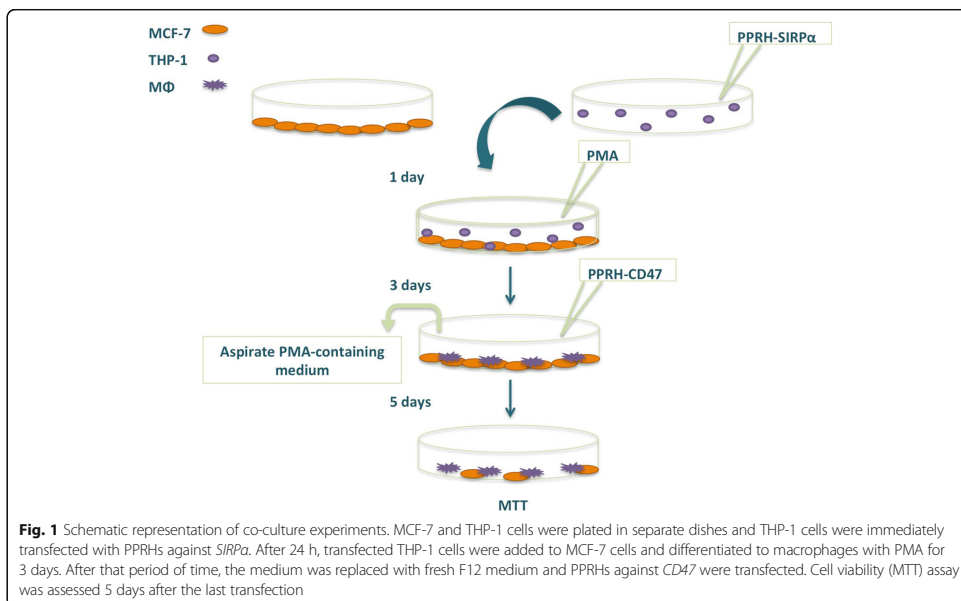- Letters in bold indicate polypirimidine interruptions in the sequence

Anti-CD47 treatment

Cells were plated in 6-well dishes. 10 μg/mL of CD47 anti-rabbit antibody (1:20 dilution; sc-25773; Santa Cruz Biotechnology) was added to the cells in a final volume of 1 mL.

Co-culture experiments

MCF-7 (60,000) and THP-1 cells (1000) were plated in 6-well dishes separately and THP-1 cells were immediately transfected with PPRHs against *SIRPα* and the negative control, as explained in the corresponding section. After 24 h, transfected THP-1 cells were added to MCF-7 cells and treated with 3 ng/ml PMA for differentiation (Fig. 1). Three days after PMA treatment, the PMA-containing medium was aspirated and PPRHs against *CD47* and the negative control were transfected

Results

Fig. 1 Schematic representation of co-culture experiments. MCF-7 and THP-1 cells were plated in separate dishes and THP-1 cells were immediately transfected with PPRHs against *SIRPα*. After 24 h, transfected THP-1 cells were added to MCF-7 cells and differentiated to macrophages with PMA for 3 days. After that period of time, the medium was replaced with fresh F12 medium and PPRHs against *CD47* were transfected. Cell viability (MTT) assay was assessed 5 days after the last transfection

in fresh F12 medium. At the same time, antibody against *CD47* was added as positive control. Cell viability was assessed 5 days after transfection by MTT assays.

MTT assays

Cells were plated in 6-well dishes in F12 medium in a total volume of 1 ml. Five days after transfection, 0.63 mM of 3-(4,5-dimethylthiazol-2-yl)- 2,5-diphenyl-tetrazolium bromide and 100 µM of sodium succinate (both from Sigma-Aldrich, Madrid, Spain) were added to the culture medium and incubated for 2.5 h at 37 °C for the reaction. After incubation, the medium was removed and the solubilization reagent (0.57 % acetic acid and 10 % sodium dodecyl sulfate in DMSO) (Sigma-Aldrich) was added. Cell viability was measured at 570 nm in a WPA S2100 Diode Array spectrophotometer. The results were expressed as the percentage of cell survival relative to the controls.

Apoptosis assay

Apoptosis was determined by the rhodamine method: 48 h after the transfection against *CD47*, rhodamine (final concentration 5 µg/mL) (Sigma-Aldrich) was added for 30 min, the cells were collected, centrifuged at 800 g at 4 °C for 5 min, and washed once in PBS. The pellet was resuspended in 500 mL of PBS with PI (final concentration 5 µg/mL; (Sigma-Aldrich). Flow cytometry analyses were performed in a CyAn™ ADP (Beckman

Coulter, Inc.) and data were analyzed using the software Summit v4.3. The percentage of Rho-negative and IP-negative cells corresponded to the apoptotic population.

RNA extraction

Total RNA was extracted from cells using TRIzol® (Life Technologies) following the manufacturer's specifications. RNA was quantified by measuring its absorbance at 260 nm using a NanoDrop ND-1000 spectrophotometer (Thermo Scientific).

Reverse transcription

cDNA was synthesized by reverse transcription in a 20 µl reaction mixture containing 500 ng of total RNA, 125 ng/µl of random hexamers (Roche), 20 units of RNAse inhibitor (Lucigen), 500 µM of each dNTP (AppliChem), 2 µL of 10× buffer, and 200 units of Moloney murine leukemia virus reverse transcriptase (Lucigen). The reaction was incubated at 42 °C for 1 h.

Real-time PCR

mRNA levels were determined by SYBR-Green Real-Time PCR in a final volume of 20 µl, containing 1× SYBR® Select Master Mix (Life Technologies), 0.25 µM of reverse and forward primers (Sigma-Aldrich), 2 or 3 µl of cDNA and H$_2$O mQ up to 20 µl. PCR cycling conditions were 10 min denaturation at 95 °C, 40 cycles

of 15 s at 95 ℃ and 1 min at 60 ℃, followed by dissociation stage for 15 s at 95 ℃, 20 s at 60 ℃ and 15 s at 95 ℃.

Fold changes in gene expression were calculated using the comparative C_T ($\Delta\Delta C_T$) method, where C_T is the threshold cycle number at which fluorescence of amplified mRNA passes the threshold. GAPDH levels were used as endogenous controls. All the primers used in these experiments are detailed in Table 2.

Western blot analyses
Cells were plated in 6-well dishes and treated with 100 nM PPRHs as described in Transfection of PPRHs section. For MCF-7 cells, 3 h after transfection, total protein extracts were obtained with deoxycholate buffer (100 mM NaCl, 10 mM NaH_2PO_4 pH 7.4, 1 μM PMSF, 1 % triton, 0.1 % SDS and 0.5 % deoxycholic acid). Cells were washed with PBS 1× and collected by scraper in 100 μL of deoxycholate buffer. Cell debris was removed by centrifugation (13,500 × g at 4 ℃ for 10 min).

For THP-1 cells, cells were collected 24 h after transfection and centrifuged for 5 min at 800 g at 4 ℃. Cells were resuspended in 50 μl of RIPA buffer (150 mM NaCl, 5 mM EDTA, 50 mM Tris–HCl pH 7.4 (all from Applichem, Barcelona, Spain), 1 % Igepal CA-630, 100 μg/ml PMSF and Protease inhibitor cocktail (all from Sigma-Aldrich). Cell lysate was kept on ice for 30 min, vortexing every 10 min. Cell debris was removed by centrifugation at 13,500 g at 4 ℃ for 10 min. The Bradford method was used to determine protein concentration using bovine serum albumin as a standard.

Whole cell extracts were resolved in 10 % SDS-polyacrylamide gels and transferred to PVDF membranes. The blocking solution was 5 % Blotto. Membranes were probed overnight at 4 ℃ with primary antibodies against CD47 (1:50 dilution; sc-25773, Santa Cruz Biotechnology, Heidelberg, Germany), SIRPα (1:50 dilution; sc-373896, Santa Cruz Biotechnology, Heidelberg, Germany) or

GAPDH (1:100 dilution; MAB374; Chemicon International, USA). Signals were detected by secondary HRP-conjugated antibodies: anti-rabbit (1:1000 dilution; Dako, Denmark) for CD47 and anti-mouse (1:1000 dilution; sc-2005, Santa Cruz Biotechnology, Heidelberg, Germany) for GAPDH and SIRPα. Chemiluminescence was detected with ImageQuant LAS 4000 mini technology (GE Healthcare).
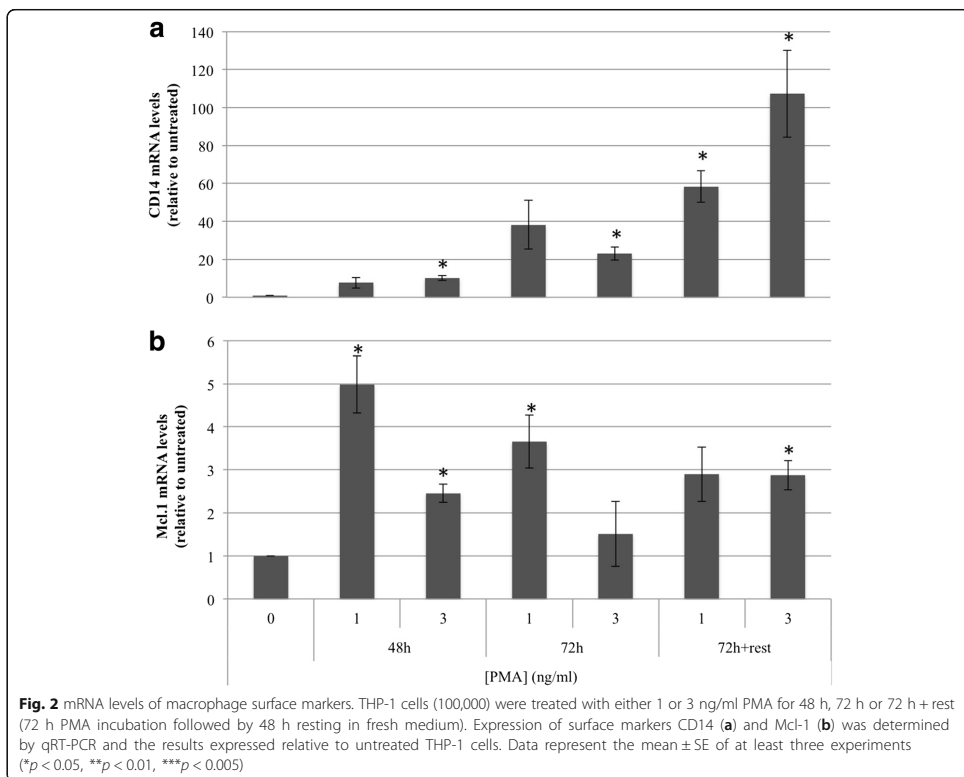
Statistical analyses
All data was recorded as mean ± standard error of the mean (SE). Analyses were performed using Student's *t* test with the software IBM SPSS Statistics v20. Significance was defined as $p < 0.05$.

Results
Expression of surface markers in PMA-treated THP-1 cells
PMA treatment of THP-1 monocytes has been commonly used to study macrophages in vitro and different differentiation protocols including variable concentration of PMA for different time periods have been reported so far [18]. We analyzed the effect of either 1 or 3 ng/ml PMA in THP-1 cells for 48 h, 72 h or 72 h + rest (72 h followed by 48 h resting in fresh medium). Cell morphology after PMA treatment was examined under the microscope for all conditions. Cell adhesion and spreading, which are hallmarks of macrophages, were observed at all indicated time points with both 1 and 3 ng/ml PMA. CD14 [19, 20, 23–25] and Mcl-1 [26] up-regulation have been reported to be differentiation markers of macrophages upon incubation of THP-1 cells with PMA. Therefore, to determine the concentration and incubation time of PMA required to differentiate THP-1 monocytes to macrophages, mRNA levels of CD14 and Mcl-1 were determined by qRT-PCR (Fig. 2). CD14 expression was highly enhanced using 3 ng/ml PMA for 72 h + rest (Fig. 2a) and Mcl-1 expression was increased at 48 h and its elevated level maintained at 72 h + rest for both concentrations of PMA (Fig. 2b).

Table 2 Sequences of the primers used in the qRT-PCR and the amplified product sizes

Target gene	Forward sequence (5'-3')	Reverse sequence (5'-3')	Product size (bp)
GAPDH	CCATGTTCGTCATGGGTGTGAACCA	GCCAGTAGAGGCAGGGATGATGTTC	251
CD14	GCAGCCGAAGAGTTCACAAG	CGCGCTCCATGGTCGATAAG	129
CD47	GAGTCTCTGTATTGCGGCGTG	GGGGTTCCTCTACAGCTTTCC	161
IL-1β	GTGGCAATGAGGATGACTTGTTC	TAGTGGTGGTCGGAGATTCGTA	124
IL-18	CCTCAGACCTTCCAGATCGC	TTCCAGGTTTTCATCATCTTCAGC	159
IL-6	CATTTGTGGTTGGGTCAGG	AGTGAGGAACAAGCCAGAGC	112
IL-8	CCACCGGAAGGAACCATCTC	TTCCTTGGGGTCCAGACAGA	279
Mcl-1	GACGAGTTGTACCGGCAGTCG	TTGATGTCCAGTTTCCGAAGC	200
SIRPα	AAATACCGCCGCTGAGAACA	TGTCCTGTGTTATTTCTCTGGCA	197
TNF-α	GCCAGAGGGCTGATTAGAG	TCAGCCTCTTCTCCTTCCTG	124

Results

Bener *et al. BMC Immunology* (2016) 17:32

Page 6 of 12

Fig. 2 mRNA levels of macrophage surface markers. THP-1 cells (100,000) were treated with either 1 or 3 ng/ml PMA for 48 h, 72 h or 72 h + rest (72 h PMA incubation followed by 48 h resting in fresh medium). Expression of surface markers CD14 (**a**) and Mcl-1 (**b**) was determined by qRT-PCR and the results expressed relative to untreated THP-1 cells. Data represent the mean ± SE of at least three experiments (*$p < 0.05$, **$p < 0.01$, ***$p < 0.005$)

PMA induced pro-inflammatory cytokines expression in a dose and time dependent manner

Increased expression of cytokines is one of the phenotypic characteristics of differentiated macrophages [19, 20, 27]. To further investigate if THP-1 cells were able to differentiate to macrophages at 1 and 3 ng/ml PMA, mRNA expression of 5 different pro-inflammatory cytokines (IL-1β, IL-18, IL-6, IL-8, and TNF-α) was analyzed by qRT-PCR (Fig. 3). After the addition of PMA, levels of pro-inflammatory cytokines were increased dose and time dependently relative to untreated THP-1 cells. It is worth noting that the levels of cytokines produced in response to PMA are not the same depending on the culture conditions [18]. IL-1β was elevated in all conditions whereas 3 ng/ml PMA induced the highest expression when treated for 72 h (Fig. 3a). IL-18 (Fig. 3b), IL-6 (Fig. 3c) and IL-8 (Fig. 3d) stimulated at the highest level with 3 ng/ml PMA for 72 h + rest and TNF-α (Fig. 3e) increased 4.4 fold with 3 ng/ml PMA for 72 h. These results suggested that THP-

1 cells could be differentiated to macrophages using 3 ng/ml PMA for 72 h and the levels of pro-inflammatory cytokines remained enhanced for the 72 h treatment followed by 48 h resting, which was also reflected in the up-regulated surface markers levels.

Effects of PPRHs on CD47 and SIRPα levels

Two types of PPRHs against *CD47* were used in the experiments, targeting either the promoter (HpCD47Pr-T) or intron 1 (HpCD47I3-T) in the template strand of the DNA (Table 1). To explore the ability of PPRHs to silence *CD47*, CD47 mRNA levels were analyzed in MCF-7 cells either in the absence or in the presence of PPRHs. Both HpCD47I3-T and HpCD47Pr-T were able to decrease CD47 mRNA levels down to 2-fold in MCF-7 cells compared to the control (Fig. 4a). To target *SIRPα*, HpSIRPαPr-C, designed against the promoter sequence and HpSIRPαI7-T, designed against the intron 7 sequence (Table 1) were transfected in THP-1 cells. A decrease in SIRPα expression was achieved with both
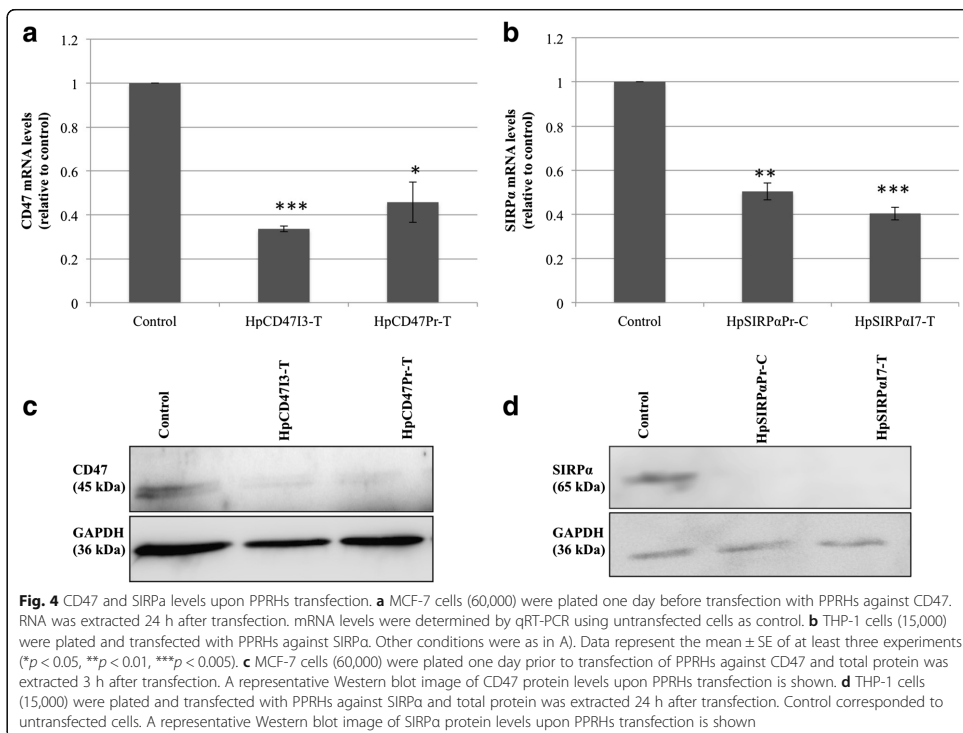
Fig. 3 mRNA levels of pro-inflammatory cytokines. THP-1 cells (100,000) were treated with either 1 or 3 ng/ml PMA for 48 h, 72 h or 72 h + rest (72 h PMA incubation followed by 48 h resting in fresh medium). Expression of IL-1β (**a**), IL-18 (**b**), IL-6 (**c**), IL-8 (**d**), and TNF-α (**e**) was determined by qRT-PCR and the results expressed relative to untreated THP-1 cells. Data represent the mean ± SE of at least three experiments (*$p < 0.05$, **$p < 0.01$, ***$p < 0.005$)

PPRHs (Fig. 4b). The effects of PPRHs on CD47 and SIRPα were also determined at the protein level in MCF-7 and THP-1 cells, respectively (Fig. 4c,d). Both PPRHs targeting CD47 decreased the protein level by 2.5 fold (Fig. 4c). Likewise, SIRPα protein levels were reduced by both HpSIRPαPr-C and HpSIRPαI7-T (Fig. 4d).

Effect of PPRHs in MCF-7 cells and in Co-culture experiments

Before proceeding to co-culture experiments, we determined the cytotoxicity of the different PPRHs against either CD47 or SIRPα in MCF-7 cells. Thus, we transfected the 4 PPRHs at the same concentration of 100 nM. Whereas HpCD47I3-T and HpSIRPαPr-C caused a cytotoxicity of 48 and 28 %, respectively, HpCD47Pr-T and HpSIRPαI7-T only caused a cytotoxicity of 8 and

18 %, respectively. Given that the last two PPRHs were practically not cytotoxic in MCF-7 cells, they were selected for the co-culture experiments. The rationale for this was that we wanted to analyze the cytotoxic effect of macrophages on MCF-7 cells that had reduced CD47 levels by PPRHs, which were not cytotoxic by themselves. Also, because it was important for the co-culture experiment, we determined the lack of CD47 expression in THP-1 cells relative to MCF-7 and of SIRPα expression in MCF-7 relative to THP-1 cells (data not shown).

Based on the patterns of pro-inflammatory cytokines and surface markers levels, 3 ng/ml of PMA was chosen for THP-1 differentiation. To decrease CD47/SIRPα interaction, CD47 and SIRPα alone or in combination were targeted by PPRHs. Scrambled PPRHs were used as negative controls and an antibody anti-CD47 as positive control to disrupt the interaction CD47/SIRPα

Results

Bener *et al. BMC Immunology* (2016) 17:32

Page 8 of 12

Fig. 4 CD47 and SIRPa levels upon PPRHs transfection. **a** MCF-7 cells (60,000) were plated one day before transfection with PPRHs against CD47. RNA was extracted 24 h after transfection. mRNA levels were determined by qRT-PCR using untransfected cells as control. **b** THP-1 cells (15,000) were plated and transfected with PPRHs against SIRPα. Other conditions were as in A). Data represent the mean ± SE of at least three experiments (*$p < 0.05$, **$p < 0.01$, ***$p < 0.005$). **c** MCF-7 cells (60,000) were plated one day prior to transfection of PPRHs against CD47 and total protein was extracted 3 h after transfection. A representative Western blot image of CD47 protein levels upon PPRHs transfection is shown. **d** THP-1 cells (15,000) were plated and transfected with PPRHs against SIRPα and total protein was extracted 24 h after transfection. Control corresponded to untransfected cells. A representative Western blot image of SIRPα protein levels upon PPRHs transfection is shown

(Fig. 5). By decreasing the level of CD47 in tumor cells, 60 % of MCF-7 cells were killed by macrophages (Fig. 5). When transfecting THP-1 cells with HpSIRPαI7-T, the decreased level of SIRPα allowed macrophages to kill 58 % of tumor cells (Fig. 5). To decrease the level of both targets in the same co-culture and to better kill tumor cells, THP-1 cells were first transfected with HpSIRPαI7-T and after differentiation, MCF-7 cells were transfected with HpCD47Pr-T in the co-culture. In these conditions, 70 % of tumor cells were eliminated. Similar results were obtained under anti-CD47 treatment. On the other hand, tumor cells escaped from macrophage killing in the absence of PPRHs and the cell viability when transfected with scrambled PPRHs was reduced by 25 % compared to that of the co-culture control (Fig. 5).

Apoptosis assay

To associate the dead mechanism to the cytotoxic effect observed in the co-culture, we measured the apoptotic effect of the PPRHs at 100 nM after 48 h of incubation using the rhodamine method (Fig. 6). Co-culture transfected with HpCD47Pr-T and HpSIRPαI1-T provoked a 3-fold increase in apoptosis compared to MCF-7 cells treated with PMA, which was higher than the apoptotic effect triggered by anti-CD47 antibody (1.7-fold) used as positive control. No significant difference was detected in the co-culture control whereas the percentage of apoptotic cells in the co-culture transfected with HpCD47-Sc and HpSIRPα-Sc was twice that of the control MCF-7 cells treated with PMA.

Discussion

In this work, we explored the usage of specific PPRHs to decrease the expression of CD47 and SIRPα to stimulate the elimination of tumor cells by macrophages, which constitutes a new approach in tumor immunotherapy.

So far, it has been shown that different concentrations and time of exposure to PMA induce THP-1 differentiation resulting in different macrophage phenotypes with altered expression of a wide range of genes at various levels. CD14 is a widely used marker to study monocyte-macrophage differentiation and its up-regulated expression is associated with macrophage phenotype [19, 20, 23–25]. The anti-apoptotic molecule Mcl-1 has also
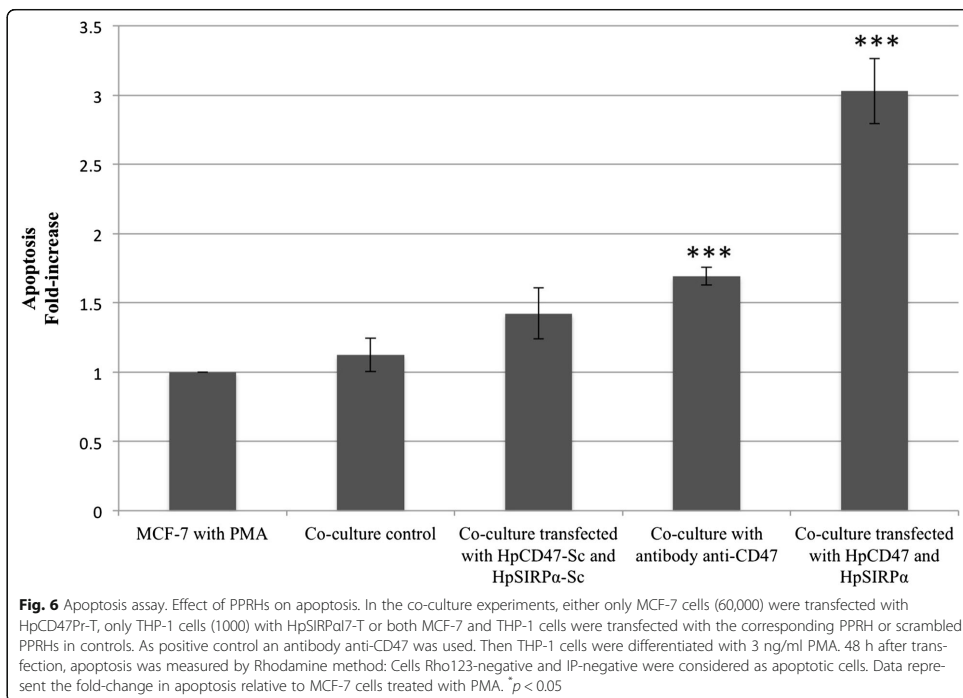
Fig. 5 Co-culture experiments. In the co-culture experiments, either only MCF-7 cells (60,000) were transfected with HpCD47Pr-T, only THP-1 cells (1000) with HpSIRPαI7-T or both MCF-7 and THP-1 cells were transfected with the corresponding PPRH or scrambled PPRHs in controls. As positive control an antibody anti-CD47 was used. Then THP-1 cells were differentiated with 3 ng/ml PMA. The percentage of viable cells was calculated relative to the control of MCF-7 cells incubated with 3 ng/ml PMA. Data represent the mean ± SE of at least three experiments (*$p < 0.05$, **$p < 0.01$, ***$p < 0.005$)

been identified as a differentiation dependent marker [22, 25]. High concentrations of PMA were previously found to induce undesirable gene up-regulation, and concentrations lower than 10 ng/ml were suggested for attain stable differentiation [18]. In the present study, we treated THP-1 cells with either 1 or 3 ng/ml PMA for incubation times commonly used in the literature (48 to 72 h), to observe the effect of different culture conditions on differentiation. Differentiation of THP-1 cells is mainly conducted with PMA treatment for 48 h or 72 h although Daigneault et al. [19] demonstrated that treating THP-1 cells with PMA followed by a period of further culture without PMA differentiates THP-1 cells to macrophages with a high capability of phagocytosis and it enhances differentiation [19]. Our data demonstrated that the highest CD14 level was reached with a PMA treatment for 72 h followed by 48 h of resting without PMA. In accordance with previous studies, we demonstrated that both CD14 and Mcl-1 levels were increased with PMA treatment in a time and dose dependent manner.

In addition to surface markers, PMA has also been reported to induce the production of pro-inflammatory cytokines in THP-1 cells [27–29]. IL-1β, IL-18, IL-6, IL-8 and TNF-α are produced by macrophages through the activation of toll-like receptor signaling, and their production is involved in the clearance of tumor cells by macrophages [30]. Our results showed the induction of several cytokines in THP-1 cells in response to PMA, depending on the duration and dose of treatment.

Cancer therapy by stimulating the patient's immune system is one of the most promising areas of cancer research. In contrast to target the adaptive immune system, therapies have been aimed to stimulate macrophages to attack cancer. Studies have demonstrated that macrophage phagocytosis is the major mechanism when treating cancer using antibody therapies aimed to abolish the interaction between CD47/SIRPα. The efficiency of macrophage mediated tumor elimination by tumor-binding antibodies has already approved for cancer therapy [30].

As a new approach in immunotherapy, we used PPRHs, which have already been proved in gene silencing in vitro

Results

Bener *et al. BMC Immunology* (2016) 17:32

Page 10 of 12

Fig. 6 Apoptosis assay. Effect of PPRHs on apoptosis. In the co-culture experiments, either only MCF-7 cells (60,000) were transfected with HpCD47Pr-T, only THP-1 cells (1000) with HpSIRPαI7-T or both MCF-7 and THP-1 cells were transfected with the corresponding PPRH or scrambled PPRHs in controls. As positive control an antibody anti-CD47 was used. Then THP-1 cells were differentiated with 3 ng/ml PMA. 48 h after transfection, apoptosis was measured by Rhodamine method: Cells Rho123-negative and IP-negative were considered as apoptotic cells. Data represent the fold-change in apoptosis relative to MCF-7 cells treated with PMA. $^{*}p < 0.05$

and in vivo [31]. PPRHs are more stable and show almost no immunogenicity, relative to siRNAs [16]. Since we previously described PPRHs as a gene silencing tool against different cancer targets in different human cell lines [15, 31–33], in this study we designed four different PPRHs to decrease the level of both CD47 and SIRPα and we demonstrated that all PPRHs were able to silence their target at both the mRNA and protein level. We showed that PMA-differentiated THP-1 cells eliminated tumor cells after decreasing CD47/SIRPα interaction whereas tumor cells remained unaffected in the absence of PPRHs. We also demonstrated that the mechanism responsible for observed cell death was apoptosis.

Elevated CD47 expression limits the killing of tumor cells through its interaction with SIRPα, whereas loss of CD47 triggers phagocytosis. So far, monoclonal antibodies directed against CD47 have been used to inhibit this interaction. Anti-CD47 antibodies have shown the preclinical activity in different cancers both in vitro and in animal models [6, 9, 34]. In addition to antibodies, targeting tumor CD47 using antisense strategies is another promising approach to inhibit CD47 function. Antisense morpholino oligonucleotides have been used

to prevent translation of CD47 mRNA and to suppress CD47 expression in mice and miniature pigs [35, 36]. Also, antisense and siRNA strategies have been suggested to offer advantages over CD47 antibodies by avoiding many of the side effects of therapeutic CD47-antibodies such as altered blood pressure [37], hemolytic anemia and pro-thrombotic or anti-thrombotic activities [38].

Recently, Chao et al. have reported the synergic effect of antibodies against CD47 with the therapeutic cancer antibody rituximab on the phagocytosis of non-Hodgkin lymphoma by macrophages in immune-deficient mice [39]. However, it was believed that this study did not provide conclusive evidence for the role of CD47/SIRPα interaction. Furthermore, it has been shown that CD47/SIRPα and SIRPα signaling negatively regulate antibody-dependent elimination of tumor cells, which supports the idea of targeting CD47/SIRPα interaction to enhance the clinical effects of cancer therapeutic antibodies [40].

SIRPα acts to inhibit in vivo clearance of CD47-expressing host cells, including red blood cells and platelets, by macrophages [41, 42]. Therefore, direct targeting of SIRPα in immune cells, rather than CD47 in tumor cells, could be considered as an alternative approach to

disrupt their interaction. A previous study showed that a novel human SIRPα-Fc fusion protein resulted in the preferential phagocytosis of acute myeloid leukemia with the blockade of CD47/SIRPα [43]. Moreover, SIRPα has been proposed as a better target due to its relatively restricted tissue expression pattern compared to CD47, which is ubiquitously expressed and binds to multiple other ligands [40].

Conclusions

Our data support the usage of PPRHs to diminish CD47/SIRPα interaction by decreasing the expression of both molecules thus resulting in an enhanced killing of tumor cells by macrophages, which might translate into beneficial effects in cancer therapy. We believe that our results encourage the use of PPRH technology as an alternative strategy, as a new and promising immunotherapeutic approach to enhance cancer therapies.

Abbreviations
DOTAP: N-[1- (2,3-dioleoyloxy)propyl]-N,N,N-trimethylammonium methylsulfate; PMA: Phorbol 12-myristate 13-acetate; PPRH: Polypurine reverse Hoogsteen hairpin; SIRPα: Signal regulatory protein α

Availability of data and materials
The data supporting the conclusions are included within the article.

Authors'contributions
GB, AJF, CSsD and IPF carried out all the experiments described in this work and drafted the manuscript. VN and CJC conceived of the study, participated in its design and coordination and helped to draft the manuscript. All authors read and approved the final manuscript.

Competing interests
The authors declare that they have no competing interests.

Consent for publication
Not applicable.

Ethics approval and consent to participate
Not applicable.

References
1. Swann JB, Smyth MJ. Review series immune surveillance of tumors. J Clin Invest. 2007;117:1137–46.
2. Jadus MR, Irwin MC, Irwin MR, Horansky RD, Sekhon S, Pepper KA, Kohn DB, Wepsic HT. Macrophages can recognize and kill tumor cells bearing the membrane isoform of macrophage colony-stimulating factor. Blood. 1996; 87:5232–41.
3. Munn DH, Cheung NK. Phagocytosis of tumor cells by human monocytes cultured in recombinant macrophage colony-stimulating factor. J Exp Med. 1990;172:231–7.
4. Jaiswal S, Jamieson CHM, Pang WW, Park CY, Chao MP, Majeti R, Traver D, van Rooijen N, Weissman IL. CD47 is upregulated on circulating hematopoietic stem cells and leukemia cells to avoid phagocytosis. Cell. 2009;138:271–85.
5. McCracken MN, Cha AC, Weissman IL. Molecular pathways: activating T cells after cancer cell phagocytosis from blockade of CD47 "Don't Eat Me" signals. Clin Cancer Res. 2015;21:3597–601.
6. Willingham SB, Volkmer J-P, Gentles AJ, Sahoo D, Dalerba P, Mitra SS, Wang J, Contreras-Trujillo H, Martin R, Cohen JD, Lovelace P, Scheeren FA, Chao MP, Weiskopf K, Tang C, Volkmer AK, Naik TJ, Storm TA, Mosley AR, Edris B, Schmid SM, Sun CK, Chua M-S, Murillo O, Rajendran P, Cha AC, Chin RK, Kim D, Adorno M, Raveh T, et al. The CD47-signal regulatory protein alpha (SIRPa) interaction is a therapeutic target for human solid tumors. Proc Natl Acad Sci. 2012;109:6662–7.
7. Lv Z, Bian Z, Shi L, Niu S, Ha B, Tremblay A, Li L, Zhang X, Paluszynski J, Liu M, Zen K, Liu Y. Loss of cell surface CD47 clustering formation and binding avidity to SIRP facilitate apoptotic cell clearance by macrophages. J Immunol. 2015; 195:661–71.
8. Chao MP, Weissman IL, Majeti R. The CD47-SIRPα pathway in cancer immune evasion and potential therapeutic implications. Curr Opin Immunol. 2012;24:225–32.
9. Oldenborg P-A. CD47: a cell surface glycoprotein which regulates multiple functions of hematopoietic cells in health and disease. ISRN Hematol. 2013;2013:614619.
10. Brown EJ, Frazier WA. Integrin-associated protein (CD47) and its ligands. Trends Cell Biol. 2001;11:130–5.
11. Poels LG, Peters D, van Megen Y, Vooijs GP, Verheyen RN, Willemen A, van Niekerk CC, Jap PH, Mungyer G, Kenemans P. Monoclonal antibody against human ovarian tumor-associated antigens. J Natl Cancer Inst. 1986;76:781–91.
12. Tsai RK, Discher DE. Inhibition of "self" engulfment through deactivation of myosin-II at the phagocytic synapse between human cells. J Cell Biol. 2008;180:989–1003.
13. Aviñó A, Frieden M, Morales JC, García de la Torre B, Güimil García R, Azorín F, Gelpí JL, Orozco M, González C, Eritja R. Properties of triple helices formed by parallel-stranded hairpins containing 8-aminopurines. Nucleic Acids Res. 2002;30:2609–19.
14. Coma S, Noé V, Eritja R, Ciudad CJ. Strand displacement of double-stranded DNA by triplex-forming antiparallel purine-hairpins. Oligonucleotides. 2005;15:269–83.
15. de Almagro MC, Coma S, Noé V, Ciudad CJ. Polypurine hairpins directed against the template strand of DNA knock down the expression of mammalian genes. J Biol Chem. 2009;284:11579–89.
16. Villalobos X, Rodríguez L, Prévot J, Oleaga C, Ciudad CJ, Noé V. Stability and immunogenicity properties of the gene-silencing polypurine reverse hoogsteen hairpins. Mol Pharm. 2014;11:254–64.
17. Tsuchiya S, Yamabe M, Yamaguchi Y, Kobayashi Y, Konno T, Tada K. Establishment and characterization of a human acute monocytic leukemia cell line (THP-1). Int J Cancer. 1980;26:171–6.
18. Park EK, Jung HS, Yang HI, Yoo MC, Kim C, Kim KS. Optimized THP-1 differentiation is required for the detection of responses to weak stimuli. Inflamm Res. 2007;56:45–50.
19. Daigneault M, Preston JA, Marriott HM, Whyte MKB, Dockrell DH. The identification of markers of macrophage differentiation in PMA-stimulated THP-1 cells and monocyte-derived macrophages. PLoS One. 2010;5:e8668.
20. Song MG, Ryoo IG, Choi HY, Choi BH, Kim ST, Heo TH, Lee JY, Park PH, Kwak MK. NRF2 signaling negatively regulates phorbol-12-myristate-13-acetate (PMA)-induced differentiation of human monocytic U937 cells into pro-inflammatory macrophages. PLoS One. 2015;10:e0134235.
21. Rovera G, Santoli D, Damsky C. Human promyelocytic leukemia cells in culture differentiate into macrophage-like cells when treated with a phorbol diester. Proc Natl Acad Sci U S A. 1979;76:2779–83.
22. Miranda MB, McGuire TF, Johnson DE. Importance of MEK-1/-2 signaling in monocytic and granulocytic differentiation of myeloid cell lines. Leukemia. 2002;16:683–92.
23. Schwende H, Fitzke E, Ambs P, Dieter P. Differences in the state of differentiation of THP-1 cells induced by phorbol ester and 1,25-dihydroxyvitamin D3. J Leukoc Biol. 1996;59:555–61.
24. Aldo PB, Craveiro V, Guller S, Mor G. Effect of culture conditions on the phenotype of THP-1 monocyte cell line. Am J Reprod Immunol. 2013;70:80–6.
25. Kohro T, Tanaka T, Murakami T, Wada Y, Aburatani H, Hamakubo T, Kodama T. A comparison of differences in the gene expression profiles of phorbol

Results

12-myristate 13-acetate differentiated THP-1 cells and human monocyte-derived macrophage. J Atheroscler Thromb. 2004;11:88–97.

26. Liu H, Perlman H, Pagliari LJ, Pope RM. Constitutively activated Akt-1 is vital for the survival of human monocyte-differentiated macrophages. Role of Mcl-1, independent of nuclear factor (NF)-kappaB, Bad, or caspase activation. J Exp Med. 2001;194:113–26.
27. Park JJ, Moon HJ, Park JH, Kwon TH, Park Y-K, Kim JH. Induction of proinflammatory cytokine production in intervertebral disc cells by macrophage-like THP-1 cells requires mitogen-activated protein kinase activity. 2015.
28. Mahmoud L, Al-Enezi F, Al-Saif M, Warsy A, Khabar KSA, Hitti EG. Sustained stabilization of Interleukin-8 mRNA in human macrophages. RNA Biol. 2014;11:124–33.
29. Lei Q, Li L, Cai J, Huang W, Qin B, Zhang S. ORF3 of hepatitis E virus inhibits the expression of proinflammatory cytokines and chemotactic factors in LPS-stimulated human PMA-THP1 cells by inhibiting NF-kB pathway. Viral Immunol. 2016;29:vim.2015.0107.
30. Weiskopf K, Weissman IL. Macrophages are critical effectors of antibody therapies for cancer. MAbs. 2015;7:303–10.
31. Rodríguez L, Villalobos X, Dakhel S, Padilla L, Hervas R, Hernández JL, Ciudad CJ, Noé V. Polypurine reverse Hoogsteen hairpins as a gene therapy tool against survivin in human prostate cancer PC3 cells in vitro and in vivo. Biochem Pharmacol. 2013;86:1541–54.
32. de Almagro MC, Mencia N, Noé V, Ciudad CJ. Coding polypurine hairpins cause target-induced cell death in breast cancer cells. Hum Gene Ther. 2011;22:451–63.
33. Villalobos X, Rodríguez L, Solé A, Lliberós C, Mencia N, Ciudad CJ, Noé V. Effect of polypurine reverse hoogsteen hairpins on relevant cancer target genes in different human cell lines. Nucleic Acid Ther. 2015;25:198–208.
34. Liu J, Wang L, Zhao F, Tseng S, Narayanan C, Shura L, Willingham S, Howard M, Prohaska S, Volkmer J, Chao M, Weissman IL, Majeti R. Pre-clinical development of a humanized anti-CD47 antibody with anti-cancer therapeutic potential. PLoS One. 2015;10:e0137345.
35. Isenberg JS, Romeo MJ, Maxhimer JB, Smedley J, Frazier WA, Roberts DD. Gene silencing of CD47 and antibody ligation of thrombospondin-1 enhance ischemic tissue survival in a porcine model: implications for human disease. Ann Surg. 2008;247:860–8.
36. Isenberg JS, Romeo MJ, Abu-Asab M, Tsokos M, Oldenborg A, Pappan L, Wink DA, Frazier WA, Roberts DD. Increasing survival of ischemic tissue by targeting CD47. Circ Res. 2007;100:712–20.
37. Bauer EM, Qin Y, Miller TW, Bandle RW, Csanyi G, Pagano PJ, Bauer PM, Schnermann J, Roberts DD, Isenberg JS. Thrombospondin-1 supports blood pressure by limiting eNOS activation and endothelial-dependent vasorelaxation. Cardiovasc Res. 2010;88:471–81.
38. Isenberg JS, Frazier WA, Krishna MC, Wink DA, Roberts DD. Enhancing cardiovascular dynamics by inhibition of thrombospondin-1/CD47 signaling. Curr Drug Targets. 2008;9:833–41.
39. Chao MP, Alizadeh AA, Tang C, Myklebust JH, Varghese B, Gill S, Jan M, Cha AC, Chan CK, Tan BT, Park CY, Zhao F, Kohrt HE, Malumbres R, Briones J, Gascoyne RD, Lossos IS, Levy R, Weissman IL, Majeti R. Anti-CD47 antibody synergizes with rituximab to promote phagocytosis and eradicate non-hodgkin lymphoma. Cell. 2010;142:699–713.
40. Zhao XW, van Beek EM, Schornagel K. CD47–signal regulatory protein-α (SIRPα) interactions form a barrier for antibody-mediated tumor cell destruction. 2011.
41. Oldenborg PA, Zheleznyak A, Fang YF, Lagenaur CF, Gresham HD, Lindberg FP. Role of CD47 as a marker of self on red blood cells. Science. 2000;288:2051–4.
42. Oldenborg P-A, Gresham HD, Lindberg FP. Cd47-signal regulatory protein α (Sirpα) regulates Fcγ and complement receptor–mediated phagocytosis. J Exp Med. 2001;193:855–62.
43. Ho JM, Danska JS, Wang JCY. Targeting SIRP α in cancer. Oncoimmunology. 2013; 22, e23081(February):6–8.

4.3 Article III:

Cancer immunotherapy using PolyPurine Reverse Hoogsteen hairpins targeting the PD-1/PD-L1 pathway in human tumor cells

Miriam Marlene Medina Enríquez*, Alex J. Félix*, Carlos J. Ciudad and Véronique Noé

*These authors contributed equally to this work

Background: Among all immunotherapy approaches, the PD-1/PD-L1 blockade has been considered one of the most successful advances in the history of cancer immunotherapy. In the tumor microenvironment, it is well established that PD-1 and its ligand PD-L1 are important in tumor progression and survival by escaping immune surveillance. In this direction, it has been reported that the blockade of PD-1/PD-L1 interaction with antibodies increased the phagocytic potency of macrophages, thus reducing tumor growth in a cancer mouse model (Gordon *et al.* 2017).

Objectives: The aim of this study was to silence *PD-1* in macrophages and *PD-L1* in different cancer cell lines using PPRHs in order to stimulate the elimination of tumor cells by macrophages in co-culture experiments.

Results: The incubation of either THP-1 or PC3 cells with PPRHs against *PD-1* and *PD-L1*, respectively, decreased PD-1/PD-L1 mRNA and protein levels. We also confirmed that the transfection of these PPRHs in either THP-1 cells or macrophages obtained by phorbol 12-myristate 13-acetate (PMA)-differentiation of THP-1 cells did not produce any effect on cell viability. In contrast, PC3 cell viability was partially decreased upon incubation with PPRHs against *PD-L1*. Regarding the PC3/macrophage co-culture experiments, the most effective combination of PPRHs against PD-1 and PD-L1 transfected into macrophages and PC3 cells, respectively, produced a 90% decrease in cell viability. This effect was also observed in other cancer cell lines such as M21, HeLa and SKBR3. The best combination of PPRHs against *PD-1/PD-L1* produced in M21, HeLa and SKBR3 co-culture experiments a decrease in cell

viability of 65%, 92% and 88%, respectively. Finally, we determined the apoptosis levels after treatment with PPRHs in co-cultures of macrophages with each one of the four different cancer cell lines. The apoptosis levels were 2.1, 2.7 and 1.8-fold increase in PC3, HeLa and SKBR3, respectively. In the case of the M21 cell line, the increase in apoptosis was more moderate (1,3-fold). In contrast, apoptosis was not detected when macrophages alone were treated with the different PPRHs.

Conclusions: We performed an *in vitro* immunotherapy approach based in silencing, by means of PPRHs, *PD-1* in macrophages and *PD-L1* in different cancer cell lines in co-culture experiments, thus inhibiting their interaction and increasing the phagocytic potency of macrophages against the tumor cells. We also showed that apoptosis was involved in this process. This study demonstrates that PPRHs could be powerful pharmacological agents to inhibit the PD-1/PD-L1 pathway.

PLOS ONE

RESEARCH ARTICLE

Cancer immunotherapy using PolyPurine Reverse Hoogsteen hairpins targeting the PD-1/PD-L1 pathway in human tumor cells

Miriam Marlene Medina Enríquez◉⬩, **Alex J. Félix**⬩, **Carlos J. Ciudad**‡, **Véronique Noé**◉‡*

Department of Biochemistry and Physiology, School of Pharmacy, and Institute of Nanoscience and Nanotechnology, University of Barcelona, Barcelona, Spain

◉ These authors contributed equally to this work.
‡ These authors are co-senior authors on this work.
* vnoe@ub.edu
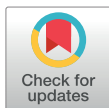
Abstract

Immunotherapy approaches stand out as innovative strategies to eradicate tumor cells. Among them, PD-1/PD-L1 immunotherapy is considered one of the most successful advances in the history of cancer immunotherapy. We used our technology of Polypurine reverse Hoogsteen hairpins (PPRHs) for silencing both genes with the aim to provoke the elimination of tumor cells by macrophages in co-culture experiments. Incubation of PPRHs against *PD-1* and *PD-L1* decreased the levels of mRNA and protein in THP-1 monocytes and PC3 prostate cancer cells, respectively. Viability of THP-1 cells and macrophages obtained by PMA-differentiation of THP-1 cells was not affected upon incubation with the different PPRHs. On the other hand, PC3 cell survival was partially decreased by PPRHs against *PD-L1*. The greatest effect in decreasing cell viability was obtained in macrophages/PC3 co-culture experiments by combining PPRHs against *PD-1* and *PD-L1*. This effect was also observed in other cancer cell lines: HeLa, SKBR3 and to a minor extent in M21. Apoptosis was not detected when macrophages were treated with the different PPRHs. However, co-cultures of macrophages with the four cancer cell lines treated with PPRHs showed an increase in apoptosis. The order of fold-increase in apoptosis was HeLa > PC3 > SKBR3 > M21. This study demonstrates that PPRHs could be powerful pharmacological agents to use in immunotherapy approaches for the inhibition of PD-1 and PD-L1.

Introduction

It is well known that the immune system can prevent the formation and progression of tumors by (i) eliminating viral infections that could lead to tumor formation, (ii) solving inflammation processes to avoid tumorigenesis and (iii) identifying and eliminating tumor cells depending on the expression of tumor-specific antigens (immune surveillance). Macrophages are one of the most important components involved in tumor elimination within the immune surveillance process [1,2]. Although macrophage cytotoxicity in tumors can be achieved by cytokine secretion, phagocytosis is the main process involved in tumor clearance [3,4]. One of the

mechanisms of macrophages to trigger phagocytosis against tumor cells but avoiding normal tissues relies on distinguishing between non-self-molecules from self-molecules. When macrophages do not recognize tumor cells, these are not eliminated by the immune system, which represents one of the hallmarks of cancer [5].

During the last decade, immunotherapy approaches arose as innovative strategies to eradicate tumor cells. There is a wide spectrum of available immunotherapies ranging from cytokines such as IL-2 and IFN-α [6], cell-based therapies like vaccines [7] or adoptive cellular therapy to stimulate host's immune system [8–11], and immune checkpoint blockade strategies using anti-CTLA-4 [12] or anti-PD-1 and anti-PD-L1 antibodies to trigger new immune responses against the tumor. Among them, PD-1/PD-L1 pathway has been the focus of extensive research in the recent years and it is considered one of the most successful advances in the history of cancer immunotherapy [12–14].

Programmed cell death protein 1 (PD-1) is an immunoinhibitory receptor that belongs to the CD28 family and it is expressed on B cells, activated T cells, dendritic cells, natural killer cells, tumor-infiltrating lymphocytes and activated monocytes. PD-1 has two main ligands: programmed cell death-ligand 1 (PD-L1) and programmed cell death-ligand 2 (PD-L2) [15,16]. However, research is more focused on PD-L1 because of its overexpression in different types of tumors [17,18].

In the tumor microenvironment, it is well established that PD-1 and its ligand PD-L1 are important in tumor progression and survival by escaping tumor neutralizing immune surveillance. Gordon *et al.* demonstrated that, by blocking PD-1/PD-L1 interaction with antibodies, the phagocytic potency of macrophages increased *in vivo*, thus reducing tumor growth in a cancer mouse model [19]. Giving the importance of PD-1/PD-L1 interaction to avoid phagocytosis, we used Polypurine reverse Hoogsteen hairpins (PPRHs) to silence both genes with the aim to provoke the elimination of tumor cells by macrophages.

PPRHs are non-modified single-stranded deoxyoligonucleotides formed by two antiparallel polypurine stretches linked by a pentathymidine loop. The intramolecular linkage consists of reverse Hoogsteen bonds that are formed between guanines and adenines, originating the hairpin structure. PPRHs can bind to polypyrimidine domains in the double-stranded DNA (dsDNA) via Watson-Crick bonds, thus displacing the fourth strand of the dsDNA and producing a triplex structure. That conformation leads to a transcriptional disruption that provokes the gene silencing effect [20,21]. Therefore, it is essential for PPRH design to find polypyrimidine tracts within the target gene sequence, which are mainly present in promoter or intronic regions [22].

In a previous study, we used this technology to conduct an immunotherapy approach based on silencing the *SIRPα* gene in macrophages and the *CD47* gene in breast cancer MCF-7 cells, to avoid their interaction and provoke the elimination of tumor cells by macrophages in co-culture experiments [23]. In addition, we demonstrated that PPRHs can act as pharmacological agents without causing hepatotoxicity or nephrotoxicity [24].

The aim of the present study was to eliminate tumor cells by macrophages in co-culture experiments by decreasing both the levels of PD-1 in macrophages and those of PD-L1 in different cancer cells using PPRHs and to evaluate the involvement of apoptosis in this approach.

Materials and methods

Cell culture and PMA induced differentiation

Prostate cancer PC3, melanoma M21, ovarian cancer HeLa, breast cancer SKBR3, and monocyte THP-1 cell lines were grown in Ham´s F-12 medium supplemented with 10% fetal bovine serum (both from Gibco, Barcelona, Spain) at 37°C in a 5% CO_2-controlled humidified

atmosphere. Trypsinization of cancer cells was performed using 0.05% Trypsin in PBS 1X (154 mM NaCl, 3.88 mM H_2NaPO_4 and 6.1 mM $HNaPO_4$ pH 7.4) (Sigma-Aldrich, Madrid, Spain). THP-1 monocytes grew on suspension.

THP-1 cells were incubated with 2 ng/mL phorbol12-myristate 13-acetate (PMA) (Sigma-Aldrich, Madrid, Spain) for differentiation into macrophages. This concentration was chosen due to the patterns of pro-inflammatory cytokines and surface marker levels observed after three days of differentiation [23]. We routinely checked THP-1 differentiation by monitoring their adhesion to the plate and changes in cell morphology.

Design of PPRHs

PPRHs were designed using The Triplex Oligonucleotide Target Sequence Search Software (http://utw10685.utweb.utexas.edu/tfo/, Austin, Texas, USA).

PPRHs were synthesized as non-modified desalted oligodeoxynucleotides by Sigma-Aldrich (HaverHill, United Kingdom). Lyophilized PPRHs were resuspended in sterile Tris-EDTA buffer (1 mM EDTA and 10 mM Tris, pH 8.0) (Sigma-Aldrich, Madrid, Spain) and stored at −20˚C until use.

As a negative control, we used a Watson-Crick hairpin (Hp-WC) that forms intramolecular Watson–Crick bonds instead of reverse Hoogsteen bonds, and therefore the polypurine domain of the hairpin cannot bind to the polypyrimidine target sequence in the DNA.

The sequences of the PPRHs and the negative control hairpin and their abbreviations are described in Fig 1.

Transfection of PPRHs

Cells were plated in 6-well dishes. Transfection consisted in mixing 100 nM of PPRH with 10 μM of the cationic liposome N-[1-(2,3-dioleoyloxy)propil]-N,N,N-trimethylammonium methylsulfate (DOTAP) (Biontex, München, Germany) in a final volume of 200 μL of culture medium. The mixture was incubated for 20 min at room temperature. Finally, the PPRH/liposome complex was added to the cells to attain a final volume of 1 mL.

RNA extraction

Total RNA was extracted from PC3 and THP-1 cells 24 h and 48 h after transfection, respectively, using TRIzol (Life Technologies, Barcelona, Spain) following the manufacturer's specifications. RNA was quantified by measuring its absorbance at 260 nm using a NanoDrop ND-1000 spectrophotometer (Thermo Fisher Scientific, Barcelona, Spain).

Reverse transcription

cDNA was synthesized by reverse transcription in a 20 μl reaction mixture containing 1 μg of total RNA, 125 ng of random hexamers (Roche, Madrid, Spain), 500 μM of each dNTP (Panreac Applichem, Barcelona, Spain), 2 μL of 10X buffer, 20 units of RNAse inhibitor and 200 units of Moloney murine leukemia virus reverse transcriptase (Last three from Lucigen, Wisconsin, USA). The reaction was incubated at 42˚C for 1 h.

Real-time PCR

The StepOnePlus Real-Time PCR Systems (Applied Biosystems, Barcelona, Spain) was used to perform these experiments. The primer sequences to determine *PD1* mRNA levels were 5'GGATTTCCAGTGGCGAGAGA3' and 5'CAGACGGAGTATGCCACCATT3'. TATA box binding protein (TBP) was used as endogenous control and the primer sequences were

Name	Sequence (5´- 3´)	Position
PPRHs against *PD-1* gene		
HpPD1-Pr	GAGCAGAGACACAGAGGAGGAAGGG T T T GAGCAGAGACACAGAGGAGGAAGGG T T	Promoter
HpPD1-E1	AGGCGGAGGTGAGCGGAAGGGAAA T T T AGGCGGAGGTGAGCGGAAGGGAAA T T	Exon 1
PPRHs against *PD-L1* gene		
HpPDL1-I1	GGGATGGAGAGAGGAGAAGGGAAAGGGAA T T T GGGATGGAGAGAGGAGAAGGGAAAGGGAA T T	Intron 1
HpPDL1-I2	AGTGGTGAAGGGAGGAGGGACA T T T AGTGGTGAAGGGAGGAGGGACA T T	Intron 2
Negative control		
Hp-WC	CCCTCCTTCCCTCGCTCCC T T T GGGAGGAAGGGAGCGAGGG T T	-----

Fig 1. PPRHs designed against *PD-1* and *PD-L1* genes, as well as the negative control hairpin. Abbreviations are (i) Hp, hairpin; (ii) I, intron; (iii) Pr, promoter; (iv) E, exon. WC stands for the Watson-Crick negative control.

https://doi.org/10.1371/journal.pone.0206818.g001

5'GAGCTGTGATGTGAAGTTTCC3' and 5'TCTGGGTTTGATCATTCTGTAG3'. The reaction was performed in a final volume of 20 μl, containing 1 X SYBR Universal PCR Master mix (Applied Biosystems, Barcelona, Spain), 0.25 μM of reverse and forward primers (Sigma-Aldrich, Madrid, Spain), 5 μl of cDNA and H_2O mQ. PCR cycling conditions were 10 min denaturation at 95°C, 40 cycles of 15 s at 95°C and 1 min at 64°C.

To determine *PD-L1* mRNA levels in PC3 cells, *PD-L1* Taqman probe (Assay ID: Hs00204257_m1) was used. Cyclophilin A Taqman probe (PPIA) (Assay ID: Hs04194521-s1) was used as endogenous control. The reaction contained 1x TaqMan Universal PCR Master mix, 1x TaqMan probe (both from Applied Biosystems, Barcelona, Spain), 3 μL of cDNA and H_2O mQ to a final volume of 20 μL. PCR cycling conditions were 10 min denaturation at 95°C, followed by 40 cycles of 15 s at 95°C and 1 min at 60°C.

The mRNA quantification was performed using the ΔΔCt method, where Ct is the threshold cycle that corresponds to the cycle where the amount of amplified mRNA reaches the

106

threshold of fluorescence. Data were expressed as mRNA levels relative to the cells treated with the negative control Hp-WC.

Western blot analyses

Total protein extracts from PC3 cells (90,000) were obtained 24 h after transfection. Cells were washed once with PBS 1X and collected by scrapping in 100 μL of Lysis buffer [150 mM NaCl, 1 mM EDTA, 50 mM Tris-HCl pH 8.0, 1.0% Igepal CA-630 (NP-40), 0.5% sodium deoxycholate, 0.1% sodium docecyl sulfate, 1 mM PMSF, 10 mM NAF and Protease inhibitor cocktail (all from Sigma Aldrich, Madrid, Spain)]. Cell debris was removed by centrifugation (12,000 x g at 4˚C for 10 min).

In the case of THP-1 monocytes (90,000), cells were collected 48 h after transfection and centrifuged for 5 min at 800 x g at room temperature. Then, cells were resuspended in 50 μL of RIPA buffer [150 mM NaCl, 5 mM EDTA, 50 mM Tris-HCl pH 7,4, 1.0% Igepal CA-630 (NP-40), 100 μg/mL PMSF and Protease inhibitor cocktail (all from Sigma Aldrich, Madrid, Spain)]. Cell lysate was kept on ice for 30 min, vortexing every 10 min. Cell debris was removed by centrifugation at 12,000 x g at 4˚C for 10 min. The Bradford method was used to determine protein concentration using bovine serum albumin as a standard.

Whole cell extracts were resolved in 10% SDS-polyacrylamide gels and transferred to PVDF membranes. The blocking solution was 5% Blotto. Membranes were probed during 90 min at room temperature with primary antibodies against PD-L1 (1:250 dilution; PA5-28115, Thermo Fisher Scientific, Barcelona, Spain), PD-1 (Pdcd-1L1, 1C10; 1:50 dilution; sc-293425, Santa Cruz Biotechnology, Heidelberg, Germany) and GAPDH (1:200 dilution; sc-47724, Santa Cruz Biotechnology, Heidelberg, Germany) to normalize the results. Detection was achieved by secondary HRP-conjugated antibodies: anti-rabbit (1:1000 dilution; Dako, Denkmark) for PD-L1 and anti-mouse (1:1000; sc-516102, Santa Cruz Biotechnology, Heidelberg, Germany) for PD-1 and GAPDH. Chemiluminescence was detected with Image Quant LAS 4000 mini technology (GE Healthcare, Barcelona, Spain). Quantification was performed using Image Studio Lite Software. Data were represented as protein levels relative to the control cells (untransfected cells).

Cell titration

Before performing the co-culture experiments, we set up the number of cells to be used for each cell line. Cell titration was carried out by increasing either the number of macrophages or the number of cancer cells. In the case of macrophages/PC3 co-cultures, we opted to start with 80,000 PC3 cells that were cultured with an increasing number of macrophages, observing that the best ratio was obtained with 10,000 cells (Table 1). Regarding macrophages/SKBR3 co-cultures, we selected 10,000 macrophages with an increasing number of SKBR3 cells and the best ratio was established at 1:6 (Table 2). When using macrophages/M21 co-cultures, since M21 were more resistant to the treatment, we opted for increasing the number of macrophages to

Table 1. Co-culture titration of PC3 cells with increasing number of macrophages.

Macrophages/PC3 Co-culture titration with 80,000 PC3 cells	
N˚ of macrophages	Cell viability (%)
1,000	66%
5,000	32%
10,000	10%
20,000	60%

https://doi.org/10.1371/journal.pone.0206818.t001

Table 2. Co-culture titration of macrophages with increasing number of SKBR3 cells.

Macrophages/SKBR3 Co-culture titration with 10,000 macrophages	
N° of SKBR3 cells	Cell viability (%)
60,000	12%
90,000	22%
120,000	32%

https://doi.org/10.1371/journal.pone.0206818.t002

60,000, thus establishing a macrophages/M21 ratio of 1:1. Finally, in the macrophages/HeLa co-cultures, the experiments were performed using the same conditions that with macrophages/PC3 co-cultures.

Co-culture experiments

THP-1 cells were plated in 6-well dishes and transfected with different PPRHs against *PD-1*. After 24 h, transfected THP-1 cells were treated with 2 ng/mL of PMA for differentiation. Three days after PMA treatment, the PMA-containing medium was replaced with fresh medium and different number of cancer cells were added to the plates containing the macrophages, as indicated in Table 3. After 6 h, cells were transfected with different PPRHs against *PD-L1*. Cell viability was assessed 4 days after the last transfection by MTT assays. The co-culture procedure is depicted in Fig 2.

MTT assays

Four days after the last transfection, 500 μg/mL of 3-(4,5-Dimethylthiazol-2-yl)-2,5-Diphenyl-tetrazolium Bromide (MTT) and 100 μM of sodium succinate (both from Sigma-Aldrich, Madrid, Spain) were added to the culture medium and incubated for 2.5 h at 37°C for the reaction. After incubation, the medium was removed and the solubilization reagent (0.57% acetic acid and 10% sodium dodecyl sulfate in DMSO) (Sigma-Aldrich, Madrid, Spain) was added. Cell survival was measured at 570 nm in a Modulus Microplate luminometer (Turner BioSystems; Promega, Madrid, Spain). Results were expressed as the percentage of cell survival relative to cells transfected with the negative control (Hp-WC).

Apoptosis assay

Apoptosis was determined by the rhodamine method: 48 h after the last transfection, rhodamine 123 (final concentration 5 μg/mL) (Sigma-Aldrich, Madrid, Spain) was added for 30 min. Then, cells were collected, centrifuged at 800 x g at 4°C for 5 min and washed once in PBS. The pellet was resuspended in 500 μL of cold PBS and Propidium Iodide at a final concentration of 5 μg/mL (Sigma-Aldrich, Madrid, Spain) was added. Flow cytometry analyses were performed in a Beckman Coulter CyAn ADP cytometer (Beckman Coulter Inc., Madrid, Spain) and data were analyzed using the software Summit v4.3. The percentage of propidium

Table 3. Number of macrophages and cancer cells plated in each co-culture experiment.

Cancer cell line	Number of cancer cells in co-culture experiments	Number of macrophages in co-culture experiments
PC3	80,000	10,000
M21	60,000	60,000
SKBR3	60,000	10,000
HeLa	80,000	10,000

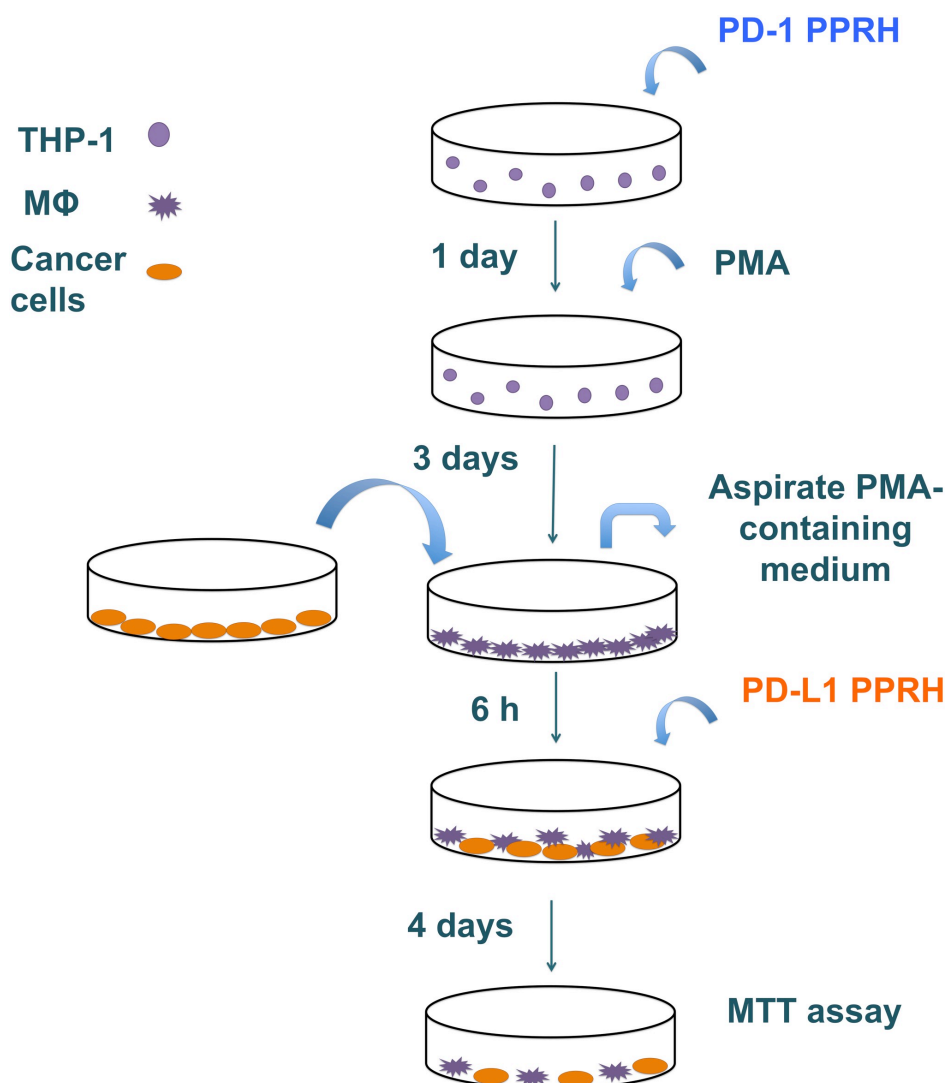https://doi.org/10.1371/journal.pone.0206818.t003

108

Fig 2. Schematic representation of co-culture experiments. THP-1 cells were plated and immediately transfected with PPRHs against *PD-1*. After 24 h, transfected THP-1 cells were differentiated to macrophages (Mφ) with PMA for 3 days. At that time, the PMA-containing medium was replaced with fresh medium and cancer cells were added to the dishes containing the macrophages. After 6 h, cells were transfected with different PPRHs against *PD-L1*. Cell viability (MTT) assay was performed 4 days after transfection with PPRHs against *PD-L1*.

https://doi.org/10.1371/journal.pone.0206818.g002

109

iodide-negative and rhodamine-negative cells corresponded to the apoptotic population. Data were expressed as the apoptosis fold-increase levels relative to the co-culture transfected with the negative control Hp-WC.

Statistical analyses

Statistical analyses were carried out using GraphPad Prism 5 (GraphPad Software, California, USA). All data are shown as the mean ± SEM of three independent experiments. Statistical significance was determined using one-way analysis of variance, followed by Dunnett's multiple comparison test. In the apoptosis experiments, a two-way ANOVA with Sidak's multiple comparisons test was used. Differences were considered significant when $p < 0.05$.

Results

Effect of PPRHs on *PD-1* and *PD-L1* mRNA and protein levels

PPRHs against *PD-1* were tested in THP-1 cells. *PD-1* mRNA levels were determined upon cell incubation with two different PPRHs against *PD-1*, HpPD1-Pr and HpPD1-E1, whose sequences are shown in Fig 1. These PPRHs were able to decrease *PD-1* mRNA levels by 2.4 and 2.7-fold, respectively, compared to the negative control Hp-WC (Fig 3A). On the other hand, when targeting *PD-L1* in PC3 cells, two different PPRHs were used, HpPDL1-I1 and HpPDL1-I2 (Fig 1), which decreased *PD-L1* mRNA levels by 2.2 and 1.8-fold, respectively, compared to the negative control (Fig 3B). When analyzing PD-1 protein levels in THP-1 cells, HpPD1-Pr and HpPD1-E1 decreased PD-1 protein by 78% and 66%, respectively, relative to the control (Fig 4A). HpPDL1-I1 and HpPDL1-I2 decreased PD-L1 protein levels in PC3 cells by 69% and 71%, respectively, compared to the control (Fig 4B).
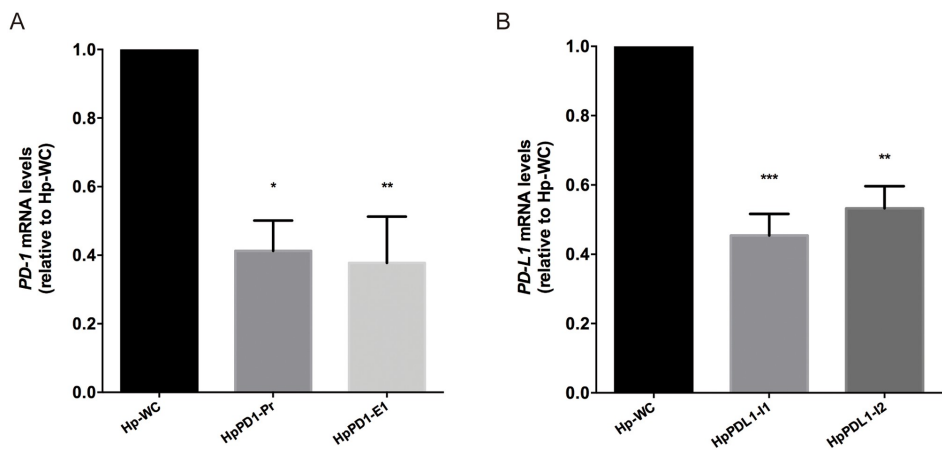
Fig 3. Effect of PPRHs on *PD-1* and *PD-L1* mRNA levels. A) THP-1 cells (90,000) were transfected with two PPRHs against *PD-1* and mRNA levels were determined 48 h after transfection. B) PC3 cells (90,000) were transfected with two PPRHs against *PD-L1* and mRNA levels were assessed 24 h after transfection. mRNA levels are plotted relative to the cells treated with the negative control (Hp-WC). Data represent the mean ± SEM of three experiments. (*p < 0.05, **p < 0.01, ***p < 0.005).
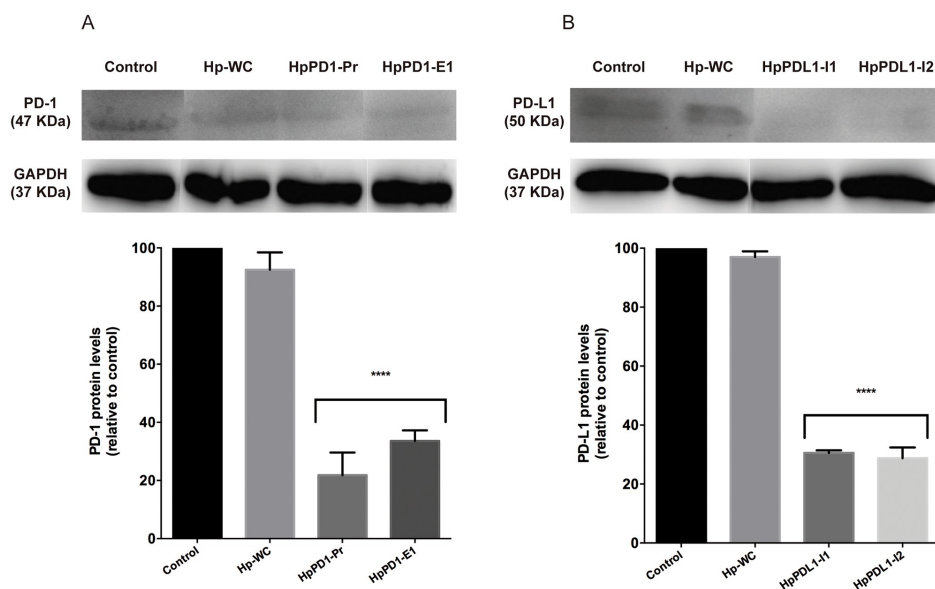
110

Fig 4. Effect of PPRHs on PD-1 and PD-L1 protein levels. A) THP-1 cells (90,000) were transfected with two PPRHs against PD-1 and protein extracts were obtained after 48 h. B) PC3 cells (90,000) were transfected with two PPRHs against PD-L1 and proteins were extracted after 24 h. Representative Western blot images of PD-1 and PD-L1 are shown. The quantification of the changes in protein levels were determined upon normalization with the signal corresponding to GAPDH protein. Non-transfected cells and cells treated with the negative control hairpin were used as controls. Data represent the mean ± SEM of three experiments. (****p < 0.001).

https://doi.org/10.1371/journal.pone.0206818.g004

Effect of PPRHs on cell viability in PC3 and THP-1 cells

We determined whether the different PPRHs against *PD-1* and *PD-L1* could provoke, on their own, any cytotoxic effect in THP-1 and PC3 cells. The transfection of the different PPRHs separately and their combinations did not cause any significant effect on cell viability in either THP-1 (Fig 5A) or macrophages (Fig 5B). However, in PC3 cells, HpPDL1-I1 and HpPDL1-I2 directed against *PD-L1*, provoked a decrease in cell viability of 65% and 45%, respectively, confirming the role of PD-L1 in tumor cell progression (Fig 5C). In contrast, PPRHs against PD-1 did not cause any effect in PC3 cells (Fig 5C).

Effect of PPRHs on PC3 cell viability in co-culture experiments

First, we tested the effect of HpPD1-Pr and HpPD1-E1 against *PD-1* and HpPDL1-I1 and HpPDL1-I2 against *PD-L1* in co-culture experiments with macrophages and PC3 cells. When silencing *PD-1* in macrophages with HpPD1-Pr or HpPD1-E1, macrophages were able to kill 37% and 39% of PC3 cells, respectively (Fig 6A). When *PD-L1* was silenced with HpPDL1-I1 or HpPDL1-I2 in PC3 cells, 62% and 66% of the cells were killed by macrophages (Fig 6A). To assess whether the inhibition of both target genes could lead to an enhanced effect, macrophages and PC3 cells were transfected together in co-culture experiments with the four combinations of PPRHs such as each of the two hairpins against *PD-1* was combined with each one
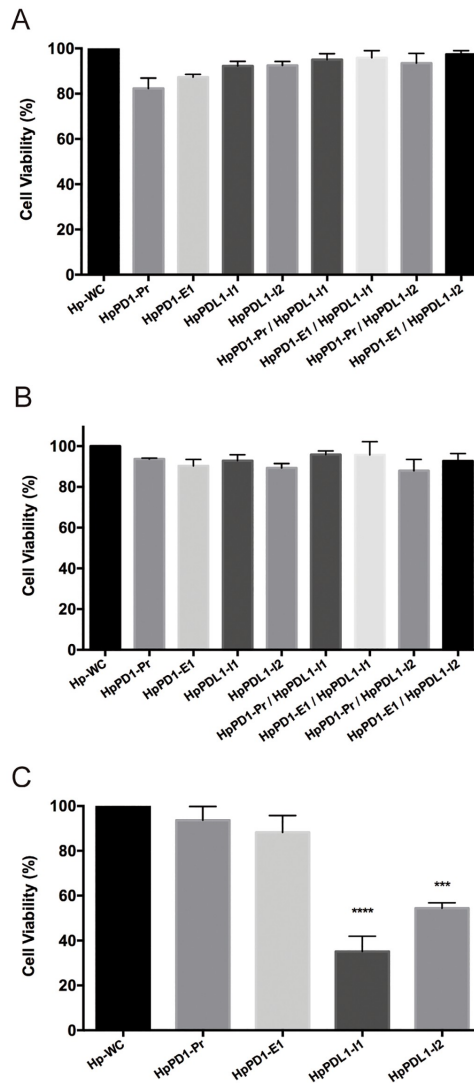
111

Results

Fig 5. Effect on cell viability upon incubation with PPRHs against *PD-1* and *PD-L1*. A) THP-1 cells (10,000) were treated with PPRHs against *PD-1*, *PD-L1* or in combination. B) Macrophages (10,000) were treated with PPRHs against *PD-1*, *PD-L1* or in combination. C) PC3 cells (80,000) were transfected with PPRHs against *PD-1* and *PD-L1*. Cell viability was assessed 5 days after transfection. Cells treated with the negative control hairpin (Hp-WC) were used as control. Data represent the mean ± SEM of three independent experiments performed on different days. (***p<0.005, ****p< 0.001).

112
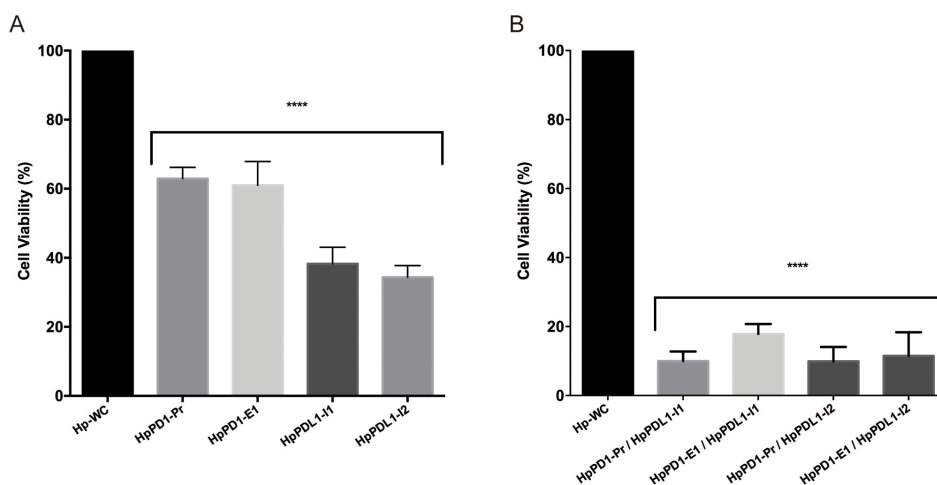
Fig 6. Macrophages/PC3 co-culture experiments. A) Effect on cell viability of PPRHs against *PD-1* transfected only in 10,000 macrophages or PPRHs against *PD-L1* transfected only in 80,000 PC3 cells, in co-culture experiments. B) Effect on cell viability, in co-culture experiments, of PPRHs against PD-1 transfected in macrophages plus PPRHs against PD-L1 transfected in PC3 cells, making a total of four combinations of PPRHs. Co-cultures incubated with the negative control hairpin (Hp-WC) were used as controls. Data represent the mean ± SEM of three independent experiments. (****p< 0.001).

against *PD-L1*. In these conditions, we observed that the best combination of PPRHs against *PD-1/PD-L1* was HpPD1-Pr/HpPDL1-I1 that provoked 90% cell death in co-culture (Fig 6B).

Effect of PPRHs on cell viability in co-culture experiments with M21, HeLa and SKBR3 cells

To extend the results observed in PC3 cells, we incubated all the combinations of PPRHs against *PD-1* and *PD-L1* in three other cancer cell lines, M21, HeLa and SKBR3, in co-culture experiments. In M21 cells, the best combination of PPRHs was HpPD1-E1/HpPDL1-I1, which provoked 65% cell death (Fig 7A). In HeLa cells, the HpPD1-E1/HpPDL1-I1 combination led to a reduction of 92% in cell viability (Fig 7B). Finally, the combination HpPD1-E1/HpPDL-I2 in SKBR3 cells was able to reduce cell viability by 88% (Fig 7C).

Level of apoptosis in co-culture experiments with PC3, M21, HeLa and SKBR3 cells

To gain insight into the mechanism that provoked cancer cells death in the co-culture experiments, we determined the levels of apoptosis in the different cell lines upon 48 hours of incubation with the different PPRHs. The most effective combinations of PPRHs against *PD-1* and *PD-L1* determined in the cell viability assays for each cancer cell line were selected for the apoptosis studies. First of all, we checked the effect on apoptosis of the different combinations of PPRHs in macrophages. We did not observe any increase in the apoptotic levels (Fig 8A), thus demonstrating that macrophages were not affected by the transfection of the different PPRHs. However, co-cultures of macrophages with either PC3, HeLa or SKBR3 cells showed 2.1, 2.7
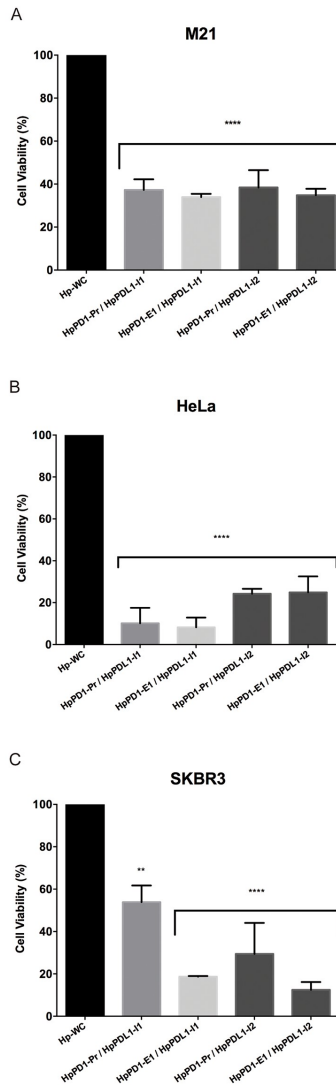
Results

Fig 7. Co-culture experiments with other cancer cell lines. M21 (60,000) (A), HeLa (80,000) (B) or SKBR3 (60,000) (C) cells were co-cultured with 60,000, 10,000 and 10,000 macrophages, respectively. Macrophages were treated with either HpPD1-Pr or HpPD1-E1 whereas cancer cells were transfected with either HpPDL1-I1 or HpPDL1-I2 against *PD-L1*. Co-cultures treated with the negative control hairpin (Hp-WC) were used as control. Data represent the mean ± SEM of at least three experiments. ($**$p < 0.01, $****$p < 0.001).

https://doi.org/10.1371/journal.pone.0206818.g007

114
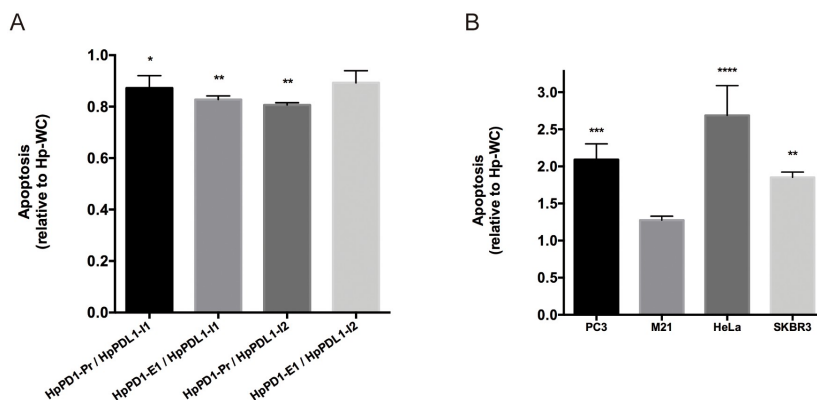
Fig 8. Apoptosis determination. A) Apoptotic levels in macrophages treated with the different combinations of PPRHs. B) Apoptotic levels in co-culture experiments using the most effective combination of PPRHs for each cancer cell line. Changes in apoptosis are represented relative to co-cultures transfected with the negative control hairpin (Hp-WC). Data represent the mean ± SEM of three experiments performed on different days. (*p < 0.05, **p < 0.01, ***p < 0.005, ****p < 0.001).

https://doi.org/10.1371/journal.pone.0206818.g008

and 1.8-fold increase in apoptosis, respectively, when compared to their respective negative controls (Fig 8B). Finally, co-culture of macrophages with M21 cancer cell line showed a moderate increase (1.3-fold) in the apoptotic population after the treatment (Fig 8B), in accordance with the observed results in cell viability.

Discussion

In this work we describe an immunotherapy approach using PPRHs directed against *PD-1* and *PD-L1* in PMA-differentiated THP-1 cells and PC3 cancer cells, respectively, to favor the elimination of tumor cells by macrophages. It has been previously demonstrated that these molecules represent a novel gene silencing tool against different cancer targets, both *in vitro* [20,25–27] and *in vivo* [28]. In addition, PPRHs are more stable, showing a half-life much longer than that of siRNAs, and they do not activate the innate inflammatory response [29]. We have used this gene silencing tool to conduct an immunotherapy approach against both *CD47* in MCF-7 cells and *SIRPα* in macrophages, respectively, achieving a large decrease in cell viability [23].

In the present study, we showed that different cancer cells were killed by macrophages in co-culture experiments upon silencing of *PD-1/PD-L1* interaction with four different PPRHs, whereas tumor cells remain unaffected when treated with the negative control.

A first step consisted in determining at the molecular level that the designed PPRHs were able to decrease the expression at the level of mRNA and protein of *PD-1* and *PD-L1* in THP-1 monocytes and PC3 cells, respectively, thus demonstrating the specific gene silencing effect of the four PPRHs used.

An important point was to verify whether any of the four PPRHs used in the study was able to produce a cytotoxic effect *per se* due to the specific silencing of either *PD-1* or *PD-L1* in both THP-1 and PC3 cells, in the absence of co-culture. The rationale for this control was to state the contribution of macrophages in the co-culture experiments to eliminate cancer cells after silencing PD-1 and PD-L1 in THP-1 and PC3 cells, respectively, and not by the effect that the PPRHs could provoke by themselves. In the case of THP-1 cells and macrophages, none of the

Results

four PPRHs, two against *PD-1* and two against *PD-L1*, produced a significant effect on cell viability. However, in PC3 cells, the two PPRHs directed against *PD-L1* were able to decrease cell viability by themselves. It has been reported that, aside from avoiding tumor immunity, PD-1/PD-L1 inhibition has also cancer cell-intrinsic functions that promote tumor growth and survival such as mTOR signaling. Therefore, suppressing either PD-1 or PD-L1 could attenuate the growth of PD-L1+ cancer cells [30,31]. In this direction, in a recent study Li *et al.* reported that the inhibition of *PD-L1* with a siRNA in gastric cancer cells suppressed cell proliferation, migration and tumorigenicity both *in vitro* and *in vivo* [32]. Another study also demonstrated that silencing *PD-L1* in colon cancer cells with a siRNA reduced cell progression and led to an increase in apoptosis [33]. Similarly, Song *et al.* reported that knocking down PD-L1 in pancreatic ductal adenocarcinoma decreased cell proliferation [34]. Finally, a recent study of Kwak and collaborators showed that silencing of PD-L1 with a siRNA in melanoma cells provoked a 25% decrease in cell viability *in vitro*. When the siRNA complexed with a polymeric carrier was injected in a xenograft mouse model, tumor growth was reduced by 60% approximately [35].

Cerignoli and collaborators showed that stimulated PBMCs previously treated with an anti-PD-1 antibody provoked a maximum cytolysis of 80% in PC3 cells later in co-culture experiments [36]. In this direction, in our co-culture approach, when *PD-1* was silenced in macrophages with non-transfected PC3 cells, the reduction in cell viability was about 40%.

When comparing the effect of silencing *PD-L1* with HpPDL1-I2 in PC3 cells alone with that produced in PC3 cells co-cultured with non-transfected macrophages, the reduction of cell viability in the latter was 20% higher. Since PD-1/PD-L1 interaction prevents the phagocytosis of tumor cells by macrophages, our hypothesis was to achieve an additional effect by inhibiting PD1/PD-L1 interaction acting on both genes in their respective cell lines, thus increasing the efficacy of the immunotherapeutic treatment. Therefore, an important conclusion of our work is that silencing *PD-1* and *PD-L1* in THP-1 and PC3 cells, respectively, led to death of the vast majority of PC3 cells (90%) by macrophages in each of the four possible combinations of PPRHs.

At this point, we wanted to expand our results in PC3 cells to additional cancer cell lines. In this regard the same approach was applied in M21, HeLa and SKBR3 cancer cell lines, observing that silencing of PD-1 and PD-L1 in co-culture experiments produced a high degree of cell mortality in all cases. HeLa cells were the most affected by the treatment, followed by SKBR3 and M21 cells. Based on data from The Human Protein Atlas (https://www.proteinatlas.org/), both cervix and prostate tissues present a higher expression of PD-L1 compared with breast and skin tissues. For that reason, we believe that the differences in the outcome of the treatment in the different cancer cell lines could be due to the differential expression of *PD-L1*. Iwamura *et al.* described that when suppressing *PD-L1* expression with a siRNA in a lung adenocarcinoma cell line, the specific lysis of tumor cells conducted by CD8+ T cells was 10% [37]. However, in our case, when silencing PD-L1 with PPRHs in PC3 cells, macrophages were able to kill two thirds (66%) of the cancer cell population. Juneja *et al.* also determined that *PD-L1* expression in murine colon adenocarcinoma MC38 cells inhibited CD8+ T cell response and cytotoxicity against tumor cells. However, CD8+ T cells were still able to kill tumor cells that did not express *PD-L1*, demonstrating its significant suppressing effect [38].

Another conclusion from our study is that apoptosis is part of the mechanism of killing in co-culture incubations with differentiated macrophages and cancer cells treated with their respective PPRHs targeting either PD-1 or PD-L1, in agreement with those reported in [36]. The levels of apoptosis in each cell line correlate with its observed decrease in cell viability.

There are currently two anti-PD-1 and three anti-PD-L1 antibodies approved for the treatment of different types of cancer and some other molecules are still in clinical trials [39].

116

Cancer immunotherapy using PolyPurine Reverse Hoogsteen hairpins targeting the PD-1/PD-L1 pathway

Several anti-CD47 antibodies are also in Phase I clinical trials [40]. In a recent study, anti-CD47 and anti-PD-L1 monotherapies were used against tumor mice models. Although both treatments were able to reduce tumor size, combination of anti-CD47 and anti-PD-L1 treatments showed the greatest reduction, thus increasing the survival of the animals more than either monotherapy [19]. Therefore, CD47 and PD-L1 are good targets for immunotherapy strategies, as we also demonstrated using PPRHs against these genes in the present work and in [23].

In conclusion, we performed an *in vitro* immunotherapy approach based in silencing, by means of PPRHs, *PD-1* in macrophages and *PD-L1* in different cancer cells in co-culture experiments to inhibit their interaction, thus increasing the phagocytic potency of macrophages against the tumor. Therefore, this work extends the usage of PPRHs as alternative pharmacological agents in immunotherapy against PD-1 and PD-L1.

Author Contributions

Conceptualization: Carlos J. Ciudad, Véronique Noé.

Data curation: Miriam Marlene Medina Enríquez, Alex J. Félix.

Formal analysis: Miriam Marlene Medina Enríquez, Alex J. Félix, Carlos J. Ciudad.

Funding acquisition: Véronique Noé.

Investigation: Miriam Marlene Medina Enríquez, Alex J. Félix, Véronique Noé.

Methodology: Miriam Marlene Medina Enríquez, Alex J. Félix.

Project administration: Véronique Noé.

Supervision: Carlos J. Ciudad, Véronique Noé.

Writing – original draft: Miriam Marlene Medina Enríquez, Alex J. Félix, Véronique Noé.

Writing – review & editing: Carlos J. Ciudad, Véronique Noé.

References

1. Dunn GP, Bruce AT, Ikeda H, Old LJ, Schreiber RD. Cancer immunoediting: From immunosurveillance to tumor escape. Nat Immunol. 2002; 3(11):991–8. https://doi.org/10.1038/ni1102-991 PMID: 12407406

2. Swann JB, Smyth MJ. Review series Immune surveillance of tumors. J Clin Invest. 2007; 117(5): 1137–46. https://doi.org/10.1172/JCI31405 PMID: 17476343

3. Munn DH, Cheung NK. Phagocytosis of tumor cells by human monocytes cultured in recombinant macrophage colony-stimulating factor. J Exp Med [Internet]. 1990; 172(1):231–7. Available from: http://www.pubmedcentral.nih.gov/articlerender.fcgi?artid=2188164&tool=pmcentrez&rendertype=abstract PMID: 2193096

4. Jadus MR, Irwin MC, Irwin MR, Horansky RD, Sekhon S, Pepper K a, et al. Macrophages can recognize and kill tumor cells bearing the membrane isoform of macrophage colony-stimulating factor. Blood [Internet]. 1996; 87(12):5232–41. Available from: http://www.ncbi.nlm.nih.gov/pubmed/8652838 PMID: 8652838

5. Jaiswal S, Jamieson CHM, Pang WW, Park CY, Chao MP, Majeti R, et al. CD47 Is Upregulated on Circulating Hematopoietic Stem Cells and Leukemia Cells to Avoid Phagocytosis. Cell [Internet]. 2009; 138(2):271–85. Available from: http://dx.doi.org/10.1016/j.cell.2009.05.046 PMID: 19632178

6. Sharma P, Wagner K, Wolchok JD, Allison JP. Novel cancer immunotherapy agents with survival benefit: recent successes and next steps. Nat Publ Gr [Internet]. 2011; 11(11):805–12. Available from: http://dx.doi.org/10.1038/nrc3153

7. Yaddanapudi K, Mitchell RA, Eaton JW. Cancer vaccines: Looking to the future. Oncoimmunology. 2013; 2(3).

117

PLOS ONE

Cancer immunotherapy using PolyPurine Reverse Hoogsteen hairpins targeting the PD-1/PD-L1 pathway

8. Qian X, Wang X, Jin H. Cell Transfer Therapy for Cancer: Past, Present, and Future. J Immunol Res. 2014;525913(Dc):9 pages.

9. Yee C. Adoptive T-cell therapy for cancer: Boutique therapy or treatment modality? Clin Cancer Res. 2013; 19(17):4550–2. https://doi.org/10.1158/1078-0432.CCR-13-1367 PMID: 23922301

10. Rosenberg SA, Yang JC, Sherry RM, Kammula US, Hughes MS, Phan GQ, et al. Durable complete responses in heavily pretreated patients with metastatic melanoma using T-cell transfer immunotherapy. Clin Cancer Res. 2011; 17(13):4550–7. https://doi.org/10.1158/1078-0432.CCR-11-0116 PMID: 21498393

11. Mellman I, Coukos G, Dranoff G. Cancer immunotherapy comes of age. Nature [Internet]. 2011; 480(7378):480–9. Available from: http://dx.doi.org/10.1038/nature10673 PMID: 22193102

12. Ribas A, Wolchok JD. Cancer immunotherapy using checkpoint blockade. Science (80-) [Internet]. 2018; 359(6382):1350–5. Available from: http://www.sciencemag.org/lookup/doi/10.1126/science.aar4060

13. Mahoney KM, Rennert PD, Freeman GJ. Combination cancer immunotherapy and new immunomodulatory targets. Nat Rev Drug Discov. 2015; 14(8):561–84. https://doi.org/10.1038/nrd4591 PMID: 26228759

14. Brahmer JR, Tykodi SS., Chow Q. M. L, Hwu W-J, Topalian SL., Hwu P, et al. Safety and activity of anti-PD-L1 antibody in patients with advanced cancer. N Engl J Med [Internet]. 2012; 366:2455–65. Available from: http://dx.doi.org/10.1056/NEJMoa1200694 PMID: 22658128

15. Alsaab HO, Sau S, Alzhrani R, Tatiparti K, Bhise K, Kashaw SK, et al. PD-1 and PD-L1 checkpoint signaling inhibition for cancer immunotherapy: mechanism, combinations, and clinical outcome. Front Pharmacol. 2017; 8(AUG):1–15.

16. Li Y, Li F, Jiang F, Lv X, Zhang R, Lu A, et al. A mini-review for cancer immunotherapy: Molecular understanding of PD-1/ PD-L1 pathway & translational blockade of immune checkpoints. Int J Mol Sci. 2016; 17(7):1–22.

17. Guan J, Lim KS, Mekhail T, Chang CC. Programmed death ligand-1 (PD-L1) expression in the programmed death receptor-1 (PD-1)/PD-L1 blockade a key player against various cancers. Arch Pathol Lab Med. 2017; 141(6):851–61. https://doi.org/10.5858/arpa.2016-0361-RA PMID: 28418281

18. Wang X, Teng F, Kong L, Yu J. PD-L1 expression in human cancers and its association with clinical outcomes. Onco Targets Ther. 2016; 9:5023–39. https://doi.org/10.2147/OTT.S105862 PMID: 27574444

19. Gordon SR, Maute RL, Dulken BW, Hutter G, George BM, McCracken MN, et al. PD-1 expression by tumour-associated macrophages inhibits phagocytosis and tumour immunity. Nature [Internet]. 2017; 545(7655):495–9. Available from: http://dx.doi.org/10.1038/nature22396 PMID: 28514441

20. de Almagro MC, Coma S, Noé V, Ciudad CJ. Polypurine hairpins directed against the template strand of DNA knock down the expression of mammalian genes. J Biol Chem. 2009; 284(17):11579–89. https://doi.org/10.1074/jbc.M900981200 PMID: 19261618

21. Ciudad CJ, Rodríguez L, Villalobos X, Félix AJ, Noé V. Polypurine Reverse Hoogsteen Hairpins as a Gene Silencing Tool for Cancer. Curr Med Chem [Internet]. 2017; 24(26):2809–26. Available from: http://www.ncbi.nlm.nih.gov/pubmed/28260512%0Ahttp://www.eurekaselect.com/150562/article PMID: 28260512

22. Goñi JR, de la Cruz X, Orozco M. Triplex-forming oligonucleotide target sequences in the human genome. Nucleic Acids Res. 2004; 32(1):354–60. https://doi.org/10.1093/nar/gkh188 PMID: 14726484

23. Bener G, Félix AJ., Sánchez de Diego C, Pascual Fabregat I, Ciudad CJ, Noé V. Silencing of CD47 and SIRPα by Polypurine reverse Hoogsteen hairpins to promote MCF-7 breast cancer cells death by PMA-differentiated THP-1 cells. BMC Immunol [Internet]. 2016; 17(1):32. Available from: http://bmcimmunol.biomedcentral.com/articles/10.1186/s12865-016-0170-z PMID: 27671753

24. Félix AJ, Ciudad CJ, Noé V. Functional pharmacogenomics and toxicity of PolyPurine Reverse Hoogsteen hairpins directed against survivin in human cells. Biochem Pharmacol [Internet]. 2018; 155(June):8–20. Available from: https://linkinghub.elsevier.com/retrieve/pii/S0006295218302338

25. de Almagro MC, Mencia N, Noé V, Ciudad CJ. Coding Polypurine Hairpins Cause Target-Induced Cell Death in Breast Cancer Cells. Hum Gene Ther [Internet]. 2011 Apr [cited 2016 Dec 7]; 22(4):451–63. Available from: http://www.ncbi.nlm.nih.gov/pubmed/20942657 PMID: 20942657

26. Villalobos X, Rodríguez L, Solé A, Lliberós C, Mencia N, Ciudad CJ, et al. Effect of Polypurine Reverse Hoogsteen Hairpins on Relevant Cancer Target Genes in Different Human Cell Lines. Nucleic Acid Ther [Internet]. 2015 Aug [cited 2016 May 2]; 25(4):198–208. Available from: http://www.ncbi.nlm.nih.gov/pubmed/26042602 PMID: 26042602

27. Rodríguez L, Villalobos X, Solé A, Lliberós C, Ciudad CJ, Noé V. Improved design of PPRHs for gene silencing. Mol Pharm. 2015; 12(3):867–77. https://doi.org/10.1021/mp5007008 PMID: 25615267

118

28. Rodríguez L, Villalobos X, Dakhel S, Padilla L, Hervas R, Hernández JL, et al. Polypurine reverse Hoogsteen hairpins as a gene therapy tool against survivin in human prostate cancer PC3 cells in vitro and in vivo. Biochem Pharmacol. 2013; 86(11):1541–54. https://doi.org/10.1016/j.bcp.2013.09.013 PMID: 24070653

29. Villalobos X, Rodríguez L, Prévot J, Oleaga C, Ciudad CJ, Noé V. Stability and immunogenicity properties of the gene-silencing polypurine reverse hoogsteen hairpins. Mol Pharm. 2014; 11(1):254–64. https://doi.org/10.1021/mp400431f PMID: 24251728

30. Kleffel S, Posch C, Barthel SR, Mueller H, Schlapbach C, Guenova E, et al. Melanoma Cell-Intrinsic PD-1 Receptor Functions Promote Tumor Growth. Cell [Internet]. 2015; 162(6):1242–56. Available from: http://dx.doi.org/10.1016/j.cell.2015.08.052 PMID: 26359984

31. Clark CA, Gupta HB, Sareddy G, Pandeswara S, Lao S, Yuan B, et al. Tumor-intrinsic PD-L1 signals regulate cell growth, pathogenesis, and autophagy in ovarian cancer and melanoma. Cancer Res. 2016; 76(23):6964–74. https://doi.org/10.1158/0008-5472.CAN-16-0258 PMID: 27671674

32. Li J, Chen L, Xiong Y, Zheng X, Xie Q, Zhou Q, et al. Knockdown of PD-L1 in Human Gastric Cancer Cells Inhibits Tumor Progression and Improves the Cytotoxic Sensitivity to CIK Therapy. Cell Physiol Biochem. 2017; 41(3):907–20. https://doi.org/10.1159/000460504 PMID: 28222426

33. Shi SJ, Wang LJ, Wang GD, Guo ZY, Wei M, Meng YL, et al. B7-H1 Expression Is Associated with Poor Prognosis in Colorectal Carcinoma and Regulates the Proliferation and Invasion of HCT116 Colorectal Cancer Cells. PLoS One. 2013; 8(10):1–11.

34. Song X, Liu J, Lu Y, Jin H, Huang D. Overexpression of B7-H1 correlates with malignant cell proliferation in pancreatic cancer. Oncol Rep. 2014; 31(3):1191–8. https://doi.org/10.3892/or.2013.2955 PMID: 24378899

35. Kwak G, Kim D, Nam G, Young Wang S, Kim I-S, Hwa Kim S, et al. Programmed Cell Death Protein Ligand-1 (PD-L1) Silencing with Polyethylenimine-Dermatan Sulfate Complex for Dual Inhibition of Melanoma Growth. ACS Nano. 2017; 11(10):10135–46. https://doi.org/10.1021/acsnano.7b04717 PMID: 28985469

36. Cerignoli F, Abassi YA, Lamarche BJ, Guenther G, Ana DS, Guimet D, et al. In vitro immunotherapy potency assays using real-time cell analysis. PLoS One. 2018; 13(3):1–21.

37. Iwamura K, Kato T, Miyahara Y, Naota H, Mineno J, Ikeda H, et al. SiRNA-mediated silencing of PD-1 ligands enhances tumor-specific human T-cell effector functions. Gene Ther [Internet]. 2012; 19(10):959–66. Available from: http://dx.doi.org/10.1038/gt.2011.185 PMID: 22113316

38. Juneja VR, McGuire KA, Manguso RT, LaFleur MW, Collins N, Haining WN, et al. PD-L1 on tumor cells is sufficient for immune evasion in immunogenic tumors and inhibits CD8 T cell cytotoxicity. J Exp Med [Internet]. 2017; 214(4):895–904. Available from: http://www.jem.org/lookup/doi/10.1084/jem.20160801 PMID: 28302645

39. Gong J, Chehrazi-Raffle A, Reddi S, Salgia R. Development of PD-1 and PD-L1 inhibitors as a form of cancer immunotherapy: A comprehensive review of registration trials and future considerations. J Immunother Cancer. 2018; 6(1):1–18.

40. Weiskopf K. Cancer immunotherapy targeting the CD47/SIRPα axis. Eur J Cancer [Internet]. 2017; 76:100–9. Available from: http://dx.doi.org/10.1016/j.ejca.2017.02.013 PMID: 28286286

Results

4.4 Article IV:

Silencing PD-1 and PD-L1: the potential of PolyPurine Reverse Hoogsteen hairpins for the elimination of tumor cells

Carlos J. Ciudad, Miriam Marlene Medina Enriquez, Alex J. Félix, Gizem Bener and Véronique Noé.

Results

Commentary

Immunotherapy

Silencing PD-1 and PD-L1: the potential of PolyPurine Reverse Hoogsteen hairpins for the elimination of tumor cells

Carlos J Ciudad[1], Mariam Marlene Medina Enriquez[1], Alex J Félix[1], Gizem Bener[1] & Véronique Noé*[,1]

[1]Department of Biochemistry & Physiology School of Pharmacy & Food Sciences & Institute of Nanoscience & Nanotechnology
IN2UB University of Barcelona 08028 Barcelona, Spain
*Author for correspondence: vnoe@ub.edu

❝the *in vitro* approach based on PPRH-mediated silencing of *PD-L1* in cancer cells and *PD-1* in macrophages proves that PPRHs can be alternative pharmacological agents in immunotherapy against PD-1 and PD-L1❞

The PD-1/PD-L1 pathway in cancer

The success or failure of the immune system to reject the tumor depends on the tumor immune tolerance. By mimicking signaling pathways of the immune system itself, tumors create conditions that favor their escape, survival and dissemination. Since the discovery of immune checkpoints, or brakes of the immune system, which was the theme for the Nobel Prize award in Physiology or Medicine in November 2018, checkpoint inhibitors are becoming standard of care for various malignancies for their ability to discriminate between 'self' from 'non-self'. Releasing these brakes shows striking effects in patients with several types of cancer, including lung cancer, renal cancer, lymphoma and melanoma, setting the basis for cancer therapy by inhibition of negative immune regulation.

PD-1 expression is induced when T cells become activated, and thus it may enhance their proliferation in the presence of ligand. When an inflammatory response is triggered, the main function of PD-1 in peripheral tissues is to regulate the activity of T cells to control autoimmunity. This results in a major immune resistance in the tumors.

The two ligands for PD-1 are PD-1 ligand 1 (PD-L1) and PD-L2. PD-L1, the primary PD-1 ligand, is overexpressed on the cell surface from many different human tumors. In these conditions, PD-L1 binds to PD-1 receptors on the activated T cells, thus inhibiting these T cells and blocking cytokine production and the cytolytic activity of PD-1+, tumor-infiltrating CD4$^+$ and CD8$^+$ T cells.

Inhibition of PD-1/PD-L1 as immunotherapy approach

The PD-1/PD-L1 pathway has become a promising target for cancer immunotherapy. Avoiding the interaction between PD-L1 and PD-1 increases immune responses *in vitro* [1] and promotes preclinical antitumor activity [2]. Inhibition of PD-L1 by a monoclonal antibody produces both tumor regression and disease stabilization in patients with metastatic non-small-cell lung cancer, melanoma, renal cell cancer and ovarian cancer [3]. The first PD-1 inhibitors, nivolumab and pembrolizumab, were approved by the US FDA in 2014 and now are being routinely used for previously treated squamous non-small-cell lung carcinoma and metastatic melanoma. A new anti-PD-L1 drug (MEDI4736) is effective in early clinical trials and atezolizumab (MPDL3280A), which is another anti-PD-L1 candidate drug, is also showing significant benefits in clinical trials. Nowadays and according to the Cancer Research Institute, there are over 1500 clinical trials testing checkpoint inhibitors. However, in spite of the significant advancement in therapy approaches based on monoclonal antibodies targeting these checkpoint molecules, manufacturing complexity and repeated dosing may represent some limitations for the use of this technology.

Future Medicine

PolyPurine Reverse Hoogsteen hairpins technology

Bearing in mind that the cost of a checkpoint inhibitor therapy represents $150,000 per year, the search for alternatives to monoclonal antibodies is more than justified. In this direction, PolyPurine Reverse Hoogsteen (PPRH) hairpins are nonmodified DNA molecules, thus very economical, composed of two antiparallel polypurine mirror repeat sequences linked by a five-thymidine loop, thus forming intramolecular reverse-Hoogsteen bonds between both domains. One of the strands of the PPRH binds to a specific polypyrimidine stretch in the double-stranded DNA (dsDNA) by Watson–Crick bonds but maintaining the hairpin structure. Upon binding their polypyrimidine target in the dsDNA, PPRHs provoke strand displacement of the polypurine tract of the duplex [4] producing inhibition of transcription or altering splicing, thus causing specific gene silencing. Therefore, to design a PPRH, it is needed to look for polypyrimidine/polypurine tracts within the gene sequence. These sequences can be found in the genome with higher frequency than initially predicted by random models [5]; they are preferentially located in promoters and introns, although they are also found in exons at lower frequency. The target sequences may contain up to three purine interruptions.

Since the polypyrimidine domains can be located in either strand of the dsDNA, PPRHs can be designed to target the appropriate strand of genomic DNA. Template-PPRHs are those PPRHs directed against the template strand of the gene, and coding-PPRHs the ones targeting the coding strand of the dsDNA of the gene. All these molecules are able to decrease gene expression using different mechanisms [6,7]. On the one hand, template-PPRHs inhibit transcription, thus decreasing the expression of the target gene at the level of mRNA and protein. On the other hand, coding-PPRHs can also bind to the mRNA in addition to the coding strand of the gene, because both have the same sequence and orientation. A coding-PPRH against an intron sequence of the *dhfr* gene produced a splicing alteration of the DHFR mRNA by inhibiting the binding of a pre-mRNA splicing factor (U2AF65), thus decreasing gene expression [7]. In addition, both template- and coding-PPRHs can inhibit transcription by interfering with the binding of transcription factors to promoter sequences [8].

Stability experiments performed in fetal calf serum revealed that the half-life of PPRHs was ten-times longer than that of siRNAs. Similar results were obtained in mouse and human serum and were also longer in cultured PC3 cells. Regarding the innate immune response, different determinations indicated that PPRHs, unlike siRNAs, do not activate the innate inflammatory response, neither at the levels of transcription factors IRF3 and NF-κB nor at the expression levels of several proinflammatory cytokines [9]. Different characteristics of PPRHs to improve their usage as a tool for gene silencing were determined, such as the role of PPRH length from 20 to 30 nucleotides, observing an increase in activity in parallel with the length in that range. PPRHs showed a higher affinity of binding and efficacy on cell viability compared with nonmodified triplex-forming oligonucleotides. To overcome possible off-target effects, wild-type (WT) PPRHs, containing the complementary bases to purine interruptions in the target sequence were tested (up to 3 pyrimidines). These WT-PPRHs could bind to their target sequence with higher affinity and higher effect in terms of decreasing cell viability. Additionally, a brand-new molecule termed Wedge-PPRH was developed with the ability to lock the dsDNA into the displaced structure. The efficacy of these PPRHs was demonstrated in prostate and breast cancer cell lines [10]. To design a Wedge-PPRH the 5′ flank of the sequence is extended with the corresponding polypyrimidine stretch complementary to the polypurine strand. The rationale of this construction was that such PPRH would open the dsDNA and the extension sequence could bind to the displaced strand.

Recently, a pharmacogenomics study of specific and unspecific hairpins against the *survivin* gene was performed. The specific PPRH generated 244 differentially expressed genes that clustered in gene sets of regulation of cell proliferation, cellular response to stress, apoptosis and prostate cancer. However, an unspecific hairpin or control Hp-WC did not originate differentially expressed genes demonstrating the lack of off-target effects. Additionally, the unspecific hairpin did not cause toxicity in cell survival assays and produced minor changes in gene expression for selected genes in RT-qPCR arrays specifically developed for hepatic and renal toxicity screening when tested in HepG2 and 786-O cell lines, respectively [11].

Cancer therapy using PPRHs

The ability of PPRHs to silence a variety of relevant cancer-related genes, in addition to *DHFR, telomerase* and *survivin* [6,8] was determined in several human cell lines [12]. PPRHs against *BCL2, MYC, mTOR, TOP1* and *MDM2* were designed and assayed for target mRNA levels, cytotoxicity and apoptosis in pancreas, colon, breast and prostate cancer cell lines. These PPRHs were effective in reducing mRNA levels and cell survival and increasing apoptosis in cancer cells. In addition, to demonstrate the gene silencing effectiveness of PPRHs *in vitro*, two *in*

124

vivo efficacy assays were conducted using two different routes of administration, intratumorally and intravenously, in a subcutaneous xenograft tumor model of PC3 prostate cancer cells. Regardless the route of administration, the specific coding-PPRH targeting *survivin* caused a decrease in tumor volume, survivin protein levels and blood vessel formation, establishing the proof of principle for their use as a therapeutic tool [8].

Immunotherapy using PPRHs

In the context of immunotherapy, PPRHs were also previously used to inhibit the expression of *SIRPα* in macrophages and *CD47* in tumor cells with the purpose to eliminate tumor cells by macrophages in co-culture experiments [13]. The specific PPRHs decreased *SIRPα* expression in macrophages and *CD47* expression in the breast cancer cell line MCF-7 both at the mRNA and protein levels. Upon treatment with these PPRHs, macrophages eliminated MCF-7 cells in co-culture experiments, thus supporting the usage of PPRHs in immunotherapy approaches. More recently, a similar strategy of cancer immunotherapy was applied, this time targeting the tandem *PD-1* and *PD-L1* expressed in macrophages and PC3 prostate cancer cells, respectively. PPRHs were able to decrease mRNA and protein levels of PD-1 and PD-L1 provoking an increase in cytotoxicity in co-culture experiments using macrophages and cancer cells. This approach was also successfully tested in HeLa, SKBR3 and M21 cancer cell lines [14].

More in detail, the results showed that PPRHs against *PD-1* tested in THP-1 cells and PPRHs against *PD-L1* tested in PC3 cells were able to decrease mRNA levels of both targets by twofold. PD-1 protein levels in THP-1 cells and PD-L1 protein levels in prostate cancer PC3 cells were reduced by 70% in both cases. In co-culture experiments, the best combination of PPRHs against *PD-1/PD-L1* caused the death of 90% of prostate cancer PC3 cells, 65% of melanoma M21 cells, 92% of cervix cancer HeLa cells and 88% of breast cancer SKBR3 cells. The mechanism by which the cancer cells were killed by macrophages was partly due to an increase in apoptosis.

In summary, the *in vitro* approach based on PPRH-mediated silencing of *PD-L1* in cancer cells and *PD-1* in macrophages proves that PPRHs can be alternative pharmacological agents in immunotherapy against PD-1 and PD-L1.

Conclusion

The PD-1/PD-L1 pathway is relevant in cancer since it is involved in the ability of tumor cells to escape immune surveillance. Thus, this pathway constitutes a novel target approach in cancer therapy. In this direction, PPRHs are a silencing technology that have shown their efficacy in *in vitro* and *in vivo* cancer models. Moreover, PPRH synthesis is economical, their stability is higher than siRNAs and they showed a low toxicity profile without off-target effects. This technology has been used in the field of immunotherapy against SIRPα in macrophages and CD47 in tumor cells and more recently against the tandem PD-1 and PD-L1 expressed in macrophages and prostate, melanoma cervix and breast cancer cells. Therefore, PPRHs could be envisaged as alternative pharmacological agents in immunotherapy.

Author contributions

MMM Enriquez performed acquisition, analysis and interpretation of data for the work and drafted the manuscript. AJ Felix performed acquisition, analysis and interpretation of data for the work and drafted the manuscript. G Bener performed acquisition, analysis and interpretation of data for the work and drafted the manuscript. CJ Ciudad performed conceptualization, funding acquisition, investigation, formal analysis, supervision and writing. V Noé performed conceptualization, funding acquisition, investigation, project administration, supervision and writing

References

1. Fife BT, Pauken KE, Eagar TN *et al.* Interactions between PD-1 and PD-L1 promote tolerance by blocking the TCR-induced stop signal. *Nat. Immunol.* 10(11), 1185–1192 (2009).

2. Iwai Y, Ishida M, Tanaka Y, Okazaki T, Honjo T, Minato N. Involvement of PD-L1 on tumor cells in the escape from host immune system and tumor immunotherapy by PD-L1 blockade. *Proc. Natl Acad. Sci. USA* 99(19), 12293–12297 (2002).

3. Brahmer JR, Pardoll DM. Immune checkpoint inhibitors: making immunotherapy a reality for the treatment of lung cancer. *Cancer Immunol. Res.* 1(2), 85–91 (2013).

4. Coma S, Noe V, Eritja R, Ciudad CJ. Strand displacement of double-stranded DNA by triplex-forming antiparallel purine-hairpins. *Oligonucleotides* 15(4), 269–283 (2005).

5. Goni JR, De La Cruz X, Orozco M. Triplex-forming oligonucleotide target sequences in the human genome. *Nucleic Acids Res.* 32(1), 354–360 (2004).

6. De Almagro MC, Coma S, Noe V, Ciudad CJ. Polypurine hairpins directed against the template strand of DNA knock down the expression of mammalian genes. *J. Biol. Chem.* 284(17), 11579–11589 (2009).

7. De Almagro MC, Mencia N, Noe V, Ciudad CJ. Coding polypurine hairpins cause target-induced cell death in breast cancer cells. *Hum. Gene Ther.* 22(4), 451–463 (2011).

8. Rodriguez L, Villalobos X, Dakhel S *et al.* Polypurine reverse Hoogsteen hairpins as a gene therapy tool against survivin in human prostate cancer PC3 cells *in vitro* and *in vivo*. *Biochem. Pharmacol.* 86(11), 1541–1554 (2013).

9. Villalobos X, Rodriguez L, Prevot J, Oleaga C, Ciudad CJ, Noe V. Stability and immunogenicity properties of the gene-silencing polypurine reverse Hoogsteen hairpins. *Mol. Pharm.* 11(1), 254–264 (2014).

10. Rodriguez L, Villalobos X, Sole A, Lliberos C, Ciudad CJ, Noe V. Improved design of PPRHs for gene silencing. *Mol. Pharm.* 12(3), 867–877 (2015).

11. Felix AJ, Ciudad CJ, Noe V. Functional pharmacogenomics and toxicity of PolyPurine Reverse Hoogsteen hairpins directed against survivin in human cells. *Biochem. Pharmacol.* 155, 8–20 (2018).

12. Villalobos X, Rodriguez L, Sole A *et al.* Effect of polypurine reverse hoogsteen hairpins on relevant cancer target genes in different human cell lines. *Nucleic Acid Ther.* 25(4), 198–208 (2015).

13. Bener G, Felix AJ, Sanchez De Diego C, Pascual Fabregat I, Ciudad CJ, Noe V. Silencing of CD47 and SIRPalpha by Polypurine reverse Hoogsteen hairpins to promote MCF-7 breast cancer cells death by PMA-differentiated THP-1 cells. *BMC Immunol.* 17(1), 32 (2016).

14. Medina Enriquez MM, Felix AJ, Ciudad CJ, Noe V. Cancer immunotherapy using PolyPurine Reverse Hoogsteen hairpins targeting the PD-1/PD-L1 pathway in human tumor cells. *PLoS ONE* 13(11), e0206818 (2018).

126

4.5 Article V:

Correction of the *aprt* gene using Repair-PolyPurine Reverse Hoogsteen hairpins in mammalian cells

Alex J. Félix, Carlos J. Ciudad and Véronique Noé

Background: Repair of point mutations in the DNA is one of the strategies for the treatment of monogenic diseases. A Repair-PPRH consists of a PPRH hairpin core bearing an extension sequence at one end, which is homologous to the DNA sequence to be repaired but containing the wild type nucleotide instead of the mutated one. We previously used different repair-PPRHs to correct deletions, insertions, substitutions and a double substitution present in a collection of CHO mutant cell lines deficient for the *dhfr* gene (Solé *et al.* 2014, 2016).

Objectives: The main aim of this work was to demonstrate the generality of action of repair-PPRH by correcting different point mutations in the endogenous *locus* of the *aprt* gene in CHO mutant cells. Additionally, we wanted to explore the possible off-target effects of this technology and gain insight into the molecular mechanism responsible for the repair event.

Results: Different repair-PPRHs were designed targeting three different single substitutions present in three different *aprt* mutants (S23, S62 and S1 cell lines). We demonstrated that these repair-PPRH were able to correct the targeted mutation contained in their respective cell line by DNA sequencing. Gene correction was also confirmed by an increase in APRT mRNA levels of the repaired clones compared to the mutant cells. In the same way, repaired clones showed very high levels of APRT enzymatic activity, whereas the mutant APRT enzyme did not present any. We also determined that the gene correction frequency when cells were transfected in S phase of the cell cycle was increased compared to cells transfected in asynchronous state. Regarding the possible off-target effects, we performed a Whole-Genome Sequencing analysis comparing S23 mutant cells and S23 cells repaired with the repair-PPRH. We did not detect any off-target effects in the genome of the repaired cells. No random insertions

nor deletions were detected, and the repair-PPRH itself was not inserted in any region of the repaired genome. Finally, we performed gel-shift assays demonstrating the binding of the repair-PPRH to the target sequence and the subsequent formation of a displacement loop (D-loop) structure that can be responsible for an homologous recombination event.

Conclusions: This work demonstrated the generality of repair-PPRHs to specifically correct point mutations at their endogenous *locus* in mammalian cells without detecting off-target modifications in the genome. We also showed the formation of a D-loop structure upon the binding of the PPRH to its target sequence that is involved in the homology directed repair pathway, giving information about the mechanism by which the repair event may occur.

AMERICAN SOCIETY of
GENE & CELL
THERAPY

Correction of the *aprt* Gene Using Repair-Polypurine Reverse Hoogsteen Hairpins in Mammalian Cells

Alex J. Félix,[1,2] Carlos J. Ciudad,[1,2] and Véronique Noé[1,2]

[1]Department of Biochemistry and Physiology, School of Pharmacy and Food Sciences, University of Barcelona, 08028 Barcelona, Spain; [2]Institute for Nanoscience and Nanotechnology IN2UB, University of Barcelona, 08028 Barcelona, Spain

In this study, we describe the correction of single-point mutations in mammalian cells by repair-polypurine reverse Hoogsteen hairpins (repair-PPRHs). These molecules consist of (1) a PPRH hairpin core that binds to a polypyrimidine target sequence in the double-stranded DNA (dsDNA), producing a triplex structure, and (2) an extension sequence homologous to the DNA sequence to be repaired but containing the wild-type nucleotide instead of the mutation and acting as a donor DNA to correct the mutation. We repaired different point mutations in the adenosyl phosphoribosyl transferase (*aprt*) gene contained in different *aprt*-deficient Chinese hamster ovary (CHO) cell lines. Because we had previously corrected mutations in the dihydrofolate reductase (*dhfr*) gene, in this study, we demonstrate the generality of action of the repair-PPRHs. Repaired cells were analyzed by DNA sequencing, mRNA expression, and enzymatic activity to confirm the correction of the mutation. Moreover, whole-genome sequencing analyses did not detect any off-target effect in the repaired genome. We also performed gel-shift assays to show the binding of the repair-PPRH to the target sequence and the formation of a displacement-loop (D-loop) structure that can trigger a homologous recombination event. Overall, we demonstrate that repair-PPRHs achieve the permanent correction of point mutations in the dsDNA at the endogenous level in mammalian cells without off-target activity.

INTRODUCTION

Monogenic disorders present a global prevalence at birth of 10 out of 1,000 cases, thus affecting millions of people worldwide.[1] These diseases are the result of single-point mutations in the DNA sequence of a specific gene that lead to the production of nonfunctional versions of the protein. In recent years, different gene-editing tools have been developed to correct mutations in the double-stranded DNA (dsDNA). On the one hand, several molecular tools such as zinc-finger nucleases (ZFNs),[2–5] transcription activator-like nucleases (TALENs),[6–10] and CRISPR/Cas9 RNA-guided nucleases[11–15] have been used to conduct gene correction therapies. These editing technologies rely on the usage of nucleases to generate locus-specific dsDNA breaks near the mutation and a donor DNA sequence that acts as a template for the correction. However, new CRISPR/Cas9 ap-

proaches such as base editing and prime editing that do not rely on dsDNA breaks to produce the correction have been also developed. Briefly, base editing is based on the deamination of the purine or pyrimidine base to eventually convert one base pair to another in the dsDNA.[16–18] Prime editing technology can directly write new genetic information into a specific DNA site by a Cas9 endonuclease fused to a reverse transcriptase programmed with a guide RNA that both specifies the target and encodes the desired editing.[19] In this case, it is necessary to generate a nick in one of the strands (protospacer-adjacent motif strand). Nevertheless, one of the main concerns upon using these nuclease-dependent technologies is the appearance of off-target effects in the genome of the host after the treatment.[20,21] On the other hand, modified or non-modified single-stranded oligodeoxynucleotides (ssODNs) have also been developed to produce the correction of single-point mutations in the dsDNA. In some cases, the ssODN containing the corrected sequence binds to its target dsDNA in a sequence-specific manner, leading to a recombination event that incorporates the corrected nucleotide.[22–25] In other cases, modified molecules such as peptide nucleic acids (PNAs) and their derivatives (e.g., γPNAs) are presently used to bind to the dsDNA, creating a triplex helical structure that stimulates the recombination between a nearby sequence and a provided donor DNA that contains the corrected nucleotide.[26–30]

Polypurine reverse Hoogsteen hairpins (PPRHs) are single-stranded and non-modified oligodeoxynucleotides composed of two antiparallel polypurine mirror repeat domains linked by a five-thymidine loop. The intramolecular linkage consists of reverse-Hoogsteen bonds between the purines, allowing the formation of the hairpin structure. PPRHs bind in a sequence-specific manner to polypyrimidine stretches in the dsDNA via Watson-Crick bonds while maintaining the hairpin conformation, thus producing a triplex structure and displacing the fourth strand of the dsDNA.[31,32] During the last decade,
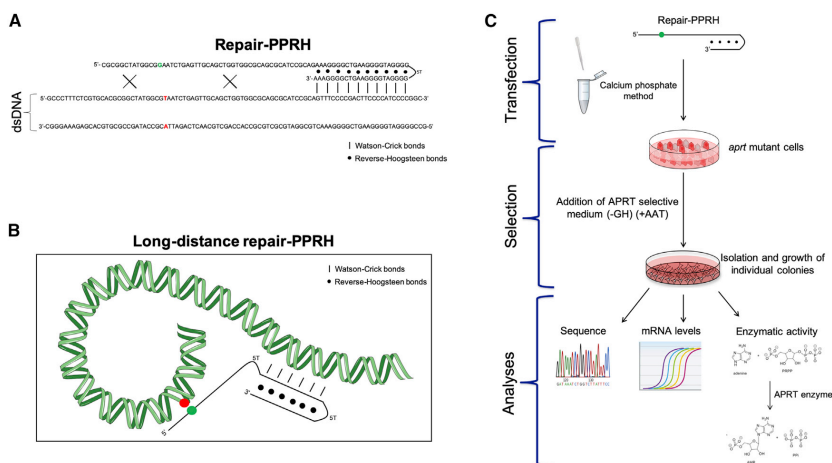
Results

Figure 1. Gene Correction Strategy Using Repair-PPRHs

(A) Structure of a repair-PPRH, consisting of a hairpin core linked to a repair domain. The core is formed by two polypurine domains linked by five thymidines, which are bound intramolecularly by reverse-Hoogsteen bonds that bind to its polypyrimidine target sequence in the dsDNA via Watson-Crick bonds. The repair domain is a sequence homologous to the DNA sequence to be repaired but containing the corrected nucleotide instead of the mutation. Mutation in the dsDNA is represented in red, whereas the correct nucleotide contained in the repair-PPRH is shown in green. (B) Scheme of a long-distance repair-PPRH containing a hairpin core that binds to a polypyrimidine target sequence away from the location of the mutation. This hairpin core is linked to a repair domain containing the wild-type nucleotide (green) by five additional thymidines (5T). Mutation in the DNA is represented in red. (C) General procedure for the targeted correction using repair-PPRHs of the adenosyl phosphoribosyl transferase (*aprt*) gene in a collection of *aprt*-deficient CHO cell lines. The approach involved transfection and selection (+AAT) of the repaired cells followed by sequencing analyses and determination of mRNA levels and enzymatic activity.

PPRHs have been used to silence genes involved in resistance to chemotherapeutic drugs,[33] cancer progression,[32,34–37] and immunotherapy approaches.[38–40] Recently, we performed a pharmacogenomic study showing the specificity of the PPRH toward its target sequence and the absence of off-target effects when using a negative DNA hairpin. We also demonstrated that PPRHs do not cause hepatotoxicity or nephrotoxicity *in vitro*.[41]

Repair-PPRHs are hairpins that bear an extension sequence at one end of the molecule (usually the 5′ end) that is homologous to the DNA sequence to be corrected but contains the wild-type nucleotide instead of the mutated one. A previous study performed in our laboratory demonstrated that repair-PPRHs were able to correct a single-point mutation in a plasmid containing a mutated version of the dihydrofolate reductase (*dhfr*) minigene. The correction was also achieved when the plasmid was stably transfected into a *dhfr*-deficient Chinese hamster ovary (CHO) cell line.[42] Furthermore, we also corrected different types of point mutations (substitutions, insertions, and deletions) at the endogenous locus of the *dhfr* gene using repair-PPRHs in various *dhfr* mutant CHO cell lines.[43]

In this work, we show the generality of action of repair-PPRHs by correcting single-point mutations at the endogenous locus of the *aprt* gene in mammalian cells (Figure 1), and we assess the absence of off-target effects of this gene-editing technology. Moreover, we gain insight into the molecular mechanism involving homologous recombination that could be responsible for the gene correction event.

RESULTS

Targeted Correction of Point Mutations at the Endogenous Locus of the *aprt* Gene

Our goal was to correct three *aprt*-deficient CHO cell lines presenting different point mutations in the *aprt* locus, leading to premature stop codons. For that reason, we designed different repair-PPRHs as described in the Materials and Methods and shown in Table S2. Each repair-PPRH contained a hairpin core that binds to a specific polypyrimidine sequence near the mutation to direct the repair domain.

The first cell line to be corrected was the S23 mutant, in which the substitution of a guanine for a thymidine in exon 1 led to a TAA stop codon (ochre) *in situ*. The repair-PPRH (HpS23E1rep) contained three pyrimidine interruptions in the hairpin core, and the repair domain contained a 51-nt sequence as an extension of the hairpin core. Upon transfection and selection, the analyzed colonies
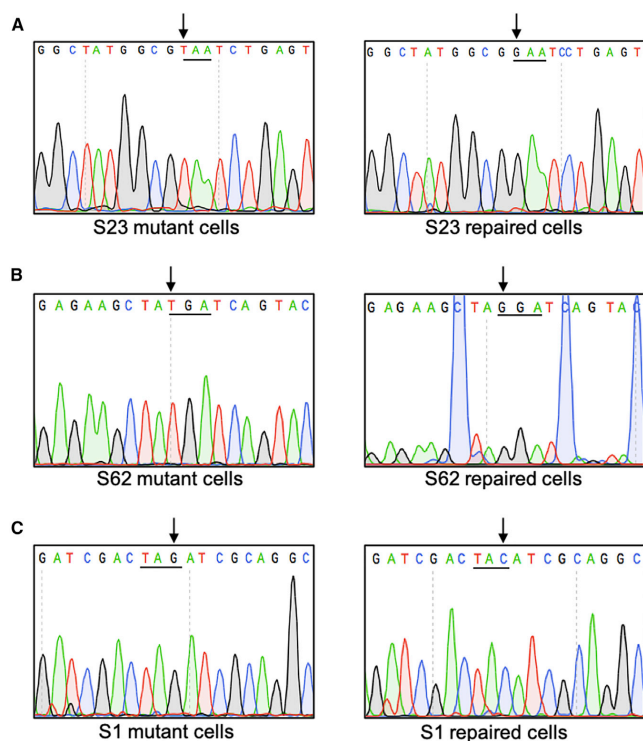
Figure 2. DNA Sequencing Results

(A–C) DNA sequences from mutants S23 (A), S62 (B), and S1 (C) and their repaired counterparts obtained after transfection with the corresponding repair-PPRH and subsequent selection. The underlined nucleotides represent the mutated/repaired codon, and the arrows indicate the specific nucleotide subjected to correction. Each experiment was conducted a minimum of three times, and a minimum of three different colonies were analyzed.

bore the corrected nucleotide, rescuing the wild-type triplet (GAA) encoding for a glutamic acid (Figure 2A).

The next mutant, S62, contained a substitution of a guanine for a thymidine in exon 5 that led to a TGA stop codon (opal) in place. The repair-PPRH (HpS62E5rep) contained two pyrimidine interruptions in the hairpin core, and the length of the repair domain was 57 nt. We confirmed the restoration of the wild-type codon (glycine) in the analyzed colonies (Figure 2B).

Finally, the S1 mutant bore a substitution of a cytosine for a guanine in exon 2, producing a TAG premature stop codon (amber). The repair-PPRH (HpS1E2rep) contained one pyrimidine interruption in the hairpin core and a 57-nt repair domain, restoring the wild-type codon (tyrosine) (Figure 2C).

To test the requirement of the hairpin core to correct the mutation, the repair domains of the different repair-PPRHs were transfected alone in their respective mutant cell lines. No surviving colonies were observed after transfecting the RD-S23E1rep, RD-S62E5rep,

and RD-S1E2rep in the S23, S62, and S1 mutant cell lines, respectively. As an additional negative control, we transfected a full repair-PPRH containing a scrambled polypurine hairpin attached to the specific repair domain of the S23 mutant (HpS23E1rep-Sc) into S23 cells, and we did not obtain any surviving cell colony.

All of the previous repair-PPRHs contained repair domains attached directly to the hairpin core, which was close to the mutation site. We wanted to explore whether we could repair a mutation using a hairpin core that was binding farther away from the mutation site and connected to the repair domain through an additional pentathymidine loop. Therefore, we designed a long-distance repair-PPRH (LD-HpS1E2rep) oligonucleotide in which the target sequence of the repair domain was located 24 nt upstream of the polypyrimidine target sequence of the hairpin core. This long-distance repair-PPRH containing a 52-nt repair domain was also able to correct the mutation, restoring the wild-type nucleotide.

APRT mRNA Levels Are Increased in the Repaired Cells

We assessed the restoration of APRT mRNA levels in the repaired cells in comparison with the mutant cell lines and the wild-type D422 cell line. In S23 repaired clones, APRT mRNA levels were increased between 1.25- and 2-fold when compared with those of the S23 mutant cell line (Figure 3A). Regarding S62 repaired clones, APRT mRNA levels were similar to those of the mutant, since the mutation is located in the last exon of the gene (exon 5) and, therefore, non-sense-mediated decay does not take place (Figure 3B). The increase in APRT mRNA levels was also observed in the case of S1 repaired colonies (Figure 3C). There were no significant differences between APRT mRNA levels from clones repaired by the HpS1E2rep repair-PPRH and by the LD-HpS1E2rep long-distance repair-PPRH (Figure 3C).

APRT Enzymatic Activity Is Restored in Repaired Cells

We determined the enzymatic activity of APRT protein in the mutant cell lines and the repaired clones. S23 and S62 mutants
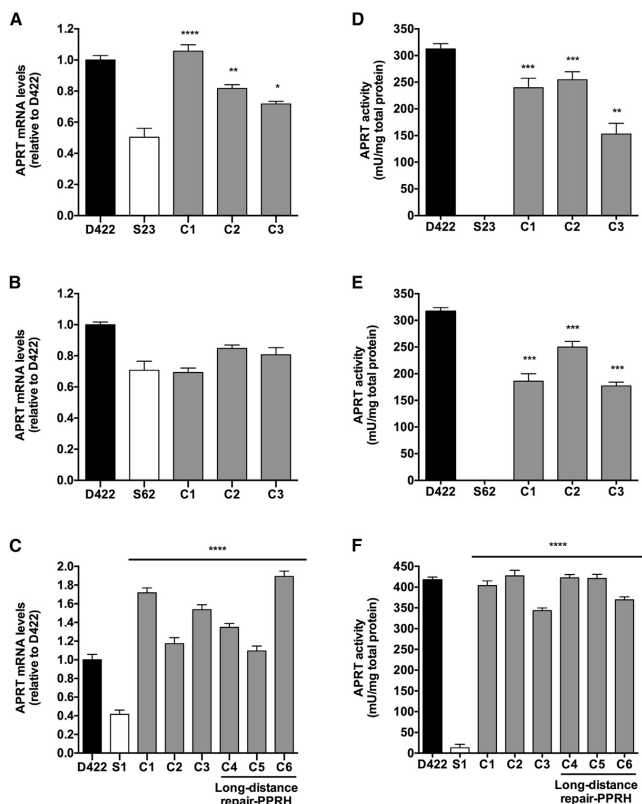
Results

Figure 3. APRT mRNA and Enzymatic Analyses

(A–C) APRT mRNA levels of mutants S23 (A), S62 (B), and S1 (C) and their repaired counterparts obtained after transfection with the corresponding repair-PPRHs and subsequent selection are shown. In (C), also represented are the *aprt* mRNA levels in three clones repaired using the long-distance repair-PPRH (LD-HpS1E2rep). APRT mRNA levels were determined by qRT-PCR and normalized with TBP mRNA. Data are plotted relative to the wild-type cell line D422. (D–F) APRT enzymatic activity was determined for mutants S23 (D), S62 (E), and S1 (F) and their repaired counterparts obtained after transfection with the corresponding repair-PPRHs and subsequent selection. In (F), also shown are the APRT enzymatic activity levels of three clones repaired with the long-distance repair-PPRH (LD-HpS1E2rep). The D422 wild-type cell line was included in the determination as the positive control. Data are represented as mU of APRT enzyme divided by the mg of total protein extract. Error bars represent the standard error of the mean of three experiments. Statistical analysis was performed comparing the mean value of each clone with the mean value of the mutant sample. *$p < 0.05$, **$p < 0.01$, ***$p < 0.001$, ****$p < 0.0001$.

did not show any APRT activity, whereas the activity levels in their respective repaired clones were similar to those of the parental cell line D422 (Figures 3D and 3E). The S1 mutant presented a very low activity in contrast with the repaired clones that showed a very similar activity to the D422 cell line (Figure 3F). There were no differences in APRT activity levels between the clones repaired by the HpS1E2rep repair-PPRH and by the LD-HpS1E2rep repair-PPRH (Figure 3F).

Gene Correction Frequency Increases in S Phase

The determination of the gene correction frequency was performed using the HpS23E1rep repair-PPRH in the S23 mutant cell line. The frequency of correction was 0.1% in the asynchronous condition. However, when cells were transfected in S phase the frequency was 0.25%, corresponding to a 2.5-fold increase compared with cells transfected in the asynchronous state (Figure 4).

Whole-Genome Sequencing Analyses Reveal No Off-Target Effects

The sequenced reads that aligned at position 960,367 in contig NW_003613583 confirmed that the sample S23 mutant had a T in that genomic position and that in S23 repaired cells the T was replaced with a G. To check whether there was any major difference in the S23 repaired cells in comparison with original mutant cells, we looked at (1) the number of total variants and (2) if there was any evidence of the insertion of the construct in other genomic locations. Regarding the total number of variants, we compared the number of variants (single-nucleotide variants, insertions, and deletions) in the genomic positions with enough coverage in both samples and we did not find any major discrepancy. Therefore, we did not see any clear evidence of a major increase in the number of variants in the S23 repaired sample (Table 1). To investigate the possible integration of HpS23E1rep in multiple genomic regions, reads with similarity to the construct were scrutinized. Under the assumption that if multiple insertions occur, the genomic fragments with this new insertion would have been sequenced but not mapped, because the sequence would not be found in the reference genome, we searched within all of the original reads (before mapping) for those with similarity with the construct using BLAST, as explained in "Whole-Genome Sequencing Analyses" in the Materials and Methods. Table 2 shows the reads with similarity to the construct in both samples. All the found reads were mapped in the target region in contig NW_003613583 (Table 2). No unmapped reads or mapped reads anywhere else with similarity were found.
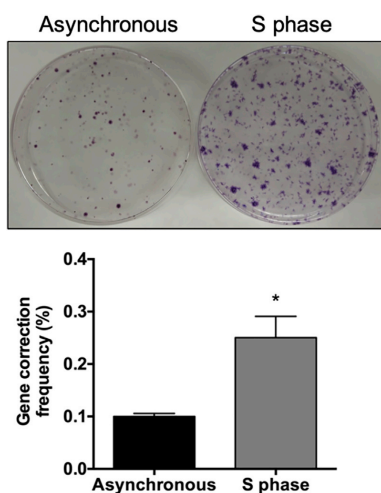
Figure 4. Gene Correction Frequency

Gene correction frequency values were calculated as the ratio between the number of surviving colonies and the total number of cells initially plated. Also shown is a representative image of the number of S23 repaired colonies obtained after the treatment with HpS23E1rep repair-PPRH in cells transfected either in asynchronous conditions or in S phase. After selection, surviving cell colonies were fixed with formaldehyde and stained with crystal violet. Error bars represent the standard error of the mean of three experiments. *p < 0.05.

Repair-PPRHs Bind to Their Target Sequence

To test the binding of repair-PPRHs to their polypyrimidine target sequence in the *aprt* locus, we performed gel-shift assays using a 160-bp radioactive probe containing the mutation present in S23 cells and its adjacent sequences (dsDNA-S23). The binding of the HpS23E1-core to its polypyrimidine target sequence produced two shifted bands corresponding to two different molecular species (Figure 5A, lane 2). The shifted band with the highest mobility corresponded to a triplex structure in which the HpS23E1-core was binding only to the polypyrimidine target sequence located in one of the two DNA strands of the probe (Figure 5A, red panel). The shifted bands with the lowest mobility corresponded to the binding of the HpS23E1-core to its polypyrimidine target sequence together with the rest of the dsDNA probe that was still bound by intramolecular Watson-Crick bonds (Figure 5A, green panel). However, we did not observe any shifted band when incubating the probe only with the RD-S23E1rep repair domain (Figure 5A, lane 3). The incubation of the full HpS23E1rep repair-PPRH produced three shifted bands (Figure 5A, lane 4). The two highest mobility-shifted bands corresponded to the same molecular species shown in lane 2. The lowest mobility-shifted band corresponded to the binding of the HpS23E1rep repair-PPRH to its polypyrimidine sequence together with the repair domain bound to its complementary strand (Figure 5A, blue panel). As negative controls, we used a hairpin core, a repair domain, or a scrambled full repair-PPRH (Figure 5A, lanes 5–7). We only observed one shifted band with the incubation of the scramble hairpin core with the probe that corresponded to an unspecific and/or partial binding of the hairpin to the sequence, but with different mobility than that of the specific hairpin core (Figure 5A, lane 5).

To confirm the nature of the lowest mobility-shifted band that appeared when incubating the full repair-PPRH with the probe (Figure 5A, lane 4), we performed a competition assay (Figure 5B). The amount of radiolabeled probe incubated with the HpS23E1rep repair-PPRH was competed with 20-fold of the HpS23E1rep-core hairpin core (Figure 5B, lane 3), which resulted in the decrease of the band that corresponded to the structure depicted in the blue panel, thus demonstrating that the full repair-PPRH is needed to produce this structure.

Binding of the PPRH to Its Target Sequence Produces a Displacement Loop

To study the molecular mechanism responsible for the repair event, we performed gel-shift assays incubating the HpS23E1-core of the repair-PPRH with the radioactive probe dsDNA-S23. To check whether this binding led to the formation of a displacement-loop (D-loop) structure, we designed three invading oligonucleotides of different lengths (O-16, O-40, and O-60) that were complementary to the displaced strand of the probe (Figure 6A). The hypothesis was that the binding of the HpS23E1-core to its polypyrimidine target sequence would form a D-loop structure, allowing the binding of the invading oligonucleotides to the displaced strand and thus producing different migration patterns in the gel shifts depending on the length of the oligonucleotide. As shown in Figure 6B, lane 2, when incubating the probe with the HpS23E1-core, two shifted bands that reproduced the same pattern as in Figure 5A, lane 2, were obtained. The incubation of each invading oligonucleotide, either O-16, O-40, or O-60, with the probe alone in the absence of the hairpin produced two shifted bands (Figure 6B, lanes 3, 5, and 7). The shifted band with the highest mobility corresponded to the binding of the invading oligonucleotide to its complementary strand present in the probe, whereas the one with the lowest mobility represented the sandwich structure between the invading oligonucleotide and the probe. Finally, when the probe was first incubated with the HpS23E1-core and then the different invading oligonucleotides were added, prominent shifted bands appeared (color arrows) with different mobilities depending on the length of the invading oligonucleotide (Figure 6B, lanes 4, 6, and 8). Therefore, the binding of the hairpin core to the probe provoked the formation of a D-loop structure of a determined length (Figure 6B, color panels). The invading oligonucleotides can be bound to the probe either completely (red panel, O-16) or partially (green and blue panels, O-40 and O-60, respectively) depending on their length. This would form structures in which the ends of the longest invading oligonucleotides would be overhanging the complex.

Results

Table 1. Number of Variants per Sample

S23 Mutant	S23 Repaired	All Variants	Filtered Variants	Filtered SNV	Filtered Del	Filtered Insert
0/0	0/1	66,758	46,002	36,147	4,681	5,174
0/1	0/0	67,563	46,414	36,637	4,684	5,093
0/0	1/1	8,579	644	105	307	232
1/1	0/0	8,414	729	92	345	292
0/1	1/1	23,814	6,322	4,490	890	942
1/1	0/1	22,472	5,675	4,046	769	860
0/1	0/1	1,074,296	971,609	798,079	92,812	80,718
1/1	1/1	1,036,972	549,872	441,444	35,296	73,132
Total		2,308,868	1,627,267	1,321,040	139,784	166,443

The genotype conventions were followed: "0/0" refers to homozygous reference position (no variant), "0/1" heterozygous, and "1/1" homozygous alternative. "Filtered" refers to the minimum coverage of 10 in both samples and a minimum of three for the alternative alleles, which reduces the number of variants by 30% but ensures that both samples have a good coverage. We can observe that the new variants in sample S23 repaired (0/0 0/1 or 0/0 1/1) and the new variants in sample S23 mutant (0/1 0/0 or 1/1 0/0) are very similar. Thus, we cannot see a big increase or decrease in the overall number of variants between these two samples. SNV, single nucleotide variant; Del, deletions; Insert, insertions.

DISCUSSION

In this study, we demonstrate the generality of action of the repair-PPRHs technology that we previously used to correct six different point mutations (single substitutions, insertions, deletions, and a double substitution) in a different gene that codes for the DHFR. In that study, we used different polypurine hairpin cores against polypyrimidine target sequences ranging from 10 to 23 nt for the successful correction of the *dhfr* gene.[43] In the present work, we carried out gene correction experiments in *aprt*-deficient cell lines that contained different single-point substitutions in the endogenous locus of the *aprt* gene, serving as a model of a disease mutation in CHO cells, because its deficiency in humans is an inherited condition that affects the kidneys and urinary tract.[44,45] In this study, we designed polypurine hairpins containing between 19 and 22 nt to assure the specificity toward its polypyrimidine target sequence and reduce the possible off-target effects. In all of the cases we demonstrated the correction of the mutation not only at the genomic level, but also at the mRNA and enzymatic activity levels, showing that the translated protein was functional. One limitation of the repair-PPRHs is the requirement of a polypyrimidine tract near the mutation to be corrected. Although the frequency of these polypyrimidine stretches around the human genome is more abundant than that predicted by simple random models,[46] it can be difficult to find an appropriate sequence adjacent to the location of the point mutation. We dealt with this situation by designing a long-distance repair-PPRH in which the target for the repair domain was located 24 nt upstream of the hairpin core. In this case, the repair domain was linked to the hairpin core by an additional pentathymidine loop. The long-distance repair-PPRH was able to correct its targeted mutation, indicating that adjacency between the repair domain and the hairpin core was not necessary to achieve the correction. This is in accordance with our previous data showing that a long-distance repair-PPRH containing a hairpin core binding 662 nt away from the mutation was able to produce the correction.[43]

The highest level of gene repair was achieved when cells were transfected just after release from S phase synchronization. We had already observed an increase in repair efficiency after synchronization when we corrected a point mutation in the *dhfr* gene using repair-PPRHs.[42] This is also consistent with the work of Brachman and Kmiec[47] that showed increased repair frequencies when using modified ssODNs by lengthening the S phase and stalling the replication fork, thus inducing the homologous recombination pathway. Other reports also determined gene correction frequencies among different cell cycle stages, confirming that the S phase stage was the most prone to achieve the correction of the mutation.[48,49] We did not obtain any surviving cell colony when cells were transfected only with the repair domain of the repair-PPRH or when this domain was attached to the scrambled polypurine hairpin that did not show any binding to the target dsDNA, establishing the requirement of the specific hairpin core to induce the triplex structure and stimulate the gene repair event. This fact corroborates our previous observation that repair domains bearing hairpin cores bound by intramolecular Watson-Crick bonds (unable to bind to the target dsDNA) instead of Hoogsteen bonds did not produce the correction.[42]

Nowadays, most popular gene-editing technologies (CRISPR/Cas9, ZFN, and TALEN systems) rely on the activity of nucleases that create extrinsic breaks in the dsDNA to achieve the correction of the mutation. One of the main concerns with these gene-editing tools is the presence of off-target effects in the repaired genome such as small insertions, deletions, or substitutions,[50–54] usually produced by unspecific cuts of the nuclease. Haapaniemi et al.[55] showed that CRISPR/cas9 genome editing induced a p53-mediated DNA damage response and cell cycle arrest in human retinal pigment epithelial cells. On-target mutagenesis such as large deletions in the target site[56] and unexpected chromosomal truncations[57] have also been reported. In this regard, repair-PPRHs did not produce any off-target effects in the genome of the repaired cells. No random insertions or deletions caused by the repair-PPRH were detected, and the repair-PPRH itself was not inserted in any region of the repaired genome. Moreover, the

Table 2. Genomic Integration of the Repair-PPRH

S23 Mutant						
Read ID	**Identity %**	**Align Length**	**Exp. Val.**	**In Region**	**CIGAR**	**mapQ**
J00148:62:HMFTCBBXX:7:1205:28544:42583	98	50	4.99e−16	yes	151M	60
J00148:62:HMFTCBBXX:7:1228:19431:11143	98	50	4.99e−16	yes	151M	60
K00310:156:HMFGLBBXX:8:1222:4980:29677	98	50	5.47e−16	yes	1S150M	30
K00310:156:HMFGLBBXX:8:2107:11464:21500	98	50	5.47e−16	yes	151M	30
K00310:158:HMFF5BBXX:6:1115:14154:37800	98	50	5.47e−16	yes	151M	60
K00310:158:HMFF5BBXX:6:1208:21846:33475	98	50	5.47e−16	yes	151M	60
K00310:158:HMFF5BBXX:6:1215:8471:30450	98	50	5.47e−16	yes	151M	60
K00310:156:HMFGLBBXX:8:1120:27011:20762	98	49	1.88e−15	yes	151M	60
J00148:62:HMFTCBBXX:7:2208:23876:43779	96	49	2.32e−14	yes	1S147M3S	60
K00310:156:HMFGLBBXX:8:2218:24728:11425	95	42	1.90e−10	yes	151M	60
K00310:158:HMFF5BBXX:6:2204:26210:16770	98	50	5.47e−16	yes	74M77S	0
K00310:158:HMFF5BBXX:6:1115:20811:45010	96	47	3.29e−13	yes	31S115M5S	0
J00148:60:HLL3CBBXX:7:2222:31598:29624	86	44	5.15e−06	yes	101M50S	0
S23 Repaired						
Read ID	Identity %	Align Length	Exp. Val.	In Region	CIGAR	mapQ
K00310:157:HMFGJBBXX:3:1104:7476:24085	100	51	1.08e−17	yes	151M	60
K00310:157:HMFGJBBXX:3:1227:21734:7468	100	51	1.08e−17	yes	151M	60
K00310:159:HMFFVBBXX:4:2125:23957:2527	100	51	1.10e−17	yes	151M	60
K00310:157:HMFGJBBXX:3:2228:25915:42812	100	51	1.08e−17	yes	41M110S	0
K00310:159:HMFFVBBXX:3:1101:10338:27567	100	51	1.10e−17	yes	43M108S	0
J00148:61:HMFGCBBXX:3:1218:21521:21869	100	20	5.08e−06	yes	55S96M	0
K00310:159:HMFFVBBXX:3:1117:27661:25474	100	27	2.41e−04	yes	151M	60

Reads are similar to the construct HpS23E1rep found with BLAST before being mapped into the genome. "Identity %," "Align Length" (alignment length), and "Exp. Val." (experimental value) refer to the values obtained in the BLAST search. Accordingly, at the most, only the 51 bases that are identical to the complementary genome region were found in the reads. In the S23 repaired we can observe that the alignment length is 51 and the identity is 100% because it contains the replaced G. The columns "In Region," "CIGAR," and "mapQ" refer to the statistics of the reads when mapped into the genome using GEM3. In region means that the read has been mapped in the region near position 960,367 in contig NW_003613583. CIGAR refers to the alignment code, and mapQ refers to the mapping quality score. Most of the reads have a quality score of 60, but some have lower quality due to bad score qualities in the bases of the read. In any case, all reads were mapped uniquely to the expected genomic region. Therefore, we could not find any evidence of integration of the construct in the genome.

presence of a preexisting effector T cell response directed toward Cas9 proteins in human beings has been described since *Staphylococcus aureus* and *Staphylococcus pyogenes* cause infections in the human population at high frequencies.[58,59] In contrast, PPRHs are non-modified, economical, and non-immunogenic DNA molecules that do not activate the innate inflammatory response.[60] Additionally, it has already been described that natural oligonucleotides,[61,62] oligonucleotides including phosphorothioate bonds,[63] morpholinos,[64] and locked nucleic acids[65] are not genotoxic.

One of the aims of this work was to get an insight into the molecular mechanism behind the repair event. On the one hand, we demonstrated the specific binding of the hairpin core of the repair-PPRH to the polypyrimidine target sequence in the dsDNA, thus producing the triplex structure. On the other hand, we explored the formation of a D-loop upon the incubation of the hairpin core of the repair-PPRH to the target sequence that could eventually stimulate the repair event. We designed different invading oligonucleotides vary-ing in length and complementary to the displaced strand of the dsDNA upon formation of the triplex by the action of the hairpin core. We showed that after the binding of the hairpin core to the target sequence there was indeed a displacement of the complementary strand, which allowed the different invading oligonucleotides to bind, generating structures with retarded mobility that indicated the formation of a D-loop. In this regard, it is known that the potential of molecules such as triplex-forming oligonucleotides to stimulate recombination with donor DNAs depends on the homology-directed repair (HDR)[66,67] and the nucleotide excision repair (NER) pathways.[67–69] Concerning the HDR pathway, RAD51 is one of the main proteins involved in this process by promoting the homologous pairing of a single-stranded DNA to a duplex DNA in a structure similar to a D-loop,[70–72] as the one shown in the present work. Therefore, this structure can stimulate the HDR pathway to finally achieve the correction of the mutation using the repair domain attached to the hairpin core of the repair-PPRH. Our previous data showed that the transfection of a repair-PPRH along with a
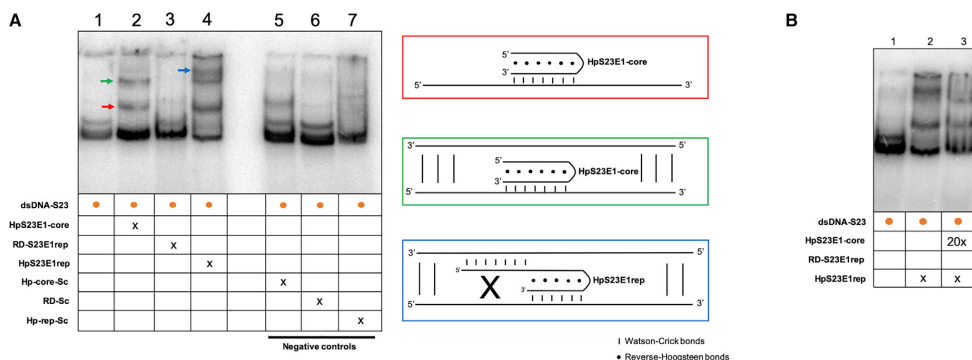
Figure 5. Binding of the Repair-PPRH to Its Target Sequence

Gel-shift assays using a 160-bp ^{32}P-radiolabeled dsDNA probe (dsDNA-S23) containing the mutation present in the S23 mutant and its flanking regions. The unlabeled oligodeoxynucleotides present in each binding reaction are indicated. (A) Lane 1, dsDNA-S23 probe alone; lane 2, dsDNA-S23 plus HpS23E1-core (100 nM); lane 3, dsDNA-S23 plus RD-S23E1rep (100 nM); lane 4, dsDNA-S23 plus HpS23E1rep repair-PPRH (100 nM); lane 5, dsDNA-S23 plus Hp-core-Sc (100 nM); lane 6, dsDNA-S23 plus RD-Sc (100 nM); lane 7, dsDNA-S23 plus Hp-rep-Sc (100 nM). Color arrows indicated the different molecular species that are generated upon incubation with the different oligodeoxynucleotides. The color of the arrows matches those of the panels corresponding to the proposed structures shown on the right panel. (B) Competition assay. Lane 1, dsDNA-S23 probe alone; lane 2, dsDNA-S23 probe plus HpS23E1rep repair-PPRH (100 nM); lane 3, dsDNA-S23 probe plus HpS23E1rep (100 nM) competed with HpS23E1-core (2 μM). 20x indicates that the oligonucleotide was added in a concentration 20 times greater than x.

Rad51 expression vector increased gene correction frequency by 10-fold,[42] thus confirming that the HDR pathway is involved in the repair process triggered by the repair-PPRH. Regarding the NER pathway, it has been reported that noncanonical DNA structures such as triple helices can be identified by the XPA/RPA DNA damage recognition complex that recruits NER machinery to these distorted sites, leading to DNA repair activity that generates recombination intermediates.[73] However, the entire mechanism by which these triplex structures stimulate recombination remains unclear.

In summary, this work demonstrates the generality of repair-PPRHs to specifically correct point mutations in their endogenous locus in mammalian cells without detecting off-target modification in the genome. We also determined the formation of a D-loop structure upon the binding of the PPRH to its target sequence that is involved in the HDR pathway, giving information about the mechanism by which the repair event may occur. Collectively, this study provides further knowledge for the usage of this technology. We envision repair-PPRHs as an alternative gene-editing tool to correct single-point mutations responsible for monogenic diseases in human cells. These molecules can be associated with advanced delivery systems such as new liposomes and gold/polymeric nanoparticles that could improve their delivery, thus allowing the implementation of this technology for *in vivo* approaches.

MATERIALS AND METHODS

Cell Culture

Several *aprt*-deficient CHO cell lines were used for gene correction. All cell lines contained a single nucleotide substitution within the coding sequence that produced a premature stop codon (nonsense mutation), thus generating a truncated protein. The mutant cell lines were isolated using different mutagens from the parental cell line D422,[74] which is a CHO cell line hemizygous for the *aprt* gene.[75] The different cell lines and their corresponding mutations are described in Table S1. Cells were grown in Ham's F12 medium containing 10% fetal bovine serum (both from Gibco, Madrid, Spain) at 37°C in a 5% CO_2-controlled humidified atmosphere. Trypsinization of the cells was performed using 0.05% trypsin (Sigma-Aldrich, Madrid, Spain).

Oligodeoxynucleotides

To design the different PPRHs we used the Triplex-Forming Oligonucleotide Target Sequence Search software (http://utw10685.utweb.utexas.edu/tfo/, Austin, TX, USA), which searches for stretches of polypurines within the DNA sequence of interest. Repair-PPRHs were designed by attaching an extension sequence (repair domain) to the hairpin core that ultimately binds to the polypyrimidine target sequence (Figure 1A).

We also designed a long-distance repair-PPRH (LD-HpS1E2rep) in which the hairpin core was located 24 nt away from the repair domain. In this case, an additional pentathymidine loop between the hairpin core and the repair domain was included to provide flexibility to the repair domain (Figure 1B). All oligodeoxynucleotides were synthesized by Sigma-Aldrich (Haverhill, UK), dissolved at 10 μg/μL (stock solution) in a sterile RNase-free Tris-EDTA buffer (1 mM EDTA and 10 mM Tris, pH 8.0; both from Sigma-Aldrich, Madrid, Spain), and stored at −20°C until use.
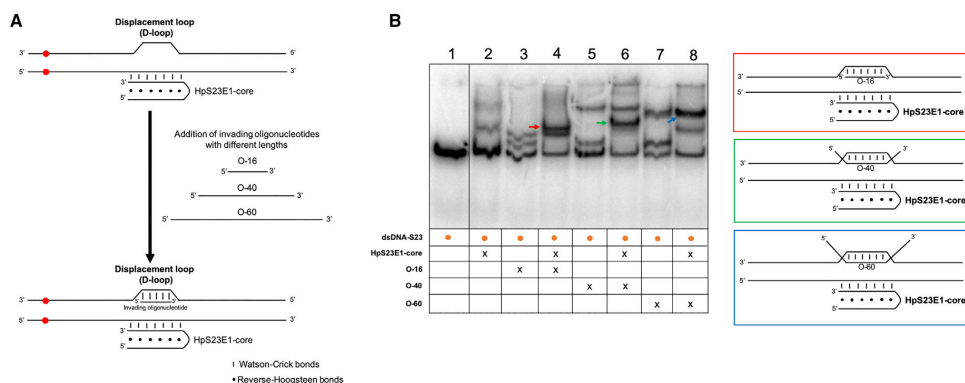
Figure 6. Strand Displacement upon Binding of the Repair-PPRH to the Target Sequence

(A) Schematic representation of the strategy used to study the formation of a displacement-loop (D-loop) structure. The hairpin core (HpS23E1-core) of the repair-PPRH was incubated with the dsDNA-S23 probe, and then different oligonucleotides varying in length and complementary to the displaced strand were added to the binding reaction. (B) Gel-shift assays using a 160-bp ^{32}P-radiolabeled dsDNA probe (dsDNA-S23) containing the mutation in S23 cells and its flanking regions. In all cases, an amount of 60 ng of each one of the unlabeled oligodeoxynucleotides was added to the binding reaction. Lane 1, dsDNA-S23 probe alone; lane 2, dsDNA-S23 plus HpS23E1-core; lane 3, dsDNA-S23 plus O-16; lane 4, dsDNA-S23 plus HpS23E1-core plus O-16; lane 5, dsDNA-S23 plus O-40; lane 6, dsDNA-S23 plus HpS23E1-core plus O-40; lane 7, dsDNA-S23 plus O-60; lane 8, dsDNA-S23 plus HpS23E1-core plus O-60. Color arrows indicate the different molecular species that are generated upon incubation with the different oligodeoxynucleotides. The colors of the arrows in the gel image match those of the panels corresponding to the proposed structures shown on the right of the figure.

As negative controls, different oligodeoxynucleotides that contained only the repair domain for each mutant, without the hairpin core, were used. In addition, a scrambled polypurine hairpin core attached to the repair domain of the S23 mutant was transfected into S23 mutant cells as an additional negative control. Sequences and abbreviations of all oligodeoxynucleotides are described in Table S2.

Transfection

Different numbers of cells ranging from 50,000 to 300,000 were plated the day before transfection. Transfections were carried out using the original calcium phosphate method.[76] Briefly, 10 μg of the repair-PPRH was mixed with 100 μL of a 2.5 M CaCl$_2$ solution and sterile Milli-Q H$_2$O in a final volume of 500 μL. This solution was added dropwise to an equal volume of a sterile 2× HEPES-buffered saline (HBS; 280 mM NaCl, 50 mM HEPES, and 1.5 mM NaH$_2$PO$_4$, pH adjusted to 7.1) while bubbling with a 1-mL sterile glass pipette. The calcium phosphate-DNA precipitate was allowed to form for 30 min at room temperature without agitation. Then, 1-mL mixtures were added dropwise to 100-mm plates containing the recipient cells in 10 mL of culture medium. After 5 h of incubation at 37°C, culture medium was replaced with fresh medium and cells were incubated for an additional 48 h before selection (Figure 1C).

Selection of the Repaired Cells

APRT selection was applied to transfected cells using RPMI 1640 selective medium (Gibco, Madrid, Spain) lacking glycine and hypoxan-

thine (−GH medium), supplemented with 50 μM adenine, 5 μM aminopterin, and 10 μM thymidine (+AAT medium) (Sigma-Aldrich, Madrid, Spain) containing 7% dialyzed fetal bovine serum (Gibco, Madrid, Spain). Each experiment was performed a minimum of three times, and a minimum of three colonies from each replicate were analyzed (Figure 1C).

DNA Sequencing

Total genomic DNA was extracted using the Wizard genomic DNA purification kit (Promega, Madrid, Spain), following the manufacturer's instructions. PCR was carried out to amplify the specific genomic region containing the mutated site. OneTaq DNA polymerase (New England Biolabs, Ipswich, MA, USA) was used following the standard PCR cycling conditions recommended by the manufacturer. The primer sequences for each amplification were as follows: 5′-TT ACCCTTGTTCCCGGACTG-3′ and 5′-TGATCTCACCTAAACAG CAC-3′ for the S23 cell line, 5′-CAGGAACCATGTGCGCTG CCTGTGAGC-3′ and 5′-GGTAAGGCTGAGCCACTGTTCAAC CG-3′ for the S62 cell line, and 5′-CTTGTTCCCAGGGA TATCTCG-3′ and 5′-GGTTGAAGAAAGAAGGGATAGG-3′ for the S1 cell line. The PCR-amplified products were sequenced by Macrogen (Amsterdam, the Netherlands).

mRNA Analyses

Total RNA was extracted using TRI Reagent (Life Technologies, Barcelona, Spain) following the instructions provided by the manufacturer. RNA concentration was determined by measuring its

137

Results

absorbance at 260 nm using a Nanodrop ND-1000 spectrophotometer (Thermo Fisher Scientific, Barcelona, Spain). cDNA was synthesized in a 20-μL reaction mixture containing 1 μg of total RNA, 125 ng of random hexamers (Roche, Barcelona, Spain), 0.5 mM of each deoxyribonucleotide triphosphate (dNTP; Bioline, London, UK), 2 μL of buffer (10×), 20 U of RNase inhibitor, and 200 U of Moloney murine leukemia virus reverse transcriptase (last three from Lucigen, Middleton, WI, USA). The reaction was incubated at 42°C for 1 h. 3 μL of the cDNA mixture was used for quantitative real-time PCR amplification.

A StepOnePlus real-time PCR system (Applied Biosystems, Barcelona, Spain) was used to perform the experiments. PCR cycling conditions were 10 min denaturation at 95°C, followed by 40 cycles of 15 s at 95°C and 1 min at 60°C. An APRT mRNA TaqMan probe (assay ID: Cg04465038_g1) was used to determine the mRNA expression of the *aprt* gene. The relative mRNA amount of the target gene was calculated using the $\Delta\Delta C_T$ method, where C_T is the threshold cycle that corresponds to the cycle where the amount of amplified mRNA reaches the threshold of fluorescence. A TATA box-binding protein (TBP) mRNA TaqMan probe (assay ID: Cg04504571_m1) was used as an endogenous control. All TaqMan probes were purchased from Life Technologies (Barcelona, Spain). The final volume of the reaction was 20 μL containing 1× TaqMan Universal PCR Master Mix II, 1× TaqMan probe (both from Life Technologies, Barcelona, Spain), 3 μL of cDNA, and nuclease-free Milli-Q H_2O.

APRT Enzymatic Activity Assay

The assay was adapted from the original paper of Johnson et al.[77] with some modifications. Basically, this method is based on the change in absorbance of adenine at 260 nm due to its conversion to AMP by APRT. First, mutant or repaired cells (5×10^6) were lysed with 200 μL of 0.1% Triton X-100 in 100 mM Tris-HCl (pH 7.4). After vortexing, cell extracts were centrifuged at $10,000 \times g$ for 10 min at 4°C and the supernatant was kept in ice until APRT activity determination. Protein concentration of the cell lysates was determined by the Bio-Rad protein assay following the instructions of the manufacturer. The 500-μL incubation mixture consisted of 0.25 mM adenine, 5 mM $MgCl_2$, 1 mM phosphoribosyl pyrophosphate, and 50 mM Tris-HCl (pH 7.4) (all from Sigma-Aldrich, Madrid, Spain). To start the reaction, 190 μL of cell lysate was added to the incubation mixture at 37°C. After vortexing, 200 μL of sample was immediately removed and placed into a new tube containing 200 μL of $LaCl_3$ (Sigma-Aldrich, Madrid, Spain), followed by rapid mixing to stop the reaction (t_0). After 30 min of reaction, another sample was removed and processed as mentioned before (t_{30}). Finally, 400 μL of 40 mM Na_2HPO_4 was added to each sample, mixed, and centrifuged at $10,000 \times g$ for 5 min at 4°C. The absorbance of the clear supernatant was measured at a wavelength of 260 nm in a UV-1700 UV-Vis spectrophotometer (Shimadzu, Duisburg, Germany). Data were represented as enzyme milliunits (mU), corresponding to the amount of enzyme that catalyzes the conversion of 1 nmol of adenine per minute, divided by the mg of total protein extract.

A scheme representing the different assays (DNA sequencing, mRNA expression, and enzymatic activity) performed to confirm the functionality of *aprt* upon repair are shown in Figure 1C.

Gene Correction Frequency

Gene correction frequency was determined for the S23 mutant cell line using the HpS23E1rep repair-PPRH. Transfection was performed either in asynchronous cells or with cells in the S phase of the cell cycle. Synchronization in S phase was achieved following the protocol described by Chin et al.,[26] which consisted basically in incubating the cells in medium supplemented with 0.1% serum for 72 h followed by incubation with 1.5 mM hydroxyurea for 15 h. After transfection and selection in +AAT medium, surviving cell colonies were fixed with 6% formaldehyde, stained with crystal violet (both from Sigma-Aldrich, Madrid, Spain), and counted.

Whole-Genome Sequencing Analyses

Total genomic DNA was extracted from both S23 mutant cells and S23 repaired cells using the method previously described in "DNA Sequencing" above. Both samples were sequenced with a whole-genome approach with an average target coverage of 26× in the facilities of the National Center for Genomic Analyses (CNAG), Barcelona, Spain. The CHO genome and annotation CHO-K1 [ATCC]_RefSeq_2014 assembly was obtained from https://chogenome.org/ and used as a reference genome. The sequenced reads were mapped into the CHO-K1[ATCC]_RefSeq_2014 assembly using the GEM3 aligner[78] with default parameters. The CHO-K1[ATCC]_RefSeq_2014 assembly was very fragmented with more than 100,000 contig fragments. To avoid mapping problems in small contigs that could lead to false-positive variant calls and to simplify the analysis, a set of 3,158 contigs longer than 100 kb covering around 90% of the genomic sequence (2.2 Gb) was used to analyze the number of variants and the genotype of both samples. For this analysis, we used the variants calls computed with HaplotypeCaller from the Genome Analysis Toolkit[79] following their best practices guidelines. As the covered regions could be different among samples and genomic regions, we applied a filter to ensure that there was enough reliable information in both samples. A set of variants with enough support in the two samples was created. Thus, we required that the genomic position had a coverage of at least 10 reads in both samples, and if there was an alternative allele, it had to have a coverage of at least three reads with the alternative variant. The filter reduced the total number of reported variants around 30% but ensured that all calls were reliable and comparable between the two samples.

To check the possible off-target effects by insertion of the repair-PPRH construct in different regions of the genome, we performed similarity searches to identify genomic sequenced reads that could contain the repair-PPRH sequence. The alignment software BLAST[80] was run with word size parameter set to 15 to speed up the search. With a word size of 15, BLAST required a seed of 15 bases from the query to be identical to the target sequence in the database to start the alignment. Only the sequences with an alignment with an expected p value lower than 1e−03 were taken for the analysis.

DNA Binding Assays

To prepare the probe for the binding assays, the target dsDNA sequence of the HpS23E1rep repair-PPRH was PCR amplified using genomic DNA from S23 mutant cells and the S23-Fw and S23-Rv primers. The dsDNA PCR product (200 ng) was 5′ end labeled with [γ-^{32}P]ATP (3,000 Ci/mmol) (PerkinElmer, Madrid, Spain) using T4 polynucleotide kinase (New England Biolabs, USA) in a 10-μL reaction mixture, according to the manufacturer's protocol. After incubation at 37°C for 1 h, 90 μL of Tris-EDTA buffer (1 mM EDTA and 10 mM Tris, pH 8.0; Sigma-Aldrich, Madrid, Spain) was added to the reaction mixture, which was subsequently filtered through a Sephadex G-50 (Sigma-Aldrich, Madrid, Spain) spin column to eliminate the unincorporated [γ-^{32}P]ATP.

Binding experiments were carried out by incubating the radiolabeled DNA probe (20,000 cpm) with a length of 160 bp with different unlabeled oligodeoxynucleotides in a buffer containing 10 mM $MgCl_2$, 100 mM NaCl, and 50 mM HEPES (pH 7.2). Binding reactions (20 μL) were incubated 5 min at 92°C followed by 25 min of cooling down until reaching room temperature. In the case of the D-loop formation gel-shift assays, binding reactions were incubated 5 min at 92°C and 5 min at 37°C (invading oligonucleotides were added to the mix at this point) and 20 min of cooling down until reaching room temperature. Unspecific DNA (poly(dI:dC)) was included in each condition at a 1:2 unspecific DNA/specific DNA ratio. Electrophoresis was performed on a nondenaturing 10% polyacrylamide gels containing 10 mM $MgCl_2$, 5% glycerol, and 50 mM HEPES (pH 7.2). Gels were run at a fixed voltage of 220 V (4°C) using a running buffer containing 10 mM $MgCl_2$ and 50 mM HEPES (pH 7.2). Finally, gels were dried at 80°C, exposed to photostimulable phosphor plates, and visualized on a Storm 840 Phosphorimager (Molecular Dynamics, GE Healthcare, Barcelona, Spain). ImageQuant software v5.2 was used to visualize the results.

Statistical Analyses

Data are represented as the mean ± SEM values of three experiments. Statistical analyses were performed using ordinary one-way ANOVA with Dunnett's multiple comparison tests. Gene frequency data were analyzed with an unpaired Student's t test. Analyses and representation of the data were carried out using GraphPad Prism version 6.0 software (GraphPad, La Jolla, CA, USA).

SUPPLEMENTAL INFORMATION

Supplemental Information can be found online at https://doi.org/10.1016/j.omtn.2019.12.015.

AUTHOR CONTRIBUTIONS

A.J.F. designed and performed the experiments and wrote the manuscript. C.J.C. and V.N. conceived the study, participated in its design and supervision, and revised the manuscript.

CONFLICTS OF INTEREST

The authors declare no competing interests.

ACKNOWLEDGMENTS

REFERENCES

1. (1996). Control of hereditary diseases. Report of a WHO Scientific Group. World Health Organ. Tech. Rep. Ser. 865, 1–84.

2. Urnov, F.D., Miller, J.C., Lee, Y.L., Beausejour, C.M., Rock, J.M., Augustus, S., Jamieson, A.C., Porteus, M.H., Gregory, P.D., and Holmes, M.C. (2005). Highly efficient endogenous human gene correction using designed zinc-finger nucleases. Nature 435, 646–651.

3. Yusa, K., Rashid, S.T., Strick-Marchand, H., Varela, I., Liu, P.Q., Paschon, D.E., Miranda, E., Ordóñez, A., Hannan, N.R., Rouhani, F.J., et al. (2011). Targeted gene correction of α1-antitrypsin deficiency in induced pluripotent stem cells. Nature 478, 391–394.

4. Chen, F., Pruett-Miller, S.M., Huang, Y., Gjoka, M., Duda, K., Taunton, J., Collingwood, T.N., Frodin, M., and Davis, G.D. (2011). High-frequency genome editing using ssDNA oligonucleotides with zinc-finger nucleases. Nat. Methods 8, 753–755.

5. Mori, T., Mori, K., Tobimatsu, T., and Sera, T. (2014). Sandwiched zinc-finger nucleases demonstrating higher homologous recombination rates than conventional zinc-finger nucleases in mammalian cells. Bioorg. Med. Chem. Lett. 24, 813–816.

6. Ding, Q., Lee, Y.K., Schaefer, E.A.K., Peters, D.T., Veres, A., Kim, K., Kuperwasser, N., Motola, D.L., Meissner, T.B., Hendriks, W.T., et al. (2013). A TALEN genome-editing system for generating human stem cell-based disease models. Cell Stem Cell 12, 238–251.

7. Mosbach, V., Poggi, L., Viterbo, D., Charpentier, M., and Richard, G.F. (2018). TALEN-induced double-strand break repair of CTG trinucleotide repeats. Cell Rep. 22, 2146–2159.

8. Yahata, N., Matsumoto, Y., Omi, M., Yamamoto, N., and Hata, R. (2017). TALEN-mediated shift of mitochondrial DNA heteroplasmy in MELAS-iPSCs with m.13513G>A mutation. Sci. Rep. 7, 15557.

9. Bedell, V.M., Wang, Y., Campbell, J.M., Poshusta, T.L., Starker, C.G., Krug, R.G., 2nd, Tan, W., Penheiter, S.G., Ma, A.C., Leung, A.Y., et al. (2012). In vivo genome editing using a high-efficiency TALEN system. Nature 491, 114–118.

10. Low, B.E., Krebs, M.P., Joung, J.K., Tsai, S.Q., Nishina, P.M., and Wiles, M.V. (2014). Correction of the Crb1^{rd8} allele and retinal phenotype in C57BL/6N mice via TALEN-mediated homology-directed repair. Invest. Ophthalmol. Vis. Sci. 55, 387–395.

11. Jain, A., Zode, G., Kasetti, R.B., Ran, F.A., Yan, W., Sharma, T.P., Bugge, K., Searby, C.C., Fingert, J.H., Zhang, F., et al. (2017). CRISPR-Cas9-based treatment of myocilin-associated glaucoma. Proc. Natl. Acad. Sci. USA 114, 11199–11204.

12. Park, H., Oh, J., Shim, G., Cho, B., Chang, Y., Kim, S., Baek, S., Kim, H., Shin, J., Choi, H., et al. (2019). In vivo neuronal gene editing via CRISPR-Cas9 amphiphilic nanocomplexes alleviates deficits in mouse models of Alzheimer's disease. Nat. Neurosci. 22, 524–528.

13. Amoasii, L., Li, H., Sanchez-Ortiz, E., Mireault, A., Caballero, D., Bassel-Duby, R., Harron, R., Stathopoulou, T.R., Massey, C., Shelton, J.M., et al. (2018). Gene editing restores dystrophin expression in a canine model of Duchenne muscular dystrophy. Science 362, 86–91.

14. Ousterout, D.G., Kabadi, A.M., Thakore, P.I., Majoros, W.H., Reddy, T.E., and Gersbach, C.A. (2015). Multiplex CRISPR/Cas9-based genome editing for correction of dystrophin mutations that cause Duchenne muscular dystrophy. Nat. Commun. 6, 6244.

15. Ruan, J., Hirai, H., Yang, D., Ma, L., Hou, X., Jiang, H., Wei, H., Rajagopalan, C., Mou, H., Wang, G., et al. (2019). Efficient gene editing at major CFTR mutation loci. Mol. Ther. Nucleic Acids 16, 73–81.

Results

16. Komor, A.C., Kim, Y.B., Packer, M.S., Zuris, J.A., and Liu, D.R. (2016). Programmable editing of a target base in genomic DNA without double-stranded DNA cleavage. Nature 533, 420–424.

17. Gaudelli, N.M., Komor, A.C., Rees, H.A., Packer, M.S., Badran, A.H., Bryson, D.I., and Liu, D.R. (2017). Programmable base editing of A●T to G●C in genomic DNA without DNA cleavage. Nature 551, 464–471.

18. Komor, A.C., Badran, A.H., and Liu, D.R. (2018). Editing the genome without double-stranded DNA breaks. ACS Chem. Biol. 13, 383–388.

19. Anzalone, A.V., Randolph, P.B., Davis, J.R., Sousa, A.A., Koblan, L.W., Levy, J.M., Chen, P.J., Wilson, C., Newby, G.A., Raguram, A., and Liu, D.R. (2019). Search-and-replace genome editing without double-strand breaks or donor DNA. Nature 576, 149–157.

20. Zhang, X.H., Tee, L.Y., Wang, X.G., Huang, Q.S., and Yang, S.H. (2015). Off-target effects in CRISPR/Cas9-mediated genome engineering. Mol. Ther. Nucleic Acids 4, e264.

21. Shin, H.Y., Wang, C., Lee, H.K., Yoo, K.H., Zeng, X., Kuhns, T., Yang, C.M., Mohr, T., Liu, C., and Hennighausen, L. (2017). CRISPR/Cas9 targeting events cause complex deletions and insertions at 17 sites in the mouse genome. Nat. Commun. 8, 15464.

22. van Ravesteyn, T.W., Dekker, M., Fish, A., Sixma, T.K., Wolters, A., Dekker, R.J., and Te Riele, H.P. (2016). LNA modification of single-stranded DNA oligonucleotides allows subtle gene modification in mismatch-repair-proficient cells. Proc. Natl. Acad. Sci. USA 113, 4122–4127.

23. Igoucheva, O., Alexeev, V., and Yoon, K. (2001). Targeted gene correction by small single-stranded oligonucleotides in mammalian cells. Gene Ther. 8, 391–399.

24. Ellis, H.M., Yu, D., DiTizio, T., and Court, D.L. (2001). High efficiency mutagenesis, repair, and engineering of chromosomal DNA using single-stranded oligonucleotides. Proc. Natl. Acad. Sci. USA 98, 6742–6746.

25. McLachlan, J., Fernandez, S., Helleday, T., and Bryant, H.E. (2009). Specific targeted gene repair using single-stranded DNA oligonucleotides at an endogenous locus in mammalian cells uses homologous recombination. DNA Repair (Amst.) 8, 1424–1433.

26. Chin, J.Y., Kuan, J.Y., Lonkar, P.S., Krause, D.S., Seidman, M.M., Peterson, K.R., Nielsen, P.E., Kole, R., and Glazer, P.M. (2008). Correction of a splice-site mutation in the beta-globin gene stimulated by triplex-forming peptide nucleic acids. Proc. Natl. Acad. Sci. USA 105, 13514–13519.

27. Lonkar, P., Kim, K.H., Kuan, J.Y., Chin, J.Y., Rogers, F.A., Knauert, M.P., Kole, R., Nielsen, P.E., and Glazer, P.M. (2009). Targeted correction of a thalassemia-associated β-globin mutation induced by pseudo-complementary peptide nucleic acids. Nucleic Acids Res. 37, 3635–3644.

28. Bahal, R., Ali McNeer, N., Quijano, E., Liu, Y., Sulkowski, P., Turchick, A., Lu, Y.C., Bhunia, D.C., Manna, A., Greiner, D.L., et al. (2016). In vivo correction of anaemia in β-thalassemic mice by γPNA-mediated gene editing with nanoparticle delivery. Nat. Commun. 7, 13304.

29. Ricciardi, A.S., Bahal, R., Farrelly, J.S., Quijano, E., Bianchi, A.H., Luks, V.L., Putman, R., López-Giráldez, F., Coşkun, S., Song, E., et al. (2018). In utero nanoparticle delivery for site-specific genome editing. Nat. Commun. 9, 2481.

30. McNeer, N.A., Anandalingam, K., Fields, R.J., Caputo, C., Kopic, S., Gupta, A., Quijano, E., Polikoff, L., Kong, Y., Bahal, R., et al. (2015). Nanoparticles that deliver triplex-forming peptide nucleic acid molecules correct F508del CFTR in airway epithelium. Nat. Commun. 6, 6952.

31. de Almagro, M.C., Coma, S., Noé, V., and Ciudad, C.J. (2009). Polypurine hairpins directed against the template strand of DNA knock down the expression of mammalian genes. J. Biol. Chem. 284, 11579–11589.

32. Ciudad, C.J., Rodríguez, L., Villalobos, X., Félix, A.J., and Noé, V. (2017). Polypurine reverse Hoogsteen hairpins as a gene silencing tool for cancer. Curr. Med. Chem. 24, 2809–2826.

33. Mencia, N., Selga, E., Noé, V., and Ciudad, C.J. (2011). Underexpression of miR-224 in methotrexate resistant human colon cancer cells. Biochem. Pharmacol. 82, 1572–1582.

34. Rodríguez, L., Villalobos, X., Dakhel, S., Padilla, L., Hervas, R., Hernández, J.L., Ciudad, C.J., and Noé, V. (2013). Polypurine reverse Hoogsteen hairpins as a gene

35. Oleaga, C., Welten, S., Belloc, A., Solé, A., Rodriguez, L., Mencia, N., Selga, E., Tapias, A., Noé, V., and Ciudad, C.J. (2012). Identification of novel Sp1 targets involved in proliferation and cancer by functional genomics. Biochem. Pharmacol. 84, 1581–1591.

36. Villalobos, X., Rodríguez, L., Solé, A., Lliberós, C., Mencia, N., Ciudad, C.J., and Noé, V. (2015). Effect of polypurine reverse Hoogsteen hairpins on relevant cancer target genes in different human cell lines. Nucleic Acid Ther. 25, 198–208.

37. de Almagro, M.C., Mencia, N., Noé, V., and Ciudad, C.J. (2011). Coding polypurine hairpins cause target-induced cell death in breast cancer cells. Hum. Gene Ther. 22, 451–463.

38. Bener, G., J Félix, A., Sánchez de Diego, C., Pascual Fabregat, I., Ciudad, C.J., and Noé, V. (2016). Silencing of CD47 and SIRPα by polypurine reverse Hoogsteen hairpins to promote MCF-7 breast cancer cells death by PMA-differentiated THP-1 cells. BMC Immunol. 17, 32.

39. Medina Enríquez, M.M., Félix, A.J., Ciudad, C.J., and Noé, V. (2018). Cancer immunotherapy using Polypurine reverse Hoogsteen hairpins targeting the PD-1/PD-L1 pathway in human tumor cells. PLoS One 13, e0206818.

40. Ciudad, C.J., Medina Enriquez, M.M., Félix, A.J., Bener, G., and Noé, V. (2019). Silencing PD-1 and PD-L1: the potential of PolyPurine Reverse Hoogsteen hairpins for the elimination of tumor cells. Immunotherapy 11, 369–372.

41. Félix, A.J., Ciudad, C.J., and Noé, V. (2018). Functional pharmacogenomics and toxicity of PolyPurine Reverse Hoogsteen hairpins directed against survivin in human cells. Biochem. Pharmacol. 155, 8–20.

42. Solé, A., Villalobos, X., Ciudad, C.J., and Noé, V. (2014). Repair of single-point mutations by polypurine reverse Hoogsteen hairpins. Hum. Gene Ther. Methods 25, 288–302.

43. Solé, A., Ciudad, C.J., Chasin, L.A., and Noé, V. (2016). Correction of point mutations at the endogenous locus of the dihydrofolate reductase gene using repair-PolyPurine Reverse Hoogsteen hairpins in mammalian cells. Biochem. Pharmacol. 110–111, 16–24.

44. Edvardsson, V.O., Sahota, A., and Palsson, R. (2019). Adenine phosphoribosyltransferase deficiency. In GeneReviews (University of Washington), https://www.ncbi.nlm.nih.gov/books/NBK100238/.

45. Bollée, G., Harambat, J., Bensman, A., Knebelmann, B., Daudon, M., and Ceballos-Picot, I. (2012). Adenine phosphoribosyltransferase deficiency. Clin. J. Am. Soc. Nephrol. 7, 1521–1527.

46. Goñi, J.R., de la Cruz, X., and Orozco, M. (2004). Triplex-forming oligonucleotide target sequences in the human genome. Nucleic Acids Res. 32, 354–360.

47. Brachman, E.E., and Kmiec, E.B. (2005). Gene repair in mammalian cells is stimulated by the elongation of S phase and transient stalling of replication forks. DNA Repair (Amst.) 4, 445–457.

48. Majumdar, A., Puri, N., Cuenoud, B., Natt, F., Martin, P., Khorlin, A., Dyatkina, N., George, A.J., Miller, P.S., and Seidman, M.M. (2003). Cell cycle modulation of gene targeting by a triple helix-forming oligonucleotide. J. Biol. Chem. 278, 11072–11077.

49. Olsen, P.A., Randol, M., and Krauss, S. (2005). Implications of cell cycle progression on functional sequence correction by short single-stranded DNA oligonucleotides. Gene Ther. 12, 546–551.

50. Cradick, T.J., Fine, E.J., Antico, C.J., and Bao, G. (2013). CRISPR/Cas9 systems targeting β-globin and CCR5 genes have substantial off-target activity. Nucleic Acids Res. 41, 9584–9592.

51. Allen, F., Crepaldi, L., Alsinet, C., Strong, A.J., Kleshchevnikov, V., De Angeli, P., Páleníková, P., Khodak, A., Kiselev, V., Kosicki, M., et al. (2018). Predicting the mutations generated by repair of Cas9-induced double-strand breaks. Nat. Biotechnol. 37, 64–82.

52. Anderson, K.R., Haeussler, M., Watanabe, C., Janakiraman, V., Lund, J., Modrusan, Z., Stinson, J., Bei, Q., Buechler, A., Yu, C., et al. (2018). CRISPR off-target analysis in genetically engineered rats and mice. Nat. Methods 15, 512–514.

53. Lin, Y., Cradick, T.J., Brown, M.T., Deshmukh, H., Ranjan, P., Sarode, N., Wile, B.M., Vertino, P.M., Stewart, F.J., and Bao, G. (2014). CRISPR/Cas9 systems have off-target

140

activity with insertions or deletions between target DNA and guide RNA sequences. Nucleic Acids Res. *42*, 7473–7485.

54. Schaefer, K.A., Wu, W.H., Colgan, D.F., Tsang, S.H., Bassuk, A.G., and Mahajan, V.B. (2017). Unexpected mutations after CRISPR-Cas9 editing in vivo. Nat. Methods *14*, 547–548.

55. Haapaniemi, E., Botla, S., Persson, J., Schmierer, B., and Taipale, J. (2018). CRISPR-Cas9 genome editing induces a p53-mediated DNA damage response. Nat. Med. *24*, 927–930.

56. Kosicki, M., Tomberg, K., and Bradley, A. (2018). Repair of double-strand breaks induced by CRISPR-Cas9 leads to large deletions and complex rearrangements. Nat. Biotechnol. *36*, 765–771.

57. Cullot, G., Boutin, J., Toutain, J., Prat, F., Pennamen, P., Rooryck, C., Teichmann, M., Rousseau, E., Lamrissi-Garcia, I., Guyonnet-Duperat, V., et al. (2019). CRISPR-Cas9 genome editing induces megabase-scale chromosomal truncations. Nat. Commun. *10*, 1136.

58. Wagner, D.L., Amini, L., Wendering, D.J., Burkhardt, L.M., Akyüz, L., Reinke, P., Volk, H.D., and Schmueck-Henneresse, M. (2019). High prevalence of *Streptococcus pyogenes* Cas9-reactive T cells within the adult human population. Nat. Med. *25*, 242–248.

59. Charlesworth, C.T., Deshpande, P.S., Dever, D.P., Camarena, J., Lemgart, V.T., Cromer, M.K., Vakulskas, C.A., Collingwood, M.A., Zhang, L., Bode, N.M., et al. (2019). Identification of preexisting adaptive immunity to Cas9 proteins in humans. Nat. Med. *25*, 249–254.

60. Villalobos, X., Rodríguez, L., Prévot, J., Oleaga, C., Ciudad, C.J., and Noé, V. (2014). Stability and immunogenicity properties of the gene-silencing polypurine reverse Hoogsteen hairpins. Mol. Pharm. *11*, 254–264.

61. Berman, C.L., Barros, S.A., Galloway, S.M., Kasper, P., Oleson, F.B., Priestley, C.C., Sweder, K.S., Schlosser, M.J., and Sobol, Z. (2016). OSWG recommendations for genotoxicity testing of novel oligonucleotide-based therapeutics. Nucleic Acid Ther. *26*, 73–85.

62. European Medicines Agency (2005). CHMP SWP reflection paper on the assessment of the genotoxic potential of antisense oligodeoxynucleotides, https://www.ema.europa.eu/en/documents/scientific-guideline/chmp-swp-reflection-paper-assessment-genotoxic-potential-antisense-oligodeoxynucleotides_en.pdf.

63. Henry, S.P., Monteith, D.K., Matson, J.E., Mathison, B.H., Loveday, K.S., Winegar, R.A., Matson, J.E., Lee, P.S., Riccio, E.S., Bakke, J.P., and Levin, A.A. (2002). Assessment of the genotoxic potential of ISIS 2302: a phosphorothioate oligodeoxynucleotide. Mutagenesis *17*, 201–209.

64. Sazani, P., Weller, D.L., and Shrewsbury, S.B. (2010). Safety pharmacology and genotoxicity evaluation of AVI-4658. Int. J. Toxicol. *29*, 143–156.

65. Guérard, M., Andreas, Z., Erich, K., Christine, M., Martina, M.B., Christian, W., Franz, S., Thomas, S., and Yann, T. (2017). Locked nucleic acid (LNA): based single-stranded oligonucleotides are not genotoxic. Environ. Mol. Mutagen. *58*, 112–121.

66. Knauert, M.P., Kalish, J.M., Hegan, D.C., and Glazer, P.M. (2006). Triplex-stimulated intermolecular recombination at a single-copy genomic target. Mol. Ther. *14*, 392–400.

67. Datta, H.J., Chan, P.P., Vasquez, K.M., Gupta, R.C., and Glazer, P.M. (2001). Triplex-induced recombination in human cell-free extracts. Dependence on XPA and HsRad51. J. Biol. Chem. *276*, 18018–18023.

68. Rogers, F.A., Vasquez, K.M., Egholm, M., and Glazer, P.M. (2002). Site-directed recombination via bifunctional PNA-DNA conjugates. Proc. Natl. Acad. Sci. USA *99*, 16695–16700.

69. Faruqi, A.F., Datta, H.J., Carroll, D., Seidman, M.M., and Glazer, P.M. (2000). Triple-helix formation induces recombination in mammalian cells via a nucleotide excision repair-dependent pathway. Mol. Cell. Biol. *20*, 990–1000.

70. Papaioannou, I., Simons, J.P., and Owen, J.S. (2012). Oligonucleotide-directed gene-editing technology: mechanisms and future prospects. Expert Opin. Biol. Ther. *12*, 329–342.

71. Gupta, R.C., Bazemore, L.R., Golub, E.I., and Radding, C.M. (1997). Activities of human recombination protein Rad51. Proc. Natl. Acad. Sci. USA *94*, 463–468.

72. Krejci, L., Altmannova, V., Spirek, M., and Zhao, X. (2012). Homologous recombination and its regulation. Nucleic Acids Res. *40*, 5795–5818.

73. Vasquez, K.M., Christensen, J., Li, L., Finch, R.A., and Glazer, P.M. (2002). Human XPA and RPA DNA repair proteins participate in specific recognition of triplex-induced helical distortions. Proc. Natl. Acad. Sci. USA *99*, 5848–5853.

74. Phear, G., Armstrong, W., and Meuth, M. (1989). Molecular basis of spontaneous mutation at the *aprt* locus of hamster cells. J. Mol. Biol. *209*, 577–582.

75. Simon, A.E., Taylor, M.W., Bradley, W.E., and Thompson, L.H. (1982). Model involving gene inactivation in the generation of autosomal recessive mutants in mammalian cells in culture. Mol. Cell. Biol. *2*, 1126–1133.

76. Wigler, M., Pellicer, A., Silverstein, S., Axel, R., Urlaub, G., and Chasin, L. (1979). DNA-mediated transfer of the adenine phosphoribosyltransferase locus into mammalian cells. Proc. Natl. Acad. Sci. USA *76*, 1373–1376.

77. Johnson, L.A., Gordon, R.B., and Emmerson, B.T. (1977). Adenine phosphoribosyltransferase: a simple spectrophotometric assay and the incidence of mutation in the normal population. Biochem. Genet. *15*, 265–272.

78. Marco-Sola, S., Sammeth, M., Guigó, R., and Ribeca, P. (2012). The GEM mapper: fast, accurate and versatile alignment by filtration. Nat. Methods *9*, 1185–1188.

79. McKenna, A., Hanna, M., Banks, E., Sivachenko, A., Cibulskis, K., Kernytsky, A., Garimella, K., Altshuler, D., Gabriel, S., Daly, M., and DePristo, M.A. (2010). The Genome Analysis Toolkit: a MapReduce framework for analyzing next-generation DNA sequencing data. Genome Res. *20*, 1297–1303.

80. Altschul, S.F., Gish, W., Miller, W., Myers, E.W., and Lipman, D.J. (1990). Basic local alignment search tool. J. Mol. Biol. *215*, 403–410.

Results

4.5.1 Additional results to article V

Some additional experiments were performed to study the implication of homologous recombination in the repair event triggered by the repair-PPRH. Moreover, the hypothetical involvement of a replication process in the correction of the mutation was also addressed by PCR experiments.

4.5.1.1 Repair frequency is increased with RAD51 overexpression

To check whether homologous recombination could be involved in the repair event triggered by the repair-PPRH, we transfected S23 cells either with the HpS23E1rep repair-PPRH alone or in combination with a pRad51 expression vector. After selecting the cells in +AAT medium, we stained the cell surviving colonies to calculate the repair frequency. As shown in Figure 18, we observed a 2.8-fold increase in the repair frequency when co-transfecting the HpS23E1rep with the pRad51 expression vector.
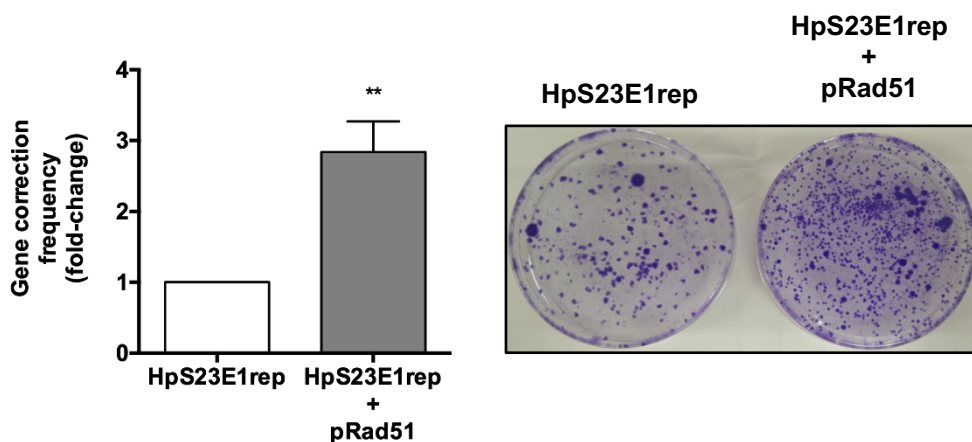
Figure 18. Gene correction frequency data. Comparison of gene correction frequency values between S23 cells transfected with either the HpS23E1rep alone or in combination with 5 µg of a RAD51 expression vector (left). A representative image of each condition is also shown (right). Data are represented as the mean ± SEM values of four experiments. Statistical analyses were performed using unpaired Student's t test. (**) $p < 0.01$.

4.5.1.2. Involvement of replication in the repair event

To test the possible implication of a replication process in the repair event, we performed an *in vitro* approach consisting in a PCR amplification of the S23 mutation site using a standard forward primer and the HpS23repli repair-PPRH. Our hypothesis was that the HpS23repli repair-PPRH would be able to act as reverse primer, thus amplifying the target site but incorporating the corrected nucleotide. As shown in Figure 19, the PCR reaction showed a 137 bp product corresponding to the size of the desired amplified region. This PCR product was purified and sequenced, demonstrating that it contained the corrected nucleotide.
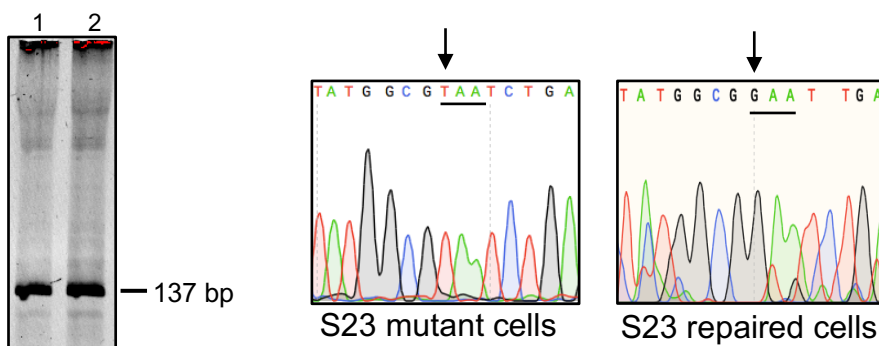
Figure 19. PCR reactions. Polyacrylamide gel electrophoresis showing the 137 bp PCR product corresponding to the target mutation site (left). The amplified product was purified and sequenced, demonstrating that it contained the corrected nucleotide instead of the original mutation (right).

4.6 Correction of the *FANCA* gene in FA cells

4.6.1 MMC sensitivity of FANCA- vs FANCA+ cells

To determine MMC sensitivity in both FA-55 cells and CP1 cells, we incubated both cell lines with increasing concentrations of MMC. As shown in Figure 20, CP1 cells (FANCA$^+$) were more resistant to MMC, especially in the 10-100 nM concentration range, whereas FA-55 cells (FANCA$^-$) were less prone to survive in the same range of concentration.
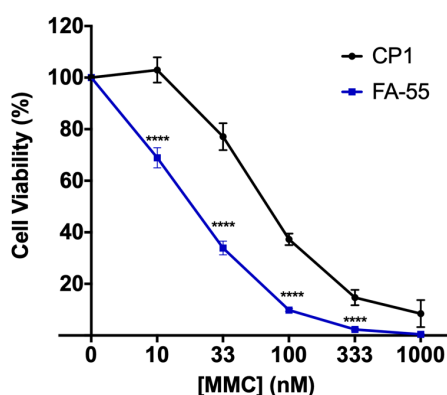

Figure 20. MMC dose-response. Both CP1 and FA-55 cells were incubated with increasing concentrations of MMC. Six days after incubation, cell viability was determined by MTT assay. Data are represented as the mean ± SEM values of three experiments. Statistical analyses were performed using 2way ANOVA. (****) $p < 0.001$.

4.6.2 DNA binding assays

We performed DNA binding assays to test the capacity of the HpFANCA-short repair-PPRH to form the triplex with its polypyrimidine target sequence in the *FANCA* mutation site. Increasing amounts of HpFANCA-short (150-1500 ng) were incubated with the dsDNA-FANCA probe, showing a shifted band corresponding to the repair-PPRH/dsDNA triplex structure (Figure 21). The incubation of the probe with the Hp-Sc6 scrambled PPRH did not produce any shift, thus demonstrating that the binding of the repair-PPRH to the target site was sequence-specific.
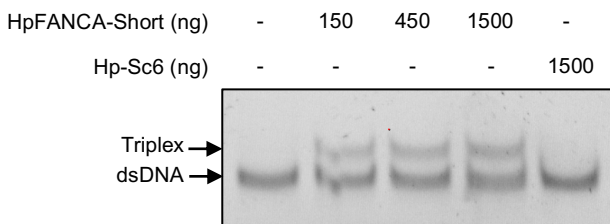
Figure 21. DNA binding assays. The 6-FAM-labeled dsDNA-FANCA probe (75 ng) was incubated with increasing amounts of the HpFANCA-short repair-PPRH. The Hp-Sc6 scrambled PPRH was used as negative control.

4.6.3 Correction of the c.295 C>T mutation in the FANCA gene

We transfected FA-55 cells with the different repair-PPRHs directed against the c.295 C>T mutation in the *FANCA* gene. After 72 h of incubation, 33 nM MMC were added to enrich the FANCA[+] cell population. Then, gDNA from each condition was extracted and gene correction frequency was determined by deep sequencing. LD-HpFANCA-1 and LD-HpFANCA-2 repair-PPRHs were not able to repair the mutation (Figure 22). However, the HpFANCA-short repair-PPRH showed significant repair frequencies, achieving a 0.6% in the best case (Figure 22).
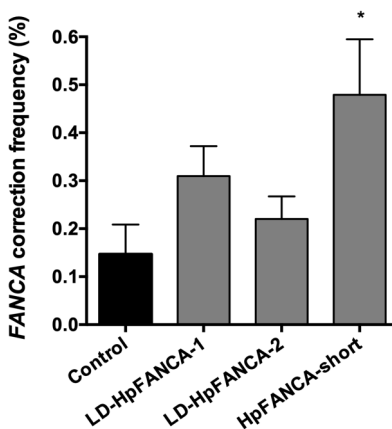
Figure 22. *FANCA* gene correction frequency. FA-55 cells were transfected with different repair-PPRHs. gDNA was extracted for each condition and the *FANCA* target site was amplified by PCR and deep-sequenced. Data are represented as the mean ± SEM values of three experiments. Statistical analyses were performed using ordinary one-way ANOVA with Dunnett's multiple comparison tests. (*) $p < 0.05$.

As positive control, we sequenced DF42 cell pools at two different time points, 14 and 21 days after transfection with HpDE6rep repair-PPRH and selection in -GHT medium. Deep-sequencing analyses confirmed that the percentage of corrected DF42 cells in the pool increased over time. Data showed 81% and 95% of corrected DF42 cells at 14 and 21 days after transfection, respectively.

5. DISCUSSION

5.1 PPRHs as gene silencing tools

One of the aims of our laboratory is to demonstrate that PPRHs can be used as alternative gene silencing tools. For that reason, the objectives of this work were to study the specificity and toxicity of these molecules and to explore new applications such as cancer immunotherapy.

5.1.1 Specificity and toxicity of PPRHs

Although PPRHs are a recent gene silencing tool, we have already validated their functionality both *in vitro* and *in vivo*. We have used PPRHs against different target genes involved in cancer progression such as *DHFR* (de Almagro *et al.* 2011)*, telomerase* (de Almagro *et al.* 2009, 2011), *BCL2*, *TOP1*, *MDM2*, *C-MYC* and *mTOR* in pancreatic, prostate, colon and breast cancer cell lines (Villalobos *et al.* 2015). In all cases, PPRHs were able to decrease the mRNA and protein levels of the targeted genes, thus producing a huge reduction of cancer cells viability. In addition, we tested different PPRHs against the *survivin* gene, which is an inhibitor of apoptosis overexpressed in different types of tumors that also promotes angiogenesis, metastasis and chemoresistance (Garg *et al.* 2016). PPRHs directed against *survivin* were transfected into PC3 prostate cancer cells, showing an increase in apoptosis that led to a final reduction of 90% on cell viability. The most effective PPRH against *survivin in vitro* was selected for the *in vivo* efficacy assays in a subcutaneous xenograft tumor model of PC3 prostate cancer cells. This PPRH directed against the *survivin* promoter (HpsPr-C) was able to decrease the tumor volume and reduce angiogenesis, thus validating the effect of PPRHs *in vivo* (Rodríguez *et al.* 2013).

In this work, we performed a functional pharmacogenomics study in prostate cancer cells upon incubation with the PPRH directed against *survivin* since the effects at the transcriptomic level and the possible off-target effects had not been extensively explored yet. We addressed the gene expression response in PC3 prostate cancer cells upon incubation with either the HpsPr-C-WT PPRH directed against the *survivin* promoter or the Watson-Crick negative hairpin. One of our first conclusions was that incubation with the negative hairpin did not produce any differentially expressed genes compared to the untreated cells. These results demonstrate that the PPRH (hairpin) molecule does not produce any off-target effect in the cell by itself, thus extending previous studies performed in our lab where we analyzed the expression of five non-related genes

chosen randomly (Rodríguez *et al.* 2013). In contrast, PC3 cells incubated with HpsPr-C-WT PPRH showed 244 differentially expressed genes when compared to the negative hairpin.

The 244 differentially expressed genes were classified by Gene Ontology mainly into the categories of binding and catalytic activities within molecular function, and cellular and metabolic within biological processes. Moreover, according to the Gene Set Enrichment Analysis, *survivin* underexpression led to the alteration of the gene sets belonging to cellular response to stress, regulation of cell proliferation, prostate cancer and apoptosis, thus confirming the proapoptotic wave produced by silencing the *survivin* gene with HpsPr-C-WT PPRH. In addition, we evaluated the possible relationships among the differentially expressed genes upon *survivin* underexpression using the STRING software for functional protein association networks. We identified the top ten more interrelated gene-nodes and analyzed their function to find out the pathways affected by the treatment with HpsPr-C-WT PPRH. Some of the most relevant genes identified in the analysis were *general transcription factor IIE* (*GTF2E2)*, *subunit G* of *RNA polymerase II* (*POLR2G*), histones (*HIST1H2AI* and *HIST1H2BE* genes), *DDX56* and *HELZ2* helicases and *SF3A1* splicing factor, among others. In summary, we determined that the genes included in the gene-nodes were involved in the regulation of vital cellular processes such as transcription and splicing, as well as genomic maintenance.

The primary routes of administration of therapeutic oligonucleotides for systemic applications are either subcutaneous or intravenous injection. After injection, oligonucleotides are absorbed into the circulation, showing peak plasma concentrations within 3-4 h. Following the peak plasma concentration, oligonucleotides rapidly distribute from circulation to tissues in minutes or few hours. In the case of naked administration, the clearance of the oligonucleotides depends on their metabolism by blood nucleases, their renal filtration and their accumulation in tissues (Geary *et al.* 2015). However, the bioavailability of oligonucleotides depends on their chemical properties. In the case of oligonucleotides that contain a phosphorothioate backbone, they extensively bind to plasma proteins, especially albumin, with low affinity. This prevents the loss of oligonucleotide to renal filtration, facilitating its uptake in tissues (Crooke 2008). In contrast, oligonucleotides that lack charge or more weakly bind to plasma proteins such as morpholinos, PNAs or siRNAs present more rapid clearance from blood primarily due to degradation in blood or excretion in urine, resulting in much lower tissue uptake (McMahon *et al.* 2002). Therefore, lower

binding oligonucleotides are presented at higher concentrations in the kidney than those with higher plasma protein binding. Nevertheless, the accumulation of oligonucleotides has also been observed in liver, lymph nodes, spleen, adipocytes and bone marrow (Geary 2009).

Since liver and kidney are two of the organs that present more accumulation of oligonucleotides after systemic administration, we wanted to test the possible toxicity of PPRHs in hepatic and renal models. In this regard, cell lines are a valuable tool to screen for cell toxicity mechanisms (Allen *et al.* 2005). They have the potential to serve as the primary choice for toxicity screening of drugs since are convenient, cost and time efficient and do not involve ethical issues (An & Tolliday 2010). Therefore, we explored the possible effects of PPRHs on toxicity *in vitro* at the hepatic and renal levels, using RT-qPCR arrays specifically developed for either hepatic or renal toxicity screening in HepG2 and 786-O cell lines, respectively. Our results showed the absence of relevant toxicity in liver and kidney since 94% and 86% of the genes present in the RT-qPCR arrays, respectively, were not significantly affected at their expression levels upon incubation with the Watson-Crick hairpin. Additionally, the incubation of either HepG2 or 786-O cells with the Watson-Crick hairpin did not produce any effect on cell viability.

These new properties of PPRHs along with other particularities that we had previously demonstrated in our lab, make PPRHs an alternative gene silencing tool with some advantages when compared to other molecules such as TFOs, ASOs or siRNAs. PPRHs are nonmodified DNA molecules that inhibit gene expression at lower concentrations than those needed for ASOs (de Almagro *et al.* 2009) or TFOs (Rodríguez *et al.* 2015). Additionally, we demonstrated that PPRHs were at least as efficient as siRNA in terms of cytotoxicity and decrease of target protein levels in the same range of concentration (de Almagro *et al.* 2009). However, PPRHs present advantages over siRNAs regarding their stability, economy and lack of immunogenicity (Villalobos *et al.* 2014). The extended half-life of PPRHs could be explained by the nature of their structure. PPRHs are single-stranded DNA molecules with a hairpin conformation due to the presence of intramolecular reverse Hoogsteen bonds. Therefore, PPRHs are not regular ssDNA molecules since they are protected by the pentathymidine loop on one side of the molecule that links both polypurine domains. This higher stability of PPRHs, even without chemical modifications, is a remarkable advantage. It is also important to consider that PPRHs follow the antigene strategy, which presents some additional

advantages compared to the antisense effect exerted by ASOs or siRNAs. First, when targeting the gene, there are only two targets per cell corresponding to the two alleles of the same gene, compared to the multiple copies of mRNA. Secondly, inhibition of transcription avoids formation of new mRNA transcrits, while molecules that inhibit translation do not stop mRNA synthesis and act in a more transient fashion. Finally, targeting DNA can impair the binding of proteins to the DNA (e.g. TFs), leading to high alterations in gene expression (Praseuth *et al.* 1999).

5.1.2 Immunotherapy approaches

Since we already validated the functionality of PPRHs as gene silencing tools both *in vitro* and *in vivo*, one of the aims of this work was to expand their applicability. In recent years, different immunotherapy approaches have been developed to trigger host's immune response to defeat tumors. In this regard, immune checkpoint blockade strategies using antibodies against checkpoint inhibitors such as the CD47/SIRPα and PD-1/PD-L1 pathways have been the focus of extensive research (Zhang *et al.* 2018; Ribas & Wolchok 2018). In this work, we have performed two different immunotherapy strategies using PPRHs to silence either the *CD47/SIRPα* or the *PD-1/PD-L1* tandem in order to stimulate the elimination of cancer cells by macrophages in co-culture experiments.

5.1.2.1 CD47/SIRPα

We explored the usage of PPRHs to decrease the expression of *SIRPα* and *CD47* in macrophages and MCF7 breast cancer cells, respectively. A total of four PPRHs were designed, two against the *SIRPα* gene and two against the *CD47* gene. All PPRHs were able to decrease either SIRPα or CD47 mRNA and protein levels in THP-1 and MCF7 cells, respectively. We also confirmed that THP-1 cells were PMA-differentiated into macrophages by analyzing the mRNA expression of specific macrophage markers including CD14, MCL-1, IL-1ß, IL-18, IL-6, IL-8 and TNF-α. In the MCF7/macrophage co-culture experiments, we showed that macrophages were able to eliminate tumor cells by decreasing the CD47/SIRPα interaction, whereas tumor cells remained unaffected in the absence of treatment with PPRHs. It is important to note that when an anti-CD47 antibody was used in the co-culture experiments, we obtained the same effect on cell viability that the co-culture transfected with the PPRHs, thus

demonstrating that PPRHs were at least as effective as the antibody. In addition, we determined that the mechanism responsible for the observed cell death was apoptosis.

Different monoclonal antibodies have been developed to inhibit the interaction between CD47 and SIRPα. Anti-CD47 antibodies have shown their efficacy both *in vitro* and *in vivo* in different types of cancer (Liu *et al.* 2015; Gu *et al.* 2018; Jain *et al.* 2019; Sun *et al.* 2020). It has also been determined the synergic effect of antibodies against CD47 and other therapeutic antibodies (e.g. rituximab) on the phagocytosis of non-Hodgkin lymphoma by macrophages in immune-deficient mice (Chao *et al.* 2010b), thus supporting the idea that blocking the CD47/SIRPα interaction can enhance the clinical effects of other cancer therapeutic antibodies (Zhao *et al.* 2011). Remarkably, some anti-CD47 antibodies like Hu5F9-G4 are currently being tested in clinical trials to treat patients with advanced cancers (Sikic *et al.* 2019). In a similar way, some approaches using antibodies to block SIRPα have also been developed to potentiate antitumor immunity (Liu *et al.* 2016; Yanagita *et al.* 2017).

However, treatment with these antibodies can present some side effects such as pro-thrombotic or anti-thrombotic activities (Isenberg *et al.* 2008) and altered blood pressure (Bauer *et al.* 2010). Moreover, it has been reported that mice that received an acute infusion of antibodies exhibited temporary anemia (Willingham *et al.* 2012) or neutropenia (Majeti *et al.* 2009). For that reason, alternative strategies like the usage of antisense molecules have also been tested to target CD47 in tumor cells. For instance, siRNAs were used to inhibit CD47 in the tumor to stimulate phagocytosis, demonstrating its efficacy both *in vitro* and *in vivo* (Wang *et al.* 2013). Schwartz et. al. also showed that the inhibition of CD47 using a blocking morpholino enhanced the killing of melanoma cells (Schwartz *et al.* 2019).

5.1.2.2 PD-1/PD-L1

Since we had already validated the usage of PPRHs against the CD47/SIRPα tandem, we wanted to further explore the application of PPRHs in immunotherapy approaches. Therefore, we described the usage of PPRHs directed against the *PD-1* and *PD-L1* genes in macrophages and cancer cells, respectively, to favor the elimination of tumor cells by macrophages.

A total of four PPRHs were designed: two against *PD-1* and two against *PD-L1*. These PPRHs were able to highly reduce PD-1 and PD-L1 mRNA and protein levels in THP-1 and PC3 prostate cancer cells, respectively. Prior to perform the co-culture experiments, we tested the different PPRHs directed against *PD-1* and *PD-L1* either alone or in combination in THP-1 cells and PMA-differentiated macrophages, demonstrating that the incubation of these cells with these PPRHs did not produce any effect on cell viability. This was an important point since the rationale was to assess the contribution of macrophages in co-culture experiments to eliminate cancer cells after inhibiting the PD-1/PD-L1 interaction and not by the effect of PPRHs *per se*. However, PC3 cells treated with PPRHs against *PD-L1* showed a reduction on cell viability. These results can be explained since, aside from avoiding tumor immunity, PD-1/PD-L1 inhibition presents cell-intrinsic functions such as mTOR signaling that promote tumor growth and survival (Kleffel *et al.* 2015; Clark *et al.* 2016). Our results are also in accordance with other works determining that knockdown of *PD-L1* in different types of cancer using siRNAs provoked a reduction on cell proliferation (Shi *et al.* 2013; Song *et al.* 2014; Kwak *et al.* 2017; Li *et al.* 2017).

Regarding the PC3/macrophage co-culture experiments, when only one of the two target genes (*PD-1* or *PD-L1*) was inhibited with their corresponding PPRHs, macrophages were able to kill half of the cancer cells present in the co-culture. Interestingly, when both PD-1 and PD-L1 were inhibited, macrophages killed the vast majority of PC3 cancer cells present in the co-culture, thus supporting our hypothesis that blocking PD-1/PD-L1 interaction from both sides could lead to a greater effect.

At this point, we expanded our results obtained in prostate cancer cells to other cancer cell lines such as melanoma M21, ovarian cancer HeLa and breast cancer SKBR3. In all cases, when PPRHs against *PD-1* and *PD-L1* were transfected into macrophages and cancer cells, respectively, in co-culture experiments, we obtained a high degree of cell mortality. However, M21 cancer cells were less affected compared to HeLa and SKBR3 cancer cells. These differences in the outcome among the different cancer cell lines could be explained since both cervix and prostate tissues present a higher *PD-L1* expression compared to breast and skin tissues (Uhlen *et al.* 2015). Other studies have also demonstrated that inhibition of the PD-1/PD-L1 pathway using gene silencing molecules (e.g. siRNAs) stimulate the immune response against tumor cells. For instance, Iwamura et al. described that suppression of PD-L1

using a siRNA in a lung adenocarcinoma cell line triggered the lysis of tumor cells conducted by CD8$^+$ T cells (Iwamura *et al.* 2012). Juneja et al. also determined that *PD-L1* expression in murine colon adenocarcinoma MC38 cells inhibited CD8$^+$ T cell response and cytotoxicity against tumor cells. However, CD8$^+$ T cells were still able to kill tumor cells that did not express *PD-L1*, demonstrating its significant suppressing effect (Juneja *et al.* 2017).

Finally, we demonstrated that the mechanism responsible for the killing of cancer cells by macrophages in the co-culture experiments was apoptosis, which was in accordance with our previous data regarding the inhibition of the CD47/SIRPα tandem. All these determinations were also in agreement with observations made by Cerignoli and collaborators, showing an increase in apoptosis when using anti-PD-1 antibodies (Cerignoli *et al.* 2018).

The search for alternatives to cell-based therapies or monoclonal antibodies is more than justified since the cost for an immunotherapy treatment could represent up to \$475,000 per patient (Dolgin 2018). In this direction, PPRHs represent a gene silencing technology that have demonstrated their efficacy both *in vitro* and *in vivo* in different cancer models. Moreover, PPRH synthesis is very economical since they are ssODNs with no modifications and they are non-immunogenic and more stable than siRNAs. PPRHs also present a low toxicity profile without off-target effects, therefore, they could be used as an alternative pharmacological agent in immunotherapy approaches for the inhibition of both the CD47/SIRPα and PD-1/PD-L1 pathways.

5.2 PPRHs as gene editing tools

In recent years, we have demonstrated that PPRHs can also be used as gene editing tools since we were able to correct different point mutations in the dsDNA in *dhfr*-deficient CHO cell lines (Solé *et al.* 2014, 2016). In this regard, the aims of this work were to prove the generality of action of repair-PPRHs by correcting different mutations in the *aprt* gene, to evaluate the possible off-target effects of this technology and to get insight into the mechanism responsible for the gene correction. Finally, we applied the repair-PPRHs to correct a single point mutation in the *FANCA* gene responsible for Fanconi anemia in a patient-derived human cell line.

5.2.1 Gene correction of the *aprt* gene

In this work, we performed gene correction experiments in *aprt*-deficient CHO cell lines (S23, S62 and S1) that contained different single-point substitutions in the endogenous *locus* of the *aprt* gene. We designed repair-PPRHs against three different mutations and, in all cases, they were able to correct the target mutation at the genomic level. Moreover, gene correction was also determined at the mRNA and enzymatic activity levels, thus demonstrating that the translated APRT protein was completely functional. Since one of the limitations of repair-PPRHs is the requirement of a polypyrimidine tract near the mutation to be corrected, we dealt with this situation by designing a long-distance repair-PPRH in which the target sequence for the repair domain was located 24 nt upstream of the hairpin core. This long-distance repair-PPRH was able to correct the mutation contained in the S23 cell line, thus indicating that adjacency between the hairpin core and the repair domain was not necessary to produce the repair. These results were in accordance with our previous data showing that a long-distance repair-PPRH containing a hairpin core binding 662 nt away from the mutation site was able to produce the correction (Solé *et al.* 2016). Nevertheless, the frequency of polypyrimidine stretches around the human genome is more abundant than that predicted by simple random models (Goñi *et al.* 2004). Therefore, it is not difficult to find an appropriate sequence adjacent to the location of the mutation.

We tested different negative controls to demonstrate that both the polypurine hairpin and the repair domain of the repair-PPRH were necessary to achieve the correction. No surviving cell colonies were obtained when cells were transfected only with the repair domain of the repair-PPRH or when this domain was attached to a scrambled polypurine hairpin. This fact corroborated with our previous observation that repair domains bearing hairpin cores bound by intramolecular WC bonds instead of Hoogsteen bonds did not produce the correction (Solé *et al.* 2014).

We also studied the influence of the cell cycle stage in the repair frequency. In this regard, the highest level of gene correction was attained when cells were transfected just after release from S phase upon synchronization. These results correlated with our previous data regarding the correction of point mutations in the *dhfr* gene after releasing the cells to S phase (Solé *et al.* 2014), and also with the work of Brachman and Kmiec (Brachman & Kmiec 2005) that showed increased repair frequencies by lengthening the S phase and stalling

the replication fork, thus inducing the HDR pathway. Other studies also demonstrated that the S phase stage was the most prone to achieve the correction of the mutation (Majumdar *et al.* 2003; Olsen *et al.* 2005).

The most popular gene-editing technologies these days such as ZFNs, TALENs and specially CRISPR/Cas systems rely on the activity of nucleases that produce extrinsic DSBs to achieve the correction of the mutation. Although it is known that CRISPR/Cas systems can obtain good gene editing frequencies (Nambiar *et al.* 2019), one of the concerns with these nuclease-based technologies is the presence of off-target effects in the repaired genome such as small deletions, insertions or substitutions, usually produced by unspecific DSBs of the nuclease (Cradick *et al.* 2013; Lin *et al.* 2014; Schaefer *et al.* 2017; Anderson *et al.* 2018; Allen *et al.* 2019). It has also been reported that these DSBs can induce a p53-mediated DNA damage response, thus leading to cell cycle arrest (Haapaniemi *et al.* 2018). Aside from off-target effects, on-target mutagenesis such as unexpected chromosomal truncations (Cullot *et al.* 2019) and large deletions in the target site (Kosicki *et al.* 2018) have also been described. In this work, we demonstrated by whole genome sequencing that repair-PPRHs did not produce any off-target effects in the genome of the repaired cells. We did not detect any random deletions or insertions caused by the repair-PPRH, and we did not find any insertion of the repair-PPRH itself in the repaired genome. Another concern about the CRISPR/Cas system is the presence of a preexisting effector T cell response directed towards Cas9 proteins in human beings since *Staphylococcus pyogenes* and *Staphylococcus aureus* cause infections in the human population at high frequencies (Charlesworth *et al.* 2019; Wagner *et al.* 2019). In contrast, PPRHs are very economical, non-modified and non-immunogenic DNA molecules that do not activate the innate inflammatory response (Villalobos *et al.* 2014).

In addition, we wanted to study the molecular mechanism responsible for the repair event. First, we showed a triplex structure generated by the specific binding of the hairpin core of the repair-PPRH to the polypyrimidine target sequence in the dsDNA. Then, we determined the formation of a D-loop structure upon incubation of the hairpin core of the repair-PPRH to the target sequence that could eventually stimulate the repair event. The general mechanism of action of a repair-PPRH is depicted in Figure 23. It is known that both the HDR (Datta *et al.* 2001; Knauert *et al.* 2006) and the NER (Faruqi *et al.* 2000; Datta *et al.* 2001; Rogers *et al.* 2002b) pathways are involved in gene repair processes induced by triplex-forming oligonucleotides.

Regarding the HDR pathway, RAD51 is one of the main proteins involved in this process by promoting the homologous pairing of a single-stranded DNA to a duplex DNA in a structure similar to a D-loop (Gupta *et al.* 2002; Krejci *et al.* 2012; Papaioannou *et al.* 2012). Therefore, this D-loop structure as the one shown in this work can stimulate the HDR pathway, thus correcting the targeted mutation. Moreover, transfection of the repair-PPRH directed against the S23 mutation along with a Rad51 expression vector increased the gene correction frequency by 3-fold, thus confirming that the HDR pathway is involved in the repair process triggered by the repair-PPRH. This is in agreement with our previous data showing a 10-fold increase in gene correction frequency after transfecting a repair-PPRH directed against a mutation in the *dhfr* gene along with the Rad51 expression vector (Solé *et al.* 2014).

Concerning the NER pathway, it is known that triple helix structures can be identified by the XPA/RPA DNA damage recognition complex that recruits NER machinery to these distorted sites, leading to DNA repair activity that generates recombination intermediates (Vasquez *et al.* 2002). However, the entire mechanism by which these triplex structures stimulate recombination remains unclear.

Finally, since we hypothesized that a replication mechanism could also be involved in the repair event, we performed a PCR amplification of the targeted mutation site using a standard forward primer and the repair-PPRH acting like a reverse primer. In these experiments, we observed that the repair-PPRH was able to amplify the desired PCR product and we determined by DNA sequencing that the amplicon contained the corrected nucleotide instead of the mutated one. This is in agreement with the "annealing-integration" proposed model reported by Court and collaborators, in which the oligonucleotide anneals to a single-stranded region at the replication fork, where DNA polymerase and ligase complete the gene repair process by extending the annealed oligonucleotide (serving as a primer) and joining it to the chromosomal DNA (Ellis *et al.* 2001; Huen *et al.* 2006).
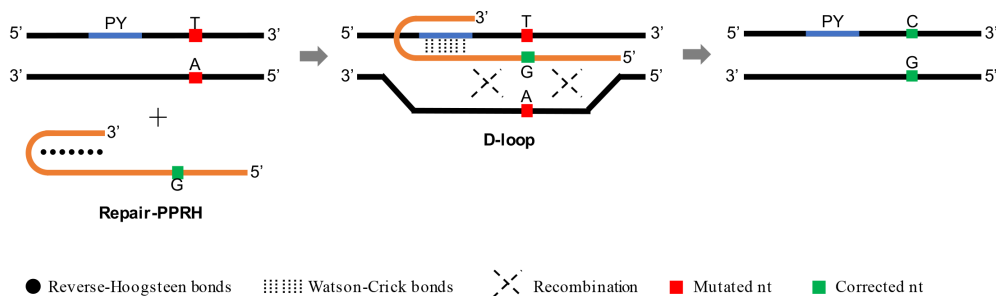
Figure 23. Mechanism of action of a repair-PPRH. The polypurine hairpin core of the repair-PPRH binds to the polypyrimidine target sequence (PY) through WC bonds, thus producing the triplex. This binding generates the formation of a D-loop structure in the dsDNA that stimulates the recombination between the mutation site and the corrected sequence contained in the repair-PPRH.

5.2.2 Gene correction of the *FANCA* gene.

We envision repair-PPRHs as an alternative gene-editing tool to correct single point mutations responsible for human monogenic diseases. For that reason, we designed repair-PPRHs to correct a mutation responsible for FA in human cells.

Although FA is a complex disease that can be caused by mutations in 21 different genes of the *FANC* family (Palovcak *et al.* 2017), 60% of total FA patients bear mutations in the *FANCA* gene (Antonio Casado *et al.* 2007; Auerbach 2009). For that reason, we applied the repair-PPRHs technology to correct a single point substitution (c.295 C>T) in the *FANCA* gene that generated a premature stop codon in a patient-derived lymphoblastic cell line (FA-55). We designed three different repair-PPRHs directed against the mutation: two following the long-distance approach because the polypyrimidine target sequence was located far away from the mutation, and the other one consisting of a regular design (or short-distance) since the polypyrimidine target sequence was located near the mutation. The two long-distance repair-PPRHs were not able to repair the mutation in FA-55 cells. However, the HpFANCA-short repair-PPRH obtained a slight but significant repair frequency value compared to the control cells. Although these gene correction frequency values seem too low to be phenotypically and clinically relevant, it has been demonstrated that *FANCA* gene-corrected hematopoietic stem cells (HSCs) present an *in vivo* proliferative

advantage once they are transplanted into immunodeficient mice, thus repopulating the hematopoietic cells of the organism (Río *et al.* 2017). Recently, it has also been reported that lentiviral-mediated hematopoietic gene therapy conferred engraftment and proliferation advantages of gene-corrected HSCs in non-conditioned patients with FA subtype A (Río *et al.* 2019). Therefore, we could hypothetically use repair-PPRHs *ex vivo* to correct some HSCs and eventually obtain an *in vivo* corrected FA phenotype regardless of the initial percentage of repaired cells.

A recent work from Río and collaborators also demonstrated the functional correction of different *FANC* genes by exploiting the NHEJ pathway, which is the preferred repair mechanism used by HSCs. The strategy consisted in inducing DNA breaks by CRISPR/Cas9 near to the target mutation to trigger a NHEJ-mediated repair, thus generating compensatory insertions or deletions that restored the coding frame of the mutated gene. Interestingly, they obtained a 0,41% of therapeutic indels 5 days after the treatment of the cells. However, 60 days after the treatment, the percentage of edited cells was 47,53% due to the proliferative advantage of functional cells versus the mutated population (Román-Rodríguez *et al.* 2019). In contrast, our approach using repair-PPRHs could specifically correct the point mutation in the endogenous *locus* and restore the wild-type *FANCA* gene without inducing any DSBs, thus avoiding the possible generation of off-target effect in the edited cells. Nevertheless, the application of repair-PPRHs for the *FANCA* gene is currently in preliminary stages and further experiments need to be conducted to achieve the correction in a more reliable way.

6. CONCLUSIONS

1. The PPRH directed against the promoter of the antiapoptotic gene *survivin* specifically alter the expression of genes involved in cell proliferation, cellular response to stress and apoptosis in PC3 prostate cancer cells. On the other hand, the Watson-Crick DNA hairpin, used as the negative control, does not alter gene expression nor produces any effect on cell viability.

2. PPRH molecules do not present hepatotoxicity nor nephrotoxicity in HepG2 hepatic and 786-O renal cells, respectively.

3. PPRHs can decrease the expression of CD47 and SIRPα in MCF7 and THP-1 cells, respectively. The decrease in CD47/SIRPα interaction leads to an enhanced killing of MCF7 cells by macrophages in co-culture experiments, caused by an increase in apoptosis.

4. PPRHs can decrease the expression of PD-1 and PD-L1 in THP-1 and PC3 cells, respectively. The inhibition of PD-1/PD-L1 interaction produces a great reduction in cell viability in PC3, HeLa, SKBR3 and M21 cancer cells, caused by an increased killing of macrophages in co-culture experiments.

5. Repair-PPRHs are able to correct different single-point mutations in the endogenous *locus* of the *aprt* gene, thus demonstrating their generality of action. The gene correction event mediated by repair-PPRHs was specific and did not produce any off-target effect in the repaired genome as revealed by whole genome sequencing.

6. The binding of the repair-PPRH to its polypyrimidine target sequence produces a D-loop structure, which promotes homologous recombination. Rad51, which is involved in homologous recombination, plays an important role in the gene correction process triggered by repair-PPRHs.

7. The correction of mutations responsible for monogenic diseases in human cells could be achieved using repair-PPRHs.

7. BIBLIOGRAPHY

Ahmadzada, T., Reid, G., & McKenzie, D. R. (2018). Fundamentals of siRNA and miRNA therapeutics and a review of targeted nanoparticle delivery systems in breast cancer. *Biophysical Reviews*, **10**(1), 69–86.

Ahmed, S., & Rai, K. R. (2003). Interferon in the treatment of hairy-cell leukemia. *Best Practice and Research: Clinical Haematology*, Bailliere Tindall Ltd, pp. 69–81.

Ahn, J. D., Morishita, R., Kaneda, Y., … Lee, I. K. (2004). Transcription factor decoy for AP-1 reduces mesangial cell proliferation and extracellular matrix production in vitro and in vivo. *Gene Therapy*, **11**(11), 916–923.

Alexeev, V., Igoucheva, O., Domashenko, A., Cotsarelis, G., & Yoon, K. (2000). Localized in vivo genotypic and phenotypic correction of the albino mutation in skin by RNA-DNA oligonucleotide. *Nature Biotechnology*, **18**(1), 43–47.

Allen, D. D., Caviedes, R., Cárdenas, A. M., Shimahara, T., Segura-Aguilar, J., & Caviedes, P. A. (2005). Cell lines as in vitro models for drug screening and toxicity studies. *Drug Development and Industrial Pharmacy*, **31**(8), 757–768.

Allen, F., Crepaldi, L., Alsinet, C., … Parts, L. (2019). Predicting the mutations generated by repair of Cas9-induced double-strand breaks. *Nature Biotechnology*, **37**(1), 64–82.

Alsaab, H. O., Sau, S., Alzhrani, R., … Iyer, A. K. (2017). PD-1 and PD-L1 Checkpoint Signaling Inhibition for Cancer Immunotherapy: Mechanism, Combinations, and Clinical Outcome. *Frontiers in Pharmacology*, **8**. doi:10.3389/fphar.2017.00561

Altmann, D. M. (2018). A Nobel Prize-worthy pursuit: cancer immunology and harnessing immunity to tumour neoantigens. *Immunology*, **155**(3), 283–284.

Alvey, C. M., Spinler, K. R., Irianto, J., … Discher, D. E. (2017). SIRPA-Inhibited, Marrow-Derived Macrophages Engorge, Accumulate, and Differentiate in Antibody-Targeted Regression of Solid Tumors. *Current Biology*, **27**(14), 2065-2077.e6.

An, W. F., & Tolliday, N. (2010, June). Cell-based assays for high-throughput screening. *Molecular Biotechnology*, pp. 180–186.

Anderson, K. R., Haeussler, M., Watanabe, C., … Warming, S. (2018). CRISPR off-target analysis in genetically engineered rats and mice. *Nature Methods*, **15**(7), 512–514.

Andrieu-Soler, C., Casas, M., Faussat, A. M., … Concordet, J. P. (2005). Stable transmission of targeted gene modification using single-stranded oligonucleotides with flanking LNAs. *Nucleic Acids Research*, **33**(12), 3733–3742.

Antonio Casado, J., Callén, E., Jacome, A., … Bueren, J. A. (2007). A comprehensive strategy for the subtyping of patients with Fanconi anaemia: conclusions from the Spanish Fanconi Anemia Research Network. *Journal of Medical Genetics*, **44**(4), 241–249.

Anzalone, A. V, Randolph, P. B., Davis, J. R., … Liu, D. R. (2019). Search-and-replace genome editing without double-strand breaks or donor DNA. *Nature*, (August). doi:10.1038/s41586-

019-1711-4

Auerbach, A. D. (2009). Fanconi anemia and its diagnosis. *Mutation Research - Fundamental and Molecular Mechanisms of Mutagenesis*, **668**(1–2), 4–10.

Avery, O. T., Macleod, C. M., & McCarty, M. (1944). Studies on the chemical nature of the substance inducing transformation of pneumococcal types: Induction of transformation by a desoxyribonucleic acid fraction isolated from pneumococcus type iii. *Journal of Experimental Medicine*, **79**(2), 137–158.

Bahal, R., Ali McNeer, N., Quijano, E., … Glazer, P. M. (2016). In vivo correction of anaemia in β-thalassemic mice by γ3PNA-mediated gene editing with nanoparticle delivery. *Nature Communications*, **7**. doi:10.1038/ncomms13304

Barrangou, R., Fremaux, C., Deveau, H., … Horvath, P. (2007). CRISPR provides acquired resistance against viruses in prokaryotes. *Science*, **315**(5819), 1709–1712.

Bartlett, R. J., Stockinger, S., Denis, M. M., … Kornegay, J. N. (2000). In vivo targeted repair of a point mutation in the canine dystrophin gene by a chimeric RNA/DNA oligonucleotide. *Nature Biotechnology*, **18**(6), 615–622.

Bauer, E. M., Qin, Y., Miller, T. W., … Isenberg, J. S. (2010). Thrombospondin-1 supports blood pressure by limiting eNOS activation and endothelial-dependent vasorelaxation. *Cardiovascular Research*, **88**(3), 471–81.

Bell, D. A., Hooper, A. J., & Burnett, J. R. (2011). Mipomersen, an antisense apolipoprotein B synthesis inhibitor. *Expert Opinion on Investigational Drugs*, **20**(2), 265–272.

Ben-Sasson, S. Z., Hu-Li, J., Quiel, J., … Paul, W. E. (2009). IL-1 acts directly on CD4 T cells to enhance their antigen-driven expansion and differentiation. *Proceedings of the National Academy of Sciences of the United States of America*, **106**(17), 7119–7124.

Boch, J., & Bonas, U. (2010). Xanthomonas AvrBs3 Family-Type III Effectors: Discovery and Function . *Annual Review of Phytopathology*, **48**(1), 419–436.

Bollée, G., Harambat, J., Bensman, A., Knebelmann, B., Daudon, M., & Ceballos-Picot, I. (2012, September 1). Adenine phosphoribosyltransferase deficiency. *Clinical Journal of the American Society of Nephrology*, pp. 1521–1527.

Brachman, E. E., & Kmiec, E. B. (2003). Targeted nucleotide repair of cyc1 mutations in Saccharomyces cerevisiae directed by modified single-stranded DNA oligonucleotides. *Genetics*, **163**(2), 527–538.

Brachman, E. E., & Kmiec, E. B. (2005). Gene repair in mammalian cells is stimulated by the elongation of S phase and transient stalling of replication forks. *DNA Repair*, **4**(4), 445–457.

Brandsma, I., & Gent, D. C. (2012). Pathway choice in DNA double strand break repair: Observations of a balancing act. *Genome Integrity*, **3**(1), 1.

Broitman, S. L., Im, D. D., & Fresco, J. R. (1987). Formation of the triple-stranded polynucleotide helix, poly(A.A.U). *Proceedings of the National Academy of Sciences of the United States of America*, **84**(15), 5120–5124.

Brouns, S. J. J., Jore, M. M., Lundgren, M., … Van Der Oost, J. (2008). Small CRISPR RNAs guide antiviral defense in prokaryotes. *Science*, **321**(5891), 960–964.

Brown, A. J., Mainwaring, D. O., Sweeney, B., & James, D. C. (2013). Block decoys: Transcription-factor decoys designed for in vitro gene regulation studies. *Analytical Biochemistry*, **443**(2), 205–210.

Cabrales, P. (2019). RRx-001 Acts as a Dual Small Molecule Checkpoint Inhibitor by Downregulating CD47 on Cancer Cells and SIRP-α on Monocytes/Macrophages. *Translational Oncology*, **12**(4), 626–632.

Campbell, C. R., Keown, W., Lowe, L., Kirschling, D., & Kucherlapati, R. (1989). Homologous recombination involving small single-stranded oligonucleotides in human cells. *The New Biologist*, **1**(2), 223–7.

Carlson, D. F., Tan, W., Lillico, S. G., … Fahrenkrug, S. C. (2012). Efficient TALEN-mediated gene knockout in livestock. *Proceedings of the National Academy of Sciences of the United States of America*, **109**(43), 17382–17387.

Cerignoli, F., Abassi, Y. A., Lamarche, B. J., … Xi, B. (2018). In vitro immunotherapy potency assays using real-time cell analysis. *PLoS ONE*, **13**(3), 1–21.

Chao, M. P., Alizadeh, A. a., Tang, C., … Majeti, R. (2010a). Anti-CD47 Antibody Synergizes with Rituximab to Promote Phagocytosis and Eradicate Non-Hodgkin Lymphoma. *Cell*, **142**(5), 699–713.

Chao, M. P., Alizadeh, A. A., Tang, C., … Majeti, R. (2010b). Anti-CD47 Antibody Synergizes with Rituximab to Promote Phagocytosis and Eradicate Non-Hodgkin Lymphoma. *Cell*, **142**(5), 699–713.

Charlesworth, C. T., Deshpande, P. S., Dever, D. P., … Porteus, M. H. (2019). Identification of preexisting adaptive immunity to Cas9 proteins in humans. *Nature Medicine*, **25**(2), 249–254.

Chatterjee, N., & Walker, G. C. (2017, June 1). Mechanisms of DNA damage, repair, and mutagenesis. *Environmental and Molecular Mutagenesis*, John Wiley and Sons Inc., pp. 235–263.

Cheng, C. J., Bahal, R., Babar, I. A., … Slack, F. J. (2015). MicroRNA silencing for cancer therapy targeted to the tumour microenvironment. *Nature*, **518**(7537), 107–110.

Chernikov, I. V., Vlassov, V. V., & Chernolovskaya, E. L. (2019). Current development of siRNA bioconjugates: From research to the clinic. *Frontiers in Pharmacology*, **10**(APR). doi:10.3389/fphar.2019.00444

Chin, J. Y., Kuan, J. Y., Lonkar, P. S., … Glazer, P. M. (2008). Correction of a splice-site mutation in the beta-globin gene stimulated by triplex-forming peptide nucleic acids. *Proceedings of the National Academy of Sciences of the United States of America*, **105**(36), 13514–13519.

Choo, Y., & Isalan, M. (2000). Advances in zinc finger engineering. *Current Opinion in Structural Biology*, **10**(4), 411–416.

Ciavatta, V. T., Padove, S. A., Boatright, J. H., & Nickerson, J. M. (2005). Mouse retina has oligonucleotide-induced gene repair activity. *Investigative Ophthalmology and Visual Science*, **46**(7), 2291–2299.

Ciccia, A., & Elledge, S. J. (2010). The DNA Damage Response: Making It Safe to Play with Knives. *Molecular Cell*, **40**(2), 179–204.

Ciudad, C. J., Rodríguez, L., Villalobos, X., Félix, A. J., & Noé, V. (2017). Polypurine Reverse Hoogsteen Hairpins as a Gene Silencing Tool for Cancer. *Current Medicinal Chemistry*, **24**(26), 2809–2826.

Clark, C. A., Gupta, H. B., Sareddy, G., … Curiel, T. J. (2016). Tumor-intrinsic PD-L1 signals regulate cell growth, pathogenesis, and autophagy in ovarian cancer and melanoma. *Cancer Research*, **76**(23), 6964–6974.

Cole-Strauss, A., Gamper, H., Holloman, W. K., Muñoz, M., Cheng, N., & Kmiec, E. B. (1999). Targeted gene repair directed by the chimeric RNA/DNA oligonucleotide in a mammalian cell-free extract. *Nucleic Acids Research*, **27**(5), 1323–1330.

Cole-Strauss, A., Yoon, K., Xiang, Y., … Kmiec, E. B. (1996). Correction of the mutation responsible for sickle cell anemia by an RNA- DNA oligonucleotide. *Science*, **273**(5280), 1386–1389.

Coma, S., Noé, V., Eritja, R., Ciudad, C. J., & Noe, V. (2005). Strand displacement of double-stranded DNA by triplex-forming antiparallel purine-hairpins. *Oligonucleotides*, **15**(4), 269–283.

Control of hereditary diseases. Report of a WHO Scientific Group. (1996). *World Health Organization Technical Report Series*, **865**, 1–84.

Cooney, M., Czernuszewicz, G., Postel, E. H., Flint, S. J., & Hogan, M. E. (1988). Site-specific oligonucleotide binding represses transcription of the human c-myc gene in vitro. *Science*, **241**(4864), 456–459.

Costa, R. M. A., Chiganças, V., Galhardo, R. D. S., Carvalho, H., & Menck, C. F. M. (2003). The eukaryotic nucleotide excision repair pathway. *Biochimie*, **85**(11), 1083–1099.

Cox, M. A., Harrington, L. E., & Zajac, A. J. (2011, April). Cytokines and the inception of CD8 T cell responses. *Trends in Immunology*, pp. 180–186.

Cradick, T. J., Fine, E. J., Antico, C. J., & Bao, G. (2013). CRISPR/Cas9 systems targeting β-

globin and CCR5 genes have substantial off-target activity. *Nucleic Acids Research*, **41**(20), 9584–9592.

Crooke, S. T. (2008). *Antisense drug technology : principles, strategies, and applications*, CRC Press.

Crooke, S. T. (2017). Molecular Mechanisms of Antisense Oligonucleotides. *Nucleic Acid Therapeutics*, **27**(2), 70–77.

Crooke, S. T., Witztum, J. L., Bennett, C. F., & Baker, B. F. (2018). RNA-Targeted Therapeutics. *Cell Metabolism*, **27**(4), 714–739.

Cullot, G., Boutin, J., Toutain, J., … Bedel, A. (2019). CRISPR-Cas9 genome editing induces megabase-scale chromosomal truncations. *Nature Communications*, **10**(1), 1–14.

Curcio, L. D., Bouffard, D. Y., & Scanlon, K. J. (1997). Oligonucleotides as modulators of cancer gene expression. *Pharmacology and Therapeutics*, **74**(3), 317–332.

D'Acquisto, F., Ialenti, A., Ianaro, A., Di Vaio, R., & Carnuccio, R. (2000). Local administration of transcription factor decoy oligonucleotides to nuclear factor-κB prevents carrageenin-induced inflammation in rat hind paw. *Gene Therapy*, **7**(20), 1731–1737.

Daley, J. M., Palmbos, P. L., Wu, D., & Wilson, T. E. (2005). Nonhomologous End Joining in Yeast. *Annual Review of Genetics*, **39**(1), 431–451.

Dana, H., Chalbatani, G. M., Mahmoodzadeh, H., … Gharagouzlo, E. (2017). Molecular Mechanisms and Biological Functions of siRNA. *International Journal of Biomedical Science : IJBS*, **13**(2), 48–57.

Datta, H. J., Chan, P. P., Vasquez, K. M., Gupta, R. C., & Glazer, P. M. (2001). Triplex-induced Recombination in Human Cell-free Extracts. *Journal of Biological Chemistry*, **276**(21), 18018–18023.

de Almagro, M. C., Coma, S., Noé, V., & Ciudad, C. J. (2009). Polypurine hairpins directed against the template strand of DNA knock down the expression of mammalian genes. *Journal of Biological Chemistry*, **284**(17), 11579–11589.

de Almagro, M. C., Mencia, N., Noé, V., & Ciudad, C. J. (2011). Coding Polypurine Hairpins Cause Target-Induced Cell Death in Breast Cancer Cells. *Human Gene Therapy*, **22**(4), 451–463.

Dekker, M., Brouwers, C., Aarts, M., … te Riele, H. (2006). Effective oligonucleotide-mediated gene disruption in ES cells lacking the mismatch repair protein MSH3. *Gene Therapy*, **13**(8), 686–694.

Del Prete, G. Q., Haggarty, B., Leslie, G. J., … Hoxie, J. A. (2009). Derivation and characterization of a simian immunodeficiency virus SIVmac239 variant with tropism for CXCR4. *Journal of Virology*, **83**(19), 9911–22.

Deng, D., Yan, C., Pan, X., … Yan, N. (2012). Structural basis for sequence-specific recognition

of DNA by TAL effectors. *Science*, **335**(6069), 720–723.

Dever, D. P., Bak, R. O., Reinisch, A., … Porteus, M. H. (2016). CRISPR/Cas9 β-globin gene targeting in human haematopoietic stem cells. *Nature*, **539**(7629), 384–389.

Dip, R., Camenisch, U., & Naegeli, H. (2004). Mechanisms of DNA damage recognition and strand discrimination in human nucleotide excision repair. *DNA Repair*, **3**(11), 1409–1423.

Diviacco, S., Rapozzi, V., Xodo, L., Hélène, C., Quadrifoglio, F., & Giovannangeli, C. (2001). Site-directed inhibition of DNA replication by triple helix formation. *FASEB Journal*, **15**(14), 2660–2668.

Dolgin, E. (2018). Bringing down the cost of cancer treatment. *Nature 2020 555:7695*.

Doudna, J. A. (2020). The promise and challenge of therapeutic genome editing. *Nature*, **578**(7794), 229–236.

Duan, W., Guo, M., Yi, L., … Li, C. (2019). The deletion of mutant SOD1 via CRISPR/Cas9/sgRNA prolongs survival in an amyotrophic lateral sclerosis mouse model. *Gene Therapy*. doi:10.1038/s41434-019-0116-1

Duca, M., Vekhoff, P., Oussedik, K., Halby, L., & Arimondo, P. B. (2008). The triple helix: 50 years later, the outcome. *Nucleic Acids Research*, **36**(16), 5123–5138.

Ekman, F. K., Ojala, D. S., Adil, M. M., Lopez, P. A., Schaffer, D. V., & Gaj, T. (2019). CRISPR-Cas9-Mediated Genome Editing Increases Lifespan and Improves Motor Deficits in a Huntington's Disease Mouse Model. *Molecular Therapy - Nucleic Acids*, **17**(September), 829–839.

Ellington, a D., & Szostak, J. W. (1990). In vitro selection of RNA molecules that bind specific ligands. *Nature*, **346**(6287), 818–822.

Ellis, H. M., Yu, D., DiTizio, T., & Court, D. L. (2001). High efficiency mutagenesis, repair, and engineering of chromosomal DNA using single-stranded oligonucleotides. *Proceedings of the National Academy of Sciences of the United States of America*, **98**(12), 6742–6746.

Ellis, P. M., Vella, E. T., & Ung, Y. C. (2017, September 1). Immune Checkpoint Inhibitors for Patients With Advanced Non–Small-Cell Lung Cancer: A Systematic Review. *Clinical Lung Cancer*, Elsevier Inc., pp. 444-459.e1.

Faruqi, A. F., Datta, H. J., Carroll, D., Seidman, M. M., & Glazer, P. M. (2000). Triple-helix formation induces recombination in mammalian cells via a nucleotide excision repair-dependent pathway. *Molecular and Cellular Biology*, **20**(3), 990–1000.

Faruqi, A. F., Seidman, M. M., Segal, D. J., Carroll, D., & Glazer, P. M. (1996). Recombination induced by triple-helix-targeted DNA damage in mammalian cells. *Molecular and Cellular Biology*, **16**(12), 6820–6828.

FDA approves first treatment for inherited rare disease | FDA. (2019). Retrieved December 23, 2019, from https://www.fda.gov/news-events/press-announcements/fda-approves-first-

treatment-inherited-rare-disease

Fei, Q., Zhang, H., Fu, L., … Zhu, J. (2008). Experimental cancer gene therapy by multiple anti-survivin hammerhead ribozymes. *Acta Biochimica et Biophysica Sinica*, **40**(6), 466–477.

Felsenfeld, G., Davies, D. R., & Rich, A. (1957). Formation of a Three-Stranded Polynucleotide Molecule. *Journal of the American Chemical Society*, **79**(8), 2023–2024.

Fire, A., Xu, S., Montgomery, M. K., Kostas, S. A., Driver, S. E., & Mello, C. C. (1998). Potent and specific genetic interference by double-stranded RNA in Caenorhabditis elegans. *Nature*, **391**(February), 806–811.

Flagler, K., Alexeev, V., Pierce, E. A., & Igoucheva, O. (2008). Site-specific gene modification by oligodeoxynucleotides in mouse bone marrow-derived mesenchymal stem cells. *Gene Therapy*, **15**(14), 1035–1048.

Franklin, R. E., & Gosling, R. G. (1953). Evidence for 2-chain Helix in crystalline structure of sodium deoxyribonucleate. *Nature*, **172**(4369), 156–157.

Gamper, H. B., Parekh, H., C. Rice, M., Bruner, M., Youkey, H., & B. Kmiec, E. (2000). The DNA strand of chimeric RNA/DNA oligonucleotides can direct gene repair/conversion activity in mammalian and plant cell-free extracts. *Nucleic Acids Research*, **28**(21), 4332–4339.

Garg, A. D., Coulie, P. G., Van den Eynde, B. J., & Agostinis, P. (2017, August 1). Integrating Next-Generation Dendritic Cell Vaccines into the Current Cancer Immunotherapy Landscape. *Trends in Immunology*, Elsevier Ltd, pp. 577–593.

Garg, H., Suri, P., Gupta, J. C., Talwar, G. P., & Dubey, S. (2016). Survivin: A unique target for tumor therapy. *Cancer Cell International*, **16**(1), 1–14.

Gaudelli, N. M., Komor, A. C., Rees, H. A., … Liu, D. R. (2017). Programmable base editing of T to G C in genomic DNA without DNA cleavage. *Nature*, **551**(7681), 464–471.

Geary, R. S. (2009, April). Antisense oligonucleotide pharmacokinetics and metabolism. *Expert Opinion on Drug Metabolism and Toxicology*, Taylor & Francis, pp. 381–391.

Geary, R. S., Norris, D., Yu, R., & Bennett, C. F. (2015). Pharmacokinetics, biodistribution and cell uptake of antisense oligonucleotides. *Advanced Drug Delivery Reviews*, **87**, 46–51.

Goñi, J. R., de la Cruz, X., & Orozco, M. (2004). Triplex-forming oligonucleotide target sequences in the human genome. *Nucleic Acids Research*, **32**(1), 354–360.

Gordon, S. R., Maute, R. L., Dulken, B. W., … Weissman, I. L. (2017). PD-1 expression by tumour-associated macrophages inhibits phagocytosis and tumour immunity. *Nature*, **545**(7655), 495–499.

Goyal, N., & Narayanaswami, P. (2018). Making sense of antisense oligonucleotides: A narrative review. *Muscle and Nerve*, **57**(3), 356–370.

Graham, I. R., & Dickson, G. (2002, May 21). Gene repair and mutagenesis mediated by chimeric RNA-DNA oligonucleotides: Chimeraplasty for gene therapy and conversion of

single nucleotide polymorphisms (SNPs). *Biochimica et Biophysica Acta - Molecular Basis of Disease*, pp. 1–6.

Grupp, S. A., Kalos, M., Barrett, D., … June, C. H. (2013). Chimeric Antigen Receptor–Modified T Cells for Acute Lymphoid Leukemia. *New England Journal of Medicine*, **368**(16), 1509–1518.

Gu, S., Ni, T., Wang, J., … Wang, Y. (2018). CD47 Blockade Inhibits Tumor Progression through Promoting Phagocytosis of Tumor Cells by M2 Polarized Macrophages in Endometrial Cancer. *Journal of Immunology Research*, **2018**. doi:10.1155/2018/6156757

Guieysse, A. L., Praseuth, D., Francois, J. C., & Helene, C. (1995). Inhibition of replication initiation by triple helix-forming oligonucleotides. *Biochemical and Biophysical Research Communications*, **217**(1), 186–194.

Gupta, A., Quijano, E., Liu, Y., … Glazer, P. M. (2017). Anti-tumor Activity of miniPEG-γ-Modified PNAs to Inhibit MicroRNA-210 for Cancer Therapy. *Molecular Therapy - Nucleic Acids*, **9**(December), 111–119.

Gupta, R. C., Bazemore, L. R., Golub, E. I., & Radding, C. M. (2002). Activities of human recombination protein Rad51. *Proceedings of the National Academy of Sciences*, **94**(2), 463–468.

Haapaniemi, E., Botla, S., Persson, J., Schmierer, B., & Taipale, J. (2018). CRISPR-Cas9 genome editing induces a p53-mediated DNA damage response. *Nature Medicine*, **24**(7), 927–930.

Haber, J. E., & Moore, J. K. (1996). Cell Cycle and Genetic Requirements of Two Pathways of Nonhomologous End-Joining Repair of Double-Strand Breaks in Saccharomyces cerevisiae. *Molecular and Cellular Biology*, **16**(5), 2164–2173.

Hakem, R. (2008). DNA-damage repair; the good, the bad, and the ugly. *EMBO Journal*, **27**(4), 589–605.

Haseloff, J., & Gerlach, W. L. (1988). Simple RNA enzymes with new and highly specific endoribonuclease activities. *Nature*, **334**(6183), 585–591.

He, P., Zhu, D., Hu, J. J., Peng, J., Chen, L. S., & Lu, G. X. (2010). PcDNA3.1(-)-mediated ribozyme targeting of HER-2 suppresses breast cancer tumor growth. *Molecular Biology Reports*, **37**(3), 1597–1604.

He, T., Tang, C., Xu, S., Moyana, T., & Xiang, J. (2007). Interferon gamma stimulates cellular maturation of dendritic cell line DC2.4 leading to induction of efficient cytotoxic T cell responses and antitumor immunity. *Cellular & Molecular Immunology*, **4**(2), 105–111.

Hefferin, M. L., & Tomkinson, A. E. (2005). Mechanism of DNA double-strand break repair by non-homologous end joining. *DNA Repair*, **4**(6), 639–648.

Hoeijmakers, J. H. J. (2009). DNA Damage, Aging, and Cancer. *New England Journal of*

Medicine, **361**(15), 1475–1485.

Holt, N., Wang, J., Kim, K., … Cannon, P. M. (2010). Human hematopoietic stem/progenitor cells modified by zinc-finger nucleases targeted to CCR5 control HIV-1 in vivo. *Nature Biotechnology*, **28**(8), 839–847.

Hoogsteen, K. (1959). The structure of crystals containing a hydrogen-bonded complex of 1-methylthymine and 9-methyladenine. *Acta Crystallographica*, **12**(10), 822–823.

Hoogsteen, K. (1963). The crystal and molecular structure of a hydrogen-bonded complex between 1-methylthymine and 9-methyladenine. *Acta Crystallographica*, **16**(9), 907–916.

Huen, M. S. Y., Li, X. T., Lu, L. Y., Watt, R. M., Liu, D. P., & Huang, J. D. (2006). The involvement of replication in single stranded oligonucleotide-mediated gene repair. *Nucleic Acids Research*, **34**(21), 6183–6194.

Igoucheva, O., Alexeev, V., & Yoon, K. (2001). Targeted gene correction by small single-stranded oligonucleotides in mammalian cells. *Gene Therapy*, **8**(5), 391–399.

Isenberg, J., Frazier, W., Krishna, M., Wink, D., & Roberts, D. (2008). Enhancing Cardiovascular Dynamics by Inhibition of Thrombospondin- 1/CD47 Signaling. *Current Drug Targets*, **9**(10), 833–841.

ishida, R., & Buchwald, M. (1982). Susceptibility of Fanconi's Anemia Lymphoblasts to DNA-cross-linking and Alkylating Agents. *Cancer Research*, **42**(10), 4000–4006.

Iwamura, K., Kato, T., Miyahara, Y., … Shiku, H. (2012). SiRNA-mediated silencing of PD-1 ligands enhances tumor-specific human T-cell effector functions. *Gene Therapy*, **19**(10), 959–966.

Jabs, D. A., & Griffiths, P. D. (2002). Fomivirsen for the treatment of cytomegalovirus retinitis. *American Journal of Ophthalmology*, pp. 552–556.

Jain, S., Van Scoyk, A., Morgan, E. A., … Weinstock, D. M. (2019). Targeted inhibition of CD47-SIRPa requires Fc-FcgR interactions to maximize activity in T-cell lymphomas. *Blood*, **134**(17), 1430–1440.

Jinek, M., Chylinski, K., Fonfara, I., Hauer, M., Doudna, J. A., & Charpentier, E. (2012). A programmable dual-RNA-guided DNA endonuclease in adaptive bacterial immunity. *Science*, **337**(6096), 816–821.

Joenje, H., & Patel, K. J. (2001). The emerging genetic and molecular basis of Fanconi anaemia. *Nature Reviews Genetics*, pp. 446–457.

Jose, A. M. (2002). Ribozyme therapy: RNA enzymes to the rescue. *Yale Journal of Biology and Medicine*, **75**(4), 215–219.

Joung, J. K., & Sander, J. D. (2013, January). TALENs: A widely applicable technology for targeted genome editing. *Nature Reviews Molecular Cell Biology*, pp. 49–55.

Juliano, R. L. (2016). The delivery of therapeutic oligonucleotides. *Nucleic Acids Research*,

44(14), 6518–6548.

June, C. H., O'Connor, R. S., Kawalekar, O. U., Ghassemi, S., & Milone, M. C. (2018). CAR T cell immunotherapy for human cancer. *Science*, **359**(6382), 1361–1365.

Juneja, V. R., McGuire, K. A., Manguso, R. T., … Sharpe, A. H. (2017). PD-L1 on tumor cells is sufficient for immune evasion in immunogenic tumors and inhibits CD8 T cell cytotoxicity. *The Journal of Experimental Medicine*, **214**(4), 895–904.

Kang, H. J., Minder, P., Park, M. A., Mesquitta, W. T., Torbett, B. E., & Slukvin, I. I. (2015). CCR5 disruption in induced pluripotent stem cells using CRISPR/Cas9 provides selective resistance of immune cells to CCR5-tropic HIV-1 virus. *Molecular Therapy - Nucleic Acids*, **4**(12), e268.

Kantoff, P. W., Higano, C. S., Shore, N. D., … Schellhammer, P. F. (2010). Sipuleucel-T immunotherapy for castration-resistant prostate cancer. *New England Journal of Medicine*, **363**(5), 411–422.

Kaplan, A. R., Pham, H., Liu, Y., … Glazer, P. M. (2020). Ku80-targeted pH-sensitive peptide-PNA conjugates are tumor selective and sensitize cancer cells to ionizing radiation. *Molecular Cancer Research*, molcanres.0661.2019.

Kelley, M. R., & Fishel, M. L. (2016). *Overview of DNA repair pathways, current targets, and clinical trials bench to clinic*. *DNA Repair in Cancer Therapy: Molecular Targets and Clinical Applications: Second Edition*, Second Edi, Elsevier Inc. doi:10.1016/B978-0-12-803582-5.00001-2

Kim, Y. G., Cha, J., & Chandrasegaran, S. (1996). Hybrid restriction enzymes: Zinc finger fusions to Fok I cleavage domain. *Proceedings of the National Academy of Sciences of the United States of America*, **93**(3), 1156–1160.

Kleffel, S., Posch, C., Barthel, S. R., … Schatton, T. (2015). Melanoma Cell-Intrinsic PD-1 Receptor Functions Promote Tumor Growth. *Cell*, **162**(6), 1242–1256.

Knauert, M. P., & Glazer, P. M. (2001). Triplex forming oligonucleotides: sequence-specific tools for gene targeting. *Human Molecular Genetics*, **10**(20), 2243–2251.

Knauert, M. P., Kalish, J. M., Hegan, D. C., & Glazer, P. M. (2006). Triplex-Stimulated Intermolecular Recombination at a Single-Copy Genomic Target. *Molecular Therapy*, **14**(3), 392–400.

Komor, A. C., Kim, Y. B., Packer, M. S., Zuris, J. A., & Liu, D. R. (2016). Programmable editing of a target base in genomic DNA without double-stranded DNA cleavage. *Nature*, **533**(7603), 420–424.

Kosicki, M., Tomberg, K., & Bradley, A. (2018). Repair of double-strand breaks induced by CRISPR–Cas9 leads to large deletions and complex rearrangements. *Nature Biotechnology*, **36**(8). doi:10.1038/nbt.4192

Krejci, L., Altmannova, V., Spirek, M., & Zhao, X. (2012). Homologous recombination and its regulation. *Nucleic Acids Research*, **40**(13), 5795–5818.

Kren, B. T., Banoyopaohyay, P., & Steer, C. J. (1998). In vivo site-directed mutagenesis of the factor IX gene by chimeric RNA/DNA oligonucleotides. *Nature Medicine*, **4**(3), 285–290.

Kren, B. T., Parashar, B., Bandyopadhyay, P., Chowdhury, N. R., Chowdhury, J. R., & Steer, C. J. (1999). Correction of the UDP-glucuronosyltransferase gene defect in the Gunn rat model of Crigler-Najjar syndrome type I with a chimeric oligonucleotide. *Proceedings of the National Academy of Sciences of the United States of America*, **96**(18), 10349–10354.

Kruger, K., Grabowski, P. J., Zaug, A. J., Sands, J., Gottschling, D. E., & Cech, T. R. (1982). Self-splicing RNA: Autoexcision and autocyclization of the ribosomal RNA intervening sequence of tetrahymena. *Cell*, **31**(1), 147–157.

Kwak, G., Kim, D., Nam, G., … Yeo, Y. (2017). Programmed Cell Death Protein Ligand-1 (PD-L1) Silencing with Polyethylenimine-Dermatan Sulfate Complex for Dual Inhibition of Melanoma Growth. *ACS Nano*, **11**(10), 10135–10146.

Lai, L. W., & Lien, Y. H. H. (2002). Chimeric RNA/DNA oligonucleotide-based gene therapy. *Kidney International*, **61**(SUPPL. 1), 47–51.

Le Doan, T., Perrouault, L., Praseuth, D., … Héène, C. (1987). Sequence-specific recognition, photocrosslinking and cleavage of the DNA double helix by an oligo-(α]-thymidylate covalently linked to an azidoproflavine derivative. *Nucleic Acids Research*, **15**(19), 7749–7760.

Lee, C. M., Flynn, R., Hollywood, J. A., Scallan, M. F., & Harrison, P. T. (2012). Correction of the Δf508 mutation in the cystic fibrosis transmembrane conductance regulator gene by zinc-finger nuclease homology-directed repair. *BioResearch Open Access*, **1**(3), 99–103.

Leong, P. L., Andrews, G. A., Johnson, D. E., … Grandis, J. R. (2003). Targeted inhibition of Stat3 with a decoy oligonucleotide abrogates head and neck cancer cell growth. *Proceedings of the National Academy of Sciences of the United States of America*, **100**(7), 4138–4143.

Li, J., Chen, L., Xiong, Y., … Wang, H. (2017). Knockdown of PD-L1 in Human Gastric Cancer Cells Inhibits Tumor Progression and Improves the Cytotoxic Sensitivity to CIK Therapy. *Cellular Physiology and Biochemistry*, **41**(3), 907–920.

Lim, K. R. Q., Maruyama, R., & Yokota, T. (2017, February 28). Eteplirsen in the treatment of Duchenne muscular dystrophy. *Drug Design, Development and Therapy*, Dove Medical Press Ltd., pp. 533–545.

Lim, W. A., & June, C. H. (2017, February 9). The Principles of Engineering Immune Cells to Treat Cancer. *Cell*, Cell Press, pp. 724–740.

Lin, Y., Cradick, T. J., Brown, M. T., … Bao, G. (2014). CRISPR/Cas9 systems have off-target

activity with insertions or deletions between target DNA and guide RNA sequences. *Nucleic Acids Research*, **42**(11), 7473–7485.

Liu, J., Wang, L., Zhao, F., … Majeti, R. (2015). Pre-Clinical Development of a Humanized Anti-CD47 Antibody with Anti-Cancer Therapeutic Potential. *PloS One*, **10**(9), e0137345.

Liu, Q., Wen, W., Tang, L., … Yan, H. X. (2016). Inhibition of SIRPα in dendritic cells potentiates potent antitumor immunity. *OncoImmunology*, **5**(9), 1–12.

Liu, W. M., Scott, K. A., Shahin, S., & Propper, D. J. (2004). The in vitro effects of CRE-decoy oligonucleotides in combination with conventional chemotherapy in colorectal cancer cell lines. *European Journal of Biochemistry*, **271**(13), 2773–2781.

Liu, X. S., Wu, H., Krzisch, M., … Jaenisch, R. (2018). Rescue of Fragile X Syndrome Neurons by DNA Methylation Editing of the FMR1 Gene. *Cell*, **172**(5), 979-992.e6.

Low, B. E., Krebs, M. P., Joung, J. K., Tsai, S. Q., Nishina, P. M., & Wiles, M. V. (2013). Correction of the Crb1rd8allele and retinal phenotype in C57BL/6N mice via TALEN-mediated homology-directed repair. *Investigative Ophthalmology and Visual Science*, **55**(1), 387–395.

Luo, M., He, H., Kelley, M. R., & Georgiadis, M. M. (2010). Redox regulation of DNA repair: Implications for human health and cancer therapeutic development. *Antioxidants and Redox Signaling*, **12**(11), 1247–1269.

Maeder, M. L., Thibodeau-Begany, S., Osiak, A., … Joung, J. K. (2008). Rapid "Open-Source" Engineering of Customized Zinc-Finger Nucleases for Highly Efficient Gene Modification. *Molecular Cell*, **31**(2), 294–301.

Majeti, R., Chao, M. P., Alizadeh, A. A., … Weissman, I. L. (2009). CD47 Is an Adverse Prognostic Factor and Therapeutic Antibody Target on Human Acute Myeloid Leukemia Stem Cells. *Cell*, **138**(2), 286–299.

Majumdar, A., Puri, N., Cuenoud, B., … Seidman, M. M. (2003). Cell cycle modulation of gene targeting by a triple helix-forming oligonucleotide. *Journal of Biological Chemistry*, **278**(13), 11072–11077.

Mann, M. J. (2005). Transcription factor decoys: a new model for disease intervention. *Annals of the New York Academy of Sciences*, **1058**, 128–139.

Mathew, V., & Wang, A. K. (2019). Inotersen: New promise for the treatment of hereditary transthyretin amyloidosis. *Drug Design, Development and Therapy*, Dove Medical Press Ltd., pp. 1515–1525.

Matlung, H. L., Szilagyi, K., Barclay, N. A., & van den Berg, T. K. (2017). The CD47-SIRPα signaling axis as an innate immune checkpoint in cancer. *Immunological Reviews*, **276**(1), 145–164.

Mclachlan, J., Fernandez, S., Helleday, T., & E. Bryant, H. (2009). Specific targeted gene repair

using single-stranded DNA oligonucleotides at an endogenous locus in mammalian cells uses homologous recombination. *DNA Repair*, **8**, 1424–1433.

McMahon, B. M., Mays, D., Lipsky, J., Stewart, J. A., Fauq, A., & Richelson, E. (2002). Pharmacokinetics and tissue distribution of a peptide nucleic acid after intravenous administration. *Antisense and Nucleic Acid Drug Development*, **12**(2), 65–70.

McNamara, M. A., Nair, S. K., & Holl, E. K. (2015). RNA-Based Vaccines in Cancer Immunotherapy. *Journal of Immunology Research*, Hindawi Publishing Corporation. doi:10.1155/2015/794528

McNeer, N. A., Anandalingam, K., Fields, R. J., … Egan, M. E. (2015). Nanoparticles that deliver triplex-forming peptide nucleic acid molecules correct F508del CFTR in airway epithelium. *Nature Communications*, **6**, 1–11.

McNeer, N. A., Schleifman, E. B., Cuthbert, A., … Glazer, P. M. (2013). Systemic delivery of triplex-forming PNA and donor DNA by nanoparticles mediates site-specific genome editing of human hematopoietic cells in vivo. *Gene Therapy*, **20**(6), 658–669.

Miller, J., McLachlan, A. D., & Klug, A. (1985). Repetitive zinc-binding domains in the protein transcription factor IIIA from Xenopus oocytes. *The EMBO Journal*, **4**(6), 1609–1614.

Min, Y.-L., Bassel-Duby, R., & Olson, E. N. (2019a). CRISPR Correction of Duchenne Muscular Dystrophy. *Annual Review of Medicine*, **70**(1), 239–255.

Min, Y. L., Li, H., Rodriguez-Caycedo, C., … Olson, E. N. (2019b). CRISPR-Cas9 corrects Duchenne muscular dystrophy exon 44 deletion mutations in mice and human cells. *Science Advances*, **5**(3), 1–13.

Moerschell, R. P., Tsunasawat, S., & Sherman, F. (1988). *Transformation of yeast with synthetic oligonucleotides. Proc. Nati. Acad. Sci. USA*, Vol. 85.

Mojica, F. J. M., Díez-Villaseñor, C., García-Martínez, J., & Almendros, C. (2009). Short motif sequences determine the targets of the prokaryotic CRISPR defence system. *Microbiology*, **155**(3), 733–740.

Mojica, F. J. M., Díez-Villaseñor, C., García-Martínez, J., & Soria, E. (2005). Intervening sequences of regularly spaced prokaryotic repeats derive from foreign genetic elements. *Journal of Molecular Evolution*, **60**(2), 174–182.

Moldovan, G.-L., & D'Andrea, A. D. (2009). How the Fanconi Anemia Pathway Guards the Genome. *Annual Review of Genetics*, **43**(1), 223–249.

Morgan, A. R., & Wells, R. D. (1968). Specificity of the three-stranded complex formation between double-stranded DNA and single-stranded RNA containing repeating nucleotide sequences. *Journal of Molecular Biology*, **37**(1), 63–80.

Morishita, R., Gibbons, G. H., Horiuchi, M., … Dzau, V. J. (1995). A gene therapy strategy using a transcription factor decoy of the E2F binding site inhibits smooth muscle proliferation in

vivo. *Proceedings of the National Academy of Sciences of the United States of America*, **92**(13), 5855–5859.

Mosbach, V., Poggi, L., Viterbo, D., Charpentier, M., & Richard, G. F. (2018). TALEN-Induced Double-Strand Break Repair of CTG Trinucleotide Repeats. *Cell Reports*, **22**(8), 2094–2106.

Moser, H. E., & Dervan, P. B. (1987). Sequence - specific cleavage of double helical DNA by triple helix formation. *Science*, **238**(4827), 645–650.

Mou, H., Smith, J. L., Peng, L., … Xue, W. (2017). CRISPR/Cas9-mediated genome editing induces exon skipping by alternative splicing or exon deletion. *Genome Biology*, **18**(1), 4–11.

Mullard, A. (2018). FDA approves landmark RNAi drug. *Nature Reviews. Drug Discovery*, **17**(9), 613.

Müller, L., Aigner, P., & Stoiber, D. (2017, March 31). Type I interferons and natural killer cell regulation in cancer. *Frontiers in Immunology*, Frontiers Media S.A. doi:10.3389/fimmu.2017.00304

Müller, S. (2015). Engineering of ribozymes with useful activities in the ancient RNA world. *Annals of the New York Academy of Sciences*, **1341**(1), 54–60.

Mussolino, C., Morbitzer, R., Lütge, F., Dannemann, N., Lahaye, T., & Cathomen, T. (2011). A novel TALE nuclease scaffold enables high genome editing activity in combination with low toxicity. *Nucleic Acids Research*, **39**(21), 9283–9293.

Nambiar, T. S., Billon, P., Diedenhofen, G., … Ciccia, A. (2019). Stimulation of CRISPR-mediated homology-directed repair by an engineered RAD18 variant. *Nature Communications*, **10**(1), 1–13.

Nazari, R., Ma, X. Z., & Joshi, S. (2008). Inhibition of human immunodeficiency virus-1 entry using vectors expressing a multimeric hammerhead ribozyme targeting the CCR5 mRNA. *Journal of General Virology*, **89**(9), 2252–2261.

Ng, E. W. M., Shima, D. T., Calias, P., Cunningham, E. T., Guyer, D. R., & Adamis, A. P. (2006). Pegaptanib, a targeted anti-VEGF aptamer for ocular vascular disease. *Nature Reviews Drug Discovery*, **5**(2), 123–132.

Novak, E. M., Metzger, M., Chammas, R., … Bydlowski, S. P. (2003). Downregulation of TNF-α and VEGF expression by Sp1 decoy oligodeoxynucleotides in mouse melanoma tumor. *Gene Therapy*, **10**(23), 1992–1997.

Olsen, P., Randol, M., & Krauss, S. (2005). Implications of cell cycle progression on functional sequence correction by short single-stranded DNA oligonucleotides. *Gene Therapy*, **12**(6), 546–551.

Omer, L., Hudson, E. A., Zheng, S., Hoying, J. B., Shan, Y., & Boyd, N. L. (2017). CRISPR

correction of a homozygous low-density lipoprotein receptor mutation in familial hypercholesterolemia induced pluripotent stem cells. *Hepatology Communications*, **1**(9), 886–898.

Osborn, M. J., Gabriel, R., Webber, B. R., … Tolar, J. (2015). Fanconi anemia gene editing by the CRISPR/Cas9 system. *Human Gene Therapy*, **26**(2), 114–126.

Osborn, M. J., Starker, C. G., McElroy, A. N., … Tolar, J. (2013). TALEN-based gene correction for epidermolysis bullosa. *Molecular Therapy*, **21**(6), 1151–1159.

Ouyang, S., Xie, Y., Xiong, Z., … Sun, X. (2018). CRISPR/Cas9-Targeted deletion of polyglutamine in spinocerebellar ataxia type 3-derived induced pluripotent stem cells. *Stem Cells and Development*, **27**(11), 756–770.

Palovcak, A., Liu, W., Yuan, F., & Zhang, Y. (2017). Maintenance of genome stability by Fanconi anemia proteins. *Cell and Bioscience*, **7**(1), 1–18.

Papaioannou, I., Simons, J. P., & Owen, J. S. (2012). Oligonucleotide-directed gene-editing technology: mechanisms and future prospects. *Expert Opinion on Biological Therapy*, **12**(3), 329–342.

Pardi, N., Hogan, M. J., Porter, F. W., & Weissman, D. (2018, March 28). mRNA vaccines-a new era in vaccinology. *Nature Reviews Drug Discovery*, Nature Publishing Group, pp. 261–279.

Pardo, B., Gómez-González, B., & Aguilera, A. (2009). DNA double-strand break repair: How to fix a broken relationship. *Cellular and Molecular Life Sciences*, **66**(6), 1039–1056.

Pardoll, D. M. (2012, April). The blockade of immune checkpoints in cancer immunotherapy. *Nature Reviews Cancer*, pp. 252–264.

Park, S. H., Lee, C. M., Dever, D. P., … Bao, G. (2019). Highly efficient editing of the β-globin gene in patient-derived hematopoietic stem and progenitor cells to treat sickle cell disease. *Nucleic Acids Research*, **47**(15), 7955–7972.

Pavletich, N. P., & Pabo, C. O. (1991). Zinc finger-DNA recognition: Crystal structure of a Zif268-DNA complex at 2.1 Å. *Science*, **252**(5007), 809–817.

Perez, E. E., Wang, J., Miller, J. C., … June, C. H. (2008). Establishment of HIV-1 resistance in CD4+ T cells by genome editing using zinc-finger nucleases. *Nature Biotechnology*, **26**(7), 808–816.

Pesce, C. D., Bolacchi, F., Bongiovanni, B., … Bergamini, A. (2005). Anti-gene peptide nucleic acid targeted to proviral HIV-1 DNA inhibits in vitro HIV-1 replication. *Antiviral Research*, **66**(1), 13–22.

Phear, G., Armstrong, W., & Meuth, M. (1989). Molecular basis of spontaneous mutation at the aprt locus of hamster cells. *Journal of Molecular Biology*, **209**(4), 577–582.

Phylactou, L. A., Kilpatrick, M. W., & Wood, M. J. A. (1998). Ribozymes as therapeutic tools for

genetic disease. *Human Molecular Genetics*, **7**(10), 1649–1653.

Praseuth, D., Guieysse, A. L., & Hélène, C. (1999, December 10). Triple helix formation and the antigene strategy for sequence-specific control of gene expression. *Biochimica et Biophysica Acta - Gene Structure and Expression*, Elsevier, pp. 181–206.

Quijano, E., Bahal, R., Ricciardi, A., Saltzman, W. M., & Glazer, P. M. (2017). Therapeutic peptide nucleic acids: Principles, limitations, and opportunities. *Yale Journal of Biology and Medicine*, **90**(4), 583–598.

Quintana-Bustamante, O., Fañanas-Baquero, S., Orman, I., … Segovia, J. C. (2019). Gene editing of PKLR gene in human hematopoietic progenitors through 5' and 3' UTR modified TALEN mRNA. *PLOS ONE*, **14**(10), e0223775.

Radecke, S., Radecke, F., Peter, I., & Schwarz, K. (2006). Physical incorporation of a single-stranded oligodeoxynucleotide during targeted repair of a human chromosomal locus. *Journal of Gene Medicine*, **8**(2), 217–228.

Rando, T. A., Disatnik, M. H., & Zhou, L. Z. H. (2000). Rescue of dystrophin expression in mdx mouse muscle by RNA/DNA oligonucleotides. *Proceedings of the National Academy of Sciences of the United States of America*, **97**(10), 5363–5368.

Ribas, A., & Wolchok, J. D. (2018, March 23). Cancer immunotherapy using checkpoint blockade. *Science*, American Association for the Advancement of Science, pp. 1350–1355.

Ricciardi, A. S., Bahal, R., Farrelly, J. S., … Saltzman, W. M. (2018). In utero nanoparticle delivery for site-specific genome editing. *Nature Communications*, **9**(1), 1–11.

Ricciardi, A. S., McNeer, N. A., Anandalingam, K. K., Saltzman, W. M., & Glazer, P. M. (2014). Targeted Genome Modification via Triple Helix Formation. In *Methods in Molecular Biology*, pp. 89–106.

Rice, M. C., May, G. D., Kipp, P. B., Parekh, H., & Kmiec, E. B. (2000). Genetic repair of mutations in plant cell-free extracts directed by specific chimeric oligonucleotides. *Plant Physiology*, **123**(2), 427–437.

Riley, R. S., June, C. H., Langer, R., & Mitchell, M. J. (2019). Delivery technologies for cancer immunotherapy. *Nature Reviews Drug Discovery*, **18**(3), 175–196.

Rinaldi, C., & Wood, M. J. A. (2018). Antisense oligonucleotides: The next frontier for treatment of neurological disorders. *Nature Reviews Neurology*, **14**(1), 9–22.

Río, P., Navarro, S., Guenechea, G., … Bueren, J. A. (2017). Engraftment and in vivo proliferation advantage of gene-corrected mobilized CD34+ cells from Fanconi anemia patients. *Blood*, **130**(13), 1535–1542.

Río, P., Navarro, S., Wang, W., … Bueren, J. A. (2019). Successful engraftment of gene-corrected hematopoietic stem cells in non-conditioned patients with Fanconi anemia.

Nature Medicine, **25**(9), 1396–1401.

Rodríguez, L., Villalobos, X., Dakhel, S., … Noé, V. (2013). Polypurine reverse Hoogsteen hairpins as a gene therapy tool against survivin in human prostate cancer PC3 cells in vitro and in vivo. *Biochemical Pharmacology*, **86**(11), 1541–1554.

Rodríguez, L., Villalobos, X., Solé, A., … Noé, V. (2015). Improved design of PPRHs for gene silencing. *Molecular Pharmaceutics*, **12**(3), 867–877.

Rogers, F. A., Vasquez, K. M., Egholm, M., & Glazer, P. M. (2002a). Site-directed recombination via bifunctional PNA-DNA conjugates. *Proceedings of the National Academy of Sciences of the United States of America*, **99**(26), 16695–16700.

Rogers, F. A., Vasquez, K. M., Egholm, M., & Glazer, P. M. (2002b). Site-directed recombination via bifunctional PNA-DNA conjugates. *Proceedings of the National Academy of Sciences*, **99**(26), 16695–16700.

Román-Rodríguez, F. J., Ugalde, L., Álvarez, L., … Río, P. (2019). NHEJ-Mediated Repair of CRISPR-Cas9-Induced DNA Breaks Efficiently Corrects Mutations in HSPCs from Patients with Fanconi Anemia. *Cell Stem Cell*, **25**(5), 607-621.e7.

Rosenberg, S. A. (2014). IL-2: The First Effective Immunotherapy for Human Cancer. *The Journal of Immunology*, **192**(12), 5451–5458.

Rossidis, A. C., Stratigis, J. D., Chadwick, A. C., … Peranteau, W. H. (2018). In utero CRISPR-mediated therapeutic editing of metabolic genes. *Nature Medicine*, **24**(10), 1513–1518.

Sakamoto, N., Wu, C. H., & Wu, G. Y. (1996). Intracellular cleavage of hepatitis C virus RNA and inhibition of viral protein translation by hammerhead ribozymes. *Journal of Clinical Investigation*, **98**(12), 2720–2728.

Santiago, Y., Chan, E., Liu, P. Q., … Collingwood, T. N. (2008). Targeted gene knockout in mammalian cells by using engineered zinc-finger nucleases. *Proceedings of the National Academy of Sciences of the United States of America*, **105**(15), 5809–5814.

Schaefer, K. A., Wu, W. H., Colgan, D. F., Tsang, S. H., Bassuk, A. G., & Mahajan, V. B. (2017). Unexpected mutations after CRISPR-Cas9 editing in vivo. *Nature Methods*, **14**(6), 547–548.

Schleifman, E. B., Bindra, R., Leif, J., … Glazer, P. M. (2011). Targeted disruption of the CCR5 gene in human hematopoietic stem cells stimulated by peptide nucleic acids. *Chemistry and Biology*, **18**(9), 1189–1198.

Schwartz, A. L., Nath, P. R., Allgauer, M., … Roberts, D. D. (2019). Antisense targeting of CD47 enhances human cytotoxic T-cell activity and increases survival of mice bearing B16 melanoma when combined with anti-CTLA4 and tumor irradiation. *Cancer Immunology, Immunotherapy*, **68**(11), 1805–1817.

Seliger, B. (2005). Strategies of tumor immune evasion. *BioDrugs*, pp. 347–354.

Shabalina, S. A., & Koonin, E. V. (2008, October). Origins and evolution of eukaryotic RNA interference. *Trends in Ecology and Evolution*, pp. 578–587.

Shao, Y., Wang, L., Guo, N., … Li, D. (2018). Cas9-nickase–mediated genome editing corrects hereditary tyrosinemia in rats. *Journal of Biological Chemistry*, **293**(18), 6883–6892.

Sharpe, A. H. (2017). Introduction to checkpoint inhibitors and cancer immunotherapy. *Immunological Reviews*, **276**(1), 5–8.

Shi, S. J., Wang, L. J., Wang, G. D., … Wen, W. H. (2013). B7-H1 Expression Is Associated with Poor Prognosis in Colorectal Carcinoma and Regulates the Proliferation and Invasion of HCT116 Colorectal Cancer Cells. *PLoS ONE*, **8**(10), 1–11.

Shimayama, T., Nishikawa, S., & Taira, K. (1995). *Generality of the NUX Rule: Kinetic Analysis of the Results of Systematic Mutations in the Trinucleotide at the Cleavage Site of Hammerhead Ribozymes. Biochemistry*, Vol. 34. Retrieved from https://pubs.acs.org/sharingguidelines

Sikic, B. I., Lakhani, N., Patnaik, A., … Padda, S. K. (2019). First-in-human, first-in-class phase i trial of the anti-CD47 antibody Hu5F9-G4 in patients with advanced cancers. *Journal of Clinical Oncology*, **37**(12), 946–953.

Simon, A. E., Taylor, M. W., Bradley, W. E., & Thompson, L. H. (1982). Model involving gene inactivation in the generation of autosomal recessive mutants in mammalian cells in culture. *Molecular and Cellular Biology*, **2**(9), 1126–1133.

Solé, A., Ciudad, C. J., Chasin, L. A., & Noé, V. (2016). Correction of point mutations at the endogenous locus of the dihydrofolate reductase gene using repair-PolyPurine Reverse Hoogsteen hairpins in mammalian cells. *Biochemical Pharmacology*, **110**–**111**, 16–24.

Solé, A., Villalobos, X., Ciudad, C. J., & Noé, V. (2014). Repair of Single-Point Mutations by Polypurine Reverse Hoogsteen Hairpins. *Human Gene Therapy Methods*, **25**(5), 288–302.

Song, X., Liu, J., Lu, Y., Jin, H., & Huang, D. (2014). Overexpression of B7-H1 correlates with malignant cell proliferation in pancreatic cancer. *Oncology Reports*, **31**(3), 1191–1198.

Stephenson, M. L., & Zamecnik, P. C. (1978). Inhibition of Rous sarcoma viral RNA translation by a specific oligodeoxyribonucleotide. *Proceedings of the National Academy of Sciences of the United States of America*, **75**(1), 285–288.

Sun, J., Muz, B., Alhallak, K., … Azab, A. K. (2020). Targeting CD47 as a novel immunotherapy for multiple myeloma. *Cancers*, **12**(2), 1–12.

Svoronos, A. A., Bahal, R., Pereira, M. C., … Engelman, D. M. (2020). Tumor-Targeted, Cytoplasmic Delivery of Large, Polar Molecules Using a pH-Low Insertion Peptide. *Molecular Pharmaceutics*. doi:10.1021/acs.molpharmaceut.9b00883

Symons, R. H. (1989). Self-cleavage of RNA in the replication of small pathogens of plants and animals. *Trends in Biochemical Sciences*, **14**(11), 445–450.

Tagalakis, A. D., Dickson, J. G., Owen, J. S., & Simons, J. P. (2005). Correction of the neuropathogenic human apolipoprotein E4 (APOE4) gene to APOE3 in vitro using synthetic RNA/DNA oligonucleotides (chimeraplasts). *Journal of Molecular Neuroscience*, **25**(1), 95–103.

Taniguchi, T., & D'Andrea, A. D. (2006). Molecular pathogenesis of Fanconi anemia: Recent progress. *Blood*, **107**(11), 4223–4233.

Tomita, N., Kim, J. Y. S., Gibbons, G. H., … Dzau, V. J. (2004). Gene therapy with an E2F transcription factor decoy inhibits cell cycle progression in rat anti-Thy 1 glomerulonephritis. *International Journal of Molecular Medicine*, **13**(5), 629–636.

Tremblay, J. P., Iyombe-Engembe, J. P., Duchêne, B., & Ouellet, D. L. (2016). Gene editing for duchenne muscular dystrophy using the CRISPR/Cas9 technology: The importance of fine-tuning the approach. *Molecular Therapy*, **24**(11), 1888–1889.

Tuerk, C., & Gold, L. (1990). Systematic evolution of ligands by exponential enrichment: RNA ligands to bacteriophage T4 DNA polymerase. *Science*, **249**(4968), 505–510.

Uhlen, M., Fagerberg, L., Hallstrom, B. M., … Ponten, F. (2015). Tissue-based map of the human proteome. *Science*, **347**(6220), 1260419–1260419.

Urlaub, G., K&s, E., Carothers, A. M., & Chasin, L. A. (1983). *Deletion of the Diploid Dihydrofolate Reductase Locus from Cultured Mammalian Cells. Cell*, Vol. 33.

Urnov, F. D., Miller, J. C., Lee, Y. L., … Holmes, M. C. (2005). Highly efficient endogenous human gene correction using designed zinc-finger nucleases. *Nature*, **435**(7042), 646–651.

Valaperta, R., Rizzo, V., Lombardi, F., … Costa, E. (2014). Adenine phosphoribosyltransferase (APRT) deficiency: Identification of a novel nonsense mutation. *BMC Nephrology*, **15**(1), 1–7.

Valetdinova, K. R., Ovechkina, V. S., & Zakian, S. M. (2019). Methods for Correction of the Single-Nucleotide Substitution c.840C>T in Exon 7 of the SMN2 Gene. *Biochemistry (Moscow)*, **84**(9), 1074–1084.

van de Vrugt, H. J., Harmsen, T., Riepsaame, J., … te Riele, H. (2019). Effective CRISPR/Cas9-mediated correction of a Fanconi anemia defect by error-prone end joining or templated repair. *Scientific Reports*, **9**(1), 1–13.

van Ravesteyn, T. W., Dekker, M., Fish, A., … te Riele, H. P. J. (2016). LNA modification of single-stranded DNA oligonucleotides allows subtle gene modification in mismatch-repair-proficient cells. *Proceedings of the National Academy of Sciences*, **113**(15), 4122–4127.

Vanlith, C., Guthman, R., Nicolas, C. T., … Hickey, R. D. (2018). Curative Ex Vivo Hepatocyte-Directed Gene Editing in a Mouse Model of Hereditary Tyrosinemia Type 1. *Human Gene Therapy*, **29**(11), 1315–1326.

Vasquez, K. M., Christensen, J., Li, L., Finch, R. A., & Glazer, P. M. (2002). Human XPA and RPA DNA repair proteins participate in specific recognition of triplex-induced helical distortions. *Proceedings of the National Academy of Sciences of the United States of America*, **99**(9), 5848–5853.

Vasquez, K. M., & Glazer, P. M. (2002). Triplex-forming oligonucleotides: principles and applications. *Quarterly Reviews of Biophysics*, **35**(1), 89–107.

Vasquez, K. M., Narayanan, L., & Glazer, P. M. (2000). Specific mutations induced by triplex-forming oligonucleotides in mice. *Science*, **290**(5491), 530–533.

Vasquez, K. M., Wang, G., Havre, P. A., & Glazer, P. M. (1999). Chromosomal mutations induced by triplex-forming oligonucleotides in mammalian cells. *Nucleic Acids Research*, **27**(4), 1176–1181.

Vasquez, K. M., & Wilson, J. H. (1998). Triplex-directed modification of genes and gene activity. *Trends in Biochemical Sciences*, **23**(1), 4–9.

Veillette, A., & Chen, J. (2018). SIRPα–CD47 Immune Checkpoint Blockade in Anticancer Therapy. *Trends in Immunology*, **39**(3), 173–184.

Villalobos, X., Rodríguez, L., Prévot, J., Oleaga, C., Ciudad, C. J., & Noé, V. (2014). Stability and immunogenicity properties of the gene-silencing polypurine reverse hoogsteen hairpins. *Molecular Pharmaceutics*, **11**(1), 254–264.

Villalobos, X., Rodríguez, L., Solé, A., … Noé, V. (2015). Effect of polypurine reverse hoogsteen hairpins on relevant cancer target genes in different human cell lines. *Nucleic Acid Therapeutics*, **25**(4), 198–208.

Wagner, D. L., Amini, L., Wendering, D. J., … Schmueck-Henneresse, M. (2019). High prevalence of Streptococcus pyogenes Cas9-reactive T cells within the adult human population. *Nature Medicine*, **25**(2), 242–248.

Wang, G., Levy, D. D., Seidman, M. M., & Glazer, P. M. (1995). Targeted mutagenesis in mammalian cells mediated by intracellular triple helix formation. *Molecular and Cellular Biology*, **15**(3), 1759–1768.

Wang, G., Seidman, M. M., & Glazer, P. M. (1996). Mutagenesis in mammalian cells induced by triple helix formation and transcription-coupled repair. *Science*, **271**(5250), 802–805.

Wang, Y., Xu, Z., Guo, S., … Huang, L. (2013). Intravenous delivery of siRNA targeting CD47 effectively inhibits melanoma tumor growth and lung metastasis. *Molecular Therapy : The Journal of the American Society of Gene Therapy*, **21**(10), 1919–1929.

Watson, J. D., & Crick, F. H. C. (1953). Molecular structure of nucleic acids: A structure for deoxyribose nucleic acid. *Nature*, **171**(4356), 737–738.

Webb, E. S., Liu, P., Baleeiro, R., Lemoine, N. R., Yuan, M., & Wang, Y. (2018). Immune checkpoint inhibitors in cancer therapy. *Journal of Biomedical Research*, **32**(5), 317–326.

Weinberg, M., Passman, M., Kew, M., & Arbuthnot, P. (2000). Hammerhead ribozyme-mediated inhibition of hepatitis B virus X gene expression in cultured cells. *Journal of Hepatology*, **33**(1), 142–151.

Wells, R. D., Collier, D. A., Hanvey, J. C., Shimizu, M., & Wohlrab, F. (1988). The chemistry and biology of unusual DNA structures adopted by oligopurine.oligopyrimidine sequences. *FASEB Journal : Official Publication of the Federation of American Societies for Experimental Biology*, **2**(14), 2939–49.

Wilkins, M. H. F., Stokes, A. R., & Wilson, H. R. (1953). Molecular structure of nucleic acids: Molecular structure of deoxypentose nucleic acids. *Nature*, **171**(4356), 738–740.

Willingham, S. B., Volkmer, J. P., Gentles, A. J., … Weissman, I. L. (2012). The CD47-signal regulatory protein alpha (SIRPa) interaction is a therapeutic target for human solid tumors. *Proceedings of the National Academy of Sciences of the United States of America*, **109**(17), 6662–6667.

Wurster, C. D., & Ludolph, A. C. (2018, January 1). Nusinersen for spinal muscular atrophy. *Therapeutic Advances in Neurological Disorders*, SAGE Publications Ltd. doi:10.1177/1756285618754459

Xiong, Z., Xie, Y., Yang, Y., … Sun, X. (2019). Efficient gene correction of an aberrant splice site in β-thalassaemia iPSCs by CRISPR/Cas9 and single-strand oligodeoxynucleotides. *Journal of Cellular and Molecular Medicine*, **23**(12), 8046–8057.

Xu, P., Tong, Y., Liu, X. Z., … Liu, D. P. (2015). Both TALENs and CRISPR/Cas9 directly target the HBB IVS2-654 (C > T) mutation in β-thalassemiaderived iPSCs. *Scientific Reports*, **5**. doi:10.1038/srep12065

Yahata, N., Matsumoto, Y., Omi, M., Yamamoto, N., & Hata, R. (2017). TALEN-mediated shift of mitochondrial DNA heteroplasmy in MELAS-iPSCs with m.13513G>A mutation. *Scientific Reports*, **7**(1), 1–11.

Yamamoto, T. (2015). *Targeted genome editing using site-specific nucleases: ZFNs, TALENs, and the CRISPR/Cas9 system. Targeted Genome Editing Using Site-Specific Nucleases: ZFNs, TALENs, and the CRISPR/Cas9 System*, Springer Japan. doi:10.1007/978-4-431-55227-7

Yamamoto, T., Moerschell, R. P., Wakem, L. P., Komar-Panicucci, S., & Sherman, F. (1992a). Strand-specificity in the transformation of yeast with synthetic oligonucleotides. *Genetics*, **131**(4), 811–819.

Yamamoto, T., Moerschell, R. P., Wakem, P., Ferguson, D., & Sherman, F. (1992b). Parameters affecting the frequencies of transformation and co-transfromation with synthetic oligonucleotides in yeast. *Yeast*, **8**(11), 935–948.

Yan, W. L., Shen, K. Y., Tien, C. Y., Chen, Y. A., & Liu, S. J. (2017, March 1). Recent progress

in GM-CSF-based cancer immunotherapy. *Immunotherapy*, Future Medicine Ltd., pp. 347–360.

Yanagita, T., Murata, Y., Tanaka, D., … Matozaki, T. (2017). Anti-SIRPα antibodies as a potential new tool for cancer immunotherapy. *JCI Insight*, **2**(1), 1–15.

Yang, B., Jeang, J., Yang, A., Wu, T. C., & Hung, C. F. (2014). DNA vaccine for cancer immunotherapy. *Human Vaccines and Immunotherapeutics*, **10**(11), 3153–3164.

Ye, L., Wang, J., Beyer, A. I., … Kan, Y. W. (2014). Seamless modification of wild-type induced pluripotent stem cells to the natural CCR5Δ32 mutation confers resistance to HIV infection. *Proceedings of the National Academy of Sciences of the United States of America*, **111**(26), 9591–9596.

Yoon, K., Cole-Strauss, A., & Kmiec, E. B. (1996). Targeted gene correction of episomal DNA in mammalian cells mediated by a chimeric RNA·DNA oligonucleotide. *Proceedings of the National Academy of Sciences of the United States of America*, **93**(5), 2071–2076.

Zaug, A. J., Been, M. D., & Cech, T. R. (1986). The Tetrahymena ribozyme acts like an RNA restriction endonuclease. *Nature*, **324**(6096), 429–433.

Zhang, X., Fan, J., & Ju, D. (2018). Insights into CD47/SIRPα axis-targeting tumor immunotherapy. *Antibody Therapeutics*, **1**(2), 37–42.

Zhang, Y., Lai, B. S., & Juhas, M. (2019). Recent advances in aptamer discovery and applications. *Molecules*, **24**(5). doi:10.3390/molecules24050941

Zhao, H., Li, Y., He, L., … Zhou, B. (2019). In Vivo AAV-CRISPR/Cas9-Mediated Gene Editing Ameliorates Atherosclerosis in Familial Hypercholesterolemia. *Circulation*. doi:10.1161/CIRCULATIONAHA.119.042476

Zhao, X. W., Van Beek, E. M., Schornagel, K., … Van Den Berg, T. K. (2011). CD47-signal regulatory protein-α (SIRPα) interactions form a barrier for antibody-mediated tumor cell destruction. *Proceedings of the National Academy of Sciences of the United States of America*, **108**(45), 18342–18347.

Zhou, J., & Rossi, J. (2017). Aptamers as targeted therapeutics: Current potential and challenges. *Nature Reviews Drug Discovery*, **16**(3), 181–202.

Zhou, M., Hu, Z., Qiu, L., … Liang, D. (2018). Seamless Genetic Conversion of SMN2 to SMN1 via CRISPR/Cpf1 and Single-Stranded Oligodeoxynucleotides in Spinal Muscular Atrophy Patient-Specific Induced Pluripotent Stem Cells. *Human Gene Therapy*, **29**(11), 1252–1263.

Zu, Y., Tong, X., Wang, Z., … Lin, S. (2013). TALEN-mediated precise genome modification by homologous recombination in zebrafish. *Nature Methods*, **10**(4), 329–331.

8. APPENDIXES

In these appendixes, the PhD student has collaborated in the writing of a review article about the application of PPRH technology for gene silencing in cancer and a mini-review regarding the usage of repair-PPRHs as a tool for gene editing. In addition, we have collaborated with the group of Rosanna Paciucci from the Vall d'Hebron Research Institute in the study of a novel DNA-binding motif in the prostate tumor overexpressed-1 (PTOV1) protein that binds to specific promoter sequences of both the *aldehyde dehydrogenase* 1 (*ALDH1A1)* and the *cyclin G2 (CCNG2)* genes, thus activating their expression.

These works do not form an intrinsic part of the body of the thesis but are related to PPRHs technology and cancer.

Polypurine Reverse Hoogsteen Hairpins as a Gene Silencing Tool for Cancer

Carlos J. Ciudad, Laura Rodríguez, Xenia Villalobos, Alex J. Félix and Véronique Noé.

A novel DNA-binding motif in prostate tumor overexpressed-1 (PTOV1) required for the expression of ALDH1A1 and CCNG2 in cancer cells

Valentina Maggio, Verónica Cánovas, Alex J. Félix, Valentí Gómez, Inés de Torres, María Eugenia Semidey, Juan Morote, Verónique Noé, Carlos J. Ciudad and Rosanna Paciucci.

Gene correction of point mutations using PolyPurine reverse Hoogsteen hairpins technology

Alex J. Félix, Anna Solé, Véronique Noé and Carlos J. Ciudad.

Appendixes

8.1 Article VI:

Polypurine Reverse Hoogsteen Hairpins as a Gene Silencing Tool for Cancer

Carlos J. Ciudad, Laura Rodríguez, Xenia Villalobos, Alex J. Félix and Véronique Noé

Appendixes

REVIEW ARTICLE

Polypurine Reverse Hoogsteen Hairpins as a Gene Silencing Tool for Cancer

Carlos J. Ciudad, Laura Rodríguez, Xenia Villalobos, Alex J. Félix and Véronique Noé[*]

Department of Biochemistry and Physiology, Faculty of Pharmacy, University of Barcelona, Barcelona, Spain

Abstract: Polypurine reverse Hoogsteen (PPRH) molecules are DNA hairpins formed by two polypurine strands running in an antiparallel orientation and containing no nucleotide modifications. The two strands, linked by a pentathymidine loop, are bound through intramolecular reverse Hoogsteen bonds. Then, PPRHs can bind by Watson-Crick bonds to their corresponding polypyrimidine target in the dsDNA provoking a displacement of the polypurine strand of the duplex. We described the effect and mechanisms of action of PPRHs in cells using PPRHs designed against the template and coding strands of the *dhfr* gene. The proof of principle of PPRHs as a therapeutic tool was established using a PPRH against *survivin* in a xenograft prostate cancer tumor model. To improve the PPRHs effect, the influence of the length was studied obtaining a higher efficiency with longer molecules. To decrease the possible off-target effect, when a purine interruption is found in the pyrimidine target, the PPRH sequence should contain both strands of the complementary base opposite to the interruption. Furthermore, the stability of PPRHs is higher than that of siRNAs, as evidenced by the longer half-life of the former in different types of serum and in PC3 cells. PPRHs do not induce the levels of the transcription factors nor the proinflammatory cytokines involved in the Toll-like Receptor pathway and they do not trigger the formation of the inflammasome complex. PPRHs can be used as therapeutic tools to target genes related to cancer progression, resistance to drugs or immunotherapy approaches.

1. INTRODUCTION

The discovery of DNA double-helix structure in 1953 [1] set a landmark in molecular biology. It implied that DNA replication is possible through the complementary nature of the two strands, corroborating that the DNA is the carrier of the genetic information, as stated earlier by Avery in 1944 [2]. Ten years later, Karst Hoogsteen proposed an additional model [3] that explained the existence of a triple stranded structure (Fig. **1**) described by Felsenfeld and Rich in 1957 [4]. These discoveries established the bases for the use of nucleic acids as therapeutic tools since they allowed rationalizing the design of molecules following a set of
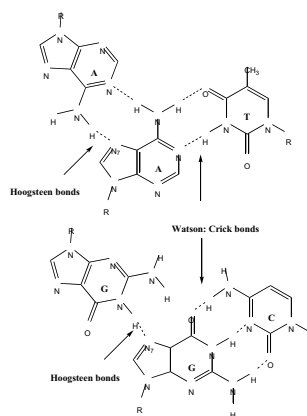
*Address correspondence to this author at the Department of Biochemistry and Physiology, Faculty of Pharmacy, University of Barcelona, Barcelona, Spain; Tel/Fax: +34-93-403-4455, +34-93-402-4520; E-mail: vnoe@ub.edu

Fig. (1). Scheme depicting the differences between Watson-Crick and Hoogsteen pairing.

pairing rules. The use of nucleic acids as disruptors of genetic flow was first described in 1978 by Zamecnik and Stephenson using an deoxy-oligonucleotide complementary to a target sequence in Rous sarcoma virus RNA which inhibited its viral replication and protein translation *in vitro* [5]. In their report, they foresaw the profound implication of this discovery, and even proposed the term "hybridon" to designate an oligonucleotide of specific sequence that acts by competitive hybridization. Today we refer to these molecules as antisense oligonucleotides (aODN).

Significant advances in organic chemistry occurred in parallel, which made possible the synthesis of relatively short fragments of oligonucleotides.

Since the late 70's, several other discoveries, such as the chemical modifications on internucleotide linkages, the automated DNA-synthesis, the description of the RNA interference pathway, or the discovery of aptamers, have remarkably amplified and pushed forward the field of antisense and antigene therapy. Finally, in the year 2001, the Human Project presented its preliminary results of the human genome sequence [6]. This opened the possibility to rationally design DNA and RNA molecules able to specifically target sequences within the genome. The full genomic sequence was completed and published in April 2003.

Nowadays, several types of oligonucleotides can be used to inhibit the expression of a given gene. They act at different levels on the flow of genetic information, allowing for the following classification:

- Oligonucleotides inhibiting the transcription process: directed against the DNA, are also named antigene oligonucleotides. In this category, we find the Triplex Forming Oligonucleotides (TFOs)

- Oligonucleotides inhibiting the translation process: are directed against the mRNA. These include antisense oligonucleotides (aODN), small interfering RNAs (siRNAs), microRNAs (miRNAs) and ribozymes.

- Oligonucleotides acting at the protein level: are able to bind to the proteins and block their activity. Aptamers are included in this category, as well as decoy oligonucleotides for transcription factors (TFs) [7].

Other oligonucleotides called antagomirs are used to aODNs.

2. GENE SILENCING OLIGONUCLEOTIDES
2.1. TFOs

TFOs are single stranded DNA molecules that bind to the major groove of the double-stranded DNA (dsDNA), forming a triplex structure. They bind in a sequence specific manner to polypurine stretches by Hoogsteen or reverse Hoogsteen hydrogen bonds. There are three types of TFOs that vary in their composition and orientation relative to the target strand:

- Pyrimidine TFOs (T,C-TFOs): are parallel to the purine target sequence and form Hoogsteen bonds. Triplets obtained are T·A*T and C·G*C^{+}.

- Purine TFOs (G,A-TFOs): are antiparallel relative to the purine target sequence and form reverse Hoogsteen bonds. Triplexes obtained are T·A*A and C·G*G.

- Mix TFOs (G,T-TFOs): can be parallel, forming Hoogsteen bonds, or antiparallel, forming reverse Hoogsteen bonds, creating the triplets T·A*T and C·G*G.

TFOs are capable of inhibiting gene transcription either by blocking the binding of transcription factors (TFs) or by distorting the normal double helical structure [8], and thus inhibiting the activity of the RNA polymerase. The dissociation constants for TFOs are comparable to those of the TFs [9], and they can compete with them for the binding to the dsDNA. It has also been reported that the binding of the TFOs can trigger the DNA repair mechanisms, which can be exploited for site-directed correction of point mutations [10-12].

It is reasonable to think that the presence of polypurine-polypyrimidine sequences in the target DNA would be a limitation. However, triple-helix target sites (TTS) are over-represented in the human genome, especially at regulatory regions such as promoters. Goñi and coworkers suggested that even if TTS are not directly targeted by TFs, they might be important for gene functionality by acting as spacing fragment to help the correct positioning of transcription factors [13, 14]. It has been reported that an intramolecular triplex modulates transcription in the human *C-MYC* promoter [15]. Nevertheless, the use of TFOs is limited by the low stability of the triplehelical structure.

2.2. Antisense Oligodeoxynucleotides

Antisense oligonucleotides are single-stranded DNA (ssDNA) molecules, typically of 20 nucleotides (nt) in length. They are designed to bind a target mRNA sequence through Watson-Crick bonds to modulate protein silence endogenous microRNAs, therefore although they modulate gene expression, they are not silencing oligonucleotides translation [16]. aODNS can be separated into two broad classes depending on their mechanism of action:

RNase H-dependent oligonucleotides, also called gapmers, have a phosphorothioate backbone with flanks that are modified in the 2′-position of the residues. The unmodified 'gap' in the aODN–mRNA duplex is recognized by ribonuclease H (RNase H), which degrades the mRNA. Since RNase H has to recognize the duplex, nucleotides can be chemically modified to a limited degree.

Steric-blocking oligonucleotides: physically prevent or inhibit the progression of splicing (spliceswitching oligonucleotide; SSO) or the translational machinery. The SSO approach is being investigated to restore the normal reading frame of dystrophin in Duchenne muscular dystrophy, a change that results in the production of a shorter although functional protein.

According to the desired application of the aODN, and to favor its effect, several modifications can be introduced in the sequence. These are directed to increase the resistance of aODN to nucleases or to improve the uptake of the aODN by the cells. In 1998, the first aODN drug, fomivirsen, was registered as a treatment for cytomegalovirus-induced retinitis [17, 18], in immunocompromised patients with AIDS and more recently, the cholesterol-reducing antisense oligonucleotide mipomersen [19] was approved by FDA in 2013.

2.3. siRNAs

Small interfering RNAs (siRNAs) are double-stranded RNA (dsRNA) oligonucleotides of 21-22 bases in length with a 3' overhang of two bases. One of the strands is called the antisense (or guide) strand, while the other one is the sense (or passenger) strand. siRNAs are the substrate of the natural intracellular protein complex called RNA induced silencing complex (RISC). Within the RISC, the siRNA is unwound and the sense strand eliminated. The antisense or guide strand binds to mRNA activating the component of RISC endonuclease argonaute 2 (AGO2) and cleaving the mRNA 10 nucleotides downstream from the 5′ end of the antisense strand. This mechanism was first demonstrated in animals in the nematode *C. elegans* [20], when the delivery of exogenous dsRNA effectively decreased the mRNA levels of the target gene (*unc22,* an abundant but nonessential myofilament protein). The RNA interference (RNAi) process is a gene silencing mechanism [21] that is conserved in eukaryotes. Its primary functions are the regulation of gene expression and the defense against virus and other exogenous genetic elements. Since the RISC complex is located in the cytoplasm, siRNAs only target mature RNA.

2.4. Ribozymes

Ribozymes derive from catalytic RNAs found in virus, bacteria and some eukaryotes. They are ssRNA molecules that catalyze the cleavage and formation of covalent bonds in RNA strands at specific sites. These sites can be located in an external RNA (trans-cleavage) or in an RNA linked to the ribozyme (cis- or self-cleavage). The catalytic domains of the different ribozymes are highly conserved and they hydrolyze the target RNA upon recognition of their specific target sequence. Cleavage occurs by nucleophilic attack of the 2′-OH group onto the neighboring phosphorus [22]. The "hammerhead" ribozyme motif has been deeply studied in gene therapy to treat cancer and viral infections, such as HIV, hepatitis B and C. Other synthetic ribozymes have been developed, such as the X-motif ribozyme or the DNA-based 10-23 deoxyribozyme.

3. OTHER THERAPEUTIC OLIGONUCLEOTIDES

Oligonucleotides are capable of interacting with other macromolecules in the cell. TFs, which bind to promoter sequences in genes, are a clear example of these interactions. Additionally, ssDNA sequences fold within themselves and acquire specific tertiary structures that enable the DNA to interact with various molecular targets. These characteristics can be exploited to design other therapeutic oligonucleotides that do not act by Watson-Crick or Hoogsteen binding.

3.1. Aptamers

Aptamers are DNA or RNA sequences that have been evolved *in vitro* to bind to a desired target – protein or small molecule– after an iterative process called Systematic Evolution of Ligands by Exponential Enrichment (SELEX). The Gold and Szostak laboratories described this process simultaneously in 1990 [23, 24]. Aptamers are a class of nucleic acid-based molecules with therapeutic potential. Indeed, in 2004 the aptamer pegaptanib (Macugen), a selective vascular endothelial growth factor (VEGF) antagonist, [25] was accepted for the treatment of age-related macular degeneration.

Like antibodies, the action of aptamers depends on their tertiary structure. Therefore changes in the sequence or chemical modifications may alter their activity. Because of their capacity to bind efficiently to specific targets, several aptamers have been developed for their use in cancer research taking advantage of the particularities of cancer cells, such as the overexpression of some membrane proteins. Whole living cells

Ciudad et al.

are also employable as selection targets. This technology is called Cell-SELEX, and it has the advantage that the aptamers recognize the native conformation of the target molecule on living cells. In this way, cell surface proteins would be targets even if their purification in native conformation is difficult. Furthermore, it is possible to prepare cell-specific aptamers without previous knowledge about cell surface molecules on the target cells. Aptamers have been conjugated to drugs [26, 27], photosensitizers [28] and liposomes [29], and can also be used for diagnostic purpose [30].

3.2. Decoys

TFs recognize sequences in DNA and in a double-stranded decoy oligonucleotide. Decoy oligonucleotides are used to draw proteins away from their binding sites in DNA. Thus, different applications for decoys have been proposed, ranging from cancer [31], graft rejection after a transplant [32], to viral replication [33].

4. POLYPURINE REVERSE HOOGSTEEN HAIRPINS

Polypurine reverse Hoogsteen (PPRH) molecules are DNA hairpins formed by two polypurine strands running in an antiparallel orientation and containing no nucleotide modifications. The two strands, linked by a pentathymidine loop, are bound through intramolecular reverse Hoogsteen bonds. Then, PPRHs can bind by Watson-Crick bonds to their corresponding polypyrimidine target in the dsDNA provoking a displacement of the polypurine strand of the duplex [34] (Fig. **2**). It was demonstrated that upon binding their polypyrimidine target in a dsDNA, PPRHs were able to displace the polypurine strand of the target duplex [35] configuration.

Because the polypyrimidine domains are located in both strands of the DNA, PPRHs can be designed to target both strands of genomic DNA. PPRHs directed against the template strand of the DNA are called template-PPRHs, while the ones targeting the coding strand of the DNA are called coding-PPRHs, which are also able to bind transcribed mRNA, since it has the same sequence and orientation than the coding strand of the DNA. PPRHs can act as antigene and antisense oligonucleotides depending on the strand they target (Fig. **3**).

4.1. Mechanism of action of PPRHs

The mechanism of action of PPRHs, shown in (Fig. **4**), depends on the location of their target. Previous works in the laboratory demonstrated that template-PPRHs inhibit transcription [36]. However, a coding-PPRH against a polypyrimidine region in intron 3 of DHFR provoked a splicing alteration by avoiding the binding of the splicing factor U2AF65 [37]. This produced the accumulation of the immature mRNA, leading to a decrease in DHFR protein levels. Subsequently, it was demonstrated that two PPRHs directed against the coding or template strand of the *survivin* promoter reduced the binding of transcription factors GATA-3 and Sp1, respectively.

4.2. Proof of principle for PPRHs as anticancer therapeutic tools.

PPRHs against different regions (promoter, exon and intron) of the *survivin* gene were designed and their effect was compared in terms of cell viability and apoptosis. The four PPRHs decreased cell viability and increased apoptosis at the range of nanomolar, in the PC3 cell line. These PPRHs did not cause a decrease in cell viability in a normal cell line (HUVEC) and two murine cancer cell lines (CT26 and 4T1).

It was observed that the most effective PPRHs were a Coding-PPRH (HpsPr-C) and a Template- (HpsPr-T)
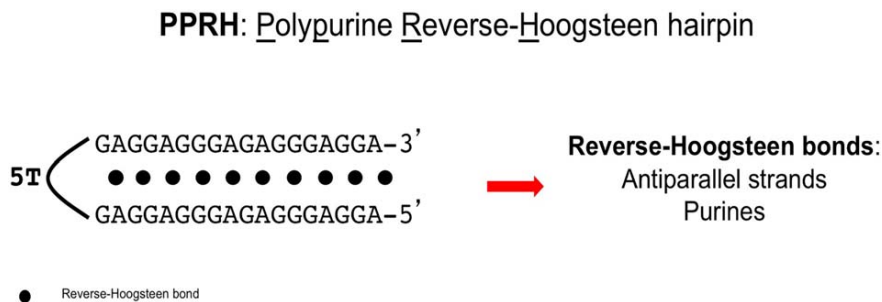

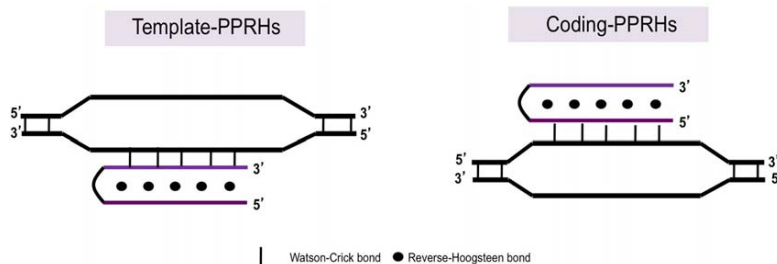**Fig. (2).** PPRH structure showing the two homopurine domains bound by Reverse Hoogsteen bonds.

Fig. (3). Template-PPRHs bind to the template strand of the dsDNA. Coding-PPRHs bind to the coding strand of the dsDNA.
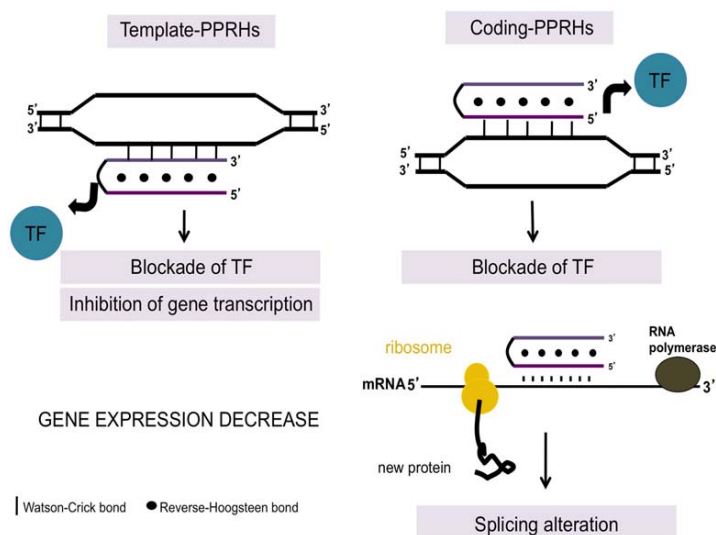

Fig. (4). Mechanism of action of template and coding PPRHs.

against two different regions of the *survivin* promoter causing a decrease in viability of more than 90% at 100 nM and an increase in apoptosis. HpsPr-C caused apoptosis in more than 50% of the cells. Both PPRHs decreased *survivin* mRNA and protein levels. HpsPr-T incubation reduced mRNA down to 38% and protein to 10%. To identify their mechanism of action EMSA assays were performed. First, their specific binding to their target sequence was confirmed. Secondly, we hypothesized that the binding of these PPRHs could interfere with the binding of putative transcription factors specific for their target sequences. After an *in silico* analysis and literature mining, the role of Sp1 and Sp3 for the Template-PPRH (HpsPr-T) and GATA for the Coding-PPRH (HpsPr-C) were studied. Using EMSA assays with nuclear extracts and competitors, it was

determined that HpsPr-T and HpsPr-C prevented the binding of Sp1/3 and GATA-3, respectively.

Finally, two *in vivo* efficacy assays were conducted using two different routes of administration, either intratumoral or intravenous, in a subcutaneous xenograft tumor model of PC3 prostate cancer cells. We compared the tumor growth throughout the administration of either HpsPr-C (the most effective one in terms of decrease in cell viability and increase in apoptosis) or Hps-Sc (a scrambled hairpin without target in the human genome). It was observed that, independently of the route of administration, the specific Coding-PPRH caused a decrease in tumor volume, in parallel with a decrease in *survivin* protein levels and blood vessel formation, which established the proof of principle as a therapeutic tool [38]. Administration of PPRHs did not

cause a decrease in body animal weight, indicating lack of toxicity.

4.3. Comparison Between Gene Silencing Molecules

Despite aODNs and siRNAs have similarities because both are nucleic acids and they both target mRNA, they have also differences in terms of cost, stability, and delivery. However, several studies have compared the activity of these two molecules and no clear choice has become apparent, much to the contrary, they argued that the choice would always depend upon the application - *in vitro* or *in vivo*-, type of administration and delivery system -systemically or locally-. Modifications such as locked nucleic acids (LNA) or 2-O-methoxyethyl (2'MOE)-RNA, among others, have increased the affinity and potency of aODNs and siRNAs while reducing undesirable responses [39].

The primary routes of administration of oligonucleotides for systemic applications are either intravenous (IV) infusion or subcutaneous (SC) injection. After these, oligonucleotides are quickly absorbed into the circulation with peak plasma concentrations reached within 3 to 4 h [40]. At this point, if no vehicle is used (gymnotic administration), the clearance of the oligonucleotides depends on their metabolism by blood nucleases, their renal filtration, and their accumulation in tissues. Therefore, the bioavailability of DNA-based molecules depends in great measure on their chemical properties. It has been clearly established that unmodified oligonucleotides, peptide nucleic acids (PNAs), morpholinos, and oligonucleotides that lack charge exhibit more rapid clearance from blood primarily due to either metabolism in blood (specially unmodified oligonucleotides) or excretion in urine [41, 42]. In contrast, oligonucleotides containing a phosphorothioate backbone are extensively bound to plasma proteins ($\geq 85\%$), especially to albumin, with relatively low affinity (Kd approximately 150 μM). This prevents loss of the oligonucleotide to renal filtration and facilitates uptake in tissues [40]. Thus, a balanced plasma protein binding is required for optimal delivery to cells and tissues systemically.

PPRHs are unmodified DNA molecules; therefore one could speculate that their PK would be similar to that of unmodified aODNs. In this case, DNase I and 3'-exonuclease are the primary enzymes to degrade circulating deoxyribonucleotides. DNase I recognizes and degrades the B form of dsDNA by single-stranded nicking mechanisms in the presence of Mg^{2+}, or by double-stranded cutting, in the presence of Mn^{2+} or

Mg^{2+} and Ca^{2+} [43, 44]. The rate of hydrolysis of this enzyme depends on the oligonucleotide conformation and sequence: extended G-G or A-T sites are quite resistant to degradation [45], as observed in G-rich anti-HIV oligonucleotides [46] and in aptamers against nucleolin [47].

In the case of siRNAs, ribonucleases belonging to the RNase A family [48] are the predominant nucleases to degrade circulating ribonucleotides. The reported half-life for unmodified siRNAs in serum ranges from minutes to 1 h [49-51]. In *in vivo* rat experiments plasma half-life was estimated to be less than 8 minutes [52]. Remarkably, the siRNAs sequence can have an impact on their own stability: regions rich in UpA clusters, which have low thermal stability, are most susceptible toward RNase A degradation [48] especially when they are located toward the end of the strands [53].

The half-lives of two different PPRHs were much longer compared to siRNA. The half-life of the PPRHs was between 7 and 10 times longer than that of siRNA, depending on the type of serum, and twice as longer when transfected to PC3 cells [54]. This extended half-life of the PPRHs could be explained by the nature of their structure. PPRHs are not standard double-stranded DNA molecules, since they are protected by the pentathymidine loop on one side and intramolecularly linked by reverse Hoogsteen bonds.

Because this susceptibility to be degraded is a serious drawback to use oligonucleotides as therapeutic agents, the higher stability of the PPRHs, even without chemical modifications, is a remarkable advantage. Generally, nuclease-resistant oligonucleotides are necessary to allow their systemic distribution. Phosphate modifications at the 3′-end and the inclusion of 2′-protected nucleosides at internal sites of the ribose are necessary to provide protection against exonucleases and endonucleases, respectively. Nevertheless, these modifications can have unintended consequences, such as the activation of the Complement system or the prolongation of clotting times [55]. Also, they increase the complexity of synthesis and the cost of the oligonucleotides.

A comparison between aODNs and siRNAs against survivin was previously performed in our group [21]. We designed two siRNAs, one targeting the coding region of the human survivin mRNA (siRNA-Surv) and the other targeting the 3'-UTR region (siRNA-3UTR), and one aODN targeting the translational start site of human survivin mRNA (aODN-Surv). aODN-Surv at 1 μM produced a downregulation effect corresponding to 80% of the initial mRNA levels. As siR-

NAs are much more potent than aODNs, a concentration of only 100 nM siRNA-Surv was needed to reduce survivin mRNA levels by 80%. This same behaviour was observed when analyzing survivin protein levels, 1μM aODN-Surv downregulated survivin by 50% whereas siRNA-Surv (100 nM) inhibited its protein levels by 50%. siRNASurv reduced cell growth by 95% at 30 nM. Moreover, treatment of endothelial cells with 30 nM siRNA-Surv caused a 4-fold induction of apoptosis, as did 800 nM aODNSurv [21]. In this direction, the effects observed with PPRHs against this same target indicate that PPRHs are at least as efficient as siRNAs in terms of cytotoxicity and decrease of protein target levels in the same range of concentration [38].

Furthermore, a comparison of the effect of a PPRH, an aODN and a siRNA against the same target was conducted in MCF-7 resistant cells. Results showed that a Template-PPRH against *DHFR* was more effective in producing cytotoxicity (70%) than an aODN (5%) and a siRNA (30%) against the same target [36].

It is important to bear in mind that PPRHs follow the antigene strategy, which presents several advantages compared to the antisense effect exerted by antisense oligonucleotides (aODNs) or small interfering RNAs (siRNAs). First, when targeting the gene, there are only two targets per cell corresponding to the two alleles, compared to the multiple copies of mRNA. Secondly, inhibition of transcription avoids formation of mRNA, while molecules that inhibit translation do not stop formation of the mRNA and are meant to act in a more transient fashion. Finally, targeting DNA might impair DNA-binding proteins that might be important for gene expression [9].

We also compared PPRHs with TFOs designed against the same region (two promoter regions within the *survivin* gene). Comparison of these two molecules provides valuable information because of their similarities. First, both molecules are directed towards the same region but to complementary sequences: the PPRH is directed against the pyrimidine strand and the TFO against the purine strand. Moreover, both molecules have the same composition of purines, except that the PPRH is double-stranded by formation of a hairpin structure and the TFO is single-stranded. Finally, both molecules form triplexes with the DNA, whereas the PPRH forms Watson-Crick bonds with the target sequence and intramolecular reverse-Hoogsteen bonds, the TFO forms reverse-Hoogsteen bonds with the purine strand of the double-stranded target sequence. This study corroborated that the presence of the hairpin structure in the PPRH have several advantages: i) the

binding affinity is higher for the PPRH than for the TFO, i.e the PPRH binds to the target sequence at lower concentrations. ii) At equal conditions, PPRHs are more potent than TFOs in terms of decrease in cell viability. iii) The difference in effect is due to the intrinsic efficacy of the molecule because the uptake is similar for both molecules. Our results are in agreement with Kool [56], indicating that the presence of the reverse-Hoogsteen strand in the PPRH, even though it does not interact with the double-stranded DNA sequence, provides an advantage for PPRHs over TFOs.

PPRHs, TFOs, aODNs, and siRNAs have in common the property of being used as gene silencing molecules. It is important to bear in mind that although PPRHs share with TFOs the formation of triplex structures, there are differences in their binding properties; while the TFOs bind to the double-stranded DNA by Hoogsteen bonds, PPRHs bind intramolecularly by reverse Hoogsteen bonds and to the dsDNA by Watson-Crick bonds. We have determined two important features regarding the differences of both PPRHs and TFOs: PPRHs have a higher binding affinity to the dsDNA target, and ii) PPRHs have a higher biological activity than TFOs. Therefore, in terms of gene expression inhibition, it was shown that PPRHs offer advantages over TFOs [57]. In addition, while working at a similar range of concentration [36] PPRHs have advantages over siRNAs taking into account stability and economy. Moreover, no off-target effects have been found when analyzing the mRNA levels for a set of randomly chosen genes, to ascertain whether PPRH directed against specific targets would affect the expression of control genes. The mRNA levels of the Telomerase, Survivin, UGT1A10, and S100A4 genes did not change significantly in SKBR3 cells incubated for 72 hr with a PPRH against DHFR [36, 37]. Likewise, in [38], the mRNA levels corresponding to APOA1, Bcl2, DHFR, PDK1 and S100A4 were not decreased when incubated with two specific PPRHs against Survivin.

4.4. Improvement of PPRH Design and Specificity

To improve the use of the PPRHs and decrease their possible off-target effects, we studied two main points conferring specificity to the PPRHs: their length and purine interruptions found in the target sequence with the aim to improve their applicability as gene silencing tools. We compared the effect in terms of binding and cell viability of three PPRHs that differed in length (20, 25 and 30 bp) directed against the same in

sequence of the *telomerase (TERT)* gene. We observed that even though all of them were able to bind to the target sequence, the longer the PPRH, the higher the effect in terms of decrease in cell viability.

It was previously stated that upon design of aODNs and TFOs, a 17-nucleotide long sequence should find one single target in the genome [58]. Indeed, the PPRHs that are normally designed in our laboratory are at least 20 bp in length, which ensures good target specificity. Regarding the length, our results conclude that whenever possible, the longer the PPRH, the higher the effect. In our hands, PPRHs from 20-nucleotide length were able to bind with high affinity to their target sequence, show effect and maintain specificity [38]. When the sequence of the gene allows for longer target sequences, such as in the case of the *TERT* gene, a longer PPRH was demonstrated to cause a higher decrease in cell viability than their shorter versions. Naturally, the longer the sequence, the less probability the molecule would bind to unintended targets.

Other authors proved that when using pyrimidine TFOs, length also played an important role. They observed that the triplex was more stabilized with longer molecules [59]. However, a similar study using G,T-TFOs showed that the optimal length was 12-mer. They explained the difference between these two molecules in the capability of G-rich oligonucleotides to self-associate, thus avoiding triplex formation. Despite that, they did not found a correlation between the formation of tetraplexes and the inability to form triplexes [60]. Arimondo *et al.* studied the importance of length in G,A-TFOs. They stated that longer TFOs bound to the target sequence with a lower K_d, meaning a higher stability of the triplex. They also studied the importance of sequence polarity, reaching to the conclusion that presence of Guanines in 3' reflected in a higher stability due to its role in the nucleation step during triplex formation [61].

There had been also studies regarding length of polypyrimidine PNAs, which form triplexes with its target sequence. Bentin *et al.* proved that PNAs of 12 and 15-mer displayed more complexity in terms of structures than 10-mer PNAs, but displayed a similar efficiency of binding [62]. Other authors proved that a 19-mer PNA inhibited expression while 15-mer and 17-mer against the same target did not, proving inhibition of gene expression is sensitive to PNA length [63].

Bhagat *et al.* studied the gene silencing activity of RNA and DNA oligonucleotides ranging from 15- to 25-mer, and found that the 19-mer DNA and RNA oligonucleotides were the most efficient ones in decreasing mRNA levels [64]. siRNAs length has also been explored. Kim *et al.* studied a set of dsRNAs ranging from 21 to 45-bp against different targets and determined that the best candidate was the 27-mer duplex, while longer duplexes lost RNAi activity [65]. Hu *et al.* studied siRNAs against *huntingtin* ranging from 15 to 21-nucleotides and concluded that when using siRNAs below 17-nt, the potency decreased [66].

For any target gene, the TFO target sequence search tool supplies different possibilities of purine sequences, susceptible to be used to design PPRHs. These sequences vary in length, percentage of Guanines, strand (forward or reverse) and location (promoter, intron, exon) within the gene. It is known that polypurine/polypyrimidine sequences are more abundant in regulatory regions, such as introns and promoters [14].

The second issue to consider is that we normally find 1-3 purine interruptions within the polypyrimidine targets. When the PPRHs were first developed it was found that adenines could be used as wild cards to place in front of the interruptions, and indeed this strategy was useful.

Coma *et al.* studied the effect of one interruption on an 11-nt hairpin by EMSA and T_m assays. They substituted the pyrimidine interruption (C) for either adenine or guanine (hairpin1-AA or hairpin1-GG) in both strands of the PPRH or used the pyrimidine of the interruption (C) in the Watson-Crick domain and its complementary base (G) in the reverse-Hoogsteen domain of the hairpin (hairpin1-CG). EMSA assays showed that the three molecules were able to bind to their double-stranded target sequence, but hairpin1-AA had the higher binding affinity, followed closely by hairpin1-CG, while hairpin1-GG displayed the lowest affinity. These results were corroborated using melting experiments, in which hairpin1-AA and hairpin1-CG had a T_m of 45ºC, while hairpin1-GG had a T_m of 40.7ºC. Using the approach of adenines, the hairpin was elongated to 20-nucleotides, which then contained 3 mismatches substituted by adenines in both strands of the molecule. Binding of this hairpin was checked in EMSA assays and they proved that in spite of interruptions, the binding occurred in just 10 minutes and with high affinity [35].

de Almagro *et al.* tested the effect of interruptions not only in terms of binding but also in functional assays. They tested two PPRHs against *DHFR*: A 20-nt PPRH carrying one interruption (T), which was substituted in both strands by either adenines (HpdI3-misTA), guanines (HpdI3-misTG) or thymidines

(HpdI3-misTT); and another PPRH of 21-nt carrying one interruption (C) substituted by adenines in both strands (HpdI3-misCA). They observed that all the PPRHs bound to their target sequence, but the PPRH using thymidines (HpdI3-misTT) was the one with the lowest affinity. Upon transfection of these PPRHs in breast cancer cells, those carrying adenines in the interruptions worked better than the others, but all of them less efficiently than the PPRH without interruptions. They concluded that adenine was the best base to use in front of the interruption to diminish the effect on instability in triplex formation [36].

Despite these PPRHs worked efficiently without causing known off-target effects, the use of PPRHs carrying adenines confronting the purine interruptions in the polypyrimidine target could raise some concern on specificity. It is important to bear in mind that target sequences usually have more than one interruption, and the higher the number, the higher the possibility of off-target effects.

In this regard, we explored the possibility of using PPRHs carrying pyrimidine interruptions, that we named Wild-type PPRHs, which bear the complementary base of the interruption in both strands of the PPRH (Fig. **5**).
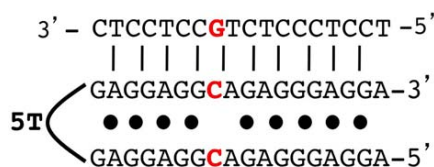
Wild Type-PPRH

Fig. (5). Wild type-PPRH: Version of PPRH containing a pyrimidine in front of purine interruptions in the DNA target.

So far, when one pyrimidine interruption occurred in the PPRH sequence, adenine was the base to use. It is obvious to deduce that the longer the target sequence, the more interruptions is meant to have. It was demonstrated that PPRHs of 20 (HpsPr-C), 26 (HpsPr-T) and 30 (HptI10-T) nucleotides carrying 3 interruptions substituted by adenines in both strands of the PPRH were able to bind to their target sequence with high affinity and cause a reduction of the targeted gene levels. However, the more interruptions are substituted by adenines, the more probability that some binding to unintended targets may occur. To enlarge the options to

design PPRHs against regions carrying interruptions without penalizing their specificity, we decided to test whether the use of the pyrimidine interruptions was detrimental for the binding affinity of the PPRH. We tested three approaches using a 26-nt PPRH against *survivin* carrying 3 interruptions: using adenines in both strands as the positive control (HpsPr-T), using the pyrimidine interruptions in both strands of the PPRH (HpsPr-T WT) or using the pyrimidine interruption in the Watson-Crick domain and its complementary base in the reverse-Hoogsteen domain. (HpsPr-T WT 2). In EMSA assays we observed that the three PPRHs were able to bind to their target sequence, thus corroborating the results from Coma and de Almagro [35, 36]. Moreover, the three PPRHs produced the same binding pattern, suggesting that the change of bases did not alter their structure. In cell viability assays, the PPRH that caused a higher decrease in cell viability was the one carrying pyrimidine interruptions in both strands of the PPRH (HpsPr-T WT) and it was the chosen approach for the follow-up experiments. So, using the best PPRHs against *survivin*, we designed their Wild-type counterparts and compared their effect in terms of binding, melting experiments, cell viability and analyzed their gene silencing capacity. We proved that Wild-type PPRHs bound with better affinity to their target sequences, exhibited by a higher intensity of binding, a higher T_m and a lower ΔG. Regarding efficacy, WT-PPRHs had a lower IC_{50} than the regular PPRHs and were able to decrease *survivin* mRNA levels. Analysis of cell viability and mRNA levels using the best candidate for *Bcl-2*, HpBcl2E1-C, in comparison with its Wild-type counterpart, showed the same behavior.

Other authors have tried to tackle the problem of interruptions in triplex binding by using either natural or synthetic analogues within the TFO sequence [67]. As an example, Aviñó *et al.* used parallel-hairpins with 8-aminopurines to increase affinity [68]. Newer approaches included using triplex intercalators, such as neomycin, to enhance affinity [69]. In our approach, nor synthetic bases nor intercalators were necessary, however, it would be interesting to study in-depth the chemical binding that takes place between this WT-PPRH and its specific target sequence. The effect of mismatches in TFOs has been studied, and the results pointed out the importance in the location of the mismatch. Specifically, interruption at the 3' end of purine TFOs destabilized the triplex because this sequence is important for the nucleation during triplex formation [61].

We decided to further improve PPRHs by designing a structure containing a polypyrimidine 5' extension that could bind to the displaced polypurine strand, as detailed in Fig. (**6**). For that reason we named this approach Wedge-PPRHs. This structure would stabilize the strand displacement in the PPRH-DNA complex, thus causing a higher silencing effect. We chose a template-PPRH to perform this approach. Two Wedge-PPRHs were designed; with 5′ extensions of 17 and 23 bases complementary to the purine sequence, linked to the hairpin structure by a 5T loop to give flexibility for the turn.

When performing binding analyses, Wedge-PPRH-23 formed two bands corresponding to a triplex and a quadruplex structure, but no quintuplex additional band was observed, which should have been appearing if the 5′ extension could bind to the displaced polypurine strand. However when we analyzed a shorter version of the Wedge-PPRH with a 5' extension of only 17 nucleotides (Wedge-PPRH-17) it hybridized to the polypurine displaced strand originating an additional shifted band corresponding to the quintuplex structure. Furthermore, Wedge-PPRH-17 was able to bind to the target sequence at a lower concentration (100 nM) than when using PPRHs and Wedge-PPRH-23.

When analyzing cell viability, the Wedge-PPRH-17 presented a lower IC50 than the parental HpsPr-T WT,

indicating that the Wedge-PPRH-17 had a higher efficacy [57] .

4.5. Immunogenicity

Immune activation by oligonucleotides has previously led to misinterpretation of data, especially when inhibition of tumor growth was not primarily due to the antisense mechanism but to the immunostimulatory properties of the oligonucleotides [70].

The innate immune system can detect pathogens using Pattern Recognition receptors (PRRs), which recognize not naturally occurring patterns in the human cell, such as dsRNA or unmethylated cytosine-phosphate-guanosine (CpG)-rich DNA in cellular compartments that are normally free of these molecules. Different PRRs recognize nucleic acids patterns out of which the toll-like receptor (TLR) family has been best characterized. TLR3, TLR7/TLR8, and TLR9 are located in the endolysosomes of macrophages and dendritic cells are responsible for the recognition of dsRNA, ssRNA, and CpG-rich DNA, respectively. After detection and binding of non-self genetic material, these TLRs lead to the phosphorylation and nuclear translocation of transcription factors, such as IRF3 controlling type 1 interferons, and NF-κB, regulating the expression of the proinflammatory cytokines IL-6, TNFα, IL-1β, and IL-18. siRNAs are recognized in a
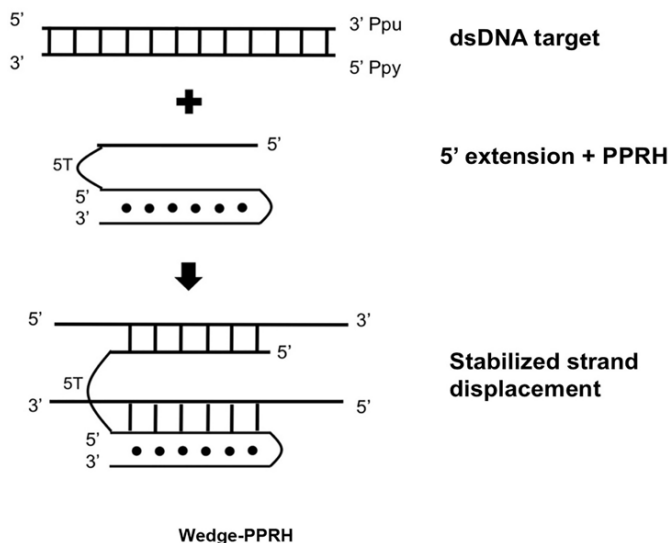

Wedge-PPRH

Fig. (6). Wedge-PPRH: Specific type of PPRH with an extension on the 5' end bearing the complementary sequence of the displaced strand of the target dsDNA.

sequence-dependent and sequence-independent manner [43, 71, 72], with immunostimulatory sequences appearing very frequently in conventionally siRNAs [71]. The length of RNAs plays a role in the activation of the immune system. Hornung *et al.* 2005 observed that 12-nt ssRNAs containing the immunostimulatory motif (GUCCUUCAA) were poor inducers of IFN-α. However, increasing the size to 16 nt or 19 nt restored cytokine induction. Our results on the immunostimulatory effect of siRNAs activating the innate immune response through the TLR pathway by the increase of IL-6, TNF-α, and IFNβ expression levels agree with previous results [71-73].

On the other hand, PPRHs did not show an immunostimulatory effect, probably because they are less than 100 bases in length, usually around 50 nucleotides. It has been reported that TLR9 recognizes unmethylated CpG-rich DNA, which is normally found in bacterial DNA provoking innate immune response [74]. In fact, peripheral blood mononuclear cells from nonhuman and human primates respond to two different types of oligonucleotides: D-ODN and K-ODN. Both of them express at least one unmethylated CpG motif. In contrast, PPRHs are unmethylated oligonucleotides and thus do not bear the unmethylated CpG sequences. This may contribute to escape TLR9 recognition and avoid the innate immune activation. Other receptors can also recognize nucleic acids in the cytoplasm such as NLR-family proteins that bind many ligands, including nucleic acids. dsRNA is sensed specifically by RIG-1 and PKR, while DAI and AIM2 recognize dsDNA. These receptors trigger a series of pathways that also ends up with the activation of proinflammatory cytokines.

The inflammasome is a multiprotein complex that mediates the proteolysis of procaspase-1 to the active caspase-1, which leads to the post-transcriptional activation of IL-1β and IL-18, and to pyroptosis, a form of programmed cell death in which immune cells die upon recognition of danger signals. Some receptors such as AIM2 do not discriminate between self and nonself DNA, so the finding that PPRHs do not produce the inflammasome response is an interesting fact. In addition, IL-18 and pro-IL-1β are limiting factors in this pathway [75], and their transcription relies on NF-κB. Regarding this matter, PPRHs have a double advantage over siRNAs: (i) they most likely do not promote the assembly of the inflammasome since they do not activate the proteolytic activity of caspase-1 and (ii) they do not induce the levels of NF-κB and therefore the levels of pro-IL-1ß nor IL-18.

In addition to the stability and immunogenic advantages of PPRHs over siRNAs, there are other aspects worth considering. For example, PPRHs do not use the intracellular RNA-processing pathways, whereas elevated concentrations of siRNA can saturate the RNAi machinery, thus perturbing miRNA-mediated regulation [76]. In mice, oversaturation of miRNA pathways with shRNA is fatal [77].

4.6. Validation of PPRHs

To evaluate if PPRHs could be used as silencing tools against different targets in several cancer cell lines, to expand the usage of PPRHs in cancer therapy and prove their general applicability, we chose a collection of therapeutic genes for the silencing activity of the PPRHs. The selected ones include a variety of biological functions: topoisomerases, antiapoptotic genes, transcription factors and protein kinases (Table **1**). We could design PPRHs directed against polypyrimidine domains of every gene to be targeted; three of these stretches were located in either a promoter region (*mtor*), an exonic sequence (*bcl2*) and mainly introns (*c-myc, mdm2, top1*), which were tested in a variety of cell lines (HCT 116, PC-3, MIAPaCa-2, SKBR3, MCF7, and MDA-MB-468).

All PPRHs were effective, yet the most remarkable results in decreasing cell survival and mRNA levels and increasing apoptosis were obtained with those against *bcl2* in PC3, MIA PaCa-2 and HCT 116 cell lines. Also, 3 out of 4 PPRHs designed against *mtor* were highly effective in HCT 116 cells. Additionally, when targeting *mtor* we performed time-course experiments, in which we observed that short incubations of 8 h after transfection already produced a 50% decrease in HCT 116 cells survival. In the case of *top1*, *mdm2*, and *c-myc*, their corresponding PPRHs showed a strong effect in reducing mRNA levels and cell viability and increasing apoptosis in the three breast cancer cell lines used.

We have determined that PPRHs produce a 40 - 70% decrease in the mRNA target levels, and that this decrease is enough to reduce cell survival significantly.

Very recently, we applied the gene silencing PPRH-technology to the area of immunotherapy, using as targets both SIRPα in macrophages and CD47 in cancer cells with the aim to eliminate tumor cells by macrophages in co-culture experiments. We demonstrated that the usage of PPRHs to decrease CD47/SIRPα interaction to reduce the expression of both proteins resulted in an enhanced killing of MCF-7 cells by

Table 1. **Compendium of the effects of PPRHs against different targets in cancer cell lines on cytotoxicity, apoptosis and mRNA and protein levels.**

Targeted gene	Cell line	PPRH	Cytotoxicity (relative to control)	mRNA levels (relative to control)	Protein levels (relative to control)	Apoptosis (Fold-change relative to control)
DHFR	SKBR3	HpdI3-A-TA	86%	50%	60%	ND
	MCF7-R	HpdI3-B	71%	58%	60%	ND
telomerase	SKBR3	HptI8-B	90%	45%	ND	ND
survivin	PC3	HpsPr-T and HpsPr-C	90%	40%	20%	1.65
	HeLa		90%	ND	ND	ND
BCL2	MIA PaCa-2	HpBcl2E1-C	95%	55%	ND	2.2
	PC3		90%	55%	ND	2.0
	HCT 116		95%	60%	ND	7.8
TOP1	SKBR3	HpTopI2-T	95%	58%	ND	2.0
	MCF7		60%	55%	ND	2.5
	MDA-MB-468		85%	68%	ND	4.2
MDM2	SKBR3	HpMdmI7-T	50%	42%	ND	4.5
	MCF7		60%	65%	ND	4
	MDA-MB-468		85%	38%	ND	13.5
MYC	SKBR3	HpMycI1-T	85%	40%	ND	4.4
	MCF7		80%	43%	ND	3.5
	MDA-MB-468		95%	72%	ND	12.5
mTOR	HCT 116	HpTorPr-C	90%	59%	ND	4.0
CD47 and *SIRPα*	MCF7 and THP-1	HpCD47Pr-T and HpSIRPαI7-T	70%*	42%	40%	3.0*
				40%	20%	

For each targeted gene, cytotoxicity, apoptosis fold-change and mRNA and protein levels upon incubation with the corresponding PPRH is shown.
*In the immunotherapy experiments targeting *CD47* in MCF-7 cells and *SIRPα* in THP-1 cells, the cytotoxicity and apoptosis fold-change corresponds to the treatment with both PPRHs in co-culture whereas the mRNA and protein levels correspond to each target separately.

macrophages, which could be translated into beneficial effects in cancer therapy [78].

4.7. Other Silencing Approaches

There are other silencing approaches being developed. One of them is based on pyrrole–imidazole polyamides, oligomers that bind to the minor groove of the DNA targeting short sequences of DNA of around 6 bp [79, 80]. In contrast, PPRHs expands a 19–25 nucleotide region, which confer a greater specificity. Concerning the potential target sites for PPRHs, TTS can generally be found in regulatory regions, specifically in introns, promoters, and to a lesser extent in exons. It is known that even if these regions are overrepresented in promoters, they are not necessarily the binding sites for

transcription factors [14]. PPRHs can bind to transcription factors response elements and also to other regions in the promoter and to both exonic and intronic sequences. In addition, PPRHs have the ability to bind to transcribed mRNA.

Programmable endonucleases such as zinc-finger nucleases (ZFN), transcription activator-like effector nucleases (TALENs) and Clustered Regulatory Interspaced Short Palindromic Repeats (CRISPR)/CRISPR-associated 9 (Cas9), are artificial proteins composed of a sequence specific DNA-binding domain fused to a nuclease, that are able to provoke double strand breaks (DSBs) in the genome, thus stimulating the cellular DNA repair-mechanisms, including error-prone non homologous end joining (NHEJ), in the absence of a

homologous DNA template, and homologous recombination (HR), in the presence of a synthetic repair template [81]. These site-specific nucleases have shown to edit DNA to disrupt, introduce, invert, or delete genes [82].

ZFNs have been used as a tool for genome editing since 2005. ZFNs are custom-designed artificial endonucleases formed by two domains: A Cys_2-His_2 zinc finger DNA-binding domain and a nuclease domain from the FokI restriction enzyme, responsible for the catalytic cleavage. When two ZFNs form a dimer, the nuclease becomes active [83, 84] and therefore, able to induced sequence-specific cleavage at a genomic *locus*, resulting on a DSB [85, 86]. ZFNs have been used in two clinical trials [87] to knockout the *chemokine (C-C motif) receptor 5* (*CCR5*) gene in CD4+ T cells thus conferring resistance to HIV-1 [88]

TALENs have emerged as an alternative to ZFNs for genome editing [89, 90]. These artificial restriction enzymes are formed by an unspecific FokI domain fused to a TAL effector DNA-binding domain, which is a naturally protein secreted by the pathogenic *Xanthomonas* bacteria, commonly located in plant cells [91]. The DNA-binding domain contains two highly variable aminoacids called repeat-variable diresidues (RVDs) out of 33-35 that are strongly conserved. RVDs are very related with the specificity of the nucleotide recognition [92, 93]. TALENs are typically used for gene disruption [94-97] and gene addition [98, 99].

The CRISPR/Cas system provides bacterial and archaeal immunity against foreign DNA by using RNAs to direct cleavage of the DNA [100]. In 2012, the type II CRISPR system was adapted for genome editing [101], and in a few years it has achieved great successes in this field. A tracrRNA-crRNA chimeric single-guide RNA (sgRNA) has been developed [102], which is able to recruit the Cas9 nuclease, responsible for introducing site-specific DSBs in target DNA [100, 101]. Cas9 protein requires a "seed" sequence within the sgRNA and a protospacer adjacent motif (PAM) [103]. By re-designing the sgRNA, almost any DNA sequence can be targeted. CRISPR/Cas system has been shown to be efficient in a variety of organisms by changing the DNA sequence at a specific *locus*. A controversial study was conducted in human embryos to modify *ß-globin*, but a high number of off-target effects were observed [104]. In somatic cells, various works have also been reported, such as the disruption of *proprotein convertase subtilisin/kexin type 9* (PCSK9) [105], or the treatment of hepatitis B virus

infection by modeling chronic infection in mouse livers with expression vectors, to be further targeted and disrupted [106]. The first clinical trial for the CRISPR–Cas9 technique targeting PD-1 started in October 2016 by a team led by oncologist Lu You at Sichuan University [107] and there are presently four other clinical trials designed against this same target in different types of cancer [87].

The initial goal for all these protein-based approaches with different degrees of complexity was genome-editing. Their mechanism of action consist in the introduction of double-strand breaks and its subsequent repair through non-homologous end joining or homology-directed repair, where the former can provoke unwanted deletions or insertions [108]. Even if these methods are considered solid platforms for genome editing, they present several drawbacks, including unwanted cytotoxic activity and potential off-target DNA cleavage [109], they are labor- and time-consuming [110, 111], and show complications linked to viral gene therapy [112]. An additional concern for these approaches could be the immune response started by the large amounts of virus necessary for the *in vivo* delivery and by the peptides from editing nucleases. On the other hand, PPRHs can be easily designed and their synthesis is inexpensive, since they are regular unmodified oligonucleotides of 50 bases approximately and can be used without further manipulation. PPRHs can be labeled in their primary synthesis with biotin or fluorophores and can also be fused to delivering or targeting agents, such as antibodies or aptamers. Finally, several PPRH-binding sites can be found per targeted gene allowing for combination therapy.

We studied the *in vivo* efficiency of the PPRHs [38] using a subcutaneous xenograft tumor model of prostate cancer. Using two different types of administration, intravenous and intratumoral, a PPRH against *survivin* promoter (HpsPr-C) was able to slow down the tumor growth, without altering mice weight. In our opinion, the best options for their clinical application considering the accumulated experience with PPRHs would be to apply this technology against cancer targets in order to inhibit anti-apoptotic, angiogenic or metastasic genes.

CONCLUSION

PPRHs have a rapid effect and work at nanomolar range, like siRNAs, and at lower concentration than that needed for aODNs or TFOs to exert their effect.

PPRHs display higher efficacy in terms of binding and effect than TFOs.

The stability of PPRHs is higher than that of siRNAs, as evidenced by the longer half-life of the former.

PPRHs proved to be target-specific and species-specific and non immunogenic.

The *in vivo* administration of a Coding-PPRH against a promoter sequence of the *survivin* gene led to a decrease in tumor growth of a PC3 xenograft compared to administration of a scrambled molecule, which constitutes the proof of principle of this technology.

PPRHs can be used as a tool to validate genes in proliferation and cancer. PPRHs can be used to target genes related to resistance, as chemosensitizers, and in immunotherapy.

LIST OF ABBREVIATIONS

2'MOE	=	2-O-Methoxyethyl
aODN	=	Antisense oligodeoxynucleotide
ARGO2	=	Endonuclease argonaute 2
Cas9	=	Clustered regularly interspaced short palindromic repeat associated 9
CpG	=	Cytosine-phosphate-guanosine
CRISPR	=	Clustered regularly interspaced short palindromic repeat
DSBs	=	Double strand breaks
dsDNA	=	Double-stranded DNA
dsRNA	=	Double-stranded RNA
HR	=	Homologous recombination
LNA	=	Locked nucleic acids
NHEJ	=	Non- homologous end joining
nt	=	Nucleotides
PNAs	=	Peptide nucleic acids
PPRH	=	Polypurine Reverse Hoogsteen hairpin
PRRs	=	Pattern Recognition receptors
RISC	=	RNA-induced silencing complex
RNase H	=	Ribonuclease H
RVDs	=	Repeat-variable diresidues
SELEX	=	Systematic evolution of ligands by exponential enrichment
sgRNA	=	Single-guide RNA
siRNA	=	Small-interfering RNA
ssDNA	=	Single-stranded DNA
SSO	=	Splice-switching oligonucleotide

TALENs	=	Transcription activator-like effector nucleases
TF	=	Transcription factor
TFO	=	Triplex forming oligonucleotide
TLR	=	Toll-like receptor
TTS	=	Triple-helix target sites
WT	=	Wild-type
ZFN	=	Zinc finger nuclease

CONSENT FOR PUBLICATION

Not applicable.

CONFLICT OF INTEREST

The authors declare no conflict of interest, financial or otherwise.

ACKNOWLEDGEMENTS

LR, XV and AJ carried out all the experiments described in this work and drafted the manuscript. VN and CC conceived the study, participated in its design and coordination and helped to draft the manuscript. All authors read and approved the final manuscript.

REFERENCES

[1]   Watson, J.D.; Crick, F.H. Molecular structure of nucleic acids; a structure for deoxyribose nucleic acid. *Nature,* **1953**, *171*(4356), 737-738.

[2]   Avery, O.T.; Macleod, C.M.; McCarty, M. studies on the chemical nature of the substance inducing transformation of pneumococcal types : Induction of transformation by a desoxyribonucleic acid fraction isolated from pneumococcus type III. *J. Exp. Med.,* **1944**, *79*(2), 137-158.

[3]   Hoogsteen, K. The crystal and molecular structure of a hydrogen-bonded complex between 1-methylthymine and 9-methyladenine. *Acta Crystallogr.,* **1963**, *16*(9), 907-916.

[4]   Felsenfeld, G.; Davies, D.R.; Rich, A. Formation of a three-stranded polynucleotide molecule. *J. Am. Chem. Soc.,* **1957**, *79*(8), 2023-2024.

[5]   Zamecnik, P.C.; Stephenson, M.L. Inhibition of Rous sarcoma virus replication and cell transformation by a specific oligodeoxynucleotide. *Proc. Natl. Acad. Sci. USA,* **1978**, *75*(1), 280-284.

[6]   Lander, E.S.; Linton, L.M.; Birren, B.; Nusbaum, C.; Zody, M.C.; Baldwin, J.; Devon, K.; Dewar, K.; Doyle, M.; Fitz-

Hugh, W.; Funke, R.; Gage, D.; Harris, K.; Heaford, A.; Howland, J.; Kann, L.; Lehoczky, J.; LeVine, R.; McEwan, P.; McKernan, K.; Meldrim, J.; Mesirov, J.P.; Miranda, C.; Morris, W.; Naylor, J.; Raymond, C.; Rosetti, M.; Santos, R.; Sheridan, A.; Sougnez, C.; Stange-Thomann, Y.; Stojanovic, N.; Subramanian, A.; Wyman, D.; Rogers, J.; Sulston, J.; Ainscough, R.; Beck, S.; Bentley, D.; Burton, J.; Clee, C.; Carter, N.; Coulson, A.; Deadman, R.; Deloukas, P.; Dunham, A.; Dunham, I.; Durbin, R.; French, L.; Grafham, D.; Gregory, S.; Hubbard, T.; Humphray, S.; Hunt, A.; Jones, M.; Lloyd, C.; McMurray, A.; Matthews, L.; Mercer, S.; Milne, S.; Mullikin, J.C.; Mungall, A.; Plumb, R.; Ross, M.; Shownkeen, R.; Sims, S.; Waterston, R.H.; Wilson, R.K.; Hillier, L.W.; McPherson, J.D.; Marra, M.A.; Mardis, E.R.; Fulton, L.A.; Chinwalla, A.T.; Pepin, K.H.; Gish, W.R.; Chissoe, S.L.; Wendl, M.C.; Delehaunty, K.D.; Miner, T.L.; Delehaunty, A.; Kramer, J.B.; Cook, L.L.; Fulton, R.S.; Johnson, D.L.; Minx, P.J.; Clifton, S.W.; Hawkins, T.; Branscomb, E.; Predki, P.; Richardson, P.; Wenning, S.; Slezak, T.; Doggett, N.; Cheng, J.F.; Olsen, A.; Lucas, S.; Elkin, C.; Uberbacher, E.; Frazier, M.; Gibbs, R.A.; Muzny, D.M.; Scherer, S.E.; Bouck, J.B.; Sodergren, E.J.; Worley, K.C.; Rives, C.M.; Gorrell, J.H.; Metzker, M.L.; Naylor, S.L.; Kucherlapati, R.S.; Nelson, D.L.; Weinstock, G.M.; Sakaki, Y.; Fujiyama, A.; Hattori, M.; Yada, T.; Toyoda, A.; Itoh, T.; Kawagoe, C.; Watanabe, H.; Totoki, Y.; Taylor, T.; Weissenbach, J.; Heilig, R.; Saurin, W.; Artiguenave, F.; Brottier, P.; Bruls, T.; Pelletier, E.; Robert, C.; Wincker, P.; Smith, D.R.; Doucette-Stamm, L.; Rubenfield, M.; Weinstock, K.; Lee, H.M.; Dubois, J.; Rosenthal, A.; Platzer, M.; Nyakatura, G.; Taudien, S.; Rump, A.; Yang, H.; Yu, J.; Wang, J.; Huang, G.; Gu, J.; Hood, L.; Rowen, L.; Madan, A.; Qin, S.; Davis, R.W.; Federspiel, N.A.; Abola, A.P.; Proctor, M.J.; Myers, R.M.; Schmutz, J.; Dickson, M.; Grimwood, J.; Cox, D.R.; Olson, M.V.; Kaul, R.; Raymond, C.; Shimizu, N.; Kawasaki, K.; Minoshima, S.; Evans, G.A.; Athanasiou, M.; Schultz, R.; Roe, B.A.; Chen, F.; Pan, H.; Ramser, J.; Lehrach, H.; Reinhardt, R.; McCombie, W.R.; de la Bastide, M.; Dedhia, N.; Blöcker, H.; Hornischer, K.; Nordsiek, G.; Agarwala, R.; Aravind, L.; Bailey, J.A.; Bateman, A.; Batzoglou, S.; Birney, E.; Bork, P.; Brown, D.G.; Burge, C.B.; Cerutti, L.; Chen, H.C.; Church, D.; Clamp, M.; Copley, R.R.; Doerks, T.; Eddy, S.R.; Eichler, E.E.; Furey, T.S.; Galagan, J.; Gilbert, J.G.; Harmon, C.; Hayashizaki, Y.; Haussler, D.; Hermjakob, H.; Hokamp, K.; Jang, W.; Johnson, L.S.; Jones, T.A.; Kasif, S.; Kaspryzk, A.; Kennedy, S.; Kent, W.J.; Kitts, P.; Koonin, E.V.; Korf, I.; Kulp, D.; Lancet, D.; Lowe, T.M.; McLysaght, A.; Mikkelsen, T.; Moran, J.V.; Mulder, N.; Pollara, V.J.; Ponting, C.P.; Schuler, G.; Schultz, J.; Slater, G.; Smit, A.F.; Stupka, E.; Szustakowki, J.; Thierry-Mieg, D.; Thierry-Mieg, J.; Wagner, L.; Wallis, J.; Wheeler, R.; Williams, A.; Wolf, Y.I.; Wolfe, K.H.; Yang, S.P.; Yeh, R.F.; Collins, F.; Guyer, M.S.; Peterson, J.; Felsenfeld, A.; Wetterstrand, K.A.; Patrinos, A.; Morgan, M.J.; de Jong, P.; Catanese, J.J.; Osoegawa, K.; Shizuya, H.; Choi, S.; Chen, Y.J.; Szustakowki, J. Initial sequencing and analysis of the human genome. *Nature,* **2001***, 409*(6822), 860-921.

[7] Hosoya, T.; Takeuchi, H.; Kanesaka, Y.; Yamakawa, H.; Miyano-Kurosaki, N.; Takai, K.; Yamamoto, N.; Takaku, H. Sequence-specific inhibition of a transcription factor by circular dumbbell DNA oligonucleotides. *FEBS Lett.,* **1999***, 461*(3), 136-140.

[8] Hartman, D.A.; Kuo, S.R.; Broker, T.R.; Chow, L.T.; Wells, R.D. Intermolecular triplex formation distorts the DNA duplex in the regulatory region of human papillomavirus type-11. *J. Biol. Chem.,* **1992***, 267*(8), 5488-5494.

[9] Praseuth, D.; Guieysse, A.L.; Hélène, C. Triple helix formation and the antigene strategy for sequence-specific control of gene expression. *Biochimica et Biophysica Acta (BBA) -. Gene Structure and Expression,* **1999***, 1489*(1), 181-206.

[10] Culver, K.W.; Hsieh, W.T.; Huyen, Y.; Chen, V.; Liu, J.; Khripine, Y.; Khorlin, A. Correction of chromosomal point mutations in human cells with bifunctional oligonucleotides. *Nat. Biotechnol.,* **1999***, 17*(10), 989-993.

[11] Faruqi, A.F.; Datta, H.J.; Carroll, D.; Seidman, M.M.; Glazer, P.M. Triple-helix formation induces recombination in mammalian cells *via* a nucleotide excision repair-dependent pathway. *Mol. Cell. Biol.,* **2000***, 20*(3), 990-1000.

[12] Kalish, J.M.; Seidman, M.M.; Weeks, D.L.; Glazer, P.M. Triplex-induced recombination and repair in the pyrimidine motif. *Nucleic Acids Res.,* **2005***, 33*(11), 3492-3502.

[13] Goñi, J.R.; de la Cruz, X.; Orozco, M. Triplex-forming oligonucleotide target sequences in the human genome. *Nucleic Acids Res.,* **2004***, 32*(1), 354-360.

[14] Goñi, J.R.; Vaquerizas, J.M.; Dopazo, J.; Orozco, M. Exploring the reasons for the large density of triplex-forming oligonucleotide target sequences in the human regulatory regions. *BMC Genomics,* **2006***, 7*, 63.

[15] Belotserkovskii, B.P.; De Silva, E.; Tornaletti, S.; Wang, G.; Vasquez, K.M.; Hanawalt, P.C. A triplex-forming sequence from the human c-MYC promoter interferes with DNA transcription. *J. Biol. Chem.,* **2007***, 282*(44), 32433-32441.

[16] Rodríguez, M.; Coma, S.; Noé, V.; Ciudad, C.J. Development and effects of immunoliposomes carrying an antisense oligonucleotide against DHFR RNA and directed toward human breast cancer cells overexpressing HER2. *Antisense Nucleic Acid Drug Dev.,* **2002***, 12*(5), 311-325.

[17] De Smet, M.D.; Meenken, C.J.; Van Den Horn, G.J. Fomivirsen - a phosphorothioate oligonucleotide for the treatment of CMV retinitis. *Ocul. Immunol. Inflamm.,* **1999***, 7*(3-4), 189-198.

[18] Roehr, B. Fomivirsen approved for CMV retinitis. *J. Int. Assoc. Physicians AIDS Care,* **1998***, 4*(10), 14-16.

[19] Furtado, J.D.; Wedel, M.K.; Sacks, F.M. Antisense inhibition of apoB synthesis with mipomersen reduces plasma apoC-III and apoC-III-containing lipoproteins. *J. Lipid Res.,* **2012***, 53*(4), 784-791.

[20] Fire, A.; Xu, S.; Montgomery, M.K.; Kostas, S.A.; Driver, S.E.; Mello, C.C. Potent and specific genetic interference by double-stranded RNA in Caenorhabditis elegans. *Nature,* **1998***, 391*(6669), 806-811.

[21] Coma, S.; Noe, V.; Lavarino, C.; Adán, J.; Rivas, M.; López-Matas, M.; Pagan, R.; Mitjans, F.; Vilaró, S.; Piulats, J.; Ciudad, C.J. Use of siRNAs and antisense oligonucleotides against survivin RNA to inhibit steps leading to tumor angiogenesis. *Oligonucleotides,* **2004***, 14*(2), 100-113.

[22] Müller, S. Engineering of ribozymes with useful activities in the ancient RNA world. *Ann. N. Y. Acad. Sci.,* **2015***, 1341*(1), 54-60.

[23] Ellington, A.D.; Szostak, J.W. *In vitro* selection of RNA molecules that bind specific ligands. *Nature,* **1990***, 346*(6287), 818-822.

[24] Tuerk, C.; Gold, L.; York, N.Y. Systematic evolution of ligands by exponential enrichment: RNA ligands to bacteriophage T4 DNA polymerase. *Science New pp,* **1990***, 249*(4968 SRC - GoogleScholar), 505-510.

[25] Gragoudas, E.S.; Adamis, A.P.; Cunningham, E.T., Jr; Feinsod, M.; Guyer, D.R. Pegaptanib for neovascular age-related macular degeneration. *N. Engl. J. Med.,* **2004***, 351*(27), 2805-2816.

[26] Ray, P.; Cheek, M.A.; Sharaf, M.L.; Li, N.; Ellington, A.D.; Sullenger, B.A.; Shaw, B.R.; White, R.R. Aptamer-

Ciudad et al.

mediated delivery of chemotherapy to pancreatic cancer cells. *Nucleic Acid Ther.,* **2012,** *22*(5), 295-305.

[27] Thiel, K.W.; Hernandez, L.I.; Dassie, J.P.; Thiel, W.H.; Liu, X.; Stockdale, K.R.; Rothman, A.M.; Hernandez, F.J.; McNamara, J.O., II; Giangrande, P.H. Delivery of chemosensitizing siRNAs to HER2+-breast cancer cells using RNA aptamers. *Nucleic Acids Res.,* **2012,** *40*(13), 6319-6337.

[28] Ferreira, C.S.; Papamichael, K.; Guilbault, G.; Schwarzacher, T.; Gariepy, J.; Missailidis, S. DNA aptamers against the MUC1 tumour marker: design of aptamer-antibody sandwich ELISA for the early diagnosis of epithelial tumours. *Anal. Bioanal. Chem.,* **2008,** *390*(4), 1039-1050.

[29] Song, X.; Ren, Y.; Zhang, J.; Wang, G.; Han, X.; Zheng, W.; Zhen, L. Targeted delivery of doxorubicin to breast cancer cells by aptamer functionalized DOTAP/DOPE liposomes. *Oncol. Rep.,* **2015,** *34*(4), 1953-1960.

[30] Shigdar, S.; Qian, C.; Lv, L.; Pu, C.; Li, Y.; Li, L.; Marappan, M.; Lin, J.; Wang, L.; Duan, W. The use of sensitive chemical antibodies for diagnosis: detection of low levels of EpCAM in breast cancer. *PLoS One,* **2013,** *8*(2), e57613.

[31] Ahn, J.D.; Kim, C-H.; Magae, J.; Kim, Y.H.; Kim, H.J.; Park, K-K.; Hong, S.; Park, K-G.; Lee, I.K.; Chang, Y-C. E2F decoy oligodeoxynucleotides effectively inhibit growth of human tumor cells. *Biochem. Biophys. Res. Commun.,* **2003,** *310*(4), 1048-1053.

[32] Suzuki, J.; Isobe, M.; Morishita, R.; Nagai, R. Applications of nucleic acid drugs for organ transplantation. *Curr. Top. Med. Chem.,* **2012,** *12*(15), 1608-1612.

[33] Nakaya, T.; Iwai, S.; Fujinaga, K.; Otsuka, E.; Ikuta, K. Inhibition of HIV-1 replication by targeting the Rev protein. *Leukemia,* **1997,** *11*(Suppl. 3), 134-137.

[34] Wikipedia contributors Polypurine reverse-Hoogsteen hairpin. https://en.wikipedia.org/w/index.php?title=Polypurine_reverse-Hoogsteen_hairpin&oldid=733028458, 3 January, 2017

[35] Coma, S.; Noé, V.; Eritja, R.; Ciudad, C.J. Strand displacement of double-stranded DNA by triplex-forming antiparallel purine-hairpins. *Oligonucleotides,* **2005,** *15*(4), 269-283.

[36] de Almagro, M.C.; Coma, S.; Noé, V.; Ciudad, C.J. Polypurine hairpins directed against the template strand of DNA knock down the expression of mammalian genes. *J. Biol. Chem.,* **2009,** *284*(17), 11579-11589.

[37] de Almagro, M.C.; Mencia, N.; Noé, V.; Ciudad, C.J. Coding polypurine hairpins cause target-induced cell death in breast cancer cells. *Hum. Gene Ther.,* **2011,** *22*(4), 451-463.

[38] Rodríguez, L.; Villalobos, X.; Dakhel, S.; Padilla, L.; Hervas, R.; Hernández, J.L.; Ciudad, C.J.; Noé, V. Polypurine reverse Hoogsteen hairpins as a gene therapy tool against survivin in human prostate cancer PC3 cells *in vitro* and *in vivo. Biochem. Pharmacol.,* **2013,** *86*(11), 1541-1554.

[39] Watts, J.K.; Corey, D.R. Silencing disease genes in the laboratory and the clinic. *J. Pathol.,* **2012,** *226*(2), 365-379.

[40] Geary, R.S.; Norris, D.; Yu, R.; Bennett, C.F. Pharmacokinetics, biodistribution and cell uptake of antisense oligonucleotides. *Adv. Drug Deliv. Rev.,* **2015,** *87*, 46-51.

[41] Amantana, A.; Iversen, P.L. Pharmacokinetics and biodistribution of phosphorodiamidate morpholino antisense oligomers. *Curr. Opin. Pharmacol.,* **2005,** *5*(5), 550-555.

[42] Dirin, M.; Winkler, J. Influence of diverse chemical modifications on the ADME characteristics and toxicology of antisense oligonucleotides. *Expert Opin. Biol. Ther.,* **2013,** *13*(6), 875-888.

[43] Blume, S.W.; Lebowitz, J.; Zacharias, W.; Guarcello, V.; Mayfield, C.A.; Ebbinghaus, S.W.; Bates, P.; Jones, D.E., Jr; Trent, J.; Vigneswaran, N.; Miller, D.M. The integral di-

valent cation within the intermolecular purine*purine.pyrimidine structure: a variable determinant of the potential for and characteristics of the triple helical association. *Nucleic Acids Res.,* **1999,** *27*(2), 695-702.

[44] Pan, C.Q.; Ulmer, J.S.; Herzka, A.; Lazarus, R.A. Mutational analysis of human DNase I at the DNA binding interface: implications for DNA recognition, catalysis, and metal ion dependence. *Protein Sci.,* **1998,** *7*(3), 628-636.

[45] Fujihara, J.; Yasuda, T.; Ueki, M.; Iida, R.; Takeshita, H. Comparative biochemical properties of vertebrate deoxyribonuclease I. *Comp. Biochem. Physiol. B Biochem. Mol. Biol.,* **2012,** *163*(3-4), 263-273.

[46] Bishop, J.S.; Guy-Caffey, J.K.; Ojwang, J.O.; Smith, S.R.; Hogan, M.E.; Cossum, P.A.; Rando, R.F.; Chaudhary, N. Intramolecular G-quartet motifs confer nuclease resistance to a potent anti-HIV oligonucleotide. *J. Biol. Chem.,* **1996,** *271*(10), 5698-5703.

[47] Bates, P.J.; Laber, D.A.; Miller, D.M.; Thomas, S.D.; Trent, J.O. Discovery and development of the G-rich oligonucleotide AS1411 as a novel treatment for cancer. *Exp. Mol. Pathol.,* **2009,** *86*(3), 151-164.

[48] Haupenthal, J.; Baehr, C.; Kiermayer, S.; Zeuzem, S.; Piiper, A. Inhibition of RNAse A family enzymes prevents degradation and loss of silencing activity of siRNAs in serum. *Biochem. Pharmacol.,* **2006,** *71*(5), 702-710.

[49] Bartlett, D.W.; Davis, M.E. Effect of siRNA nuclease stability on the *in vitro* and *in vivo* kinetics of siRNA-mediated gene silencing. *Biotechnol. Bioeng.,* **2007,** *97*(4), 909-921.

[50] Dykxhoorn, D.M.; Palliser, D.; Lieberman, J. The silent treatment: siRNAs as small molecule drugs. *Gene Ther.,* **2006,** *13*(6), 541-552.

[51] Layzer, J.M.; McCaffrey, A.P.; Tanner, A.K.; Huang, Z.; Kay, M.A.; Sullenger, B.A. *In vivo* activity of nuclease-resistant siRNAs. *RNA,* **2004,** *10*(5), 766-771.

[52] Thompson, J.D.; Kornbrust, D.J.; Foy, J.W.; Solano, E.C.; Schneider, D.J.; Feinstein, E.; Molitoris, B.A.; Erlich, S. Toxicological and pharmacokinetic properties of chemically modified siRNAs targeting p53 RNA following intravenous administration. *Nucleic Acid Ther.,* **2012,** *22*(4), 255-264.

[53] Turner, J.J.; Jones, S.W.; Moschos, S.A.; Lindsay, M.A.; Gait, M.J. MALDI-TOF mass spectral analysis of siRNA degradation in serum confirms an RNAse A-like activity. *Mol. Biosyst.,* **2007,** *3*(1), 43-50.

[54] Villalobos, X.; Rodríguez, L.; Prévot, J.; Oleaga, C.; Ciudad, C.J.; Noé, V. Stability and immunogenicity properties of the gene-silencing polypurine reverse Hoogsteen hairpins. *Mol. Pharm.,* **2014,** *11*(1), 254-264.

[55] Henry, S.P.; Jagels, M.A.; Hugli, T.E.; Manalili, S.; Geary, R.S.; Giclas, P.C.; Levin, A.A. Mechanism of alternative complement pathway dysregulation by a phosphorothioate oligonucleotide in monkey and human serum. *Nucleic Acid Ther.,* **2014,** *24*(5), 326-335.

[56] Vo, T.; Wang, S.; Kool, E.T. Targeting pyrimidine single strands by triplex formation: structural optimization of binding. *Nucleic Acids Res.,* **1995,** *23*(15), 2937-2944.

[57] Rodríguez, L.; Villalobos, X.; Solé, A.; Lliberós, C.; Ciudad, C.J.; Noé, V. Improved design of PPRHs for gene silencing. *Mol. Pharm.,* **2015,** *12*(3), 867-877.

[58] François, J-C. *Methods in Enzymology*; Elsevier BV, **2000,** pp. 74-95.

[59] Shindo, H.; Torigoe, H.; Sarai, A. Thermodynamic and kinetic studies of DNA triplex formation of an oligohomopyrimidine and a matched duplex by filter binding assay. *Biochemistry,* **1993,** *32*(34), 8963-8969.

[60] Cheng, A-J.; Van Dyke, M.W. Oligodeoxyribonucleotide length and sequence effects on intramolecular and intermolecular G-quartet formation. *Gene,* **1997,** *197*(1-2), 253-260.

[61] Arimondo, P.B.; Barcelo, F.; Sun, J-S.; Maurizot, J-C.; Garestier, T.; Hélène, C. Triple helix formation by (G,A)-containing oligonucleotides: asymmetric sequence effect. *Biochemistry,* **1998**, *37*(47), 16627-16635.

[62] Bentin, T.; Hansen, G.I.; Nielsen, P.E. Structural diversity of target-specific homopyrimidine peptide nucleic acid-dsDNA complexes. *Nucleic Acids Res.,* **2006**, *34*(20), 5790-5799.

[63] Liu, Y.; Braasch, D.A.; Nulf, C.J.; Corey, D.R. Efficient and isoform-selective inhibition of cellular gene expression by peptide nucleic acids. *Biochemistry,* **2004**, *43*(7), 1921-1927.

[64] Bhagat, L.; Putta, M.R.; Wang, D.; Yu, D.; Lan, T.; Jiang, W.; Sun, Z.; Wang, H.; Tang, J.X.; La Monica, N.; Kandimalla, E.R.; Agrawal, S. Novel oligonucleotides containing two 3-ends complementary to target mRNA show optimal gene-silencing activity. *J. Med. Chem.,* **2011**, *54*(8), 3027-3036.

[65] Kim, D-H.; Behlke, M.A.; Rose, S.D.; Chang, M-S.; Choi, S.; Rossi, J.J. Synthetic dsRNA Dicer substrates enhance RNAi potency and efficacy. *Nat. Biotechnol.,* **2005**, *23*(2), 222-226.

[66] Hu, J.; Liu, J.; Yu, D.; Aiba, Y.; Lee, S.; Pendergraff, H.; Boubaker, J.; Artates, J.W.; Lagier-Tourenne, C.; Lima, W.F.; Swayze, E.E.; Prakash, T.P.; Corey, D.R. Exploring the effect of sequence length and composition on allele-selective inhibition of human huntingtin expression by single-stranded silencing RNAs. *Nucleic Acid Ther.,* **2014**, *24*(3), 199-209.

[67] Gowers, D.M.; Fox, K.R. Towards mixed sequence recognition by triple helix formation. *Nucleic Acids Res.,* **1999**, *27*(7), 1569-1577.

[68] Aviñó, A.; Frieden, M.; Morales, J.C.; García de la Torre, B.; Güimil García, R.; Azorín, F.; Gelpí, J.L.; Orozco, M.; González, C.; Eritja, R. Properties of triple helices formed by parallel-stranded hairpins containing 8-aminopurines. *Nucleic Acids Res.,* **2002**, *30*(12), 2609-2619.

[69] Arya, D.P. New approaches toward recognition of nucleic acid triple helices. *Acc. Chem. Res.,* **2011**, *44*(2), 134-146.

[70] Moreno, P.M.; Pêgo, A.P. Therapeutic antisense oligonucleotides against cancer: hurdling to the clinic. *Front Chem.,* **2014**, *2*, 87.

[71] Judge, A.D.; Sood, V.; Shaw, J.R.; Fang, D.; McClintock, K.; MacLachlan, I. Sequence-dependent stimulation of the mammalian innate immune response by synthetic siRNA. *Nat. Biotechnol.,* **2005**, *23*(4), 457-462.

[72] Sioud, M. Induction of inflammatory cytokines and interferon responses by double-stranded and single-stranded siRNAs is sequence-dependent and requires endosomal localization. *J. Mol. Biol.,* **2005**, *348*(5), 1079-1090.

[73] Hornung, V.; Guenthner-Biller, M.; Bourquin, C.; Ablasser, A.; Schlee, M.; Uematsu, S.; Noronha, A.; Manoharan, M.; Akira, S.; de Fougerolles, A.; Endres, S.; Hartmann, G. Sequence-specific potent induction of IFN-alpha by short interfering RNA in plasmacytoid dendritic cells through TLR7. *Nat. Med.,* **2005**, *11*(3), 263-270.

[74] Hanagata, N. Structure-dependent immunostimulatory effect of CpG oligodeoxynucleotides and their delivery system. *Int. J. Nanomedicine,* **2012**, *7*, 2181-2195.

[75] Davis, B.K.; Wen, H.; Ting, J.P. The inflammasome NLRs in immunity, inflammation, and associated diseases. *Annu. Rev. Immunol.,* **2011**, *29*(1), 707-735.

[76] Khan, A.A.; Betel, D.; Miller, M.L.; Sander, C.; Leslie, C.S.; Marks, D.S. Corrigendum: Transfection of small RNAs globally perturbs gene regulation by endogenous microRNAs. *Nat. Biotechnol.,* **2009**, *27*(7), 671-671.

[77] Grimm, D.; Streetz, K.L.; Jopling, C.L.; Storm, T.A.; Pandey, K.; Davis, C.R.; Marion, P.; Salazar, F.; Kay, M.A.

[78] Fatality in mice due to oversaturation of cellular microRNA/short hairpin RNA pathways. *Nature,* **2006**, *441*(7092), 537-541.

[78] Bener, G. A, J.F.; Sanchez de Diego, C.; Pascual Fabregat, I.; Ciudad, C.J.; Noe, V. Silencing of CD47 and SIRPalpha by Polypurine reverse Hoogsteen hairpins to promote MCF-7 breast cancer cells death by PMA-differentiated THP-1 cells. *BMC Immunol.,* **2016**, *17*(1), 32.

[79] Matsuda, H.; Fukuda, N.; Ueno, T.; Tahira, Y.; Ayame, H.; Zhang, W.; Bando, T.; Sugiyama, H.; Saito, S.; Matsumoto, K.; Mugishima, H.; Serie, K. Development of gene silencing pyrrole-imidazole polyamide targeting the TGF-beta1 promoter for treatment of progressive renal diseases. *J. Am. Soc. Nephrol.,* **2006**, *17*(2), 422-432.

[80] Yang, F.; Nickols, N.G.; Li, B.C.; Szablowski, J.O.; Hamilton, S.R.; Meier, J.L.; Wang, C.M.; Dervan, P.B. Animal toxicity of hairpin pyrrole-imidazole polyamides varies with the turn unit. *J. Med. Chem.,* **2013**, *56*(18), 7449-7457.

[81] Wyman, C.; Kanaar, R. DNA double-strand break repair: alls well that ends well. *Annu. Rev. Genet.,* **2006**, *40*, 363-383.

[82] Carroll, D. Genome engineering with targetable nucleases. *Annu. Rev. Biochem.,* **2014**, *83*, 409-439.

[83] Miller, J.C.; Holmes, M.C.; Wang, J.; Guschin, D.Y.; Lee, Y.L.; Rupniewski, I.; Beausejour, C.M.; Waite, A.J.; Wang, N.S.; Kim, K.A.; Gregory, P.D.; Pabo, C.O.; Rebar, E.J. An improved zinc-finger nuclease architecture for highly specific genome editing. *Nat. Biotechnol.,* **2007**, *25*(7), 778-785.

[84] Szczepek, M.; Brondani, V.; Büchel, J.; Serrano, L.; Segal, D.J.; Cathomen, T. Structure-based redesign of the dimerization interface reduces the toxicity of zinc-finger nucleases. *Nat. Biotechnol.,* **2007**, *25*(7), 786-793.

[85] Kim, Y.G.; Cha, J.; Chandrasegaran, S. Hybrid restriction enzymes: zinc finger fusions to Fok I cleavage domain. *Proc. Natl. Acad. Sci. USA,* **1996**, *93*(3), 1156-1160.

[86] Porteus, M.H.; Carroll, D. Gene targeting using zinc finger nucleases. *Nat. Biotechnol.,* **2005**, *23*(8), 967-973.

[87] ClinicalTrials ClinicalTrials.gov. *https://clinicaltrials.gov,* 3 January, 2017

[88] Perez, E.E.; Wang, J.; Miller, J.C.; Jouvenot, Y.; Kim, K.A.; Liu, O.; Wang, N.; Lee, G.; Bartsevich, V.V.; Lee, Y.L.; Guschin, D.Y.; Rupniewski, I; Waite, A.J.; Carpenito, C.; Carroll, R.G.; Orange, J.S.; Urnov, F.D.; Rebar, E.J.; Ando, D.; Gregory, P.D.; Riley, J.L.; Holmes, M.C.; June, C.H. Establishment of HIV-1 resistance in CD4+ T cells by genome editing using zinc-finger nucleases. *Nat. Biotechnol.,* **2008**, *26*(7), 808-816.

[89] Boch, J.; Scholze, H.; Schornack, S.; Landgraf, A.; Hahn, S.; Kay, S.; Lahaye, T.; Nickstadt, A.; Bonas, U. Breaking the code of DNA binding specificity of TAL-type III effectors. *Science,* **2009**, *326*(5959), 1509-1512.

[90] Moscou, M.J.; Bogdanove, A.J. A simple cipher governs DNA recognition by TAL effectors. *Science,* **2009**, *326*(5959), 1501.

[91] Boch, J.; Bonas, U. Xanthomonas AvrBs3 family-type III effectors: discovery and function. *Annu. Rev. Phytopathol.,* **2010**, *48*, 419-436.

[92] Deng, D.; Yan, C.; Pan, X.; Mahfouz, M.; Wang, J.; Zhu, J.K.; Shi, Y.; Yan, N. Structural basis for sequence-specific recognition of DNA by TAL effectors. *Science,* **2012**, *335*(6069), 720-723.

[93] Mak, A.N.; Bradley, P.; Cernadas, R.A.; Bogdanove, A.J.; Stoddard, B.L. The crystal structure of TAL effector PthXo1 bound to its DNA target. *Science,* **2012**, *335*(6069), 716-719.

[94] Carlson, D.F.; Tan, W.; Lillico, S.G.; Stverakova, D.; Proudfoot, C.; Christian, M.; Voytas, D.F.; Long, C.R.;

Whitelaw, C.B.; Fahrenkrug, S.C. Efficient TALEN-mediated gene knockout in livestock. *Proc. Natl. Acad. Sci. USA,* **2012,** *109*(43), 17382-17387.

[95] Li, T.; Liu, B.; Spalding, M.H.; Weeks, D.P.; Yang, B. High-efficiency TALEN-based gene editing produces disease-resistant rice. *Nat. Biotechnol.,* **2012,** *30*(5), 390-392.

[96] Mussolino, C.; Morbitzer, R.; Lütge, F.; Dannemann, N.; Lahaye, T.; Cathomen, T. A novel TALE nuclease scaffold enables high genome editing activity in combination with low toxicity. *Nucleic Acids Res.,* **2011,** *39*(21), 9283-9293.

[97] Wood, A.J.; Lo, T.W.; Zeitler, B.; Pickle, C.S.; Ralston, E.J.; Lee, A.H.; Amora, R.; Miller, J.C.; Leung, E.; Meng, X.; Zhang, L.; Rebar, E.J.; Gregory, P.D.; Urnov, F.D.; Meyer, B.J. Targeted genome editing across species using ZFNs and TALENs. *Science,* **2011,** *333*(6040), 307.

[98] Hockemeyer, D.; Wang, H.; Kiani, S.; Lai, C.S.; Gao, Q.; Cassady, J.P.; Cost, G.J.; Zhang, L.; Santiago, Y.; Miller, J.C.; Zeitler, B.; Cherone, J.M.; Meng, X.; Hinkley, S.J.; Rebar, E.J.; Gregory, P.D.; Urnov, F.D.; Jaenisch, R. Genetic engineering of human pluripotent cells using TALE nucleases. *Nat. Biotechnol.,* **2011,** *29*(8), 731-734.

[99] Zu, Y.; Tong, X.; Wang, Z.; Liu, D.; Pan, R.; Li, Z.; Hu, Y.; Luo, Z.; Huang, P.; Wu, Q.; Zhu, Z.; Zhang, B.; Lin, S. TALEN-mediated precise genome modification by homologous recombination in zebrafish. *Nat. Methods,* **2013,** *10*(4), 329-331.

[100] Wiedenheft, B.; Sternberg, S.H.; Doudna, J.A. RNA-guided genetic silencing systems in bacteria and archaea. *Nature,* **2012,** *482*(7385), 331-338.

[101] Jinek, M.; Chylinski, K.; Fonfara, I.; Hauer, M.; Doudna, J.A.; Charpentier, E. A programmable dual-RNA-guided DNA endonuclease in adaptive bacterial immunity. *Science,* **2012,** *337*(6096), 816-821.

[102] Mali, P.; Yang, L.; Esvelt, K.M.; Aach, J.; Guell, M.; Di-Carlo, J.E.; Norville, J.E.; Church, G.M. RNA-guided human genome engineering *via* Cas9. *Science,* **2013,** *339*(6121), 823-826.

[103] Doudna, J.A.; Charpentier, E. Genome editing. The new frontier of genome engineering with CRISPR-Cas9. *Science,* **2014,** *346*(6213), 1258096.

[104] Liang, P.; Xu, Y.; Zhang, X.; Ding, C.; Huang, R.; Zhang, Z.; Lv, J.; Xie, X.; Chen, Y.; Li, Y.; Sun, Y.; Bai, Y.; Songyang, Z.; Ma, W.; Zhou, C.; Huang, J. CRISPR/Cas9-mediated gene editing in human tripronuclear zygotes. *Protein Cell,* **2015,** *6*(5), 363-372.

[105] Ding, Q.; Strong, A.; Patel, K.M.; Ng, S.L.; Gosis, B.S.; Regan, S.N.; Cowan, C.A.; Rader, D.J.; Musunuru, K. Permanent alteration of PCSK9 with *in vivo* CRISPR-Cas9 genome editing. *Circ. Res.,* **2014,** *115*(5), 488-492.

[106] Lin, S.R.; Yang, H.C.; Kuo, Y.T.; Liu, C.J.; Yang, T.Y.; Sung, K.C.; Lin, Y.Y.; Wang, H.Y.; Wang, C.C.; Shen, Y.C.; Wu, F.Y.; Kao, J.H.; Chen, D.S.; Chen, P.J. The CRISPR/Cas9 System Facilitates Clearance of the Intrahepatic HBV Templates *In Vivo. Mol. Ther. Nucleic Acids,* **2014,** *3*, e186.

[107] Cyranoski, D. CRISPR gene-editing tested in a person for the first time. *Nature,* **2016,** *539*(7630), 479.

[108] Lin, S.; Staahl, B.T.; Alla, R.K.; Doudna, J.A. Enhanced homology-directed human genome engineering by controlled timing of CRISPR/Cas9 delivery. *eLife,* **2014,** *3*, e04766.

[109] Fu, Y.; Foden, J.A.; Khayter, C.; Maeder, M.L.; Reyon, D.; Joung, J.K.; Sander, J.D. High-frequency off-target mutagenesis induced by CRISPR-Cas nucleases in human cells. *Nat. Biotechnol.,* **2013,** *31*(9), 822-826.

[110] Mussolino, C.; Morbitzer, R.; Lütge, F.; Dannemann, N.; Lahaye, T.; Cathomen, T. A novel TALE nuclease scaffold enables high genome editing activity in combination with low toxicity. *Nucleic Acids Res.,* **2011,** *39*(21), 9283-9293.

[111] Wijshake, T.; Baker, D.J.; van de Sluis, B. Endonucleases: new tools to edit the mouse genome. *Biochimica et Biophysica Acta (BBA) -. Molecular Basis of Disease,* **2014,** *1842*(10), 1942-1950.

[112] Cox, D.B.; Platt, R.J.; Zhang, F. Therapeutic genome editing: prospects and challenges. *Nat. Med.,* **2015,** *21*(2), 121-131.

8.2 Article VII:

A novel DNA-binding motif in prostate tumor overexpressed-1 (PTOV1) required for the expression of ALDH1A1 and CCNG2 in cancer cells

Valentina Maggio, Verónica Cánovas, Alex J. Félix, Valentí Gómez, Inés de Torres, María Eugenia Semidey, Juan Morote, Verónique Noé, Carlos J. Ciudad and Rosanna Paciucci.

Appendixes
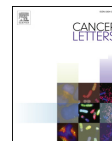
Original Articles

A novel DNA-binding motif in prostate tumor overexpressed-1 (PTOV1) required for the expression of *ALDH1A1* and *CCNG2* in cancer cells

Valentina Maggio[a,1], Verónica Cánovas[a,1], Alex J. Félix[b], Valentí Gómez[a], Inés de Torres[c], María Eugenia Semidey[c], Juan Morote[a,d], Verónique Noé[b], Carlos J. Ciudad[b], Rosanna Paciucci[a,*]

[a] Biochemistry Service, Vall d'Hebron University Hospital and Universitat Autònoma de Barcelona, Pg. Vall d'Hebron 119-129, Barcelona, 08035, Spain
[b] Department of Biochemistry and Physiology, School of Pharmacy, And Institute of Nanoscience and Nanotechnology, University of Barcelona, Avinguda Joan XXIII 27, 08028, Barcelona, Spain
[c] Department of Pathology, Vall d'Hebron University Hospital, Barcelona, Spain
[d] Deparment of Urology, Vall d'Hebron University Hospital, and Universitat Autònoma de Barcelona, Spain

ARTICLE INFO

ABSTRACT

PTOV1 is a transcription and translation regulator and a promoter of cancer progression. Its overexpression in prostate cancer induces transcription of drug resistance and self-renewal genes, and docetaxel resistance. Here we studied PTOV1 ability to directly activate the transcription of *ALDH1A1* and *CCNG2* by binding to specific promoter sequences. Chromatin immunoprecipitation and electrophoretic mobility shift assays identified a DNA-binding motif inside the PTOV-A domain with similarities to known AT-hooks that specifically interacts with *ALDH1A1* and *CCNG2* promoters. Mutation of this AT-hook-*like* sequence significantly decreased the expression of *ALDH1A1* and *CCNG2* promoted by PTOV1. Immunohistochemistry revealed the association of PTOV1 with mitotic chromosomes in high grade prostate, colon, bladder, and breast carcinomas. Overexpression of *PTOV1, ALDH1A1*, and *CCNG2* significantly correlated with poor prognosis in prostate carcinomas and with shorter relapse-free survival in colon carcinoma. The previously described interaction with translation complexes and its direct binding to *ALDH1A1* and *CCNG2* promoters found here reveal the PTOV1 capacity to modulate the expression of critical genes at multiple levels in aggressive cancers. Remarkably, the AT-hook motifs in PTOV1 open possibilities for selective targeting its nuclear and/or cytoplasmic activities.

1. Introduction

Prostate cancer (PCa) is the most frequent neoplasia in men and the third leading cause of death for cancer in western Countries [1]. The majority of patients are cured by radical prostatectomy but late-diagnosed or aggressive cancers have decreased survival rates of 29% [2]. The mainstay therapy for PCa is androgens deprivation therapy (ADT) that, although initially very effective, leads the majority of patients to develop a Castration Resistant Prostate Cancer (CRPC) with poor prognosis [3,4]. Recently, docetaxel, a taxane that arrests mitotic division, has been introduced in combination with ADT as first line therapy in metastatic hormone-naïve PCa with improved results [5]. However, the development of resistance remains the most critical

unsolved problem in prostate cancer [2,6].

Our previous findings described the action of the oncogenic protein PTOV1 in the progression of PCa to a metastatic disease and docetaxel resistance [7,8]. Suggestive of a role for PTOV1 in the acquisition of a more aggressive phenotype, we and others showed that the increased expression of this protein significantly associated with a higher grade of malignancy in PCa and numerous other cancer types [7,9–14]. The structure of the protein consists mainly of two highly homologous sequences arranged in tandem identified as PTOV-A and -B domains [15]. PTOV1 is able to shuttle between nucleus and cytoplasm, its overexpression induces cell proliferation, tumor growth, and increases the motility of PCa and breast cancer cells *in vitro*, and metastasis *in vivo* [16,17]. In the cytoplasm, PTOV1 was shown to interact with the

receptor of activated protein C kinase 1 (RACK1), and positively regulated protein synthesis, in particular c-Jun translation and activity [16]. In the nucleus, PTOV1 was shown to decrease Notch signaling in metastatic prostate tumors by repressing the transcription of Notch target genes *HES1* and *HEY1,* an action that was associated to active histone deacetylases [18]. In breast cancer cells, PTOV1 was found to repress the expression of Dickkopf 1 (DKK1), a major secreted Wnt signaling antagonist that resulted in the activation of downstream Wnt/ β catenin signaling and cancer progression [17].

Recently, PTOV1 was described able to directly bind nucleic acids through an amino acid sequence with similarities to known AT-hook motifs [19]. The first AT-hook motif, discovered in the high mobility group proteins A1 (HMGA1), confers these proteins a global role as master regulators of chromatin structure in addition to physically interact with a large variety of different transcription factors [20]. Remarkably, HMGA1 proteins are over-expressed in virtually every type of cancer, where their expression levels correlate with tumor malignancy and poor outcome [21]. An AT-hook consensus motif was defined as composed by a core of arginines (R) and prolines (P) that allows the amino acid stretch to bind the minor groove of A-T rich sequences of RNA and DNA [22]. The first 43 amino acids at the N-terminal of PTOV1 contain a new type of AT-hook motif defined as *extended AT-hook* (eAT-hook) that is 10–15 amino acids longer and differs from the canonical motif [19].

The progression of CRPC PC3 and Du145 cells to a docetaxel resistant phenotype promoted by the overexpression of PTOV1 is associated to increased expression of genes involved in resistance to docetaxel and self-renewal (*e.g. ABCB1, CCNG2* and *ALDH1A1*) [8], suggesting that through the expression of these genes PTOV1 conferred cells a higher resistance to chemotherapy and higher plasticity [8,23–26]. Here, we studied whether PTOV1 may directly bind and activate the promoter regions of these genes in LNCaP androgen-dependent prostate cancer cells. We report the identification and localization of a novel DNA-binding motif in PTOV1 that allows the protein to directly and specifically bind to *ALDH1A1* and *CCNG2* promoters and it is required for their full activation.

2. Materials and methods

2.1. Cell cultures

LNCaP androgen dependent prostate cancer cells were obtained from the American Type Culture Collection (Rockville, MD). Cells were periodically confirmed free of contaminated cell lines by in house authentication of cell cultures by STR-fingerprints comparing these with those published by ATCC. LNCaP cells were maintained in RPMI 1640 medium (Life Technologies, Inc., Grand Island, NY) supplemented with 10% heat-inactivated fetal bovine serum (Life Technologies) at 37 °C in an atmosphere of 5% CO_2. Antibodies to PTOV1 antibody were produced and purified as previously described [15,27]. Wnt3a conditioned medium was kindly provided by D. Arango (Vall d'Hebron Institute of Research, Barcelona).

2.2. Plasmid and peptides

The lentiviral HAPTOV1-ires-GFP and GFP-PTOV1 vectors were previously described [18]. Short-hairpin shRNA sequences 1397 and 1439 (Sigma-Aldrich, St. Louis, MO) targeting the human PTOV1 mRNA were as described [8] and are shown in Supplementary Table 3. PTOV1 mutant at amino acids 98–100 (the sequence KRRP was changed to EGGP) was obtained with the plasmid GFP-PTOV1 using the QuikChange™ Site-Directed Mutagenesis kit (Stratagene, La Jolla, CA) according to the manufacturer's instructions. The primers used for mutagenesis were: 5′-GAGTGGCAGGAGGAGGGCGGACCCTAGTCT GAC-3' (Forward) and 5′-GTCAGAGTAGGGTCCGCCCTCCTCCTGCCA

CTC-3' (Reverse). The eAT-hook-wild type and eAT-hook-mutant peptides were purchased from PepMic (Suzhou, China). The A-domain peptide was described previously [9].

2.3. Real time qPCR

Total RNA was extracted with the RNeasy mini kit (QIAGEN, Hilden, Germany), reverse transcribed with the Mooney Murine Leukemia Virus Reverse Transcription (M-MLV-RT) kit (Promega, Madison, USA) and real-time qPCR performed with the Universal Probe Library (Roche, Basilea, Switzerland) on a LightCycler 480 RealTime PCR instrument (Roche). Primers are shown in Supplementary Table 1. The ΔΔCt method was applied to estimate relative transcript levels. TBP, IPO8, or HMBS were used as endogenous control genes. Values are presented as mean $\pm$ SD.

2.4. Chromatin immunoprecipitation (ChIP)

Chromatin was immunoprecipitated using EZ-chip Chromatin Immuno Precipitation kit (Millipore, Burlington, USA) according to the manufacturer, as previously described [16].

Briefly, after a mild formaldehyde crosslinking step, cells were sonicated, lysates incubated with primary antibodies and precipitated with protein A/G-Sepharose. Crosslinking of DNA-protein complexes was reversed, DNA purified and used as a template for PCR reactions. Primers used for PCR in ChIP experiments are described in Supplementary Table 2.

2.5. Electrophoretic mobility shift assay (EMSA)

For binding assays, we used the following double-stranded DNAs corresponding to regions of: *ALDH1A1* promoter (from −395- to −363), *CCNG2* promoter (from −269 - to −239) and *HES1* gene (from +45 to +69). The dsDNA probes were formed by mixing 20 μg of each single-stranded oligodeoxynucleotide in a 150 mM NaCl solution. After incubation at 90 °C for 5 min, solutions were allowed to cool down slowly to room temperature. The duplexes were purified in a nondenaturing 20% polyacrylamide gel electrophoresis and DNA concentration was determined by measuring its absorbance (260 nm) at 25 °C in a Nanodrop ND-1000 spectrophotometer (Thermo Fisher Scientific, Barcelona, Spain). Duplexes were 5′-end-labeled with [γ-^{32}P]-ATP (Perkin Elmer, Madrid, Spain) by T4 polynucleotide kinase (New England BioLabs) in a 10 μL reaction mixture, according to the manufacturer's protocol. After incubation at 37 °C for 1 h, 90 μL of Tris-EDTA buffer (1 mM EDTA and 10 mM Tris, pH 8.0; Sigma-Aldrich) were added to the reaction mixture, which was subsequently filtered through a Sephadex G-25 (Sigma-Aldrich) spin-column to eliminate the unincorporated [γ-^{32}P]-ATP. Radio-labeled probes (100.000 cpm, [γ-^{32}P]-ATP) were placed in ice for 30 min with 10 μg of PTOV1 domains or 0.3 μg of peptides using either 5 μg or 0.15 μg poly (dI:dC), respectively, as unspecific competitor, in the presence of the binding buffer (5% Glycerol, 0.5 mM DTT, 4 mM $MgCl_2$, 36 mM KCl, 0.5 mM EDTA, 25 mM Tris-HCl pH 8.0; all reagents were purchased from Sigma-Aldrich). The products of the binding reactions were electrophoretically resolved in 5% polyacrylamide and 5% glycerol native gels at a fixed voltage of 220 V and 4 °C. Gels were dried at 80 °C and visualized on a Storm 840 PhosphorImager (Molecular Dynamics, GE Healthcare Life Sciences, Barcelona, Spain). ImageQuant software v5.2 was used to visualize the results.

2.6. In vivo growth of prostate cancer cells

LNCaP cells (1×10^6) in 100 μL mix of PBS and Matrigel (mix 1:1), were inoculated subcutaneously in the right flank of 6-week-old male mice (Rj:NMRI-*Foxn1*$^{nu/nu}$, n = 6) (Charles River Laboratories, Barcelona, Spain). All animal experimental procedures were approved

by the Vall d'Hebron Hospital Animal Experimentation Ethics Committee. After tumors reached 1.5 cm in diameter, mice were euthanized and tumors excised. Tumors were fixed in formol, embedded in paraffin and processed for histopathology. Hematoxylin & eosin staining to verify the histopathological findings were performed.

2.7. Immunohistochemistry

Four-micron sections from human and mice tumors were used for antigen retrieval in citrate buffer, as described [18]. After blocking endogenous peroxidase activities and non-specific labeling, sections were labeled with PTOV1 antibody for 2 h at room temperature. As a negative control, primary antibody was omitted or replaced with non-specific rabbit antibody, obtaining clean negative results in all cases (data not shown). Reaction was revealed by the avidin–biotin complex and staining with diaminobenzidine (ABC Elite kit, Burlingame, CA, USA). Nuclei were counterstained with Hematoxylin.

2.8. DNA analyses in human prostate cancer samples

The mRNA expression of *PTOV1, ALDH1A1* and *CCNG2* genes was analyzed in dataset from human prostate tumors (GSE97284 n = 188) using the R2 bioinformatics platform (http://r2.amc.nl). The most informative probeset, according to its average present signal (APS) and average value (Avg) was selected. The presence of DNA amplification, point mutations and deletions in the genes of interest were analyzed from publicly available datasets of human prostate tumors using the cBioPortal platform [28,29]. Correlations between *PTOV1, ALDH1A1,* and *CCNG2* genes and survival of patients with colon carcinoma were obtained using the dataset GSE14333 (n = 290).

2.9. Western blotting

Western blotting analyses were performed as previously described [18]. Specific reactivity to antibodies was detected with a chemiluminescent substrate (GE Healthcare). Densitometric analysis of western blot signals with antibody to PTOV1 was performed using ImageJ software.

2.10. Statistics

Results are expressed as means ± standard deviation of the means. For statistical analysis, according to whether data were sampled from a Gaussian distribution or not, unpaired t-test or Mann-Whitney U test was used to compare two groups. A p value ≤ 0.05 was taken as the level of significance. These analyses were performed using GraphPad Prism 5 software.

3. Results

3.1. PTOV1 induces the expression of self-renewal genes in prostate cancer cells

Our prior studies identified *PTOV1, ALDH1A1* and *CCNG2* genes as potential significant markers of metastasis and poor prognosis when overexpressed in primary androgen dependent prostate tumors [8]. ALDH1A1 is a hallmark of both normal and cancer stem cells (CSCs) and an enabler of drug resistance in different types of cancers [14,30], while CCNG2 is a promoter of G2/M cell cycle arrest that contributes to thiopurine and doxorubicin resistance [31,32]. In metastatic CRPC Du145 and PC3 cells, the overexpression of PTOV1 provoked an increase in the expression of these genes (Fig. 1A) [8]. Additionally, in androgen dependent LNCaP PCa cells PTOV1 also significantly induced the expression of *ALDH1A1* and *CCNG2* (Fig. 1B and C). On the other hand, the knockdown of *PTOV1* by short hairpin RNAs provoked a significant reduction of endogenous *PTOV1* levels and a parallel

significant decrease in *ALDH1A1* and *CCNG2* mRNA expression with respect to a control shRNA (Fig. 1B and C).

3.2. PTOV1 directly induces the expression of ALDH1A1 and CCNG2 in PCa cells

We next interrogated the mechanisms by which PTOV1 drives the transcription of *ALDH1A1* and *CCNG2*. Prior work had shown that the engagement of two signaling networks, Wnt/β-catenin and Jun kinase (JNK), activate PTOV1-mediated functions [16,17]. Upon inhibition of these pathways by iCRT14 or JNK inhibitor II, specific inhibitors of Wnt and JNK signaling, respectively, the expression of *ABCB1*, driven by PTOV1, was abrogated (Supplementary Fig. S1). In contrast, the PTOV1-dependent expression of *ALDH1A1* and *CCNG2* was not affected, suggesting that PTOV1 induced their transcription independently from these pathways (Supplementary Fig. S1C) [16,17]. Based on these observations, we hypothesized that PTOV1 mediates the transcription of *ALDH1A1* and *CCNG2* genes by direct association with their promoters. We thus performed chromatin immunoprecipitation (ChIP) in LNCaP cells, and observed a specific binding of PTOV1 to the chromatin of the *ALDH1A1* and *CCNG2* promoters (Fig. 2A). In contrast, the binding of PTOV1 to the *ABCB1* promoter resulted in unclear or non specific, suggesting that *ABCB1* transcriptional activation occurs through other circuits promoted by PTOV1, as suggested above (Supplementary Fig. S1). As expected, no binding of PTOV1 was observed to internal sequences of the *HES1* gene [18] .

3.3. PTOV1 directly binds to ALDH1A1 and CCNG2 promoters through a new motif in its A domain

AT-hook amino acid motifs confer proteins the ability to bind DNA or RNA. The N-terminal region of PTOV1 contained an extended AT-hook (eAT-hook) motif [19]. We tested different regions of PTOV1, including the eAT-hook motif, the A domain, and the B domain for their ability to bind the promoter sequences of *ALDH1A1* and *CCNG2* genes using electrophoretic mobility shift assays (EMSA). We synthesized small DNA probes (32 nucleotides) from the *ALDH1A1* and *CCNG2* promoters containing putative AT-hook target sequences (Fig. 3), and from the *HES1* intron-1 as negative control. These probes were labeled with [^{32}P] and used in binding reactions with recombinant glutathione-S-transferase (GST), full-lenght GST-PTOV1 protein, GST-A domain, GST-B domain, and two short peptides containing the wild type eAT-hook or the mutated eAT-hook described previously [19] (Fig. 3). A specific shifted band is detected when recombinant GST-PTOV1 is incubated with either *ALDH1A1* or *CCNG2* probes (Fig. 3B). Surprisingly, the GST-A domain of PTOV1, but not the GST-B domain, showed a strong binding activity with both *ALDH1A1* and *CCNG2* probes. However, either the wild-type or the mutated eAT peptides did not generate any shifted band with these probes, and no shifted band was visible with the *HES1* negative control probe. (Fig. 3B).

The analysis of the amino acids sequence of the A domain revealed a motif with similarities to a 'classic AT-hook' (Fig. 3A) [33]. This sequence is not conserved in the corresponding homologous B domain of PTOV1. Therefore, we synthesized a short peptide of 15 amino acids that corresponds to the motif present in the A domain (Fig. 3A). Interestingly, both labeled probes from *ALDH1A1* and *CCNG2* produced light shifted bands in the presence of this short peptide from the A domain (Fig. 3B), indicating that PTOV1 is able to bind to these promoters through a new amino acid sequence present in the A domain, but not with the eAT-hook previously described, nor with the B domain of the protein.

3.4. The new PTOV1 AT-hook-like motif is necessary to modulate ALDH1A1 and CCNG2 expression

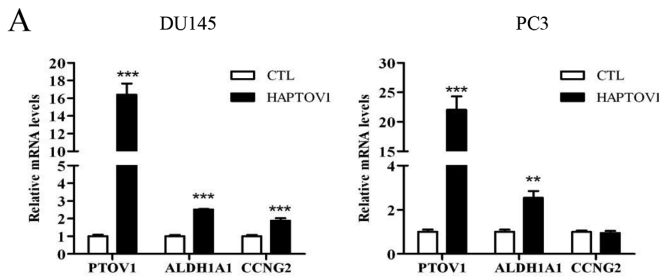In order to study the functional relevance of the KRRP sequence

160

Fig. 1. The ectopic expression of PTOV1 in prostate cancer cells promotes *ALDH1A1* and *CCNG2* expression. (**A**) CRPC Du145 and PC3 cells transduced with a lentiviral vector HAPTOV1-ires-GFP, or a control lentivirus (GFP), were analyzed by real time qPCR for *ALDH1A1* and *CCNG2* expression. (**B**) Left, LNCaP cells transduced with the lentiviral vector HAPTOV1, or the control lentivirus (GFP), were analyzed by real time qPCR for *gene* expression. Right, LNCaP cells transduced with lentiviral vectors bearing shRNA sequences (sh1397 or sh1439) and a control shRNA (shCTL) for PTOV1 knockdown, were analyzed by real time qPCR.(**C**) Immunoblots of LNCaP cells as in B, identify the endogenous or the HAPTOV1 protein. Numbers in the right panel, express the reduction of PTOV1 protein levels were quantified by densitometric analysis of the signal with respect to actin using ImageJ software. p-value: * < 0.05; ** < 0.01; *** < 0.001.
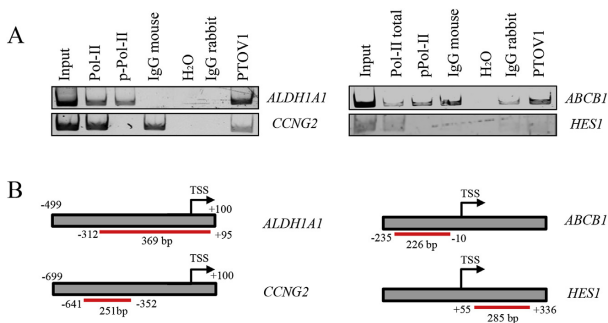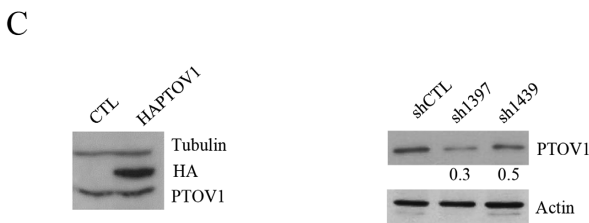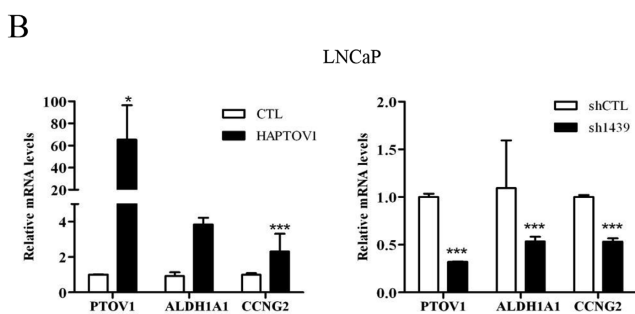
Fig. 2. PTOV1 is associated to the chromatin of *ALDH1A1* and *CCNG2* promoters. (**A**) Sheered chromatin from LNCaP cells transduced with a lentivirus encoding the fusion protein HAPTOV1 was immunoprecipitated with rabbit antibodies to PTOV1, total and phosphorylated polymerase II, and rabbit or mouse IgGs as controls. Co-immunoprecipitated DNA fragments were analyzed by PCR with specific primers for *ALDH1A1*,*CCNG2*, *ABCB1* and *HES1* promoter regions. (**B**) Graphical representation of primers localization and length of the amplified sequences on the promoters of the indicated genes. TSS: transcription start site.

resembling the core AT-hook (Fig. 3A) present in the peptide that binds to *ALDH1A1* and *CCNG2* promoters, we changed the motif to EGGP, by means of site-directed mutagenesis. This mutant was created in the GFP-full-length PTOV1 plasmid, so as to study the function of the protein as a transcription activator. As it is shown in Fig. 4, both wild-type or mutant GFP-PTOV1 were efficiently expressed in transfected cells. Importantly, the expression of the mutant caused a moderate but significant decrease in *ALDH1A1* and *CCNG2* transcript levels when
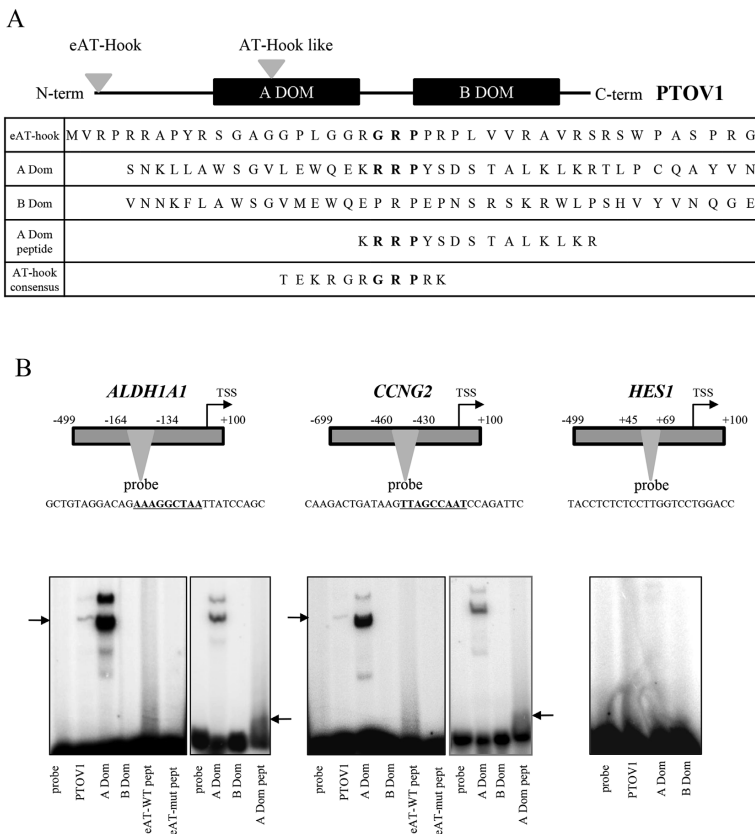
Fig. 3. EMSA identify a new AT-hook-*like* motif in the A domain of PTOV1. **(A)** Schematic of the protein structure of PTOV1 identifying the AT-hook domains present at the N-terminal (eAT-hook) and within the A domain (AT-hook-*like*) (not in scale). Bottom, eAT-hook, the first 43 amino acids from the N-terminal of PTOV1; A domain, the partial amino acid sequence (85–125) of the A domain; B domain, the partial amino acid sequence of the B domain (amino acid 249 to 292); A domain peptide, the amino acid sequence of the AT-hook-*like* motif peptide used for EMSA assays (amino acid 100 to 114); AT-hook consensus, the described AT-hook of HGMA1 (amino acid 21 to 31). Bold characters identify amino acids in the 'core' of AT-hook motifs. **(B)** Drawings show the localization of the DNA sequence probes with respect to the transcription start sites (TSS). Bottom panels: two gel shift assays are shown for each *ALDH1A1* and *CCNG2* probe: in the left gels, labeled sequences from *ALDH1A1* promoter were incubated with recombinant GST-PTOV1 (PTOV1), GST-A domain (A dom), GST-B domain (B dom), eAT-hook wild type peptide (eAT-WT pept) and mutated eAT-hook peptide (eAT-mut pept). In the right gels, labeled sequences from the *CCNG2* promoter were incubated with the GST-A domain (A dom), GST-B domain (B dom), and the A domain AT-hook-*like* peptide (A dom pept). Arrows indicate the shift provoked by the binding of protein domains or peptides to labeled DNA. A gel shift assay performed with the *HES1* probe is shown on the right panel as control.

compared to wild-type PTOV1 (Fig. 4B). The GFP-PTOV1 plasmids express comparable levels of the exogenous protein, indicating similar levels of transfection in these experiments (Fig. 4C).

Together with the above demonstration of direct binding to *ALDH1A1* and *CCNG2* promoter sequences, these results lend support to the hypothesis that the AT-hook-*like* motif in the A domain of PTOV1 is critical for the PTOV1 promoted activation of transcription of these genes.

3.5. PTOV1, ALDH1A1 and CCNG2 expression levels are associated with aggressiveness in prostate and colon carcinomas

To understand the significance of the ability of the oncoprotein

PTOV1 to directly bind and activate the expression of *ALDH1A1* and *CCNG2* genes in tumor cells, we interrogated several publicly available databases containing expression data, clinical and pathological information of untreated patients with prostate cancer for the association of expression of these genes. Data derived from micro-dissected untreated prostate tumors specimens [34] show that *PTOV1*, *ALDH1A1* and *CCNG2* transcript levels are significantly increased in patients with high Gleason Score (> 8) in comparison to patients with low Gleason score (< 7) (Fig. 5A) (GSE97284)[34]. The transcript levels of these genes are also significantly higher in prostate adenocarcinomas of patients who developed regional or distal metastasis after radical prostatectomy, suggesting their relationship with metastatic progression [8]. In addition, the expression levels of PTOV1 significantly correlated with the
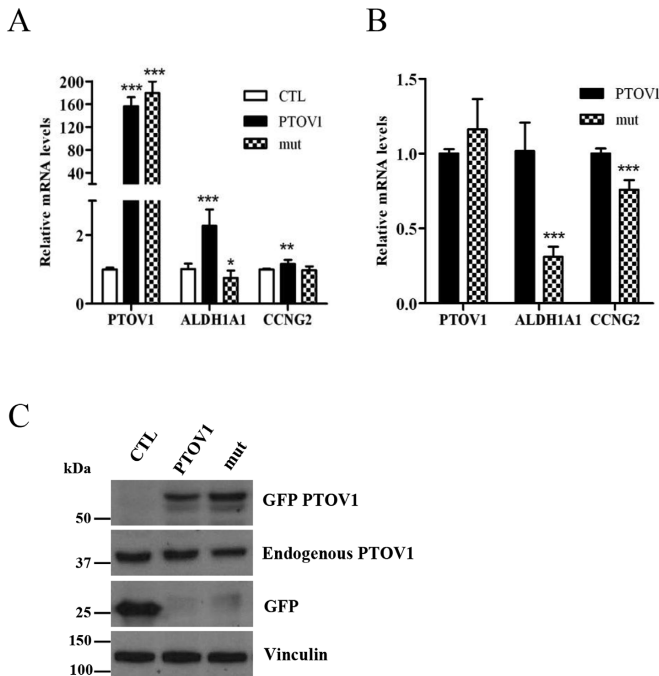
A

B

C

Fig. 4. Mutation of the newly discovered AT-hook-*like* 'core' motif of PTOV1 reduces the protein transcription capacity. The plasmid containing GFP/full-lenght PTOV1 mutated at the AT-hook (EGGP), or wild-type plasmid, and the control GFP plasmid were transfected in HEK293T cells. (**A**) Cells were analyzed for gene expression by real-time PCR 72 h after transfection. The graph shows the relative expression of *PTOV1, ALDH1A1* and *CCNG2* as compared to their endogenous levels (cells transfected with the GFP plasmid, CTL). (**B**) The levels of expression of GFP-PTOV1 (wild-type) was taken as control to compare to mutated GFP-PTOV1 from the same experiment as in A to show the effect that mutant exogenous PTOV1 has on the expression of downstream *ALDH1A1* and *CCNG2* genes in comparison to wild-type PTOV1.
(**C**) Western blot analysis of cells transfected with wild-type or mutant GFP-PTOV1 plasmids, shows similar levels of expression of the exogenous PTOV1, as indicated by the GFP antibody signals. Vinculin is shown as protein loading control.

expression of *ALDH1A1* (Spearman 0.46, $p < 0.0001$) and *CCNG2* (Spearman 0.68, $p < 0.0001$) (GSE46691). Moreover, in a cohort of patients with prostate carcinoma including data derived from 10 studies [35–44], *PTOV1, ALDH1A1* and *CCNG2* genes also showed a highly significant co-occurrence of alterations at their DNA (Table 1). These observations suggest that the expression of *PTOV1, ALDH1A1* and *CCNG2* genes is associated for a coordinated activity in aggressive prostate tumors.

Because PTOV1 can strongly and specifically bind to DNA *in vitro* and to chromatin *in vivo*, we searched for PTOV1 association with DNA in mitotic tumors cells using immunohistochemical analysis in different types of tumors. In xenografted mice tumors derived from LNCaP cells, a strong signal for PTOV1 was detected in mitotic cells where the staining appears associated to condensed chromosomes (Fig. 5B). Similarly, in colon carcinoma tissues immunohistochemical analysis reveals a clear accumulation of PTOV1 in the nuclei of mitotic cells, confirming its strong association with chromatin in aggressive tumor cells (Fig. 6A). Interrogating publicly available datasets of patients with colon carcinomas (GSE24551, GSE14333), high levels of *PTOV1, ALDH1A1* and *CCNG2* expression correlated with poor relapse-free survival and event-free survival, although for *ALDH1A1* the association did not reach significance (Fig. 6B). Furthermore, immunohistochemical analyses of high grade urothelial bladder carcinoma and ductal breast carcinoma, previously shown to express high levels of PTOV1[7], also revealed a clear association of the protein with condensed mitotic DNA (Fig. 7).

4. Discussion

Here, we provide new insights into the mechanisms used by the

protein PTOV1 to regulate the expression of *ALDH1A1* and *CCNG2,* relevant factors involved in tumor progression. Specifically, we show that PTOV1 is able to directly bind to the promoter sequences of these genes through a newly unveiled protein motif localized within the A domain of the protein [45]. This finding impacts on several aspects of the action of PTOV1 in cancer progression.

First, our findings define PTOV1 as a new nucleic acid binding protein containing two distinct motifs: one extended (eAT-hook) at the N-terminal [19] and a second AT-hook-*like* motif, identified and characterized in this work, within the A domain of PTOV1. The previously described eAT-hook does not bind to any of the DNA sequences tested here, in line with previous results that this motif has a higher affinity for RNA sequences [19]. In contrast, the newly identified AT-hook-*like* strongly binds to DNA sequences from the *ALDH1A1* and *CCNG2* promoters but not to *ABCB1* promoter or internal *HES1* gene sequences, indicating its specificity. Of note, mutations of the 'core' sequence in the AT-hook-*like* motif, decreases the expression of *ALDH1A1* and *CCNG2* indicating that this motif is functionally relevant for the transcriptional activity of PTOV1. Since PTOV1 was shown to function both at specific promoter sites to regulate transcription [17,18] and at ribosomes [16] to regulate mRNA translation, our present findings reveal potential new ways to selectively mitigate the nuclear or cytoplasmic functions of PTOV1 in cancer cells: the identification of inhibitors of these 'microhandles' in the protein could prevent its specific binding to either DNA or RNA, causing functionally diverse consequences on cell fate.

Secondly, we have shown that the transcriptional activation of *ALDH1A1* and *CCNG2* by PTOV1 is independent of the canonical Wnt or JNK pathways, being instead mechanistically explained by the direct binding of PTOV1 to specific sequences of these promoters. ALDH1A1 is an established hallmark of CSCs and promoter of drug resistance in
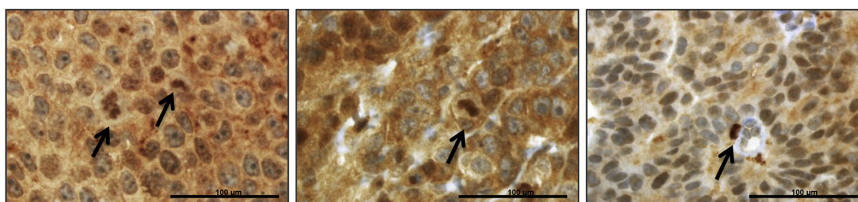
163

222
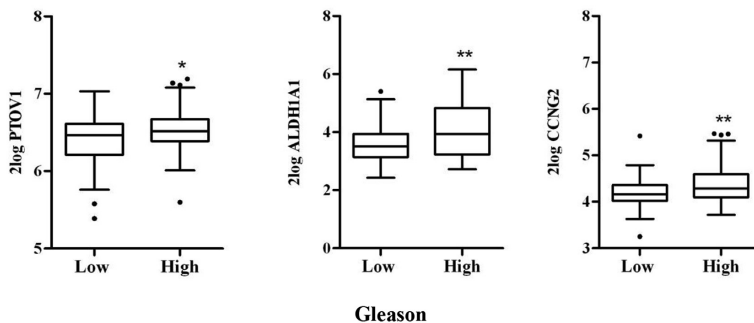
Fig. 5. The expression of *PTOV1*, *ALDH1A1* and *CCNG2* is significantly associated with the Gleason score in prostate carcinomas. (**A**) Box and whisker plots represent *PTOV1*, *ALDH1A1* and *CCNG2* expression levels in prostate tumors with different Gleason as obtained from published database (GSE 97284). Low grade represents the grade group of < 7 n = 83; High grade indicates the grade groups 4 and 5 (Gleason score: 4 + 4, 3 + 5, 5 + 3, 4 + 5, 5 + 4, 5 + 5) n = 91. (**B**) Immunohistochemical stainings of antibodies to PTOV1 in LNCaP tumors formed in immunosuppressed mice. PTOV1 associates to condensed chromatin in aggressive mitotic cells (arrows). Scale bar: 100 μm. p-value: * < 0.05; ** < 0.01; *** < 0.001.

Table 1
Co-occurrence of DNA alterations in prostate tumors.

Gene A	Gene B	Log Odds Ratio	Adjusted p-Value	Tendency
PTOV1	*ALDH1A1*	> 3	< 0.001	Co-occurrence
PTOV1	*CCNG2*	2.762	< 0.0001	Co-occurrence

different types of cancers, including colon cancer [14,30] and CCNG2 is an unconventional cyclin whose function in cancer progression remains to be determined. CCNG2 was first described as a tumor suppressor in several cancer types [46–48], being significantly upregulated in response diverse growth inhibitory stimuli, contributing to induce G2/M checkpoint and cell cycle arrest in response to doxorubicin [32] and to thiopurine resistance in lymphoblastoid cells [31]. However, it was also reported to modulate invasion in glioblastoma cells [49]. In these tumors, CCNG2 is remarkably expressed at hypoxic sites, and was shown to cooperate with actin-binding proteins providing flexibility to actin filaments for glioblastoma cell invasion. Consistent with an oncogenic role, we found that *CCNG2* is significantly co-expressed with *PTOV1* and *ALDH1A1* in aggressive prostate tumors and colon carcinomas, where overexpression of these genes is linked to progression and decreased relapse-free survival (Figs. 5A and 6B). The association of ALDH1A1 with poor survival was very recently confirmed in colon carcinomas [50]. Lastly, the significant co-occurrence of DNA alterations in *PTOV1*, *ALDH1A1* and *CCNG2* in prostate carcinomas (Table 1)

together with the above mentioned findings, indicate a concerted action of these genes in cancer progression [14,31,45,49]. These observations also suggest that, similarly to HMGA proteins, PTOV1 bound to *ALDH1A1* and *CCNG2* promoters may function as an epigenetic factor that triggers the recruitment of chromatin regulators and transcription factors to activate gene expression.

The expression of CCNG2, increased at G2-M phase, blocks the cell cycle before mitotic entry and chromosome condensation and is associated to thiopurine and doxorubicin resistance [31,32]. In addition, *ALDH1A1* is one of the most overexpressed gene in Solitary Fibrous Tumors, a rare spindle cell tumor with high mitotic counts [51]. Thus, PTOV1 action on *CCNG2* and *ALDH1A1* promoters might occur at mitotic stages and, conceivably, its binding to chromatin may be detected in condensed chromosomes of tumors cells. In fact, we observed positive PTOV1 staining in mitotic DNA in cells of prostate, colon, bladder and breast carcinomas. In mice tumors from LNCaP cells, numerous mitotic cells had a strong chromatin associated PTOV1 staining, although strong reactivity was also observed in the cytoplasm, suggesting its actions in cytoplasm and nucleus in aggressive tumor stages [27].

Thirdly, the protein structure of PTOV1 shares similarities with other proteins that interact with nucleic acids, like the β-barrel present in Ku (Ku70/Ku80) heterodimers and the SMRT/HDAC1-associated repressor protein (SHARP) [52,53]. Ku70/Ku80 are the DNA binding subunits of the DNA-PK complex necessary for the assembling of the DNA repair machinery for double strand breaks and are also implicated in transcriptional regulation [54]. SHARP is an important
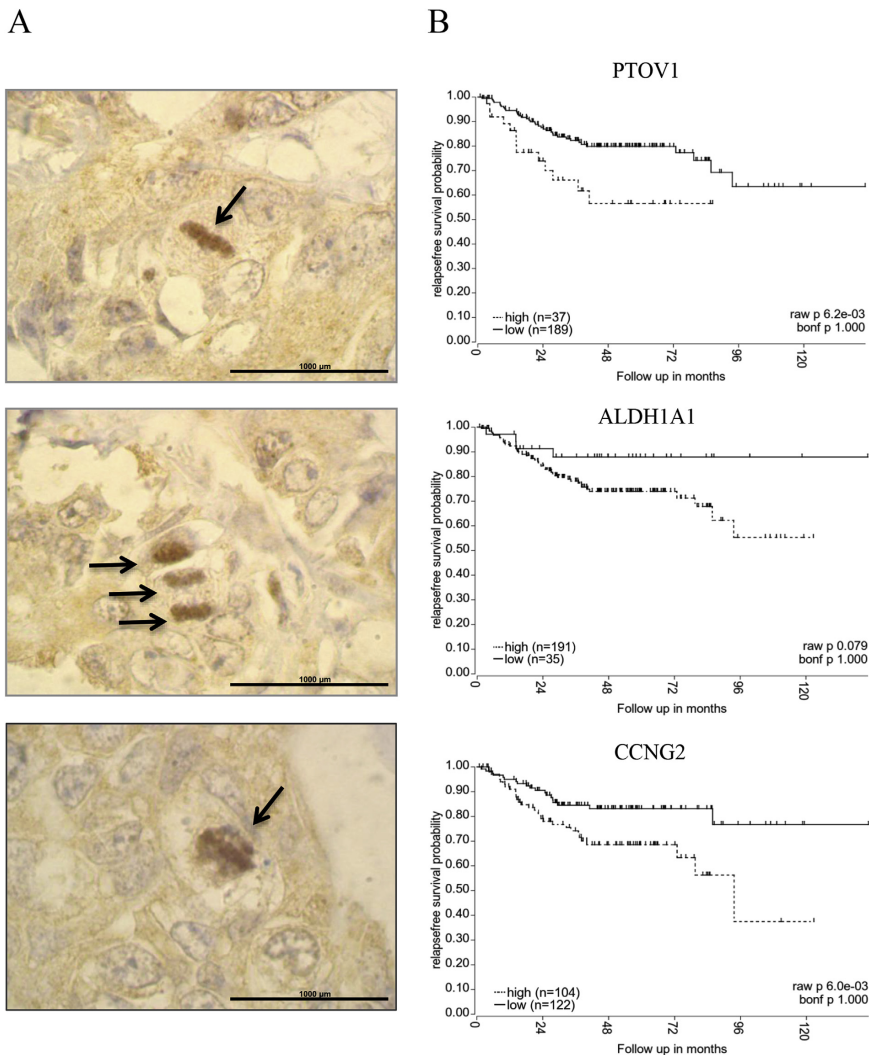
164

A

B

Fig. 6. PTOV1 accumulates in the nuclei of mitotic colon carcinoma cells. (**A**) Immunohistochemistry analyses of aggressive colon carcinoma cells show PTOV1 localized in condensed mitotic nuclei (arrows). Scale bar: 1000 μm. (**B**) The expression of PTOV1 significantly correlates with poor overall survival in colon tumors. Public datasets (GSE62452, GSE3141, GSE45547, GSE24551, GSE21653, GSE14333) containing information of survival rates in patients with colon cancer were analyzed using R2 platform.

transcriptional regulator of nuclear receptor-mediated responses, Notch-mediated transcription, and X-chromosome silencing during development [53,55]. Besides sharing characteristics like DNA binding abilities and transcription regulatory functions, the two tandem domains in PTOV1 are structurally related to the SPOC domain in Ku and SHARP [52,56]. Similarly to PTOV1, SHARP also contains RNA recognition motifs, but is not known to contain nucleic acid-binding AT-

hook-*like* motifs [53]. Members of the HMGA family of proteins also share structural (presence of several AT-hook motifs) and functional similarities with PTOV1, *e.g.* promote transcription [20,21], bind directly to gene promoters, are overexpressed in cancer, and are associated to metastasis and therapy resistance [57–59].

AT-hook variants containing modifications that still allow binding to the DNA minor groove have been discovered, suggesting that the
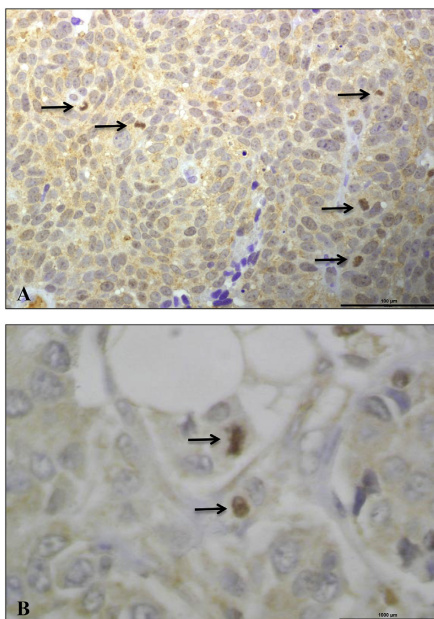
Fig. 7. PTOV1 accumulates in the nuclei of mitotic bladder carcinoma and breast carcinoma cells. Immunohistochemical staining of antibodies to PTOV1 in high grade bladder carcinoma **(A)** and breast carcinoma. Scale bar: 100 μm. **(B)** reveal strong staining associated to chromatin of mitotic cells (arrows). Scale bar: 1000 μm.

consensus core motif based on the HMGA family might not be so strict [60]. Recently, different unconventional AT-hook motifs were identified in DNA/RNA binding proteins [61,62]. Similar to the unconventional AT-hook-*like* motif reported here for PTOV1, an unconventional AT-hook domain 2 found in MeCP2 with a KRGRK core it is still able to bind AT-rich DNA sequences [63]. Another example of unconventional, AT-hook sequence is the TAF1 protein of *Drosophila melanogaster* that significantly diverges from the HGMA consensus without losing DNA affinity [60]. Moreover, Tip5, a subunit of the nucleolar remodeling complex (NoRC) that provides the link between nucleolar matrix and rDNA, also contains different AT-hook motifs for interaction with nucleic acids [64], including an *extended*-AT-hook that preferentially binds RNA to modulate the association between NoRC and promoter-associated RNA (pRNA) [65]. Finally, RNA-binding proteins Rrp12 and Srsf10 contain AT-hook motifs, suggesting that similarly to PTOV1 these proteins may have roles in DNA and RNA processes [66]. We propose that the previously identified eAT-hook and the newly unveiled AT-hook-*like* motifs have key roles in the functions of PTOV1 in mRNA translation and transcription, respectively [16–18].

In summary, we report a novel DNA binding motif in PTOV1 that allows its specific and direct binding to sequences of the *ALDH1A1* and *CCNG2* promoters, genes implicated in self-renewal and drug resistance, and their expression is associated with progression of tumors to aggressive stages and worse patients outcome. The distinct DNA and RNA-binding AT-hook motifs might direct PTOV1 nuclear and cytoplasmic actions. Noteworthy, these motifs reveal specificities potentially useful to screen for inhibitors of distinct oncogenic functions of PTOV1.

Author's contributions

VM and VC carried out the majority of the experimental work, the statistical analyses, analyses of data, and participated in the writing of the manuscript. AJ participates in the design of EMSA, realization and analysis. CC and VN designed and performed the experimental EMSA with VM. IdT and MES performed the immunohistochemistry analysis of carcinoma tissues. JM participated in data analyses and interpretation. RP conceived and designed the study, interpreted the data, and wrote the manuscript. All authors read and approved the final version of the manuscript.

Conflicts of interest

The authors declare no potential conflict of interest.

Appendix A. Supplementary data

Supplementary data to this article can be found online at https://doi.org/10.1016/j.canlet.2019.03.019.

References

[1] R.L. Siegel, K.D. Miller, Jemal, A. Cancer Stat. 68 (2018) 7–30, https://doi.org/10.3322/caac.21442 2018.
[2] G. Attard, et al., Prostate cancer, Lancet 387 (2016) 70–82, https://doi.org/10.1016/s0140-6736(14)61947-4.
[3] C. Huggins, R.E. Stevens Jr., C.V. Hodges, Studies on prostatic cancer: ii. the effects of castration on advanced carcinoma of the prostate gland, Arch. Surg. 43 (1941) 209–223, https://doi.org/10.1001/archsurg.1941.01210140043004.
[4] H. Beltran, et al., New therapies for castration-resistant prostate cancer: efficacy and safety, Eur. Urol. 60 (2011) 279–290, https://doi.org/10.1016/j.eururo.2011.04.038.
[5] N.D. James, et al., Addition of docetaxel, zoledronic acid, or both to first-line long-term hormone therapy in prostate cancer (STAMPEDE): survival results from an adaptive, multiarm, multistage, platform randomised controlled trial, Lancet 387 (2016) 1163–1177, https://doi.org/10.1016/s0140-6736(15)01037-5.
[6] N. Mottet, et al., Updated guidelines for metastatic hormone-sensitive prostate cancer: abiraterone acetate combined with castration is another standard, Eur. Urol. (2017), https://doi.org/10.1016/j.eururo.2017.09.029.
[7] S. Fernandez, et al., PTOV1 is overexpressed in human high-grade malignant tumors, Virchows Arch. Int. J. of Pathol. 458 (2011) 323–330, https://doi.org/10.1007/s00428-010-1018-1.
[8] V. Canovas, et al., Prostate Tumor Overexpressed-1 (PTOV1) promotes docetaxel-resistance and survival of castration resistant prostate cancer cells, Oncotarget 8 (2017) 59165–59180, https://doi.org/10.18632/oncotarget.19467.
[9] J. Morote, et al., PTOV1 expression predicts prostate cancer in men with isolated high-grade prostatic intraepithelial neoplasia in needle biopsy, Clin. Cancer Res.Off. J. Am. Assoc. Cancer Res. 14 (2008) 2617–2622, https://doi.org/10.1158/1078-0432.ccr-07-4987.
[10] Q. Yang, et al., Prostate tumor overexpressed 1 (PTOV1) is a novel prognostic marker for nasopharyngeal carcinoma progression and poor survival outcomes, PLoS One 10 (2015) e0136448, https://doi.org/10.1371/journal.pone.0136448.
[11] F. Guo, et al., Increased PTOV1 expression is related to poor prognosis in epithelial ovarian cancer, Tumour biol. J. Int. Soc. Oncodev. Biol. Med. 36 (2015) 453–458, https://doi.org/10.1007/s13277-014-2662-x.
[12] F. Lei, et al., Overexpression of prostate tumor overexpressed 1 correlates with tumor progression and predicts poor prognosis in breast cancer, BMC Canc. 14 (2014) 457, https://doi.org/10.1186/1471-2407-14-457.
[13] S.P. Chen, et al., Prostate tumor overexpressed 1 is a novel prognostic marker for hepatocellular carcinoma progression and overall patient survival, Medicine 94 (2015) e423, https://doi.org/10.1097/md.0000000000000423.
[14] T. Li, et al., ALDH1A1 is a marker for malignant prostate stem cells and predictor of

Appendixes

prostate cancer patients' outcome, Lab. Invest. J. Tech. Methods Pathol. 90 (2010) 234–244, https://doi.org/10.1038/labinvest.2009.127.

[15] P. Benedit, et al., PTOV1, a novel protein overexpressed in prostate cancer containing a new class of protein homology blocks, Oncogene 20 (2001) 1455–1464, https://doi.org/10.1038/sj.onc.1204233.

[16] N. Marques, et al., Regulation of protein translation and c-Jun expression by prostate tumor overexpressed 1, Oncogene 33 (2014) 1124–1134, https://doi.org/10.1038/onc.2013.51.

[17] Y. Cui, et al., Prostate tumour overexpressed-1 promotes tumourigenicity in human breast cancer via activation of Wnt/beta-catenin signalling, J. Pathol. 239 (2016) 297–308, https://doi.org/10.1002/path.4725.

[18] L. Alana, et al., Prostate tumor OVerexpressed (PTOV1) down-regulates HES1 and HEY1 notch targets genes and promotes prostate cancer progression, Mol. Canc. 13 (2014) 74, https://doi.org/10.1186/1476-4598-13-74.

[19] M. Filarsky, et al., The extended AT-hook is a novel RNA binding motif, RNA Biol. 12 (2015) 864–876, https://doi.org/10.1080/15476286.2015.1060394.

[20] A.G. Benecke, S. Eilebrecht, RNA-mediated regulation of HMGA1 function, Biomolecules 5 (2015) 943–957.

[21] S.N. Shah, L.M. Resar, High mobility group A1 and cancer: potential biomarker and therapeutic target, Histol. Histopathol. 27 (2012) 567–579, https://doi.org/10.14670/hh-27.567.

[22] J.R. Huth, et al., The solution structure of an HMG-I(Y)-DNA complex defines a new architectural minor groove binding motif, Nat. Struct. Biol. 4 (1997) 657–665.

[23] R. Demidenko, et al., Frequent down-regulation of ABC transporter genes in prostate cancer, BMC Canc. 15 (2015) 683, https://doi.org/10.1186/s12885-015-1689-8.

[24] P.E. Burger, et al., High aldehyde dehydrogenase activity: a novel functional marker of murine prostate stem/progenitor cells, Stem Cells (Dayton) 27 (2009) 2220–2228, https://doi.org/10.1002/stem.135.

[25] D. Albino, et al., Activation of the lin 28/let-7 Axis by loss of ESE3/EHF promotes a tumorigenic and stem-like phenotype in prostate cancer, Cancer Res. 76 (2016) 3629–3643, https://doi.org/10.1158/0008-5472.can-15-2665.

[26] F. Desarnaud, P. Geck, C. Parkin, G. Carpinito, A.N. Makarovskiy, Gene expression profiling of the androgen independent prostate cancer cells demonstrates complex mechanisms mediating resistance to docetaxel, Cancer Biol. Ther. 11 (2011) 204–212.

[27] A. Santamaria, et al., PTOV-1, a novel protein overexpressed in prostate cancer, shuttles between the cytoplasm and the nucleus and promotes entry into the S phase of the cell division cycle, Am. J. Pathol. 162 (2003) 897–905, https://doi.org/10.1016/s0002-9440(10)63885-0.

[28] E. Cerami, et al., The cBio cancer genomics portal: an open platform for exploring multidimensional cancer genomics data, Cancer Discov. 2 (2012) 401–404, https://doi.org/10.1158/2159-8290.cd-12-0095.

[29] J. Gao, et al., Integrative analysis of complex cancer genomics and clinical profiles using the cBioPortal, Sci. Signal. 6 (2013) pl1, https://doi.org/10.1126/scisignal.2004088.

[30] I. Ma, A.L. Allan, The role of human aldehyde dehydrogenase in normal and cancer stem cells, Stem Cell Rev. 7 (2011) 292–306, https://doi.org/10.1007/s12015-010-9208-4.

[31] L. Chouchana, et al., Molecular insight into thiopurine resistance: transcriptomic signature in lymphoblastoid cell lines, Genome Med. 7 (2015) 37, https://doi.org/10.1186/s13073-015-0150-6.

[32] M. Zimmermann, et al., Elevated cyclin G2 expression intersects with DNA damage checkpoint signaling and is required for a potent G2/M checkpoint arrest response to doxorubicin, J. Biol. Chem. 287 (2012) 22838–22853, https://doi.org/10.1074/jbc.M112.376855.

[33] R. Reeves, M.S. Nissen, A. The, T-DNA-binding domain of mammalian high mobility group I chromosomal proteins. A novel peptide motif for recognizing DNA structure, J. Biol. Chem. 265 (1990) 8573–8582.

[34] S. Tyekucheva, et al., Stromal and epithelial transcriptional map of initiation progression and metastatic potential of human prostate cancer, 8 (2017) 420, https://doi.org/10.1038/s41467-017-00460-4.

[35] D. Gao, et al., Organoid cultures derived from patients with advanced prostate cancer, Cell 159 (2014) 176–187, https://doi.org/10.1016/j.cell.2014.08.016.

[36] B.S. Taylor, et al., Integrative genomic profiling of human prostate cancer, Cancer Cell 18 (2010) 11–22, https://doi.org/10.1016/j.ccr.2010.05.026.

[37] M. Fraser, et al., Genomic hallmarks of localized, non-indolent prostate cancer, Nature 541 (2017) 359–364, https://doi.org/10.1038/nature20788.

[38] C.S. Grasso, et al., The mutational landscape of lethal castration-resistant prostate cancer, Nature 487 (2012) 239–243, https://doi.org/10.1038/nature11125.

[39] D. Robinson, et al., Integrative clinical genomics of advanced prostate cancer, Cell 161 (2015) 1215–1228, https://doi.org/10.1016/j.cell.2015.05.001.

[40] H. Beltran, et al., Divergent Clonal Evolution of Castration-Resistant Neuroendocrine Prostate Cancer vol. 22, (2016), pp. 298–305, https://doi.org/10.1038/nm.4045.

[41] S.C. Baca, et al., Punctuated evolution of prostate cancer genomes, Cell 153 (2013) 666–677, https://doi.org/10.1016/j.cell.2013.03.021.

[42] C.E. Barbieri, et al., Exome sequencing identifies recurrent SPOP, FOXA1 and MED12 mutations in prostate cancer, Nat. Genet. 44 (2012) 685–689, https://doi.org/10.1038/ng.2279.

[43] A. Kumar, et al., Substantial Interindividual and Limited Intraindividual Genomic Diversity Among Tumors from Men with Metastatic Prostate Cancer vol. 22, (2016), pp. 369–378, https://doi.org/10.1038/nm.4053.

[44] H. Hieronymus, et al., Copy number alteration burden predicts prostate cancer relapse, Proc. Natl. Acad. Sci. U. S. A 111 (2014) 11139–11144, https://doi.org/10.1073/pnas.1411446111.

[45] V. Canovas, M. Lleonart, J. Morote, R. Paciucci, The role of prostate tumor overexpressed 1 in cancer progression, Oncotarget 8 (2017) 12451–12471, https://doi.org/10.18632/oncotarget.14104.

[46] D.W. Cui, G.G. Sun, Y.J. Cheng, Change in expression of cyclin G2 in kidney cancer cell and its significance, Tumour biol. J. Int. Soc. Oncodev. Biol. Med. 35 (2014) 3177–3183, https://doi.org/10.1007/s13277-013-1415-6.

[47] G.G. Sun, W.N. Hu, D.W. Cui, J. Zhang, Decreased expression of CCNG2 is significantly linked to the malignant transformation of gastric carcinoma, Tumour biol. J. Int. Soc. Oncodev. Biol. Med. 35 (2014) 2631–2639, https://doi.org/10.1007/s13277-013-1346-2.

[48] G.G. Sun, J. Zhang, W.N. Hu, CCNG2 expression is downregulated in colorectal carcinoma and its clinical significance, Tumour biol. J. Int. Soc. Oncodev. Biol. Med. 35 (2014) 3339–3346, https://doi.org/10.1007/s13277-013-1440-5.

[49] A. Fujimura, et al., Cyclin G2 promotes hypoxia-driven local invasion of glioblastoma by orchestrating cytoskeletal dynamics, Neoplasia 15 (2013) 1272–1281.

[50] L.M. van der Waals, I.H.M. Borel Rinkes, O. Kranenburg, ALDH1A1 expression is associated with poor differentiation, 'right-sidedness' and poor survival in human colorectal cancer, PLoS One 13 (2018) e0205536, https://doi.org/10.1371/journal.pone.0205536.

[51] F. Bertucci, et al., Gene expression profiling of solitary fibrous tumors, PLoS One 8 (2013) e64497, , https://doi.org/10.1371/journal.pone.0064497.

[52] E. Vojnic, et al., Structure and VP16 binding of the Mediator Med 25 activator interaction domain, Nat. Struct. Mol. Biol. 18 (2011) 404–409, https://doi.org/10.1038/nsmb.1997.

[53] F. Oswald, et al., RBP-Jkappa/SHARP recruits CtIP/CtBP corepressors to silence Notch target genes, Mol. Cell Biol. 25 (2005) 10379–10390, https://doi.org/10.1128/mcb.25.23.10379-10390.2005.

[54] V.L. Fell, C. Schild-Poulter, The Ku heterodimer: function in DNA repair and beyond, Mut. Res. Rev. Mut. Res. 763 (2015) 15–29, https://doi.org/10.1016/j.mrrev.2014.06.002.

[55] C.A. McHugh, et al., The Xist lncRNA interacts directly with SHARP to silence transcription through HDAC3, Nature 521 (2015) 232–236, https://doi.org/10.1038/nature14443.

[56] F. Bontems, et al., NMR structure of the human Mediator MED25 domain, J. Struct. Biol. 174 (2011) 245–251, https://doi.org/10.1016/j.jsb.2010.10.011.

[57] O. Mendez, V. Peg, Extracellular HMGA1 Promotes Tumor Invasion and Metastasis in Triple-Negative Breast Cancer, (2018), https://doi.org/10.1158/1078-0432.ccr-18-0517.

[58] S.S. Liau, F. Rocha, E. Matros, M. Redston, E. Whang, High mobility group AT-hook 1 (HMGA1) is an independent prognostic factor and novel therapeutic target in pancreatic adenocarcinoma, Cancer 113 (2008) 302–314, https://doi.org/10.1002/cncr.23560.

[59] L.J. Wood, et al., HMG-I/Y, a new c-Myc target gene and potential oncogene, Mol. Cell Biol. 20 (2000) 5490–5502.

[60] C.E. Metcalf, D.A. Wassarman, DNA binding properties of TAF1 isoforms with two AT-hooks, J. Biol. Chem. 281 (2006) 30015–30023, https://doi.org/10.1074/jbc.M606289200.

[61] J. Blokken, J. De Rijck, F. Christ, Z. Debyser, Protein-protein and protein-chromatin interactions of LEDGF/p75 as novel drug targets, Drug Discov. Today Technol. 24 (2017) 25–31, https://doi.org/10.1016/j.ddtec.2017.11.002.

[62] A. Garabedian, A. Bolufer, F. Leng, Peptide Sequence Influence on the Conformational Dynamics and DNA Binding of the Intrinsically Disordered AT-Hook 3 Peptide vol. 8, (2018), https://doi.org/10.1038/s41598-018-28956-z 10783.

[63] M.J. Lyst, J. Connelly, C. Merusi, A. Bird, Sequence-specific DNA binding by AT-hook motifs in MeCP2, FEBS Lett. 590 (2016) 2927–2933, https://doi.org/10.1002/1873-3468.12328.

[64] K. Zillner, et al., Large-scale organization of ribosomal DNA chromatin is regulated by Tip5, Nucleic Acids Res. 41 (2013) 5251–5262, https://doi.org/10.1093/nar/gkt218.

[65] Y. Zhou, et al., Reversible acetylation of the chromatin remodelling complex NoRC is required for non-coding RNA-dependent silencing, Nat. Cell Biol. 11 (2009) 1010–1016, https://doi.org/10.1038/ncb1914.

[66] S. Gerstberger, M. Hafner, T. Tuschl, A census of human RNA-binding proteins, Nat. Rev. Genet. 15 (2014) 829–845, https://doi.org/10.1038/nrg3813.

8.3 Article VIII:

Gene correction of point mutations using PolyPurine reverse Hoogsteen hairpins technology

Alex J. Félix, Anna Solé, Véronique Noé and Carlos J. Ciudad

Appendixes

Gene correction of point mutations using PolyPurine reverse Hoogsteen hairpins technology

Alex J. Félix[1], Anna Solé[1], Véronique Noé[1] and Carlos J. Ciudad[1*]

[1]Department of Biochemistry and Physiology, School of Pharmacy and Food Sciences, and Institute for Nanoscience and Nanotechnology (IN2UB), University of Barcelona, Barcelona, Spain.

*Correspondence

Carlos J. Ciudad

cciudad@ub.edu

Keywords: Gene-editing, Repair-PPRH, triplex, aprt, dhfr, mutation

Abstract

Monogenic disorders are often the result of single point mutations in specific genes, leading to the production of nonfunctional proteins. Different blood disorders such as ß-thalassemia, sickle cell disease, hereditary spherocytosis, Fanconi anemia and Hemophilia A and B are usually caused by point mutations. Gene editing tools including TALENs, ZFNs or CRISPR/Cas platforms have been developed to correct mutations responsible for different diseases. However, alternative molecular tools such as triplex-forming oligonucleotides and their derivatives (e.g. peptide nucleic acids), not relying on nuclease activity, have also demonstrated their ability to correct mutations in the DNA. Here, we review the Repair-PolyPurine Reverse Hoogsteen hairpins (PPRHs) technology, which can represent an alternative gene editing tool within this field. Repair-PPRHs are non-modified single-stranded DNA molecules formed by two polypurine mirror repeat sequences linked by a five-thymidine bridge, followed by an extended sequence at one end of the molecule which is homologous to the DNA sequence to be repaired but containing the corrected nucleotide. The two polypurine arms of the PPRH are bound by intramolecular reverse-Hoogsteen bonds between the purines, thus forming a hairpin structure. This hairpin core binds to polypyrimidine tracts located relatively near the target mutation in the dsDNA in a sequence-specific manner by Watson-Crick bonds, thus producing a triplex structure which stimulates recombination. This technology has been successfully employed to repair a collection of mutants of the *dhfr* and *aprt* genes within their endogenous *loci* in mammalian cells and could be suitable for the correction of mutations responsible for blood disorders.

Scientists estimate that the global prevalence of all monogenic diseases in the human population is 1%, including over 10,000 different conditions ("Control of hereditary diseases. Report of a WHO Scientific Group." 1996). These disorders are often the result of a unique single point mutation in a specific gene that produces a nonfunctional protein. Recently, nuclease-based gene editing tools such as transcription activator like nucleases, zinc-finger nucleases or CRISPR/Cas platforms have been extensively used to correct mutations in the DNA (Gaj *et al.* 2016). Alternatively, molecules such as triplex-forming oligonucleotides (TFOs) (Seidman & Glazer 2003) or peptide nucleic acids (PNAs) (Ricciardi *et al.* 2018b) that do not rely on the activity of nucleases to produce the gene correction have been developed. In this instance, the repair event is triggered by the formation of a local triple helix structure near the mutation site that stimulates the cell's own endogenous repair machinery. Here, we will review an alternative triplex-forming molecule named PolyPurine Reverse Hoogsteen (PPRH) hairpin, which has been developed in our laboratory, to correct point mutations in the DNA.

PPRHs

PPRHs are non-modified single-stranded DNA molecules (45-55 nt) formed by two polypurine mirror repeat sequences linked by a five-thymidine bridge (5T). The formation of the hairpin structure is due to the establishment of intramolecular reverse-Hoogsteen bonds between the purines. PPRHs can bind to polypyrimidine tracts in the double-stranded DNA (dsDNA) in a sequence-specific manner via Watson-Crick bonds, thus generating a triple helix in the target site and displacing the polypurine strand of the dsDNA (Coma *et al.* 2005). This local distortion in the dsDNA interferes with DNA transcription and inhibits the expression of the targeted gene (de Almagro *et al.* 2009).

During the last decade, we have used PPRHs as gene silencing tools to inhibit genes related to cancer progression such as *dihydrofolate reductase* (*DHFR*) (de Almagro *et al.* 2009, 2011), *telomerase (TERT)* (de Almagro *et al.* 2009), *BCL2*, *topoisomerase 1* (*TOP1*), *mTOR*, *MDM2*, C-*MYC* (Villalobos *et al.* 2015)*, CHK1, WEE1* (Aubets *et al.* 2020) and s*urvivin* (*BIRC5*) *in vivo* (Rodríguez *et al.* 2013). Additionally, we applied the PPRHs technology in immunotherapy approaches by inhibiting the CD47/SIRPα (Bener *et al.* 2016) and PD-1/PD-L1 pathways (Enríquez *et al.* 2018; Ciudad *et al.* 2019). PPRHs and their advantages (low cost of production, stability and lack of immunogenicity) as gene silencing tools for cancer have been reviewed in Ciudad *et al.* 2017.

Repair-PPRHs

It is known that triplex formation can stimulate repair between a targeted *locus* and a donor DNA sequence by both homology-directed repair (HDR) (Datta *et al.* 2001; Knauert *et al.* 2006) and nucleotide excision repair (NER) (Faruqi *et al.* 2000; Datta *et al.* 2001; Rogers *et al.* 2002) pathways. For that reason, we believed that PPRHs could represent an alternative tool for gene correction due to their ability to produce triplex structures and therefore stimulate recombination (between the template and the target site) to correct point mutations in the DNA. To do so, we conceived an advanced design of the PPRH molecules that we called repair-PPRHs. These molecules are PPRH hairpins that bear an extension sequence at one end of the molecule which is

homologous to the DNA sequence to be repaired but including the corrected nucleotide instead of the mutated one (Figure 1A). In this case, the polypurine hairpin core of the repair-PPRH is designed to bind to a polypyrimidine sequence located near the target mutation, thus producing the PPRH/DNA triplex and stimulating the recombination between the extension sequence of the repair-PPRH and the mutation target site.

In our seminal paper we used repair-PPRHs to correct a point mutation in the *dhfr* gene from Chinese Hamster Ovary (CHO) cells (Solé *et al.* 2014). We selected the *dhfr* gene as a model because we could easily identify the repaired clones by applying a DHFR selective culture medium that does not contain glycine, hypoxanthine nor thymidine (-GHT).

First, DNA binding assays were performed to check the capacity of PPRHs to open the target dsDNA for the subsequent binding of a repair oligonucleotide corresponding to the extension sequence of the repair-PPRH. Two PPRHs containing 13 and 23 purines, respectively, directed against polypyrimidine sequences located in exon 6 of the *dhfr* gene were used to perform the binding experiments. We demonstrated that both PPRHs were able to bind and open their target dsDNA sequences ranging from 13 to 25 nt. Moreover, the introduction of an interruption in the duplex to simulate a point mutation did not alter the binding of the PPRH to its target sequence (Solé *et al.* 2014). The minimum concentration to obtain the binding between the PPRH and its target sequence was 3 nM. Additionally, Solé *et al.* 2017 proved that even PPRHs susceptible to fold into stable G4 structures can still bind in a sequence-specific manner to the target DNA and produce triplex formation.

Then, to assess if PPRHs were able to correct a point mutation, we designed a repair-PPRH directed against a nonsense mutation (G>C) located in exon 2 of the *dhfr* minigene contained in the p11Mut expression vector. To do so, a PPRH bearing a polypurine hairpin core of 13 nt was combined with a 25 nt extension sequence homologous to the mutation site but containing the corrected nucleotide. In cells, two different approaches were attempted to repair this mutation in p11Mut. In the first approach, gene correction was achieved by the co-transfection of both p11Mut and the repair-PPRH in *dhfr*-deficient DG44 CHO cells. After incubation, cells were selected in -GHT medium obtaining different repaired clones. The frequency of repair was approximately 0.15% (Solé *et al.* 2014). Gene correction was confirmed by DNA sequencing and by determining the levels of DHFR mRNA and protein. In the second approach, we performed the experiment in DG44 cells stably transfected with p11Mut (DG44-p11Mut cell line) since it could resemble to our final aim of correcting a point mutation in the endogenous *locus* of the gene. We confirmed that the repair-PPRH was able to correct the mutation at the same frequency (0.15%) as our first approach (Solé *et al.* 2014). The levels of DHFR mRNA and protein were recovered compared to the mutant DG44-p11Mut cell line (Solé *et al.* 2014). In a third approach, we explored the applicability of repair-PPRHs to correct point mutations at the endogenous level. There, a repair-PPRH designed against a mutation in exon 6 (G>-) of the *dhfr* gene was transfected into the DA5 cell line, which contained this specific mutation in the endogenous *locus* of the *dhfr* gene. After selection, surviving cell colonies were acquired at a frequency of 0.01% (Solé *et al.* 2014). In this case, gene correction frequency was lower than in the previous experiments since the correction was achieved for the first time in the endogenous *locus* of the gene. However, spontaneous corrections were not observed in any of the experiments. The levels of DHFR mRNA and protein were

rescued compared to the mutant DA5 cell line. Moreover, we corroborated that the DHFR protein from the repaired clones showed equal or higher DHFR activity levels than the *dhfr*[+] parental cell line, thus demonstrating that the corrected gene was completely functional (Solé *et al.* 2014).

Factors affecting gene correction frequency

The study of the influence of both hydroxyurea and aphidicolin in the repair frequency was also addressed (Solé *et al.* 2014). It is known that hydroxyurea inhibits the ribonucleotide reductase enzyme (Bianchi *et al.* 1986), thus arresting cells in the S phase of the cell cycle by blocking or retarding the movement of the replication fork caused by the dNTP pools imbalance (Saintigny *et al.* 2001). In the case of aphidicolin, it is a potent inhibitor of polymerases α, δ and ε, which leads to the blockage of the replication fork and provokes a similar effect to hydroxyurea (Wang 1991). The effect on replication caused by these agents leads to double-strand DNA breaks (DSBs), which can stimulate both the HDR and the non-homologous end joining (NHEJ) pathways to repair the DNA damage (Lundin *et al.* 2002). Accordingly, the incubation of both DG44 and DG44-p11Mut cell lines with 5 µg/mL aphidicolin or 2 mM hydroxyurea for 3 h before incubation with the repair-PPRHs increased the repair frequency by 2-fold (Solé *et al.* 2014). This is in keeping with other studies showing increased gene correction frequencies when incubating repair oligonucleotides after treatment with hydroxyurea or aphidicolin (Parekh-Olmedo *et al.* 2003; Ferrara *et al.* 2004; Wu *et al.* 2005; Chin *et al.* 2008; Engstrom & Kmiec 2008).

Finally, since the RAD51 protein plays a central role in homologous recombination (Krejci *et al.* 2012; Papaioannou *et al.* 2012) and it is required for triplex-induced recombination (Datta *et al.* 2001; Gupta *et al.* 2002), we checked its role in the repair event triggered by repair-PPRHs. Co-transfection of the repair-PPRH with a pRad51 expression vector in DA5 cells led to an increase in gene correction frequency of 10-fold compared to the transfection of the repair-PPRH alone (Solé *et al.* 2014), thus confirming that homologous recombination is involved in the repair process. Overall, this study represented the proof-of-concept for the usage of PPRHs as gene editing tools.

Correction of point mutations in the endogenous *locus*

In the following study, the usage of repair-PPRHs was expanded by correcting a representative compilation of point mutations (insertions, deletions, substitutions and a double substitution) located in the endogenous *locus* of the *dhfr* gene (Solé *et al.* 2016). For that purpose, *dhfr*-deficient CHO cell lines derived from the parental cell line UA21 (Urlaub *et al.* 1983), which carried only one copy of the *dhfr* gene (hemizygous), were selected to perform the repair experiments. DU8 (Urlaub *et al.* 1989), DF42 (Carothers *et al.* 1986), DI33A (Chasin *et al.* 1990; Carothers *et al.* 1993a), DA5 and DA7 (Carothers *et al.* 1993b) and DP12B and DP6B (Carothers *et al.* 1993a) cell lines contained premature STOP codons either in place by a nucleotide substitution or downstream due to frameshift by single deletions, insertions or by exon skipping, thus producing a nonfunctional DHFR enzyme (Table 1). Repair-PRHs were designed targeting the different mutations and transfected in their corresponding mutant cell lines. After

selection in -GHT deficient medium, repaired clones were expanded and analyzed by DNA sequencing of the targeted site, thus demonstrating the correction of the mutation. We also confirmed that the corrected *dhfr* gene was completely functional since the levels of DHFR mRNA and protein were equal or higher than the levels shown by the parental cell line, as well as DHFR enzymatic activity (Solé *et al.* 2016). In addition, we evaluated the variation in gene correction frequency depending on the number of DF42 cells initially plated to perform the experiment. The maximum frequency value was observed (7.6%) when transfection was carried out with only 1,000 cells (Solé *et al.* 2016).

One can argue that PPRH molecules present a major limitation since it is necessary to find polypyrimidine stretches relatively close to the target mutation. Despite these polypyrimidine domains are more abundant in the human genome than initially predicted by simple random models (Goñi *et al.* 2004, 2006), finding a polypyrimidine sequence adjacent to the point mutation can be complicated in some cases. To solve this issue for the DF42 mutant, we designed a long-distance repair-PPRH whose repair domain was targeting the mutation located 662 nt upstream from the polypyrimidine target sequence of the hairpin core. The repair domain of the repair-PPRH was connected to the hairpin core by another 5T loop. This long-distance repair-PPRH was able to correct its targeted mutation showing similar results to the short-distance repair-PPRH used for the correction of the same mutant, thus indicating that adjacency between the target mutation and the polypyrimidine domain was not crucial to achieve the correction.

Generality of action of repair-PPRHs

Recently, we demonstrated the generality of action of repair-PPRHs (Félix *et al.* 2020) by correcting three different mutations in the endogenous *locus* of the *aprt* gene in various *aprt*-deficient CHO cell lines (Table 1) named S23, S62 and S1 (Phear *et al.* 1989). It is worth noting that this gene also served as a disease model in CHO cells, since *aprt* deficiency in humans represents an inherited condition that severely affects the urinary tract and the kidneys (Bollée *et al.* 2012; Edvardsson *et al.* 2019). In that study, we designed repair-PPRHs containing polypurine hairpin cores composed of 19-22 nt to assure their specificity and to minimize the off-target effects as much as possible. In all the mutant cell lines we demonstrated the correction of the mutation at the DNA, mRNA and enzymatic levels, showing that the corrected APRT protein was completely functional. Moreover, we used a long-distance repair-PPRH in which the polypyrimidine target sequence was located 24 nt downstream of the S1 mutation site, however, it showed a similar effect to that of the short-distance repair-PPRH (Félix *et al.* 2020). The influence of the cell cycle phase in the repair event was also studied by performing gene correction experiments either during S phase or in asynchronous conditions. The repair frequency was increased by 2.5-fold in S phase (Félix *et al.* 2020), which is in accordance with other studies regarding gene correction with repair oligonucleotides (Majumdar *et al.* 2003; Brachman & Kmiec 2005; Olsen *et al.* 2005). Moreover, co-transfection of the repair-PPRH with the pRAD51 expression vector in S23 cells led to a 2.8-fold increase in the repair frequency (unpublished). Both factors, S phase synchronization and co-transfection with pRAD51, agree with our previous findings for the *dhfr* gene.

One of our concerns was the possible generation of off-target edits in the repaired genome caused by the treatment with repair-PPRHs. Whole genome sequencing analyses of repaired clones revealed that the repair-PPRH did not produce any random insertions or deletions (indels) in the genome. Moreover, the sequence of the repair-PPRH itself was not detected in any location of the genome (Félix *et al.* 2020). Finally, we got an insight into the molecular mechanism responsible for the gene correction event. The D-loop structure formation upon binding of the repair-PPRH to its polypyrimidine target sequence was demonstrated by DNA binding assays (Félix *et al.* 2020), thus serving as a recombination intermediate that stimulates DNA repair (Parekh-Olmedo *et al.* 2002; Drury & Kmiec 2003, 2004). The mechanism of action of repair-PPRHs is depicted in Figure 1B and 1C.

Despite the advantages of repair-PPRHs, we would like to state that the main limitations of this technology are the low repair frequency and the delivery. A way to ameliorate the low repair frequency would be to increase the rate of homologous recombination. In this direction, as stated previously, co-transfection of repair-PPRHs with a pRAD51 led to an increase in the correction frequency. Since the rate of homologous recombination is higher in the S phase of the cell cycle, synchronization in the S phase can also increase the correction frequency, as observed for the *dhfr* and *aprt* genes. Regarding the delivery of repair-PPRHs, the development of new liposome formulations (Juliano 2016) or polymeric nanoparticles (McNeer *et al.* 2015; Bahal *et al.* 2016; Ricciardi *et al.* 2018a) may contribute to improve gene repair. Finally, modification in the backbone of repair-PPRHs including phosphorothioate or locked nucleic acids (LNA) may increase the stability of the molecule and decrease its degradation by nucleases.

To date, we have only tested repair-PPRHs to correct single and double point mutations. Anyhow, most monogenic diseases are just caused by one point mutation in the responsible gene, thus making repair-PPRHs an alternative tool to correct different disorders. In this respect, we constructed Table 2 to show the versatility for designing repair-PPRHs to correct some of the most common point mutations that affect genes involved in monogenic blood disorders, with the aim of making them available for the scientific community.

CRISPR/Cas systems

Nowadays, CRISPR/Cas has become a popular gene editing tool for therapeutic purposes (Osborn *et al.* 2015; Dever *et al.* 2016; Sansbury *et al.* 2019; van de Vrugt *et al.* 2019; Xiong *et al.* 2019). Nevertheless, several studies have demonstrated the presence of off-target effects caused by unspecific activity of the CRISPR/Cas system (Cradick *et al.* 2013; Lin *et al.* 2014; Schaefer *et al.* 2017; Anderson *et al.* 2018; Allen *et al.* 2019; Cullot *et al.* 2019). Unintended on-target effects such as large deletions and complex rearrangements have also been reported (Kosicki *et al.* 2018). In this regard, Félix *et al.* showed the absence of off-target effects when using repair-PPRHs to correct point mutations in the *aprt* gene in mammalian cells. Furthermore, since *Staphylococcus pyogenes* and *Staphylococcus aureus* cause infections at high frequencies in human beings, an anti-Cas9 preexisting effector T cell response has been discovered (Charlesworth *et al.* 2019; Wagner *et al.* 2019). On the other hand, PPRHs are

nonmodified (cheap) DNA oligonucleotides that do not activate the innate inflammatory response (Villalobos *et al.* 2014).

TFOs

The ability of TFOs to stimulate recombination by triple helix formation in mammalian cells was first described in 1996 (Faruqi *et al.* 1996). Consecutive studies highlighted the potential of TFOs to correct mutations in the DNA by triplex-induced recombination between the target site and a donor DNA molecule (Chan *et al.* 1999; Culver *et al.* 1999; Datta *et al.* 2001). TFO backbone modifications have been developed to increase its binding affinity while reducing nuclease-mediated degradation. Peptide nucleic acids (PNAs) are synthetic DNA analogs composed of N-(2-aminoethyl)-glycine monomers linked by peptide bonds (Nielsen *et al.* 1991). This neutrally charged backbone allows the PNA to bind with high affinity to DNA, thus forming more stable triplex structures (Kim *et al.* 1993). Moreover, PNAs are also resistant to nuclease and protease activities (Demidov *et al.* 1994).

PNAs and their derivatives have been developed to correct mutations responsible for different monogenic diseases. Intranasal delivery of polymeric nanoparticles containing PNAs and donor DNA sequences in cystic fibrosis mice led to the correction of the F508del *CFTR* mutation *in vivo* (McNeer *et al.* 2015). More recently, PNAs delivered by polymeric nanoparticles have been used to correct the *ß-globin* gene both *in vivo* (Bahal *et al.* 2016) and *in utero* (Ricciardi *et al.* 2018a) in ß-thalassemic mice with very low off-target activity. The most recent review on PNAs as gene editing tools can be found in Economos *et al.* 2020.

Final remarks

It is evident that triplex-mediated repair of mutations in the DNA constitute a powerful gene editing approach that has demonstrated its therapeutic effect *in vivo*. Repair-PPRHs can represent a new tool in this field since they have shown their efficacy to correct different point mutations in the *dhfr* and *aprt loci* in mammalian cells with no detectable off-target activity. In addition, here we describe a collection of repair-PPRHs designed to correct 10 different blood diseases. A better understanding of the mechanisms by which the repair-PPRH triggers the recombination event may lead to improvements on PPRH design, thus increasing the frequency of correction.

Author contributions

AJF, AS and CJC wrote the original draft and VN revised the manuscript.

Funding

References

Allen, F., Crepaldi, L., Alsinet, C., … Parts, L. (2019). Predicting the mutations generated by repair of Cas9-induced double-strand breaks. *Nature Biotechnology*, **37**(1), 64–82.

Anderson, K. R., Haeussler, M., Watanabe, C., … Warming, S. (2018). CRISPR off-target analysis in genetically engineered rats and mice. *Nature Methods*, **15**(7), 512–514.

Aubets, E., Noé, V., & Ciudad, C. J. (2020). Targeting replication stress response using polypurine reverse hoogsteen hairpins directed against WEE1 and CHK1 genes in human cancer cells. *Biochemical Pharmacology*, 113911.

Bahal, R., Ali McNeer, N., Quijano, E., … Glazer, P. M. (2016). In vivo correction of anaemia in β-thalassemic mice by γ3PNA-mediated gene editing with nanoparticle delivery. *Nature Communications*, **7**. doi:10.1038/ncomms13304

Bener, G., J. Félix, A., Sánchez de Diego, C., Pascual Fabregat, I., Ciudad, C. J., & Noé, V. (2016). Silencing of CD47 and SIRPα by Polypurine reverse Hoogsteen hairpins to promote MCF-7 breast cancer cells death by PMA-differentiated THP-1 cells. *BMC Immunology*. doi:10.1186/s12865-016-0170-z

Bianchi, V., Pontis, E., & Reichard, P. (1986). Changes of deoxyribonucleoside triphosphate pools induced by hydroxyurea and their relation to DNA synthesis. *Journal of Biological Chemistry*, **261**(34), 16037–16042.

Bollée, G., Harambat, J., Bensman, A., Knebelmann, B., Daudon, M., & Ceballos-Picot, I. (2012, September 1). Adenine phosphoribosyltransferase deficiency. *Clinical Journal of the American Society of Nephrology*, pp. 1521–1527.

Brachman, E. E., & Kmiec, E. B. (2005). Gene repair in mammalian cells is stimulated by the elongation of S phase and transient stalling of replication forks. *DNA Repair*, **4**(4), 445–457.

Carothers, A. M., Urlaub, G., Grunberger, D., & Chasin, L. A. (1993a). Splicing mutants and their second-site suppressors at the dihydrofolate reductase locus in Chinese hamster ovary cells. *Molecular and Cellular Biology*, **13**(8), 5085–5098.

Carothers, A. M., Urlaub, G., Mucha, J., Yuan, W., Chasin, L. A., & Grunberger, D. (1993b). A mutational hot spot induced by N-hydroxy-aminofluorene in dihydrofolate reductase mutants of Chinese hamster ovary cells. *Carcinogenesis*, **14**(10), 2181–2184.

Carothers, A. M., Urlaub, G., Steigerwalt, R. W., Chasin, L. A., & Grunberger, D. (1986). Characterization of mutations induced by 2-(N-acetoxy-N-acetyl)aminofluorene in the dihydrofolate reductase gene of cultured hamster cells. *Proceedings of the National Academy of Sciences of the United States of America*, **83**(17), 6519–6523.

Chan, P. P., Lin, M., Fawad Faruqi, A., Powell, J., Seidman, M. M., & Glazer, P. M. (1999). Targeted correction of an episomal gene in mammalian cells by a short DNA fragment tethered to a triplex-forming oligonucleotide. *Journal of Biological Chemistry*, **274**(17), 11541–11548.

Charlesworth, C. T., Deshpande, P. S., Dever, D. P., … Porteus, M. H. (2019). Identification of preexisting adaptive immunity to Cas9 proteins in humans. *Nature Medicine*, **25**(2), 249–254.

Chasin, L. A., Urlaub, G., Mitchell, P., … Grunberger, D. (1990). RNA processing mutants at the dihydrofolate reductase locus in Chinese hamster ovary cells. *Progress in Clinical and Biological Research*, **340A**, 295–304.

Chin, J. Y., Kuan, J. Y., Lonkar, P. S., … Glazer, P. M. (2008). Correction of a splice-site mutation in the beta-globin gene stimulated by triplex-forming peptide nucleic acids. *Proceedings of the National Academy of Sciences*, **105**(36), 13514–13519.

Ciudad, C. J., Medina Enriquez, M. M., Félix, A. J., Bener, G., & Noé, V. (2019). Silencing PD-1 and PD-L1: the potential of PolyPurine Reverse Hoogsteen hairpins for the elimination of tumor cells. *Immunotherapy*, **11**(5), 369–372.

Ciudad, C. J., Rodríguez, L., Villalobos, X., Félix, A. J., & Noé, V. (2017). Polypurine Reverse Hoogsteen Hairpins as a Gene Silencing Tool for Cancer. *Current Medicinal Chemistry*, **24**(26), 2809–2826.

Coma, S., Noé, V., Eritja, R., & Ciudad, C. J. (2005). Strand displacement of double-stranded DNA by triplex-forming antiparallel purine-hairpins. *Oligonucleotides*, **15**(4), 269–283.

Control of hereditary diseases. Report of a WHO Scientific Group. (1996). *World Health Organization Technical Report Series*, **865**, 1–84.

Cradick, T. J., Fine, E. J., Antico, C. J., & Bao, G. (2013). CRISPR/Cas9 systems targeting β-globin and CCR5 genes have substantial off-target activity. *Nucleic Acids Research*, **41**(20), 9584–9592.

Cullot, G., Boutin, J., Toutain, J., … Bedel, A. (2019). CRISPR-Cas9 genome editing induces megabase-scale chromosomal truncations. *Nature Communications*, **10**(1), 1–14.

Culver, K. W., Hsieh, W.-T., Huyen, Y., … Khorlin, A. (1999). *The goal of correcting point mutations in living human Correction of chromosomal point mutations in human cells with bifunctional oligonucleotides*. *NATURE BIOTECHNOLOGY*, Vol. 17. Retrieved from http://biotech.nature.com

Datta, H. J., Chan, P. P., Vasquez, K. M., Gupta, R. C., & Glazer, P. M. (2001). Triplex-induced Recombination in Human Cell-free Extracts. *Journal of Biological Chemistry*, **276**(21), 18018–18023.

de Almagro, M. C., Coma, S., Noe, V., & Ciudad, C. J. (2009). Polypurine Hairpins Directed against the Template Strand of DNA Knock Down the Expression of Mammalian Genes. *Journal of Biological Chemistry*, **284**(17), 11579–11589.

de Almagro, M. C., Mencia, N., Noé, V., & Ciudad, C. J. (2011). Coding Polypurine Hairpins Cause Target-Induced Cell Death in Breast Cancer Cells. *Human Gene Therapy*, **22**(4), 451–463.

Demidov, V. V., Potaman, V. N., Frank-Kamenetskil, M. D., … Nlelsen, P. E. (1994). Stability of peptide nucleic acids in human serum and cellular extracts. *Biochemical Pharmacology*, **48**(6), 1310–1313.

Dever, D. P., Bak, R. O., Reinisch, A., … Porteus, M. H. (2016). CRISPR/Cas9 β-globin gene targeting in human haematopoietic stem cells. *Nature*, **539**(7629), 384–389.

Drury, M. D., & Kmiec, E. B. (2003). DNA pairing is an important step in the process of targeted nucleotide exchange. *Nucleic Acids Research*, **31**(3), 899–910.

Drury, M. D., & Kmiec, E. B. (2004). Double displacement loops (double d-loops) are templates for oligonucleotide-directed mutagenesis and gene repair. *Oligonucleotides*, **14**(4), 274–286.

Economos, N. G., Oyaghire, S., Quijano, E., Ricciardi, A. S., Mark Saltzman, W., & Glazer, P. M. (2020). Peptide nucleic acids and gene editing: Perspectives on structure and repair.

Molecules, **25**(3). doi:10.3390/molecules25030735

Edvardsson, V. O., Sahota, A., & Palsson, R. (2019). Adenine Phosphoribosyltransferase Deficiency. In *GeneReviews*, pp. 1–19.

Engstrom, J. U., & Kmiec, E. B. (2008). DNA replication, cell cycle progression and the targeted gene repair reaction. *Cell Cycle*, **7**(10), 1402–1414.

Enríquez, M. M. M., J. Félix, A., Ciudad, C. J., Noé, V., & Ahmad, A. (2018). Cancer immunotherapy using PolyPurine Reverse Hoogsteen hairpins targeting the PD-1/PD-L1 pathway in human tumor cells. *PLOS ONE*. doi:10.1371/journal.pone.0206818

Faruqi, A. F., Datta, H. J., Carroll, D., Seidman, M. M., & Glazer, P. M. (2000). Triple-helix formation induces recombination in mammalian cells via a nucleotide excision repair-dependent pathway. *Molecular and Cellular Biology*, **20**(3), 990–1000.

Faruqi, A. F., Seidman, M. M., Segal, D. J., Carroll, D., & Glazer, P. M. (1996). Recombination induced by triple-helix-targeted DNA damage in mammalian cells. *Molecular and Cellular Biology*, **16**(12), 6820–6828.

Félix, A. J., Ciudad, C. J., & Noé, V. (2020). Correction of the aprt Gene Using Repair-Polypurine Reverse Hoogsteen Hairpins in Mammalian Cells. *Molecular Therapy - Nucleic Acids*, **19**(March), 683–695.

Ferrara, L., Parekh-Olmedo, H., & Kmiec, E. B. (2004). Enhanced oligonucleotide-directed gene targeting in mammalian cells following treatment with DNA damaging agents. *Experimental Cell Research*, **300**(1), 170–179.

Gaddis, S. S., Wu, Q., Thames, H. D., … Vasquez, K. M. (2006). A web-based search engine for triplex-forming oligonucleotide target sequences. *Oligonucleotides*, **16**(2), 196–201.

Gaj, T., Sirk, S. J., Shui, S. L., & Liu, J. (2016). Genome-editing technologies: Principles and applications. *Cold Spring Harbor Perspectives in Biology*, **8**(12). doi:10.1101/cshperspect.a023754

Goñi, J. R., de la Cruz, X., & Orozco, M. (2004). Triplex-forming oligonucleotide target sequences in the human genome. *Nucleic Acids Research*, **32**(1), 354–360.

Goñi, J. R., Vaquerizas, J. M., Dopazo, J., & Orozco, M. (2006). Exploring the reasons for the large density of triplex-forming oligonucleotide target sequences in the human regulatory regions. *BMC Genomics*, **7**. doi:10.1186/1471-2164-7-63

Gupta, R. C., Bazemore, L. R., Golub, E. I., & Radding, C. M. (2002). Activities of human recombination protein Rad51. *Proceedings of the National Academy of Sciences*, **94**(2), 463–468.

Juliano, R. L. (2016). The delivery of therapeutic oligonucleotides. *Nucleic Acids Research*, **44**(14), 6518–6548.

Kim, S. K., Nordén, B., Nielsen, P. E., Egholm, M., Buchardt, O., & Berg, R. H. (1993). Right-Handed Triplex Formed between Peptide Nucleic Acid PNA-T8 and Poly(dA) Shown by Linear and Circular Dichroism Spectroscopy. *Journal of the American Chemical Society*, **115**(15), 6477–6481.

Knauert, M. P., Kalish, J. M., Hegan, D. C., & Glazer, P. M. (2006). Triplex-Stimulated Intermolecular Recombination at a Single-Copy Genomic Target. *Molecular Therapy*, **14**(3), 392–400.

Kosicki, M., Tomberg, K., & Bradley, A. (2018). Repair of double-strand breaks induced by

CRISPR–Cas9 leads to large deletions and complex rearrangements. *Nature Biotechnology*, **36**(8). doi:10.1038/nbt.4192

Krejci, L., Altmannova, V., Spirek, M., & Zhao, X. (2012). Homologous recombination and its regulation. *Nucleic Acids Research*, **40**(13), 5795–5818.

Lin, Y., Cradick, T. J., Brown, M. T., … Bao, G. (2014). CRISPR/Cas9 systems have off-target activity with insertions or deletions between target DNA and guide RNA sequences. *Nucleic Acids Research*, **42**(11), 7473–7485.

Lundin, C., Erixon, K., Arnaudeau, C., … Helleday, T. (2002). Different Roles for Nonhomologous End Joining and Homologous Recombination following Replication Arrest in Mammalian Cells. *Molecular and Cellular Biology*, **22**(16), 5869–5878.

Majumdar, A., Puri, N., Cuenoud, B., … Seidman, M. M. (2003). Cell cycle modulation of gene targeting by a triple helix-forming oligonucleotide. *Journal of Biological Chemistry*, **278**(13), 11072–11077.

McNeer, N. A., Anandalingam, K., Fields, R. J., … Egan, M. E. (2015). Nanoparticles that deliver triplex-forming peptide nucleic acid molecules correct F508del CFTR in airway epithelium. *Nature Communications*, **6**, 1–11.

Nielsen, P. E., Egholm, M., Berg, R. H., & Buchardt, O. (1991). Sequence-selective recognition of DNA by strand displacement with a thymine-substituted polyamide. *Science*, **254**(5037), 1497–1500.

Olsen, P., Randol, M., & Krauss, S. (2005). Implications of cell cycle progression on functional sequence correction by short single-stranded DNA oligonucleotides. *Gene Therapy*, **12**(6), 546–551.

Osborn, M. J., Gabriel, R., Webber, B. R., … Tolar, J. (2015). Fanconi anemia gene editing by the CRISPR/Cas9 system. *Human Gene Therapy*, **26**(2), 114–126.

Papaioannou, I., Simons, J. P., & Owen, J. S. (2012). Oligonucleotide-directed gene-editing technology: mechanisms and future prospects. *Expert Opinion on Biological Therapy*, **12**(3), 329–342.

Parekh-Olmedo, H., Drury, M., & Kmiec, E. B. (2002). Targeted nucleotide exchange in Saccharomyces cerevisiae directed by short oligonucleotides containing locked nucleic acids. *Chemistry and Biology*, **9**(10), 1073–1084.

Parekh-Olmedo, H., Engstrom, J. U., & Kmiec, E. B. (2003). The Effect of Hydroxyurea and Trichostatin A on Targeted Nucleotide Exchange in Yeast and Mammalian Cells. *Annals of the New York Academy of Sciences*, **1002**(1), 43–55.

Phear, G., Armstrong, W., & Meuth, M. (1989). Molecular basis of spontaneous mutation at the aprt locus of hamster cells. *Journal of Molecular Biology*, **209**(4), 577–582.

Ricciardi, A. S., Bahal, R., Farrelly, J. S., … Saltzman, W. M. (2018a). In utero nanoparticle delivery for site-specific genome editing. *Nature Communications*, **9**(1), 1–11.

Ricciardi, A. S., Quijano, E., Putman, R., Saltzman, W. M., & Glazer, P. M. (2018b). Peptide nucleic acids as a tool for site-specific gene editing. *Molecules*, **23**(3), 1–15.

Rodríguez, L., Villalobos, X., Dakhel, S., … Noé, V. (2013). Polypurine reverse Hoogsteen hairpins as a gene therapy tool against survivin in human prostate cancer PC3 cells in vitro and in vivo. *Biochemical Pharmacology*, **86**(11), 1541–1554.

Rogers, F. A., Vasquez, K. M., Egholm, M., & Glazer, P. M. (2002). Site-directed recombination

via bifunctional PNA-DNA conjugates. *Proceedings of the National Academy of Sciences of the United States of America*, **99**(26), 16695–16700.

Saintigny, Y., Delacôte, F., Varès, G., … Lopez, B. S. (2001). Characterization of homologous recombination induced by replication inhibition in mammalian cells. *EMBO Journal*, **20**(14), 3861–3870.

Sansbury, B. M., Hewes, A. M., & Kmiec, E. B. (2019). Understanding the diversity of genetic outcomes from CRISPR-Cas generated homology-directed repair. *Communications Biology*, **2**(1), 1–10.

Schaefer, K. A., Wu, W. H., Colgan, D. F., Tsang, S. H., Bassuk, A. G., & Mahajan, V. B. (2017). Unexpected mutations after CRISPR-Cas9 editing in vivo. *Nature Methods*, **14**(6), 547–548.

Seidman, M. M., & Glazer, P. M. (2003). The potential for gene repair via triple helix formation. *J Clin Invest*, **112**(4), 487.

Solé, A., Ciudad, C. J., Chasin, L. A., & Noé, V. (2016). Correction of point mutations at the endogenous locus of the dihydrofolate reductase gene using repair-PolyPurine Reverse Hoogsteen hairpins in mammalian cells. *Biochemical Pharmacology*, **110**–**111**, 16–24.

Solé, A., Delagoutte, E., Ciudad, C. J., Noé, V., & Alberti, P. (2017). Polypurine reverse-Hoogsteen (PPRH) oligonucleotides can form triplexes with their target sequences even under conditions where they fold into G-quadruplexes. *Scientific Reports*, **7**(January), 1–11.

Solé, A., Villalobos, X., Ciudad, C. J., & Noé, V. (2014). Repair of Single-Point Mutations by Polypurine Reverse Hoogsteen Hairpins. *Human Gene Therapy Methods*, **25**(5), 288–302.

Urlaub, G., K&s, E., Carothers, A. M., & Chasin, L. A. (1983). *Deletion of the Diploid Dihydrofolate Reductase Locus from Cultured Mammalian Cells. Cell*, Vol. 33.

Urlaub, G., Mitchell, P. J., Ciudad, C. J., & Chasin, L. A. (1989). Nonsense mutations in the dihydrofolate reductase gene affect RNA processing. *Molecular and Cellular Biology*, **9**(7), 2868–2880.

van de Vrugt, H. J., Harmsen, T., Riepsaame, J., … te Riele, H. (2019). Effective CRISPR/Cas9-mediated correction of a Fanconi anemia defect by error-prone end joining or templated repair. *Scientific Reports*, **9**(1), 1–13.

Villalobos, X., Rodríguez, L., Prévot, J., Oleaga, C., Ciudad, C. J., & Noé, V. (2014). Stability and immunogenicity properties of the gene-silencing polypurine reverse hoogsteen hairpins. *Molecular Pharmaceutics*, **11**(1), 254–264.

Villalobos, X., Rodríguez, L., Solé, A., … Noé, V. (2015). Effect of polypurine reverse hoogsteen hairpins on relevant cancer target genes in different human cell lines. *Nucleic Acid Therapeutics*, **25**(4), 198–208.

Wagner, D. L., Amini, L., Wendering, D. J., … Schmueck-Henneresse, M. (2019). High prevalence of Streptococcus pyogenes Cas9-reactive T cells within the adult human population. *Nature Medicine*, **25**(2), 242–248.

Wang, T. S. (1991). EUKARYOTIC DNA POLYMERASES. *Annual Review of Biochemistry*.

Wu, X. S., Xin, L., Yin, W. X., … Liang, C. C. (2005). Increased efficiency of oligonucleotide-mediated gene repair through slowing replication fork progression. *Proceedings of the National Academy of Sciences of the United States of America*, **102**(7), 2508–2513.

Xiong, Z., Xie, Y., Yang, Y., … Sun, X. (2019). Efficient gene correction of an aberrant splice site in β-thalassaemia iPSCs by CRISPR/Cas9 and single-strand oligodeoxynucleotides. *Journal of Cellular and Molecular Medicine*, **23**(12), 8046–8057.

Table 1. CHO mutant cell lines corrected by repair-PPRHs.

Cell line	Gene	Mutation	Base change	Coding change	References
DF42		c.541 Exon 6	Substitution G > T	STOP in place	
DA5		c. 541 Exon 6	Deletion (-G)	STOP at +584 (normal termination is at +562)	
DP12B		c.370 – 2 Intron 4	Substitution A > T	Exon 5 skipped STOP at +504	
DI33A	*dhfr*	c. 493 Exon 6	Insertion (+G)	STOP at +505	(Solé *et al.* 2016)
DU8		c. 136 + 1 Exon 2/Intron 2	Double substitution GG > AA	Exon 2 skipped STOP at +139	
DA7		c. 235 Exon 3	Substitution G > T	STOP in place	
S23		c. 7 Exon 1	Substitution G > T	STOP in place	
S1	*aprt*	c. 180 Exon 2	Substitution C > G	STOP in place	(Félix *et al.* 2020)
S62		c. 505 Exon 5	Substitution G > T	STOP in place	

Position numbers refer to the translational start site (ATG). The correction of the mutant cell lines using repair-PPRHs can be found in the referenced papers.

Table 2. Compendium of repair-PPRHs designed to correct point mutations responsible for 10 different blood disorders.

Blood disorder	Gene	Mutation	Codon change	Name and sequence (5'->3') of the Repair-PPRH
G6PD deficiency (mediterranean)	G6PD	c.563 C>T Exon 6	TCC>TTC Ser>Phe p.188	RHp-G6PD-E6-C (99 nt) GCCGTCACCAAGAACATTCACGAGTCCTGCATGAGCCAGATGTAAGGCTTGGGCAACGGGAGGGGAAGGGCGG AttttAGGGCGGGAAGGGAGGGCAACGG
Beta-Thalassemia	HBB	G>A Intron 1 (+110)	TGG>TAG	RHp-HBB-I1-C (91 nt) ACTGACTCTCTCTGCCTATTGGTCTATTTTCCCACCCTTAGtttAAAAGAAAGGGGAAGAAAAGAtttAGAAAAGAA GGGGAAAGAAAA
Sickle cell disease	HBB	c.70 A>T Exon 1	GAG>GTG Glu>Val p.7	RHp-HBB-E-T (81 nt) CATGGTGCATCTGACTCCTGAGGAGAAGTCTGCCGTTACTGCCCTGTGGGGCAAGGTGAACGtttGCAAGTGGA ACGGGG
Porphyria	HMBS	c.33+1 G>A/T Exon 1/ Intron 1	Intron retention 67 bp	RHp-HMBS-E1-T (97 nt) GCAATGCGGCTGCAACGGCGGTGAGTGCTGAGCCGGTGACCtttGGAAGGAATGGGGAAATCAGAGAGtttGAG AGACTAAAGGGGTAAGGAAGG
Ferritin Deficiency	FTL	c.310 G>T Exon 3	GAG>TAG Glu>Ter p.104	RHp-FTL-E3-C (93 nt) TGAAAGCTGCCATGGCCCTGGAGAAAAAGCTGAACCAGGCCtttGGAAAAAGAGGGGGAGAGACGAGtttGGAAAA GAGGGGGAGAGACAG
Dyserythropoietic anemia	CODAN1B	c.281 A>G Exon 5	TAT>TGT Tyr>Cys p.94	RHp-C15ORF41-E5-T (102 nt) GAGGCCATTAATGAGGGGCGCATAGTCCACCTCATTGGCCAGGTCCAGGAGCACTGGGCAGGAGAGGTAAAAAGT GGTGAGGttttGGAGTGGTGAAAAATGGAG
Hemophilia A	F8	c.6976 C>T Exon 27	CGA>TGA Arg>Ter p.2326	RHp-F8-E27 (87 nt) CGTTACTGACTCGCTACCTTCGAATTCACCCCCAGAGTTGGtttGGCAGTGGAGAGGGGAGGGAGtttGAGGAGGGA GAGGTGACGG

|				
Hemophilia B	*F9*	c.169 C>T Exon 2	CAA>TAA Gln>Ter p.57	RHp-F9-E2 (100 nt) ATTCTCTCTCAAGGTTCCCTT**G**AACAAACTCTTCCAATTTACCTttttAAGAAAAACTGAAATGTAAAAGAAttttAAGA AAATGTAAAGTCAAAAGAA
Fanconi anemia	*FANCA*	c.295 C>T Exon 4	CAG>TAG Gln>Ter p.99	RHp-FANCA-E4 (99 nt) GCCTTGAGGCTTGATCCTG**G**CAAAGCAGAGCCTTAAACttttGGGGAGAATAGATGCAAAGGGAAAAttttAAAAAGG GAAACGTAGATAAGAGGGGG
Von Willebrand	*VWF*	c.4975 C>T Exon 28	CGA>TGA Arg>Ter p.1659	RHp-VWF-E28 (103 nt) GACCGCTCCCC**C**GAGAGGCTCCTGACCTGGTGCTGCAGAGGTGCTGCTCCGGAGAGGGGCTGCAGA**A**GGGGT GGGAGAGGGGAtttAGGGGAGAGGGTGGGGA

The design of the different repair-PPRHs was performed as follows: i) Finding triplex targeting sites near the mutation using the TFO searching tool (http://utw10685.utweb.utexas.edu/tfo/) (Gaddis *et al.* 2006); ii) Devising the corresponding polypurine hairpin core (underlined sequences); iii) Determining the repair domain of the repair-PPRH corresponding to the homologous sequence of the mutation site but containing the corrected nucleotide (green). In the case of a long-distance repair-PPRH, an additional 4-5 thymidine loop is added between the hairpin core and the repair domain. The abbreviation of the gene responsible for the blood disorder, the position of the mutation and the affected codon are given for each case. The position of the mutation is referred to the translation start site (ATG). TER, termination codon.
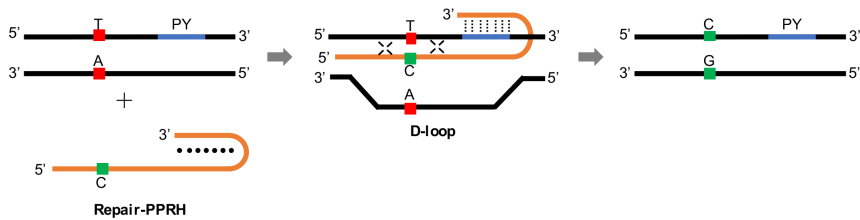
A
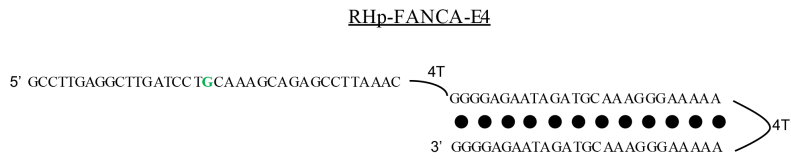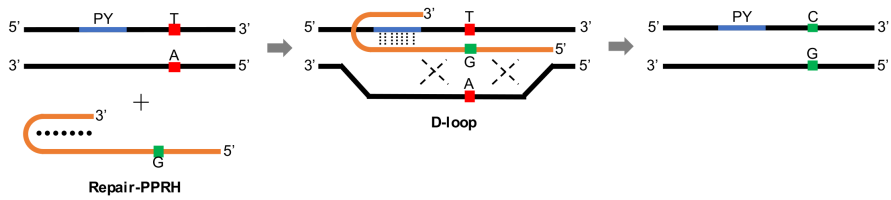
RHp-FANCA-E4

Figure 1. Mechanism of action of repair-PPRHs. (A) Representation of the RHp-FANCA-E4 repair-PPRH targeting the c.295 C>T mutation in the *FANCA* gene. In this case, the polypurine hairpin core is bound to the repair domain by an additional four-thymidine bridge following the long-distance repair-PPRH approach. Scheme depicting the mechanism of action of a repair-PPRH when the polypyrimidine target sequence (PY) is located either upstream (B) or downstream (C) of the mutation.